THE SYNTHESIS AND REACTIVITY OF CATIONIC TERMINAL BORYLENE COMPLEXES

A thesis submitted in accordance with the requirements for the degree of Doctor of Philosophy at the University of Oxford

Glesni Angharad Pierce
The Queen's College, Oxford
August 2009

This thesis is dedicated to Mam, Dad and Cerys

Abstract

This thesis describes the synthesis, structure/bonding studies and reactivity of cationic terminal borylene complexes.

Reactions of the cationic terminal borylene complexes, $[CpFe(CO)_2(BNR_2)]^+[BAr^f_4]^-$ (R = Cy, ^{i}Pr) with heteroallenes have been investigated and shown to proceed by initial coordination of the substrate at the electrophilic boron centre. Reaction with isocyanate ultimately forms $[CpFe(CO)_2(CNPh)]^+[BAr^f_4]^-$ by a net metathesis process. Dicyclohexylcarbodiimide, however, reacts by insertion into the Fe=B bond of the aminoborylene to form $[CpFe(CO)_2C(NCy)_2BNR_2]^+[BAr^f_4]^-$. An excess of the substrate yields the spirocyclic complex, $[CpFe(CO)_2C(NCy)_2B(NCy)_2BNR_2]^+[BAr^f_4]^-$ via a second insertion into the B=N bond. Computational studies investigating insertion and metathesis reaction pathways of these aminoborylene complexes are also reported.

Reactions of dicyclohexylcarbodiimide with three-coordinate aminoborane and aminoboryl complexes are described. Formation of the first boron guanidinate complexes featuring dihalide substituents, $Cy_2NC(NCy)_2BCl_2$ and $^iPr_2NC(NCy)_2BCl_2$ by both salt metathesis and carbodiimide insertion routes are reported. The aminoboryl complexes, $CpFe(CO)_2B(NPh_2)Cl$ and $CpFe(CO)_2B(NBz_2)Cl$ have also been synthesized and their reactions with carbodiimides probed.

A novel cationic terminal borylene complex, $[Cp'Fe(CO)_2(BN^iPr_2)]^+$ $[BAr^f_4]^-$ featuring a methyl-substituted Cp ring is reported and represents the first structurally characterized isopropyl substituted aminoborylene complex.

Substitution of the ancillary carbonyl ligands of cationic terminal borylene complexes has been investigated. Irradiation of the aminoboryl precursor complex, $CpFe(CO)_2B(NCy_2)Cl$ in the presence of trialkylphosphines, PR_3 (PR_3 = PMe_3, PPh_3, $P(OMe)_3$) yield the mono(phosphine) complexes, $CpFe(CO)(PR_3)B(NCy_2)Cl$. The mono(substituted) dimer $[\{CpFe(CO)(BNCy_2)\}_2(\mu\text{-dmpe})]$ was also formed from the reaction with the chelating ligand, dmpe. Replacement of the second carbonyl is prevented by the steric bulk of the dicyclohexylamino substituent, and instead $[CpFe(CO)(PR_3)_2]^+Cl^-$ is formed by extrusion of the borylene fragment. The mono(phosphine) ligated cationic terminal borylene complexes, $[CpFe(CO)(PR_3)(BNCy_2)]^+[BAr^f_4]^-$ were subsequently formed by halide abstraction. Both $[CpFe(CO)(PMe_3)(BNCy)_2]^+[BAr^f_4]^-$ and the bridging dication $[\{CpFe(CO)(BNCy_2)\}_2(\mu\text{-dmpe})]^{2+}[BAr^f_4]^-_2$ were structurally authenticated.

Replacing the bulky cyclohexyl groups of the aminoboryl precursor for methyl groups allowed synthesis of the bis(substituted) complexes, $CpFe(PMe_3)_2B(NMe_2)Cl$ and $CpFe(dmpe)B(NMe_2)Cl$. Extraction of these complexes into dichloromethane resulted in formation of the borylene, $[CpFe(PMe_3)_2(BNMe_2)]^+Cl^-$ and $[CpFe(dmpe)(BNMe_2)]^+Cl^-$ by spontaneous halide ejection.

Acknowledgements

Firstly, I would like to express my gratitude to Dr Simon Aldridge for all his ideas, guidance, support and encouragement throughout my DPhil. It truly has been a wonderful experience.

I would like to acknowledge the contributions made by the following people:
Drs Joanna Day, Li-Ling Ooi, Andreas Stasch, and Prof. Cameron Jones (Cardiff University) and Drs Amber Thompson, Dave Watkin, Drasko Vidovic and Delphine LePevelen (Oxford) for carrying out X-ray crystallography on the compounds described heirin.

Dr Natalie Coombs and Dr Dave Willock (Cardiff University) and Susmita De and Dr E. Jemmis (Bangalore) for performing the DFT calculations described in this thesis.

The technical staff in both Cardiff and Oxford for their help with keeping the lab running: Mal, Alan, Rob Jenkins, Ricky, Gaz, Dave, Robin, JoBo and Sham, Alan Roper, Andy White and Jude.

EPSRC National Crystallography and Mass Spectrometry Service Centres at Southampton and Swansea. Drs Anneke Lubben and Tom Douglas (Bath) and Romaeo Dallanegra and Becky Pawley (Oxford) for their help with Electrospray Mass Spectrometry.

A huge thank you to members of the lab for help and encouragement over the years and, most importantly, the laughs that made my DPhil some of the best years of my life – Mini, Jo, Bres, Tom, Dan, Matt, James, Praba, Carina, Maria, (Cardiff) and Dave, Alex, Hassiane, Vicky, Christina, Drasko, Angie, Jan, Mari-Carmen, Debs, Cally, Will, Mike and Ian (Oxford).

To Mam, Dad, Cerys, Taid, Gran and Grandad for their unconditional love and support and for always believing in me!

Finally, I would like to thank Geth for his love and understanding, and for always being there.

Notes

The following abbreviations were used in the text:

Ar^f = $C_6H_3(CF_3)_2$-3,5

br = broad

μ = bridged

^{n}Bu = $-CH_2CH_2CH_2CH_3$

^{t}Bu = $-C(CH_3)_3$

Bz = $CH_2C_6H_5$

calc. = calculated

cat = 1,2-$O_2C_6H_4$

Cp = cyclopentadienyl, η^5 -C_5H_5

Cp' = methylcyclopentadienyl, η^5-C_5H_4Me

Cp* = pentamethylcyclopentadienyl, η^5-C_5Me_5

Cy = cyclohexyl

Cym = (η^5-C_5R_5)$Mn(CO)_3$

δ = NMR chemical shift

d = doublet, days

d d = doublet of doublets

DFT = density functional theory

dmpe = 1,2-bis(dimethylphosphino)ethane

EI = electron ionisation

equiv. = equivalents

ES = electrospray

Fc = ferrocenyl, (C_5H_5)Fe(C_5H_4-)

FT = Fourier Transform

fwhm = frequency width at half maximum

h = hours

^{i}Pr = $-CH(CH_3)_2$

IR = infrared

J = coupling constant

λ = wavelength

m = multiplet

md = medium

Me = $-CH_3$

Mes = mesityl, 2,4,6-$Me_3C_6H_2$

min. = minutes

MS = mass spectrometry

ν = stretching frequency

NMR = nuclear magnetic resonance

obs. = observed

Ph = $-C_6H_5$

pin = 1,2-$O_2C_2Me_4$

ppm = parts per million

q = quartet

ref. = reference

RT = room temperature

s = singlet

sept = septet

sh = shoulder

st = strong

t = triplet

THF = tetrahydrofuran

Tf = triflate, OSO_2CF_3

tmg = $OCH_2CH_2CH_2O$

tmp = 2,2,6,6-tetramethylpiperidyl

Trip = 2,4,6-triisopropylphenyl

VT = variable temperature

w = weak

1 Torr = 1 mmHg = 133.3 Pa

Contents

	Page
Chapter One Introduction	1
1.1 Introduction	1
1.2 Boryl Complexes	2
1.2.1 Synthesis of Boryl Complexes	3
1.2.1.1 Salt Elimination	3
1.2.1.2 Oxidative Addition	10
1.3 Borylene Complexes	13
1.3.1 Bridging Borylene Complexes	15
1.3.1.1 Synthesis of Bridging Borylene Complexes	15
1.3.1.1.1 From Diboranes	15
1.3.1.1.2 From Dihaloboranes	17
1.3.1.1.3 Photochemical Borylene Transfer	19
1.3.1.1.4 Oxidative Addition	21
1.3.2 Terminal Borylene Complexes	22
1.3.2.1 Synthesis of Terminal Borylene Complexes	22
1.3.2.1.1 Salt Elimination	22
1.3.2.1.2 Photolytic Borylene Transfer	25
1.3.2.1.3 Halide Abstraction	28
1.3.2.1.4 α-Migration of a Boryl Substituent	33
1.3.2.1.5 Modification of Existing Borylene Systems	36
1.3.2.1.6 Miscellaneous Approaches	42

Page

1.3.2.2 Spectroscopic and Structural Aspects of Terminal Borylene Complexes 43

1.3.2.3 Reactivity of Terminal Borylene Complexes 49

1.3.2.3.1 Borylene Transfer Chemistry 49

1.3.2.3.2 Coordination at Boron 55

1.4 References for Chapter One 59

Chapter Two Experimental Techniques 68

2.1 The Manipulation of Air-Sensitive Compounds 68

2.1.1 Inert Atmosphere Techniques 68

2.1.2 High Vacuum Techniques 70

2.2 Physical Measurements 70

2.2.1 NMR Spectroscopy 70

2.2.2 Infrared Spectroscopy 71

2.2.3 Mass Spectrometry 71

2.2.4 Elemental Analysis 71

2.2.5 X-Ray Crystallography 71

2.2.6 Theoretical Calculations 72

2.3 Photolytic Experiments 72

2.4 Purification and Preparation of Essential Solvents and Reagents 72

2.4.1 Preparation of Precursors 75

2.4.1.1 Preparation of Transition Metal Anions 75

Page

2.4.1.2 Preparation of $Na\{B[3,5\text{-}(CF_3)_2C_6H_3]_4\}$ 75

2.4.1.3 Preparation of $[CpFe(CO)_2(BNR_2)]^+[BAr^f_4]^-$ (R = ^{i}Pr/Cy/Me) 76

2.5 References for Chapter Two 79

Chapter Three Insertion Reactions of Carbodiimide with Two-Coordinate Aminoborylene Complexes 80

3.1 Introduction 80

3.1.1 Aims of the Present Research 84

3.2 Experimental 84

3.3 Results and Discussion 89

3.3.1 Reaction of $[CpFe(CO)_2(BNCy_2)]^+[BAr^f_4]^-$ with CO_2 89

3.3.2 Oxygen Atom Abstraction 89

3.3.3 Insertion of Dicyclohexylcarbodiimide into Aminoborylene Complexes 93

3.3.4 Computational Studies of the Reaction of the Model Aminoborylene $[CpFe(CO)_2(BNMe_2)]^+[BAr^f_4]^-$ with Heteroallenes 103

3.3.4.1 Computational Studies of the Insertion of Carbodiimides, MeNCNMe into $[CpFe(CO)_2(BNMe_2)]^+[BAr^f_4]^-$ 105

3.3.4.1.1 Insertion of the First Equivalent of MeNCNMe 106

3.3.4.1.2 Insertion of the Second Equivalent of MeNCNMe 112

3.3.4.2 Computational Studies of the Reaction of the Isocyanate, MeNCO with $[CpFe(CO)_2(BNMe_2)]^+[BAr^f_4]^-$ 115

3.3.4.2.1 Insertion of the First Equivalent of MeNCO 116

Page

3.3.4.2.2 Insertion of the Second Equivalent of MeNCO 122

3.4 Conclusions and Suggestions for Further Research 126

3.5 References for Chapter Three 129

Chapter Four Synthesis and Reactivity of Three-Coordinate Amino Boranes and Boryls Towards Dicyclohexylcarbodiimide 132

4.1 Introduction 132

4.1.1 Aims of the Present Research 135

4.2 Experimental 137

4.3 Results and Discussion 141

4.3.1 Reactions of Carbodiimide with Aminoboryl Complexes 141

4.3.2 Rational Synthetic Routes to Guanidinate Complexes, 4.1 and 4.2 151

4.3 Conclusions and Suggestions for Further Research 154

4.4 References for Chapter Four 157

Chapter Five Studies of Ligand Variation in Cationic Terminal Borylene Complexes 161

5.1 Introduction 161

5.1.1 Aims of the Present Research 163

5.2 Experimental 164

5.3 Results and Discussion 172

5.3.1 Synthesis of $[CpFe(CO)_2(BN^iPr_2)]^+[BAr^f_4]^-$ 172

5.3.2 Mono(Substitution) of Carbonyl Ligands for Phosphines 176

5.3.3 Synthesis of Mono(Substituted) Cationic Borylene Complexes 186

5.3.4 Substitution of Both Carbonyls for Phosphines 196

5.4 Conclusions and Suggestions for Further Research 200

5.5 References for Chapter Five 204

Appendix One

Computational Methodology 208

Appendix Two

List of Publications 214

Chapter One

Introduction

1.1 Introduction

Transition metal complexes featuring a classical two-centre two-electron bond to a main group element such as carbon, silicon, or the heavy group 13 elements are very well established.[1] For boron however, this area of chemistry is relatively new, with the first such compounds being crystallographically characterized in 1990.[2] Despite this late start there has recently been a plethora of studies targeting a better understanding of the structure, bonding and reactivity of these compounds.[3] A recent exciting development by Segawa *et al.*[4] resulted in the first source of a nucleophilic boryl anion via the synthesis of a boryllithium. Many theoretical studies have also been carried out in order to determine the nature of the M-B bond and its relationship to other organometallic ligand systems (e.g. group 13, CO, N_2 etc.).[5] There are five main structural types of compound containing conventional M-B bonds, and these are shown in Figure 1.1. The classification scheme has been devised according to the coordination number of the boron atom and the number of metal-boron bonds, and include borane, boryl, bridging and terminal borylenes and metallaborylenes featuring a 'naked' boron atom between two metal centres.

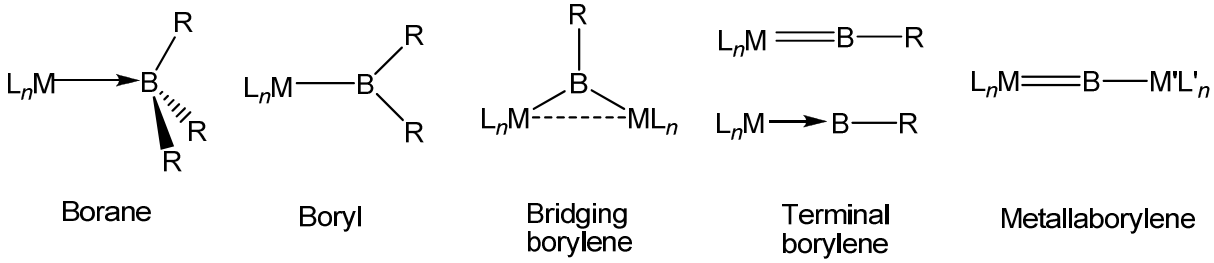


Figure 1.1 Two-centre two-electron bonded transition metal complexes of boron.

Borane complexes are Lewis acid-base adducts and feature a four-coordinate boron centre.[6] Boryl complexes, the most widely known class of compound, feature a three-coordinate boron centre.[3b,o] The borylene moiety, BR can adopt two main coordination modes, three-coordinate bridging between two transition metal centres or two-coordinate when terminally bound to a transition metal.[3]

The focus of this introduction will be on the synthesis, structure/bonding and reactivity of terminal borylene complexes, with a short section on the formation of bridging borylene complexes. The synthesis of group 8 boryl complexes will also be discussed as they are important precursors in the formation of borylene complexes.

1.2 Boryl Complexes

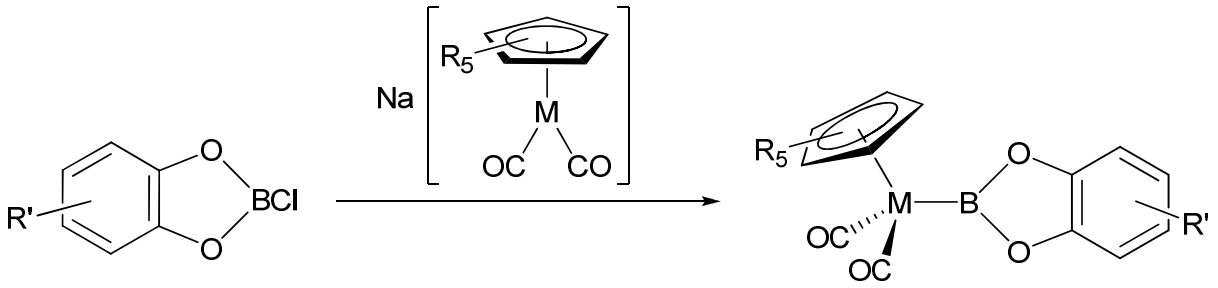
Transition metal boryl complexes were first reported by Nöth and Schmid in the 1960s.[3a,7] Unfortunately, none of the complexes were crystallographically characterized, and many were later discredited as subsequent spectroscopic data (e.g. ^{11}B NMR) obtained for structurally authenticated systems differed from that reported in these initial studies.[8] Renewed interest was sparked by the implication of boryl complexes in the functionalisation of hydrocarbons,[9] and in catalytic hydroboration[10] and diboration[11] processes. There has consequently been significant development in the chemistry of the transition metal boryl complexes, with numerous reviews appearing in the literature discussing the synthesis, structure/bonding and reactivity of these complexes.[3] This introduction will focus on the synthesis of the group 8 transition metal boryl complexes which are most relevant to the experimental work carried out.

1.2.1 Synthesis of Boryl Complexes

There are two main routes for the preparation of transition metal boryl complexes: salt elimination and oxidative addition.

1.2.1.1 Salt Elimination

In 1993 Hartwig and co-workers successfully adopted the salt elimination methodology to form $CpFe(CO)_2Bcat$ by the reaction between an anionic transition metal fragment and the corresponding haloborane precursor[8] (an alternative route to the synthesis of $CpFe(CO)_2Bcat$ involving formation of dilithiocatechol has also been reported).[12] A number of related complexes containing the catechol-type substituent have since been formed, featuring methyl, tert-butyl[9f] or chloro[12] substituents and are shown in Scheme 1.1. Related ruthenium complexes such as $Cp^*Ru(CO)_2B(3,5\text{-}Me_2cat)$ and $Cp^*Ru(CO)_2Bpin$ have also been formed via the same salt elimination route.[9f]

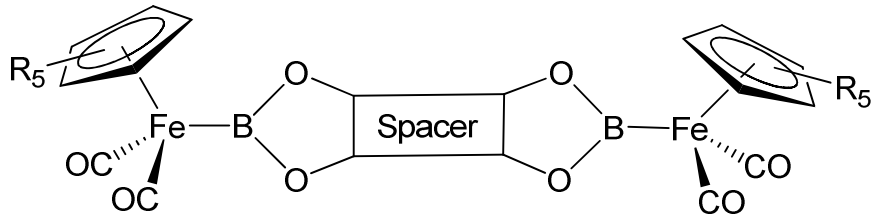


M = Fe $R_n = H_5$, R' = H_4, Cl_4, 3,5-^{t}Bu$_2$cat, 3,5-Me_2cat
$R_n = Me_5$, R' = H_4, Cl_4, 3,5-^{t}Bu$_2$cat

M = Ru R_n = 3,5-Me_2cat, pin

Scheme 1.1 Synthesis of catecholboryl systems.

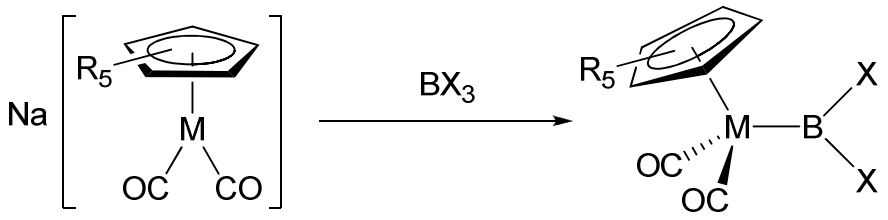
The dinuclear iron complexes (η^5-C_5R_5)Fe(CO)$_2$BO$_2$R'O$_2$BFe(CO)$_2$(η^5-C_5R_5) ($R_5 = H_5$, H_4Me, Me_5; Spacer = C_6H_2; $R_5 = H_5$, Spacer = C_5H_8) featuring a symmetrically bridging boryl ligand were reported in 2002.[13] The synthesis involves the related reactions of bifunctional boron halide reagents with two equivalents of an organometallic anion. The molecular structures of all but Cp*Fe(CO)$_2$BO$_2$C$_6$H$_2$O$_2$BFe(CO)$_2$Cp* were obtained. A related complex, Cp*Fe(CO)$_2$B(tmg) has also been structurally authenticated.[14]



$R_5 = H_5$, H_4Me, Me_5; Spacer = C_6H_2
$R_5 = H_5$, Spacer = C_5H_8

Scheme 1.2 Bifunctional complexes featuring symmetrically bridging boryl ligands.

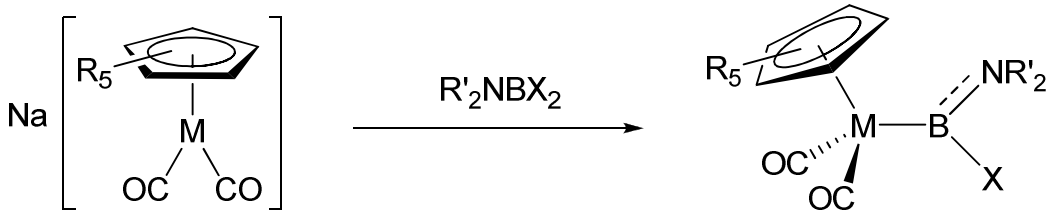
The first group 8 dihaloboryl complex, CpFe(CO)$_2$BCl$_2$ was formed in 2002[12] from the reaction of Na[CpFe(CO)$_2$] with BCl$_3$, and subsequently structurally authenticated in 2004.[15] A range of dihaloboryl complexes featuring fluoride, bromide and chloride have since been reported[16] including CpFe(CO)$_2$BX$_2$ (X = Br, F), Cp*Fe(CO)$_2$BX$_2$, (X = Cl, Br, F), Cp'Ru(CO)$_2$BCl$_2$ and CpRu(CO)$_2$BF$_2$,[17] although the iodide analogues are reported to be too labile to characterize fully.



M = Fe; R_5 = H_5, Me_5; X = Cl, Br, F
M = Ru; R_5 = H_4Me; X = Cl
M = Ru; R_5 = Me_5; X = F

Scheme 1.3 Syntheses of dihaloboryl systems.

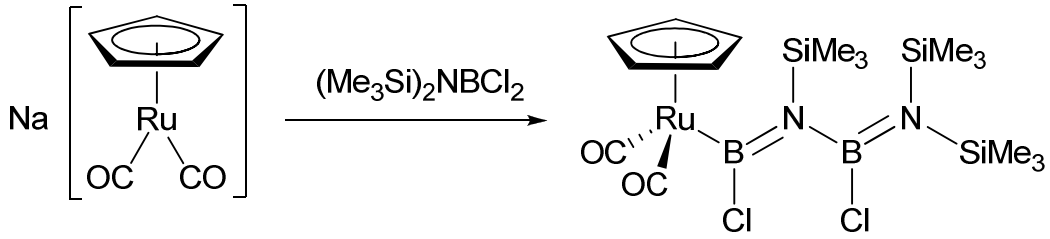
In 1998, Braunschweig and co-workers synthesised the first amino(halo)boryl complexes, (η^5-C_5R_5)$Fe(CO)_2B(NMe_2)Cl$ (R_5 = H_5, H_4Me, Me_5) from the reaction of Na[(η^5-C_5R_5)$Fe(CO)_2$ with Me_2NBCl_2 in benzene.[18] Reaction with the more reactive aminoborane, Me_2NBBr_2 yielded a 1:1 mixture of the corresponding aminoboryl complex, (η^5-C_5R_5)$Fe(CO)_2B(NMe_2)Br$ and the bridging borylene complex, [(μ-$BNMe_2$)(μ-CO){(η^5-C_5R_5)$Fe(CO)\}_2$] (*vide infra*) which could not be separated.[19] The use of more sterically bulky substituents such as ^{i}Pr and Cy allows for the selective high yielding synthesis of the boryl systems.[20-22] The ruthenium aminoboryl complexes, $CpRu(CO)_2B(NR_2)X$ (R = Me, X = Cl, Br; R = Cy, X = Cl) were also formed in this manner.[19,23]



M = Fe; R_5 = H_5, H_4Me, Me_5; R' = Me; X = Cl, Br
R_5= H_5; R' = ^{i}Pr, Cy; X = Cl
M = Ru; R_5 = H_5; R' = Me; X = Cl, Br

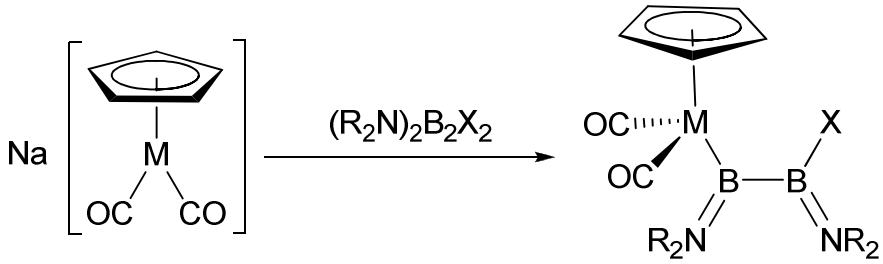
Scheme 1.4 Formation of amino(halo)boryl complexes.

Reaction of $Na[CpRu(CO)_2]$ with two equivalents of the bulkier electrophile $(Me_3Si)_2NBCl_2$ however, yielded the unusual boryl complex, $[CpRu(CO)_2\{B(Cl)NSiMe_3B(Cl)N(SiMe_3)_2\}]$ via the intramolecular elimination of Me_3SiCl.[19]



Scheme 1.5 Formation of $[CpRu(CO)_2\{B(Cl)NSiMe_3B(Cl)N(SiMe_3)_2\}]$.

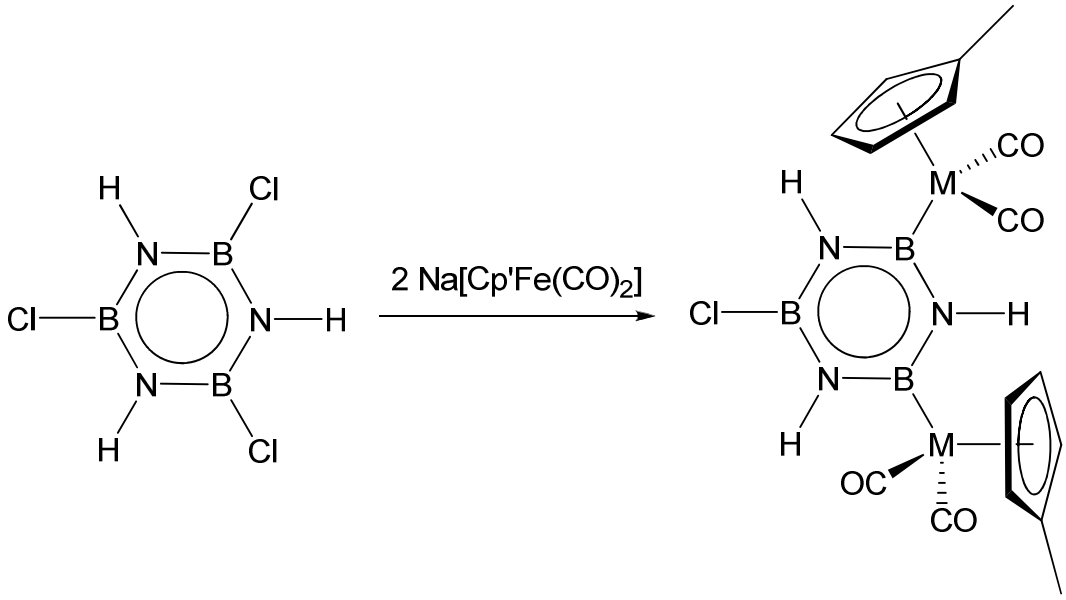
Synthesis of transition metal substituted diborane(4) complex, $CpFe(CO)_2B(NMe_2)B(NMe_2)Cl$ was reported via the reaction of $Na[CpFe(CO)_2]$, with $B_2(NMe_2)_2Cl_2$.[24] Use of the more reactive dibromo diborane(4) reagent allowed access to the corresponding ruthenium complex, $CpRu(CO)_2B(NMe_2)B(NMe_2)Br$ which was also structurally authenticated.[25] Subsequently a number of related complexes such as $CpFe(CO)_2B(NR)B(NR)Cl$ ($R = SiMe_3$, C_4H_8, C_5H_{10}) have also been synthesised.[26]



M = Fe; R = Me, C_4H_8, C_5H_{10}; X = Cl
M = Ru; R = Me; X = Br

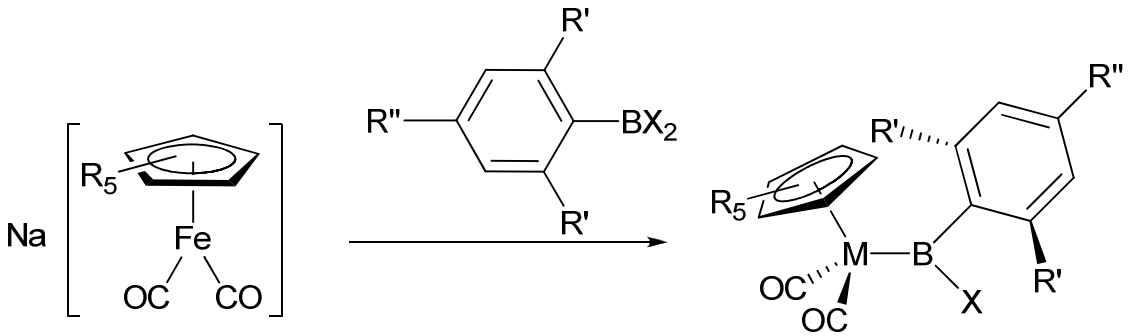
Scheme 1.6 Synthesis of aminodiboran(4yl) complexes.

The first η^1-borazine complex, $\{Cp'Fe(CO)_2\}_2(B_3N_3H_3Cl)$ was also reported by the Braunschweig group via the salt elimination reaction of $Na[Cp'Fe(CO)_2]$ with $(ClBNH)_3$.[27]



Scheme 1.7 Synthesis of the η^1-borazine complex.

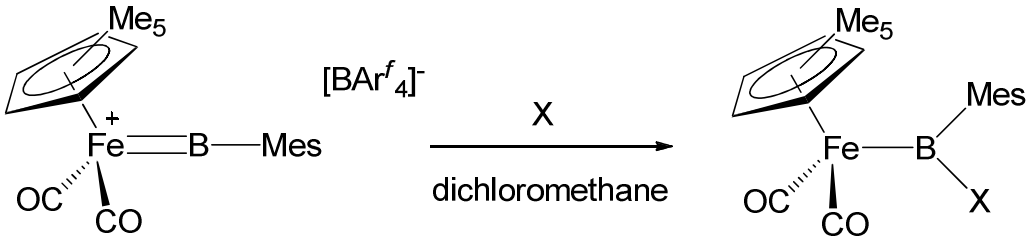
A range of asymmetric haloboryl complexes of the type, $CpM(CO)_2B(R)X$ featuring a variety of boron-bound substituents (aryl, aryloxy, silyl, germyl, dialkyl and diaryl) have been synthesised by the salt elimination route between one equivalent of an organometallic anion and the corresponding haloborane. The ferrocenyl(bromo)boryl complexes $CpFe(CO)_2B(Fc)Br$, $Cp^*Fe(CO)_2B(Fc)Br$ and $Cp'Ru(CO)_2B(Fc)Br$,[28] and the cymantrenyl boryl complexes $CpFe(CO)_2B(cym)Br$ and $Cp^*Fe(CO)_2FeB(cym)Br$[29] were all synthesised by this salt elimination route, as were the aryl substituted systems $CpFe(CO)_2B(2,6\text{-}Trip_2C_6H_3)Br$,[30] $(\eta^5\text{-}C_5R_5)Fe(CO)_2B(Mes)Br$ (R_5 = H_5, H_4Me, Me_5)[31,32] and $Cp^*Fe(CO)_2B(Ph)Cl$[33] (Scheme 1.8).



$R_5 = H_5, H_4Me, Me_5$; R'/R" = Me; X = Br
$R_5 = Me_5$; R'/R" = H; X = Cl
$R_5 = H_5$; R' = 2,4,6-$^{i}Pr_3C_6H_2$; R" = H; X = Br

Scheme 1.8 Formation of aryl(halo)complexes.

By contrast the related fluoro-, chloro- and iodo- systems, $Cp^*Fe(CO)_2B(Mes)X$ (X = F, Cl, I) were accessed in yields of 60-80% from the reaction of the cationic terminal borylene complex, $[Cp^*Fe(CO)_2BMes]^+[BAr^f_4]^-$ with an appropriate halide ion source.[34,35]

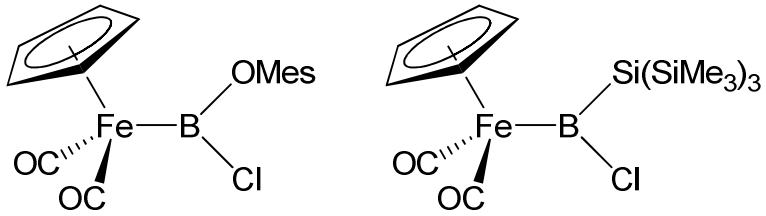


X = [PPN]Cl
X = $[Ph_4P]Br$
X = $[^{n}Bu_4N]I$
X = $[^{n}Bu_4N][BF_4]$

Scheme 1.9 Synthesis of mesityl(halo)boryl complexes via halide addition.

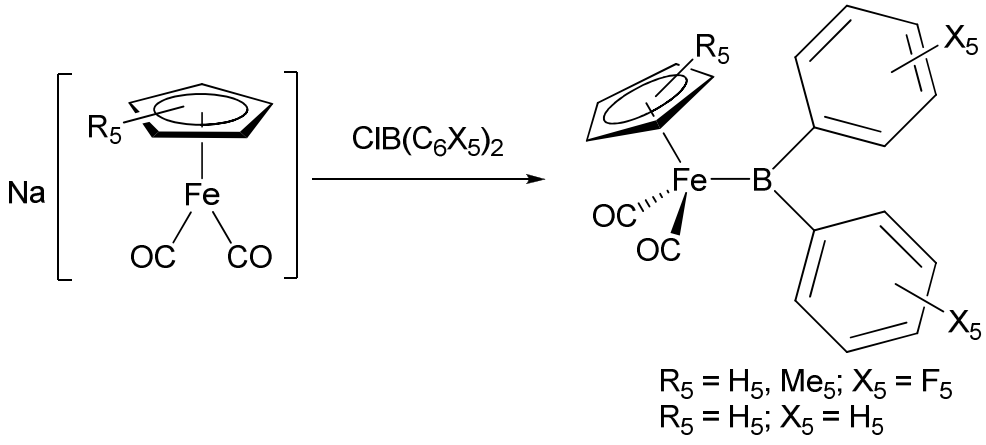
In 2006, Cowley reported the formation of $CpFe(CO)_2B(\eta^1\text{-}C_5Me_5)Cl$ via a salt elimination methodology; this complex was isolated in 67% yield and characterized spectroscopically.[36]

Aryloxy(halo)boryl systems of the type, $(\eta^5\text{-}C_5R_5)Fe(CO)_2B(OMes)X$ (R_5 = H, X = Cl, Br; R_5 = Me; X = Cl) have also been targeted by the reaction of the corresponding dihaloborane with one equivalent of $Na[(\eta^5\text{-}C_5R_5)Fe(CO)_2]$.[21] Systems featuring the heavier group 14 elements, $CpFe(CO)_2B(R)Cl$ (R = $Si(SiMe_3)_3$, $Ge(SiMe_3)_3$) have also been formed by this route and represent the first examples of silyl and germyl boryl complexes.[37]



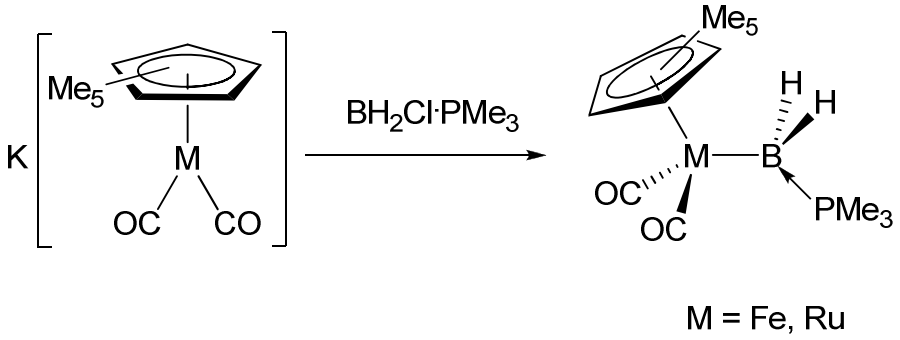
Scheme 1.10 Asymmetric boryl complexes featuring the aryloxy and silyl moieties.

Diaryl complexes of the type, $(\eta^5\text{-}C_5R_5)Fe(CO)_2B(C_6X_5)_2$ (R_5 = H_5, Me_5; X = F; R_5 = H_5; X = H)[8,38,39] have also been synthesised and fully characterized by the salt elimination route.



Scheme 1.11 Formation of diaryl complexes $(\eta^5\text{-}C_5R_5)Fe(CO)_2B(C_6X_5)_2$.

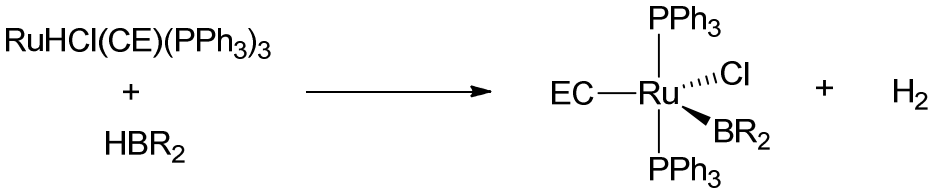
In 2000, Shimoi and co-workers reported formation of the base stabilised boryl complexes, $Cp^*M(CO)_2(BH_2{\cdot}PMe_3)$ (M = Fe, Ru) which were prepared by salt elimination (Scheme 1.12). The complexes were also prepared by photolysis of $Cp^*M(CO)_2Me$ in the presence of $BH_3{\cdot}PMe_3$ but resulted in lower yields.[40]



Scheme 1.12 Formation of a base-stabilized dihydridoboryl systems.

1.2.1.2 Oxidative Addition

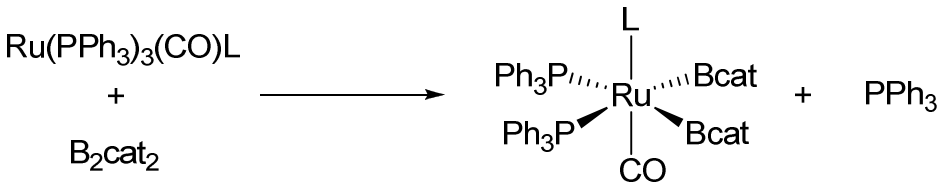
The oxidative addition of a suitable substrate to a coordinatively unsaturated transition metal centre is a fundamental reaction in organometallic chemistry and finds application in many catalytic processes.[9-11] Roper and co-workers have been instrumental in reporting the synthesis of many five- and six-coordinate ruthenium and osmium boryl complexes via B-X oxidative addition reactions. In 1997 the oxidative addition of borane B-H bonds to hydrido- and phenyl-ruthenium and phenyl-osmium complexes was investigated giving rise to a number of coordinatively unsaturated boryl complexes (Scheme 1.13).[41] $Os(Bcat)Cl(CO)(PPh_3)_2$ was structurally authenticated,[42] whereas the other complexes were spectroscopically characterized.



E = O; R_2 = cat, 1,2-$O_2C_{10}H_6$, 3-Mecat, 1,2-$(NH)_2C_6H_4$, 1-S-2-NHC_6H_4
E = S; R_2 = cat, 1-S-2-NHC_6H_4
E = N-p-tolyl, R_2 = cat

Scheme 1.13 Syntheses of ruthenium boryl complexes by B-H oxidative addition and subsequent elimination of H_2.

Related bis(catechol)boryl complexes can be formed by the reaction between a transition metal precursor and a diborane(4) species. Thus, for example, oxidative addition of B_2cat_2 to $Ru(CO)L(PPh_3)_3$ yields the six coordinate ruthenium complexes, *cis*-$Ru(Bcat)_2(CO)L(PPh_3)_2$ (L = CO, CN-p-tolyl).[43]



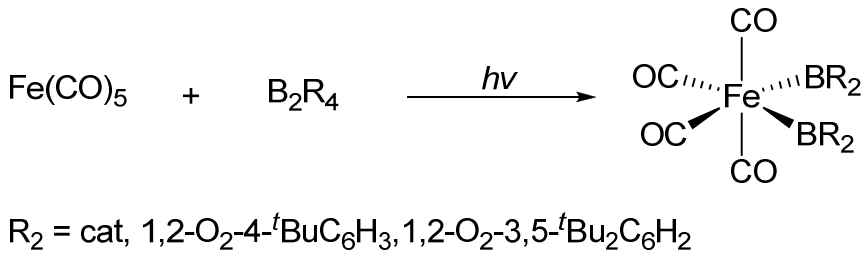
L = CO, CN-*p*-tolyl

Scheme 1.14 Syntheses of bis(catechol)boryl complexes by B-B oxidative addition.

The corresponding osmium derivatives, $Os(Bcat)_2(CO)L(PPh_3)_2$ however can only be accessed via initial reductive elimination of *o*-tolylBcat from *cis*-Os(Bcat)(*o*-tolyl)(CO)(CE)$(PPh_3)_2$ (E = O, CN-p-tolyl). This reaction occurs slowly at room temperature in benzene solution to yield the four coordinate complexes, $Os(CO)_2(PPh_3)_2$ and Os(CO)(CN-

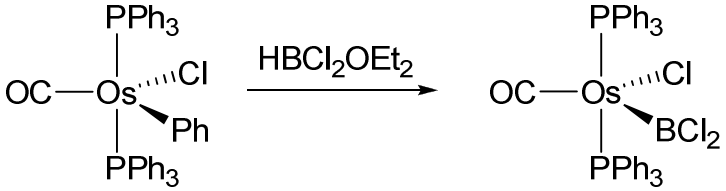
p-tolyl)$(PPh_3)_2$ respectively which, in the presence of B_2cat_2, then yield the bis(boryl) complexes, $Os(Bcat)_2(CO)_2(PPh_3)_2$ and $Os(Bcat)_2(CO)(CN\text{-}p\text{-}tolyl)(PPh_3)_2$.[43,44]

Related iron complexes, $(CO)_4Fe(BR_2)_2$ (R_2 = cat, 1,2-O_2-4-^{t}BuC_6H_3, 1,2-O_2-3,5-^{t}BuC_6H_2) can also be formed by the oxidative addition reaction of B_2R_4 to $Fe(CO)_4$ (which is accessed photolytically from $Fe(CO)_5$).[45] These complexes can also be produced by a double salt elimination route between $[Fe(CO)_4]^{2-}$ and two equivalents of the corresponding chloroborane.



Scheme 1.15 Synthesis of iron bis(boryl) complexes.

In 2000, Roper *et al*. reported the formation of the five-coordinate chloroboryl complex, $OsCl(CO)(PPh_3)_2(BCl_2)$ via the oxidative addition of the B-H bond of $HBCl_2{\cdot}OEt_2$ to $Os(Ph)Cl(CO)(PPh_3)_2$ with concomitant elimination of benzene.[46] Unfortunately, the complex was never structurally authenticated, however, it has been used as a precursor to form boryl and base stabilised borylene complexes via subsequent boron-centred chemistry.



Scheme 1.16 Synthesis of an osmium dichloroboryl complex.

1.3 Borylene Complexes

In 1967 Timms reported that fluoroborylene, BF could be accessed from elemental boron and BF_3 at temperatures of 2000˚C.[47] In 1984, West then reported the formation of free borylene as shown by chemical trapping at a temperature of -196˚C.[48] These studies highlighted the high reactivity of the "free" borylene fragment, which could only be obtained under extreme conditions.

In the absence of structural data a number of computational studies have been carried out on borylene complexes in order to compare the borylene moiety (BF) to the isoelectronic ligands CO and N_2.[5f,k]

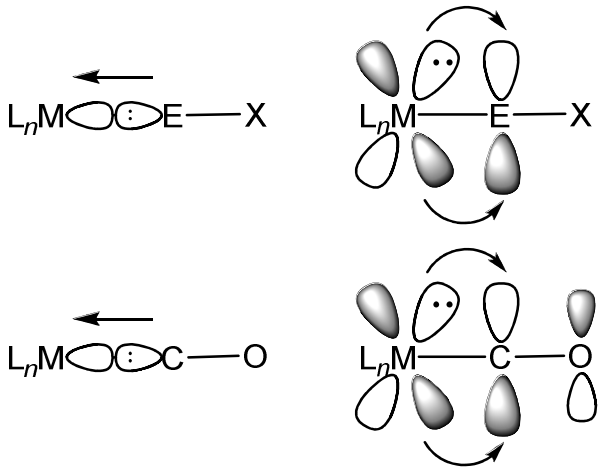
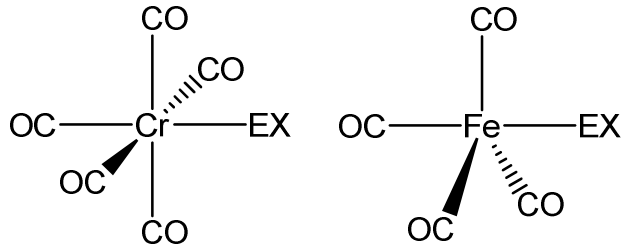


Figure 1.2 Comparison of BF and CO, reflecting the similar σ donor and π acceptor properties of both ligands.

The studies reveal that BF is a better σ donor than CO, but both are comparable π acceptors. This is due to the much higher energy of the σ-donor orbital (HOMO) on B compared to C and the similar energies of the respective π* (LUMO) orbitals. These

differences are reflected in the bond dissociation energies of BF (73.8 kcal mol^{-1}) and CO (48.4 kcal mol^{-1}) complexes of $[Fe(CO)_4]$ (Figure 1.3).[5b]



EX	BDE (D_o / kcal mol^{-1})
BF (Cr)	62.1
BF (Fe)	73.8
CO (Cr)	41.8
CO (Fe)	48.4

Figure 1.3 Bond dissociation energies for BF and CO for complexation to the $Cr(CO)_5$ and $Fe(CO)_4$ fragments.

Aside from thermodynamics, theoretical studies also predict free borylene, BF to have high kinetic lability due to the high polarity of the B-F bond and a small HOMO-LUMO gap. Complexation to a transition metal increases the HOMO-LUMO gap resulting in complexes with high bond dissociation energies. However, an imbalance between σ donation and π acceptance is predicted to lead to a build-up of positive charge on the boron centre in transition metal borylene complexes, making them attractive subjects for nucleophiles[5f,k].

A number of strategies have been suggested to circumvent the intrinsic lability of the borylene complexes including: (i) steric shielding, by using sterically demanding substituents at the boron centre; (ii) electronic stabilization, for example by the use of a strong π donor substituent on the boron centre (such as NR_2) which acts to alleviate the inherent electrophilicity at the boron centre; or (iii) base stabilization by the coordination of a Lewis base at the electrophilic boron centre.

The borylene ligand can adopt two different coordination modes, namely bridging between two metal centres with boron having a coordination number three, or terminally

bound to one metal centre with formation of a formal double bond resulting in boron having a coordination number of two. The first structurally authenticated bridging borylene complex was synthesized in 1995[49] with terminally bound analogues first realised in 1998.[50,51] Since then there has been considerable interest in the synthesis, structure/bonding and reactivity of these complexes.

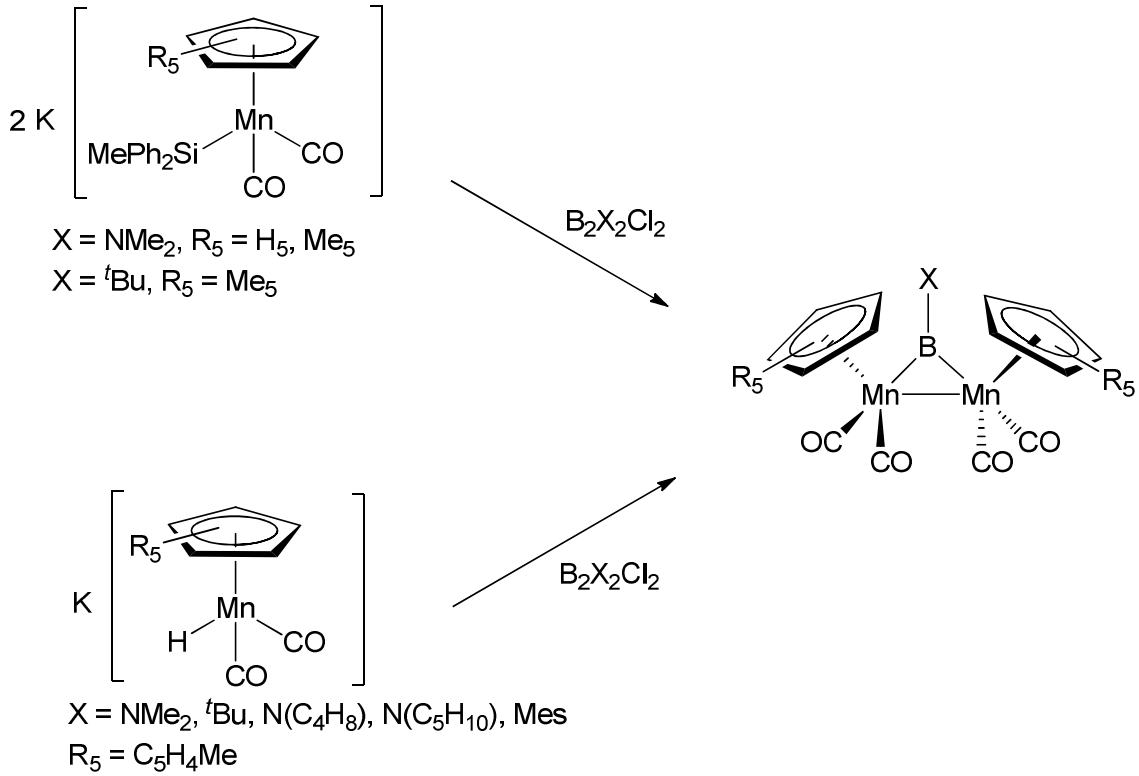
1.3.1 Bridging Borylene Complexes

1.3.1.1 Synthesis of Bridging Borylene Complexes

1.3.1.1.1 From Diboranes

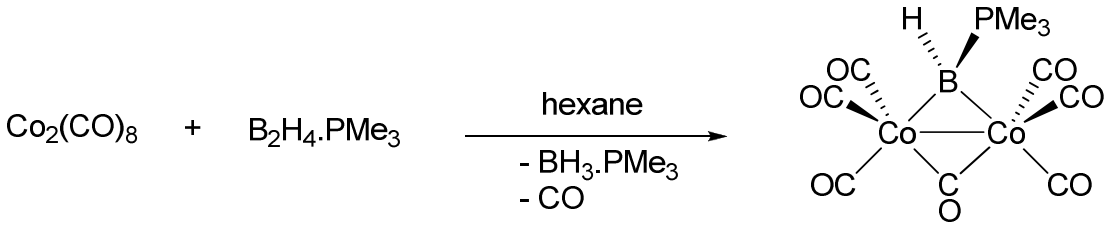
The first structurally characterized example of a bridging borylene complex was reported in 1995 by Braunschweig and co-workers.[49] The reaction between 1,2-dihalodiboranes(4), $X_2B_2Cl_2$ (X = NMe_2, ^{t}Bu) and the anionic transition metal complex, K[η^5-(C_5R_5)$Mn(CO)_2(SiMePh_2)$] (R_5 = H_5, Me_5) afforded the highly robust bridging borylene complex, [(μ-BX){(η^5-C_5R_5)$Mn(CO)_2$}$_2$] in ca. 40% yield via a complex reaction mechanism.

The synthesis however, was improved by using the anionic manganese hydride complex, K[Cp'$MnH(CO)_2$] and the products were formed in higher yields of ca. 65%.[52,53] The reaction proceeds by hydrogen transfer from manganese to boron, and studies have shown that cleavage of the boron-boron bond in the diborane(4) precursor contributes towards formation of the borylene complex, as repeating the reaction with aminodichloroboranes does not yield the bridging borylene complex. The transition metal hydride was also successfully reacted with $X_2B_2Cl_2$ (X = $N(C_4H_8)_2$, $N(C_5H_{10})_2$, Mes) to give [(μ-BX){Cp'$Mn(CO)_2$}$_2$].[26,54]



Scheme 1.17 Synthesis of $[(\mu\text{-BX})\{(\eta^5\text{-}C_5R_5)Mn(CO)_2\}_2]$.

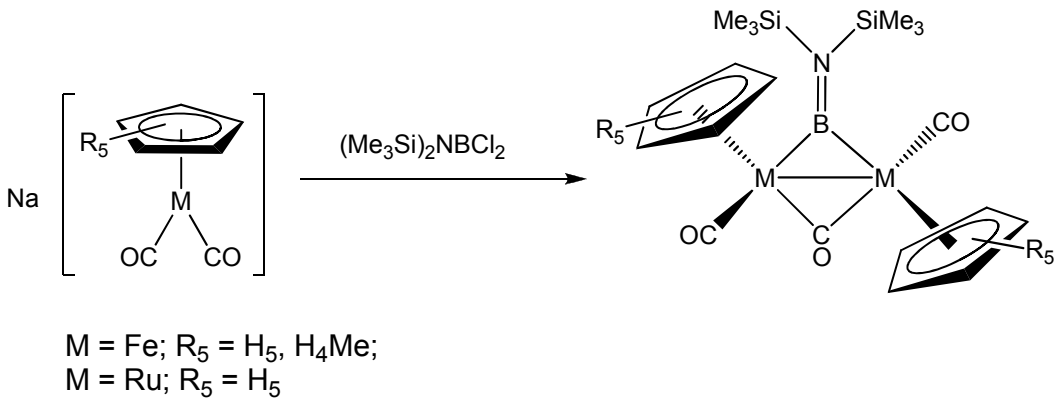
In 1998, Shimoi employed a different approach to the bridging borylene complex. Reaction of $[Co_2(CO)_8]$ with $B_2H_4{\cdot}2PMe_3$ leads to fragmentation of the diborane(4) into $BH_3{\cdot}PMe_3$ and formation of the unique donor-stabilised borylene complex, $[(\mu\text{-BH})(PMe_3)(\mu\text{-CO})\{Co(CO)_3\}_2]$ in 66% yield.[55]



Scheme 1.18 Synthesis of the donor stabilized bridging borylene.

1.3.1.1.2 From Dihaloboranes

In order to broaden the scope and accessibility to bridging borylene complexes beyond the use of diboranes, dihaloboranes were used in the salt elimination route. $[(\mu\text{-}BN(SiMe_3)_2)(\mu\text{-}CO)\{(\eta^5\text{-}C_5R_5)Fe(CO)\}_2]$ (R_5 = H_5, Me_5) and $[(\mu\text{-}BN(SiMe_3)_2)(\mu\text{-}CO)\{CpRu(CO)\}_2]$ were formed from the reaction of the aminoborane, $(Me_3Si)_2NBCl_2$ with two equivalents of $Na[(\eta^5\text{-}C_5R_5)M(CO)_2]$ (M = Fe, R_5 = Me_5, H_5; M = Ru, R_5 = H_5).[18,19] The complex, $[(\mu\text{-}B(tmp))(\mu\text{-}CO)\{CpFe(CO)\}_2]$ has also been formed by the same route.[21]



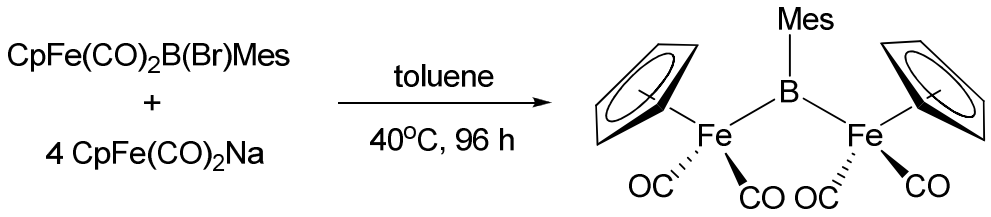
M = Fe; R_5 = H_5, H_4Me;
M = Ru; R_5 = H_5

Scheme 1.19 Formation of bridging aminoborylene complexes.

Interestingly, repeating the reaction with the less sterically demanding *dimethyl*amino borane, Me_2NBCl_2 yielded the monosubstituted haloboryl complex, $(\eta^5\text{-}C_5R_5)M(CO)_2B(NMe_2)Cl$ (M = Fe; R_5 = H_5, H_4Me, Me_5; M = Ru; R_5 = H_5) via displacement of only one halide.[18,19] It is likely that the different reactivity modes of Me_2NBCl_2 and $(Me_3Si)_2NBCl_2$ can be attributed to the increased electrophilicity of the boron centre in the latter due to the electron-withdrawing effects of the silyl groups. It should be noted however that the reaction was subsequently repeated using Me_2NBBr_2, which contains weaker B-X bonds, and although the product was never structurally authenticated, both ^{11}B

NMR and IR spectroscopy indicated formation of $[(\mu\text{-}BNMe_2)(\mu\text{-}CO)\{(\eta^5\text{-}C_5R_5)Fe(CO)\}_2]$.[19] Whilst the dimethyl bridging borylene complex, $[(\mu\text{-}BNMe_2)(\mu\text{-}CO)\{(\eta^5\text{-}C_5R_5)Fe(CO)\}_2]$ is both air and moisture stable, the silyl derivative $[(\mu\text{-}BN(SiMe_3)_2)(\mu\text{-}CO)\{(\eta^5\text{-}C_5R_5)Fe(CO)\}_2]$ was found to be extremely air and moisture sensitive, possibly due to the increased electrophilicity of the boron centre.

In 2002, Aldridge *et al*. reported the first example of an unsupported bridging borylene complex via salt elimination.[31,32] Reaction of the mesityl boryl complex, $[CpFe(CO)_2B(Br)Mes]$ with an excess of $Na[CpFe(CO)_2]$ at 40˚C for 96 h formed $[(\mu\text{-}BMes)\{CpFe(CO)_2\}_2]$ which was structurally characterized.

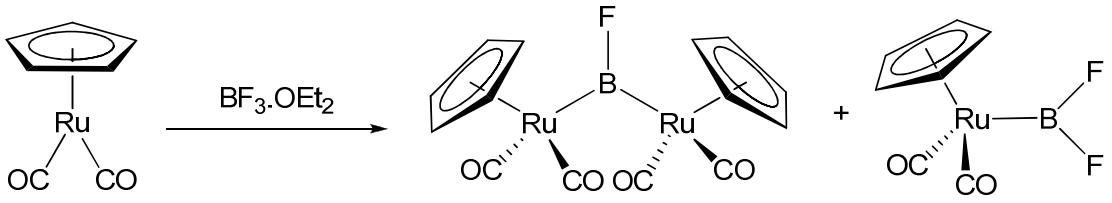


Scheme 1.20 Synthesis of the first unsupported bridging borylene.

Photolysis of $[(\mu\text{-}BMes)\{CpFe(CO)_2\}_2]$ results in the loss of CO and formation of $[(\mu\text{-}BMes)(\mu\text{-}CO)\{CpFe(CO)\}_2]$ in ca. 90% yield.[31] The phenyl substituted bridging borylene complex, $[(\mu\text{-}BPh)(\mu\text{-}CO)\{Cp^*Fe(CO)\}_2]$ was also synthesised from the corresponding reaction of $PhBCl_2$ and five equivalents of $Na[Cp^*Fe(CO)_2]$.[33]

Recently, the bridging haloborylene complexes, $[(\mu\text{-}BCl)\{CpFe(CO)_2\}_2]$, $[(\mu\text{-}BX)\{Mn(CO)_5\}_2]$ (X = Cl, Br)[56] and $[(\mu\text{-}BF)\{CpRu(CO)_2\}_2]$[17] have been synthesised and structurally characterized making use of the salt elimination route between BX_3 (X = Cl, Br, F) and two equivalents of the corresponding anion. Interestingly, in the case of $[(\mu\text{-}BF)\{CpRu(CO)_2\}_2]$, the reaction is dependent on choice of reaction solvent. In diethyl

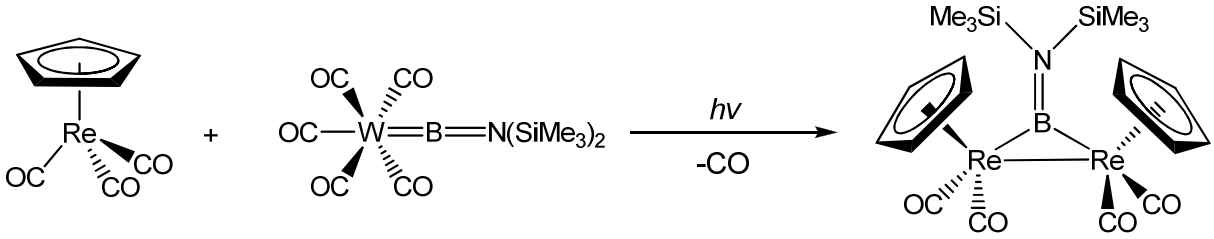
ether, the bridging borylene is formed as the major product with 10% of the corresponding boryl complex, $[CpRu(CO)_2BF_2]$, being generated as a side product. In toluene however, the selectivity for boryl and borylene products is reversed with only 10% of $[(\mu\text{-}BF)\{CpRu(CO)_2\}_2]$ being synthesised.



Scheme 1.21 Synthesis of $[(\mu\text{-}BF)\{CpRu(CO)_2\}_2]$ by salt elimination.

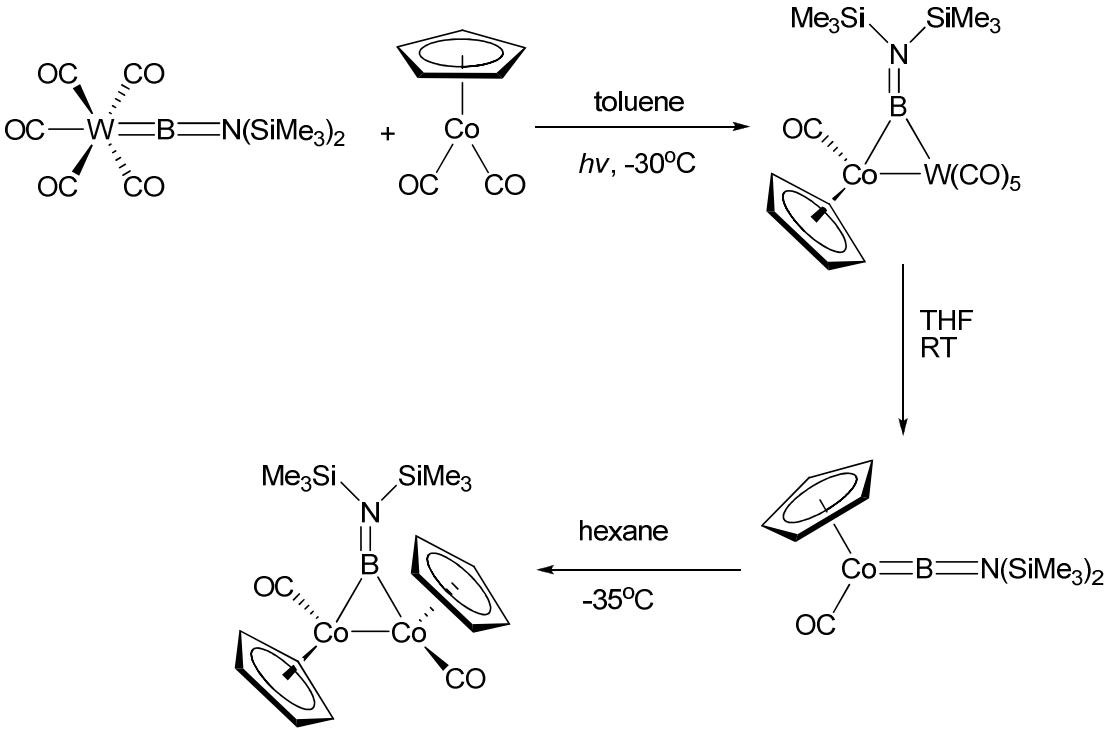
1.3.1.1.3 Photochemical Borylene Transfer

A new route to bridging borylene complexes was established by Braunschweig in 2001, which allowed access to complexes that could not be accessed via the salt elimination methodology. Photolysis of the terminal borylene complex $(OC)_5W[BN(SiMe_3)_2]$ (*vide infra*) in the presence of $[CpRe(CO)_3]$ at -10˚C for four days yielded $[(\mu\text{-}BN(SiMe_3)_2)\{CpRe(CO)_2\}_2]$ via a photochemical borylene transfer reaction.[57] Attempts to structurally authenticate the complex were unsuccessful and the structure was instead inferred from spectroscopic data.



Scheme 1.22 Synthesis of $[(\mu\text{-}BN(SiMe_3)_2)\{CpRe(CO)_2\}_2]$ via photolytic borylene transfer.

Repeating the reaction of $[(OC)_5WBN(SiMe_3)_2]$ with $[CpCo(CO)_2]$ in toluene at -30˚C for 6 h under photolytic conditions formed the heterodinuclear bridging borylene complex, $[(\mu\text{-}BN(SiMe_3)_2)\{CpCo(CO)\}\{W(CO)_5\}]$ which was proposed to be an intermediate in the complete photochemical borylene transfer reaction. Dissolving this complex in THF resulted in the formation of the terminal borylene complex, $[(OC)_5CoBN(SiMe_3)_2]$ after 14 h. However, ^{11}B NMR spectroscopy indicated this complex was unstable and after 32 days, complete conversion to a third species was observed via the homodinuclear bridging borylene, $[(\mu\text{-}BN(SiMe_3)_2)\{CpCo(CO)\}_2]$ which was structurally characterized.[58] The analogous rhodium complex, $[(\mu\text{-}BN(SiMe_3)_2)\{CpRh(CO)\}_2]$ has also recently been synthesised and structurally characterized via the same route.[59]

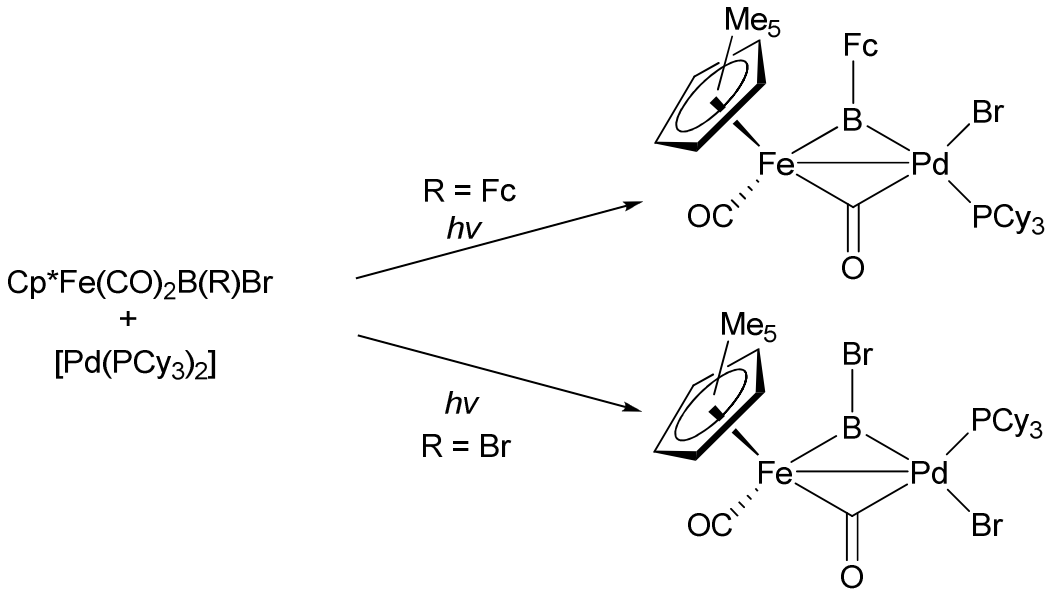


Scheme 1.23 Reaction mechanism for the synthesis of $[(\mu\text{-}BN(SiMe_3)_2)\{CpCo(CO)\}_2]$.

Recently, further examples of these heterodinuclear bridging borylene complexes have surfaced. Reaction of $[(OC)_5WBN(SiMe_3)_2]$ with $[CpRh(CO)_2]$ under photolytic conditions at room temperature formed $[(\mu\text{-}BN(SiMe_3)_2)\{CpRh(CO)\}\{W(CO)_5\}]$ in 63% yield. The reaction of the more electron rich iridium dicarbonyl complex with $[(OC)_5MBN(SiMe_3)_2]$ (M = Cr, W) also resulted in a bridging heterodinuclear complex; in this case however, structural and spectroscopic data revealed that the borylene fragment, $BN(SiMe_3)_2$ is more closely associated with the electron rich iridium centre.[60]

1.3.1.1.4 Oxidative Addition

Reaction of $[Cp^*Fe(CO)_2\{B(Fc)Br\}]$ with $[Pd(PCy_3)_2]$ in C_6D_6 led to the formation and structural characterization of $[(\mu\text{-}BFc)(\mu\text{-}CO)\{Cp^*Fe(CO)\}\{(Cy_3P)Pd(Br)\}]$. The reaction proceeds by the oxidative addition of a B-Br bond to the electron rich palladium centre, with loss of one bulky PCy_3 ligand and formation of a heterodinuclear bridging borylene complex. Repeating the reaction with $[Cp^*Fe(CO)_2BBr_2]$ formed the corresponding heterodinuclear bridging borylene complex, $[(\mu\text{-}BBr)(\mu\text{-}CO)\{Cp^*Fe(CO)\}\{(Cy_3P)Pd(Br)]$, the first example of a transition metal compound featuring the reactive B-Br borylene moiety.[61] The analogous platinum heterodinuclear complex, $[(\mu\text{-}BBr)(\mu\text{-}CO)\{Cp^*Fe(CO)\}\{(Cy_3P)Pt(Br)]$, has also been synthesized recently and characterized by multinuclear spectroscopy.[62]



Scheme 1.24 Synthesis of heterodinuclear bridging borylene complexes via oxidative addition.

1.3.2 Terminal Borylene Complexes

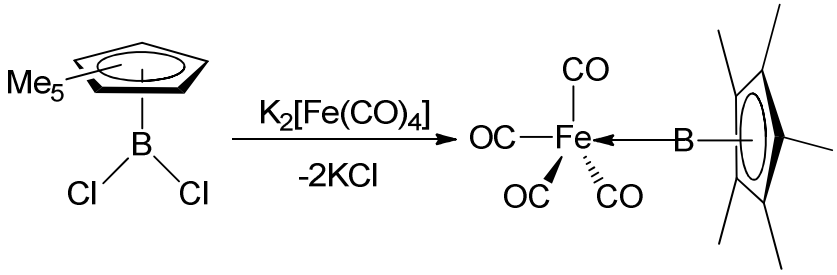
Since the formation of the first structurally characterized terminal borylene complexes in 1998, there has been significant interest into the synthesis, structure and reactivity of these elusive complexes.[50,51] The main synthetic routes available are (i) salt elimination, (ii) photolytic transfer, (iii) halide abstraction and (iv) substitution of a halide substituent at an existing boryl complex by a tethered base.

1.3.2.1 Synthesis of Terminal Borylene Complexes

1.3.2.1.1 Salt Elimination

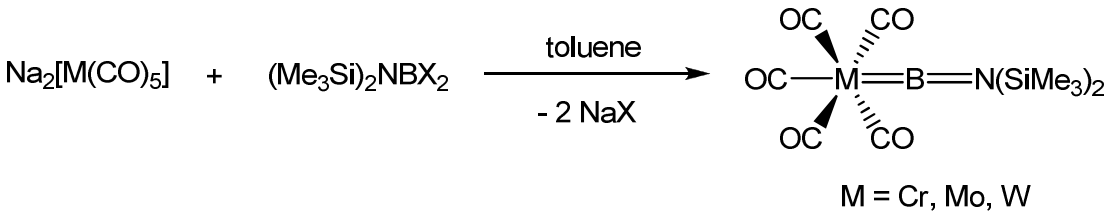
The first structurally authenticated terminal borylene complexes, $[(OC)_4Fe(BCp^*)]$ and $[(CO)_5WBN(SiMe_3)_2]$ were reported by Cowley[50] and Braunschweig[51] respectively in 1998. Both complexes were formed by a double salt elimination methodology, involving the

reactions of dianionic transition metal carbonylates, $[M(CO)_n]^{2-}$ (M = W, *n* = 5; M = Fe, *n* = 4), with dihaloboranes, RBX_2 (R = C_5Me_5, $N(SiMe_3)_2$; X = Cl, Br). A common feature of these complexes is that the boron centre is stabilized by the use of sterically encumbered and strongly electron donating substituents. $[(OC)_4Fe(BCp^*)]$ was synthesized in 30% yield by treatment of Cp^*BCl_2 with $K_2[Fe(CO)_4]$ in toluene at –78˚C, followed by warming to room temperature. The Lewis acidity of the boron centre is alleviated by the electronic and steric stability offered by the Cp* ring, which alters its coordination mode from η^1 to η^5 on formation of the borylene complex.



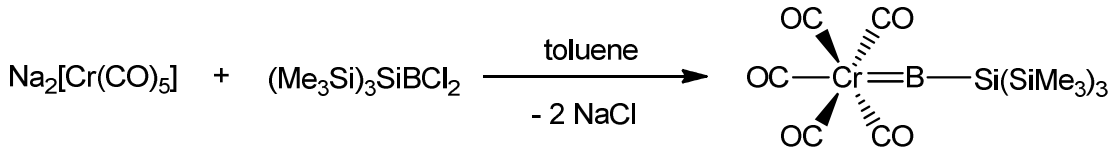
Scheme 1.25 Synthesis of $[(OC)_4Fe(BCp^*)]$.

In a similar fashion, $[(OC)_5WBN(SiMe_3)_2]$, the first terminal borylene to feature a formal double bond between boron and a transition metal, was formed by the reaction of $Na_2[W(CO)_5]$ and $(Me_3Si)_2NBBr_2$. The analogous complexes of the lighter group 6 metals, $[(OC)_5MBN(SiMe_3)_2]$, (M = Cr, Mo) (with $(Me_3Si)_2NBX_2$ where X = Cl, Br)[63] and the closely related iron compound $[(OC)_4FeBN(SiMe_3)_2]$[51] have also been synthesized using this approach, with the chromium and molybdenum complexes being structurally characterized.



Scheme 1.26 Synthesis of $[(OC)_5MBN(SiMe_3)_2]$ (M = Cr, Mo, W).

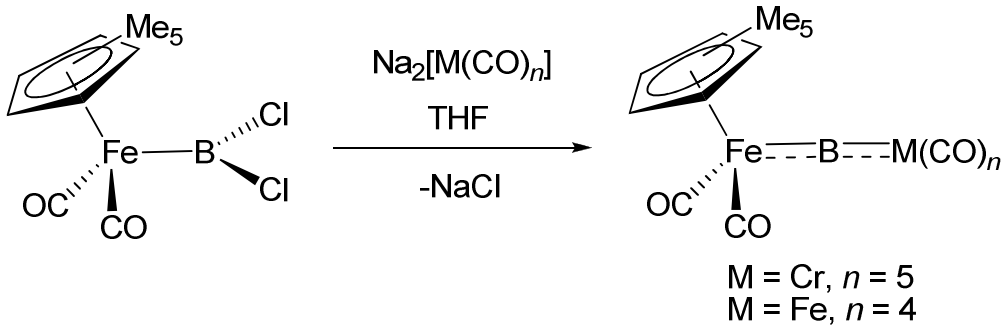
Attempts to broaden the scope of this synthetic approach by exploiting other aminodihaloboranes, have been unsuccessful. However, the use of the sterically demanding silylborane $(Me_3Si)_3SiBCl_2$ in conjunction with $Na_2[Cr(CO)_5]$ allowed for the synthesis of $[(OC)_5CrBSi(SiMe_3)_3]$ in 81% yield.[64] This complex is extremely sensitive compared to its aminoborylene analogue, and decomposes readily even in the solid state at room temperature - a characteristic attributed to its electronic unsaturation due to the non π-donating nature of the $Si(SiMe_3)_3$ substituent. Despite this, a crystal structure was obtained and the complex was fully characterized; the germanium analogue, $[(OC)_5CrBGe(SiMe_3)_3]$ was also synthesized and characterized spectroscopically.[64]



Scheme 1.27 Synthesis of $[(OC)_5CrBSi(SiMe_3)_3]$.

An alternative approach to vary the electronic/steric properties of the borylene substituent X, is to utilize not a main group substituent (NR_2, Cp* etc.) but a transition metal fragment. Thus the metallaborylenes, $[(OC)_nMBFe(CO)_2Cp^*]$ (M = Cr, n = 5, M = Fe, n = 4) featuring a 'naked' bridging boron atom between two transition metal centres, have been

formed by related double salt elimination chemistry involving [Cp*Fe(CO)$_2$BCl$_2$] and either Na$_2$[Cr(CO)$_5$] or Na$_2$[Fe(CO)$_4$] respectively.[65]

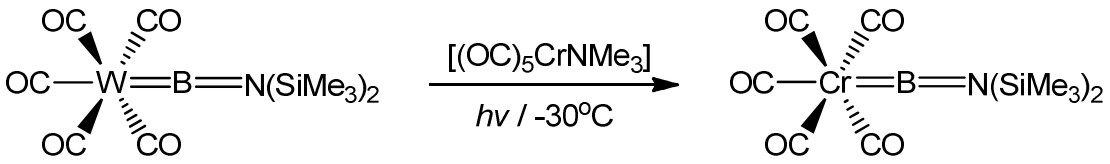


Scheme 1.28 Formation of metallaborylene complexes from dihaloboryl.

Although this salt elimination protocol is conceptually simple, closely related to methods used in the synthesis of a wide range of boryl complexes, and in theory applicable to a wide range of boron dihalide and metal carbonyl dianion reagents, its practical synthetic use has been confined (despite much work by a number of research groups) to the examples described above.

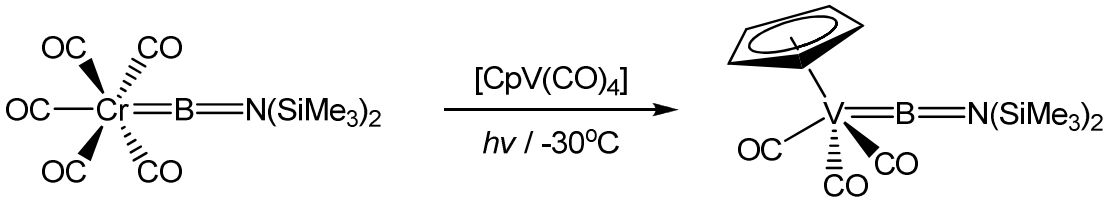
1.3.2.1.2 Photolytic Borylene Transfer

An alternative synthetic route to the formation of terminal (and bridging) borylene complexes which has been exploited extensively by Braunschweig and co-workers, involves photolytic transfer of the borylene fragment to a suitable *in situ* generated acceptor fragment. Thus, in the first example of its kind, photolytic reaction of [(OC)$_5$WBN(SiMe$_3$)$_2$] with [(OC)$_5$Cr(NMe$_3$)] at -30^{o}C led to transfer of the aminoborylene fragment BN(SiMe$_3$)$_2$ and formation of [(OC)$_5$CrBN(SiMe$_3$)$_2$].[57]



Scheme 1.29 Photolytic transfer of the aminoborylene moiety.

Thermal transfer was also observed at 60˚C, although the reaction was less clean; photolytic transfer of the aminoborylene to $[Cr(CO)_6]$ resulted in the formation of two products, with the borylene complex being formed in ca. 50% yield, probably due to the low solubility of $[Cr(CO)_6]$. Reaction of $[(OC)_5WBN(SiMe_3)_2]$ with the cyclopentadienylrhenium carbonyl substrate $[CpRe(CO)_3]$ led to the generation of the bridging borylene product $[(\mu\text{-}BN(SiMe_3)_2)\{CpRe(CO)_2\}_2]$.[57] However, use of the *chromium* complex $[(OC)_5CrBN(SiMe_3)_2]$ as the borylene source led to the formation of the first half sandwich terminal borylene, $[CpV(CO)_3BN(SiMe_3)_2]$, by photolytic reaction with $[CpV(CO)_4]$ at –30˚C over a period of 48 h.[66] Previously, the same borylene compound had been targeted using salt elimination chemistry, but to no avail, thus highlighting the need for a diverse range of synthetic approaches.

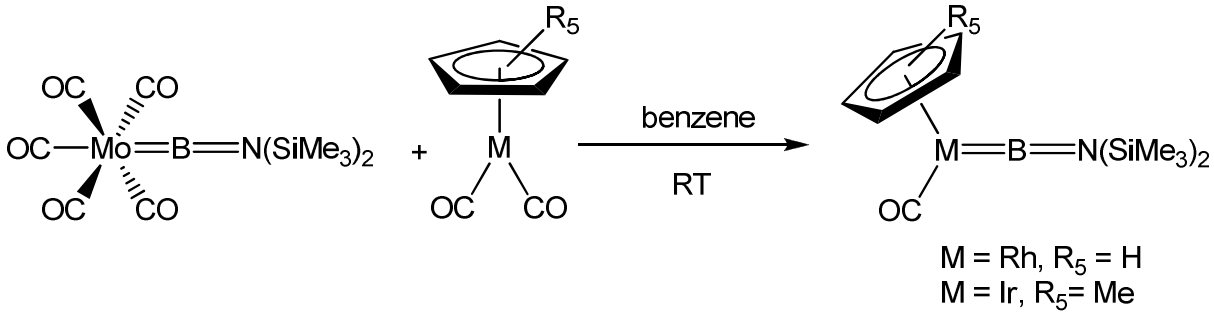


Scheme 1.30 Formation of the first half sandwich terminal borylene complex.

Analogous chemistry was also used to form the first cobalt terminal borylene complex $[CpCo(CO)BN(SiMe_3)_2]$, and although this species proved too labile to be crystallographically

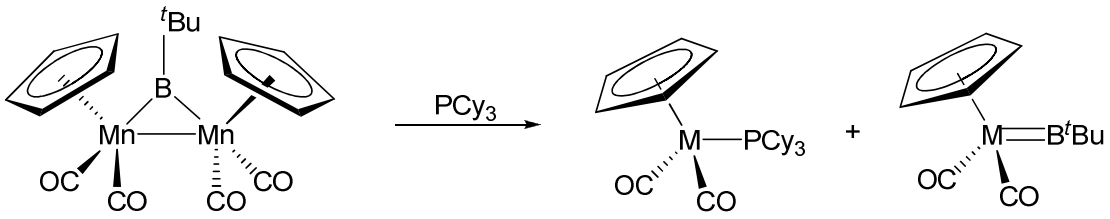
characterized, its synthesis does provide key mechanistic insight through the isolation of a mixed metal intermediate.[58] Photolysis of a mixture of $[(OC)_5WBN(SiMe_3)_2]$ and $[CpCo(CO)_2]$ yields the heterodinuclear bridging borylene, $[(\mu\text{-}BN(SiMe_3)_2)\{CpCo(CO)\}\{W(CO)_5\}]$ in 40 % yield (*vide supra*) (Scheme 1.23). Moreover a solution of this bridging species in THF undergoes complete conversion to $[CpCo(CO)BN(SiMe_3)_2]$ over a period of 14 h at room temperature. The identification of the dinuclear intermediate implies that borylene transfer proceeds via an initial associative mechanism rather than by dissociation of the borylene ligand, with photolysis serving to activate the acceptor metal fragment by loss of CO.

Although $[CpCo(CO)BN(SiMe_3)_2]$ undergoes slow decomposition even at -35°C to give $[(\mu\text{-}BN(SiMe_3)_2)\{CpCo(CO)\}_2]$, related group 9 borylene complexes have recently been formed by a similar method. Solutions of the molybdenum complex $[(CO)_5MoBN(SiMe_3)_2]$ and either $[CpRh(CO)_2]$ or $[Cp^*Ir(CO)_2]$ were stirred in C_6D_6 at ambient temperature, leading to the formation of the first terminal borylene complexes of rhodium and iridium, respectively. Of these, only the iridium complex, $[Cp^*Ir(CO)BN(SiMe_3)_2]$ was amenable to structural characterization, presumably due to the enhanced stability afforded by the sterically bulky Cp* ligand and the electron rich iridium centre.[59]



Scheme 1.31 Formation of Rh and Ir terminal borylene complexes.

Interestingly the microscopic *reverse* of the associative inter-metallic borylene transfer process has also been demonstrated. The terminal alkylborylene [$CpMn(CO)_2(B^tBu)$] is formed by phosphine-induced cleavage of [$(\mu\text{-}B^tBu)\{CpMn(CO)_2\}_2$] in refluxing benzene, together with the phosphine complex [$CpMn(CO)_2(PCy_3)$] (Scheme 1.32).

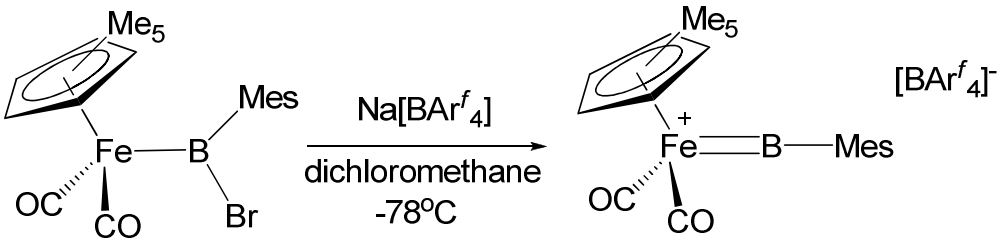


Scheme 1.32 Formation of the first terminal alkylborylene complex.

The novel alkylborylene was isolated as pale yellow crystals suitable for X-ray diffraction, and although found to be both air- and moisture-sensitive, could be manipulated further under argon despite a lack of π-donor stabilization at the boron centre.[67]

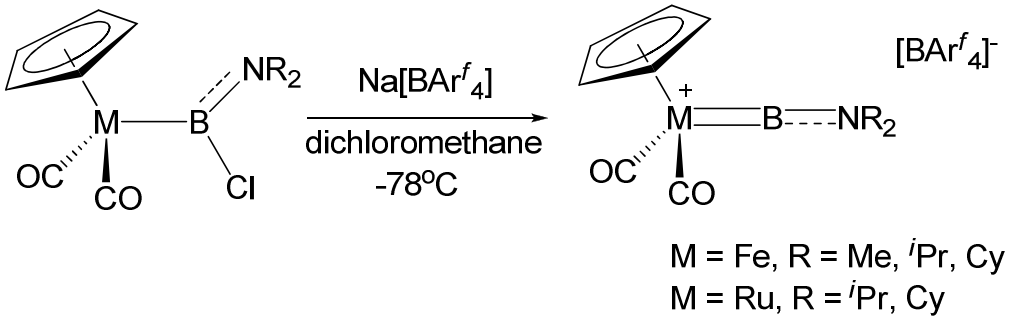
1.3.2.1.3 Halide Abstraction

In 2003 a new route to terminal borylene complexes was developed, analogous to the classical halide abstraction methodology used to access cationic silylene complexes such as $[Cp^*Ru(PMe_3)_2(SiMe_2)]^+[B(C_6F_5)_4]^-$.[68] The terminal borylene complex $[Cp^*Fe(CO)_2(BMes)]^+[BAr^f_4]^-$, the first of its kind, was synthesized by the abstraction of bromide from the corresponding asymmetric haloboryl $[Cp^*Fe(CO)_2B(Mes)Br]$ by $Na[BAr^f_4]$ in dichloromethane.[34-35] The reaction sees the complete conversion (by NMR spectroscopy) to the cationic terminal borylene with the appearance of a broad signal at δ_B 145 ppm.



Scheme 1.33 Synthesis of the cationic terminal borylene complex, $[Cp^*Fe(CO)_2(BMes)]^+[BAr^f_4]^-$.

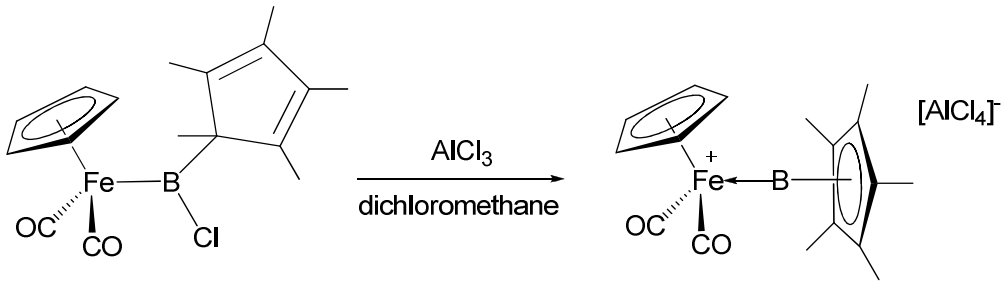
The halide abstraction methodology has also been applied to heteroatom-functionalized systems. Thus the cationic aminoborylene complexes, $[CpFe(CO)_2(BNR_2)]^+[BAr^f_4]^-$ (R = ^{i}Pr, Cy, Me)[20-22,35] have all been formed by halide abstraction from the corresponding asymmetric amino(halo)boryl complex. While the di*methyl*amino complex is thermally fragile, the bulkier dicyclohexyl- and diisopropyl-aminoborylene complexes can be isolated in reasonable yields and in the case of the cyclohexyl aminoborylene complex, crystallographically characterized. The first cationic ruthenium borylene complexes, $[CpRu(CO)_2(BNR_2)]^+[BAr^f_4]^-$ (R = Cy, ^{i}Pr) have also been synthesized by the same halide abstraction route.[23]



Scheme 1.34 Synthesis of cationic aminoborylene complexes.

By contrast, the interaction of $[CpFe(CO)_2B(OMes)Cl]$ with $Na[BAr^f_4]$, yields $[CpFe(CO)_2B(OMes)F]$ as a red oil.[21] The reaction is thought to occur via the abstraction of fluoride from $Na[BAr^f_4]$, a reaction which has subsequently been demonstrated explicitly for related cationic manganese systems. Presumably the putative mesityloxy substituent does not offer either the immediate steric bulk of mesityl or the electronic stabilization inherent in amino substituents.

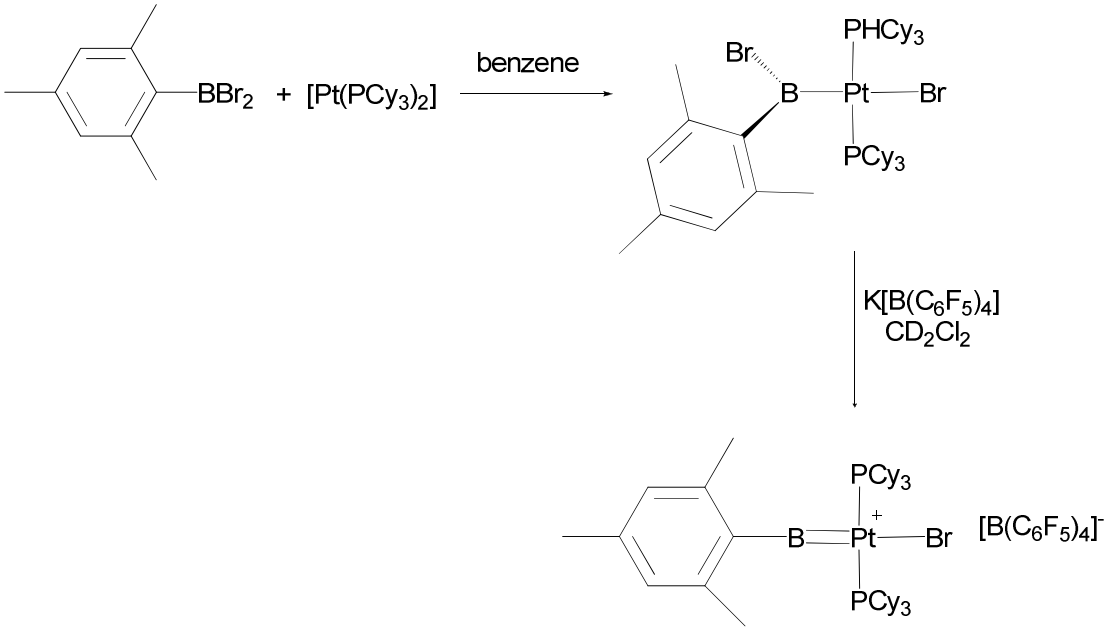
The use of pentamethylcyclopentadienyl as the boron-bound substituent has also been examined and yields a cationic complex featuring a metal-boron single bond. $[CpFe(CO)_2Fe(BCp^*)]^+[AlCl_4]^-$ was synthesised from the haloboryl precursor, $CpFe(CO)_2B(\eta^1\text{-}Cp^*)Cl$, and $AlCl_3$ with the ability of the Cp* substituent to alter its coordination mode at boron (as with $[(OC)_4Fe(BCp^*)]$) presumably being a key factor in the stability of the borylene product.[36]



Scheme 1.35 Synthesis of $[CpFe(CO)_2Fe(BCp^*)]^+[AlCl_4]^-$.

In conjunction with certain substituents, the halide abstraction methodology can be used to access cationic borylene complexes from boryl precursors, which in turn have been generated by B-Br oxidative addition. Thus, the cationic platinum complex, *trans*-$[(Cy_3P)_2Pt(BMes)Br]^+[B(C_6F_5)_4]^-$ can be synthesised from *trans*-$[(Cy_3P)_2Pt\{B(Mes)Br\}Br]$ using a closely related halide abstraction approach. In this case the reaction with $Na[BAr^f_4]$

failed to produce crystals suitable for X-ray diffraction; however, the use of $K[B(C_6F_5)_4]$ in CD_2Cl_2 led to the isolation and structural characterization of the terminal borylene complex.[69]

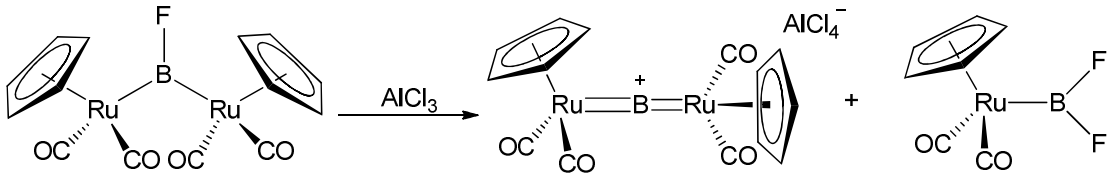


Scheme 1.36 Formation of the cationic complex, *trans*-$[(Cy_3P)_2Pt(BMes)Br]^+[B(C_6F_5)_4]^-$.

A further twist on the abstraction methodology is to remove the halide from a bridged halo-borylene complex rather than an asymmetric boryl. Such an approach generates a cationic system featuring a 'naked' bridging boron atom, and mirrors previous reports leading to the syntheses of the heavier congeners $[(\mu\text{-E})\{Cp^*Fe(CO)_2\}]^+[BAr^f_4]^-$ (E = Ga, In).[70]

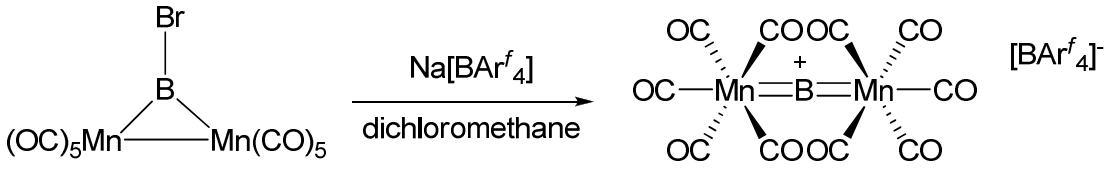
Recently Aldridge and co-workers reported formation of the cationic metallaborylene, $[(\mu\text{-B})\{CpRu(CO)_2\}_2]^+$ by heterolytic cleavage of the B-F bond in $[(\mu\text{-BF})\{CpRu(CO)_2\}_2]$ with either $B(C_6F_5)_3$ or $AlCl_3$. During the reaction, the fluoroboryl, $[CpRu(CO)_2BF_2]$ is produced by halide abstraction. However, the metallaborylene is produced cleanly by using a three-fold excess of $AlCl_3$. Interestingly the group also investigated the reactivity of the bridging complex, $[\{CpRu(CO)(\mu\text{-CO})\}_2]$ with $AlCl_3$ which proceeded by formation of a

simple donor-acceptor adduct rather than by cleavage of the Ru-CO bond, presumably due to the less polar and more strongly π-bonded nature of the CO ligand versus BF.[17]



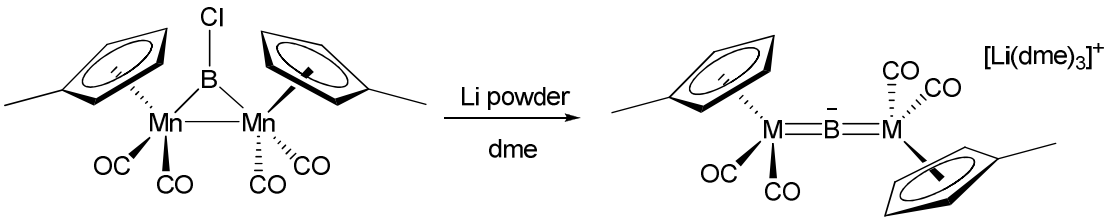
Scheme 1.37 Formation of the cationic metallaborylene, $[(\mu\text{-B})\{CpRu(CO)_2\}_2]^+$.

The reaction of $[(\mu\text{-BBr})\{Mn(CO)_5\}_2]$ with $Na[BAr^f_4]$ generates the extremely air- and moisture-sensitive cationic metallaborylene, $[(\mu\text{-B})\{Mn(CO)_5\}_2]^+$ which abstracts fluoride from the $[BAr^f_4]^-$ counterion over a period of 2 h to give $[(\mu\text{-BF})\{Mn(CO)_5\}_2]$.[71] The related iron complexes, $[(\mu\text{-B})\{(\eta^5\text{-}C_5R_5)Fe(CO)_2\}]^+[BAr^f_4]^-$ ($R_5 = H_5$, Me_5) were also synthesized by the same method.



Scheme 1.38 Formation of a metallaborylene by halide abstraction.

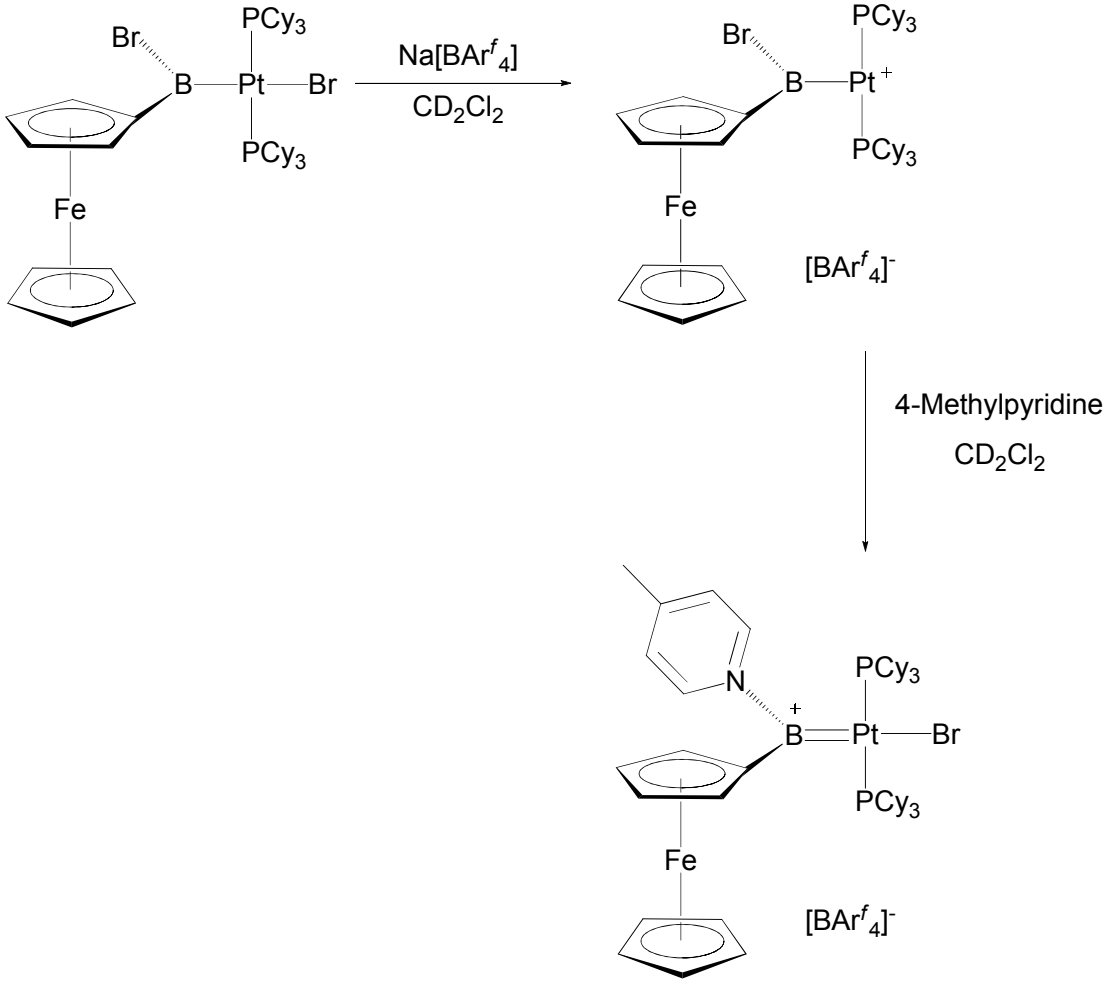
In addition, the isoelectronic dimanganese anion, $[Li(dme)_3]^+[(\mu\text{-B})\{Cp'Mn(CO)_2\}_2]^-$, has also recently been synthesized by Braunschweig and co-workers.[72] Rather than halide abstraction, *reduction* of the chloroborylene, $[(\mu\text{-BCl})\{Cp'Mn(CO)_2\}_2]$ with lithium sand at -10˚C results in a downfield shift in the ^{11}B NMR from 134 ppm to 195 ppm, and to the isolation of the dimanganese anion as the $[Li(dme)_3]^+$ salt (Scheme 1.39).



Scheme 1.39 Synthesis of the metallaborylene $[Li(dme)_3]^+[(\mu\text{-}B)\{Cp'Mn(CO)_2\}_2]^-$.

1.3.2.1.4 α-Migration of a Boryl Substituent

α-Migration of a boron-bound substituent has also been exploited synthetically, although to date only in the synthesis of base-stabilized systems by halide migration. The square planar Pt(II) system *trans*-$[(Cy_3P)_2Pt\{B(Fc)Br\}Br]$ is one of a number of systems accessible by B-Br oxidative addition to $Pt(PCy_3)_2$. The B(Fc)Br fragment has a notable *trans* influence, exerting a strong *trans*-labilizing effect on the bromide ligand;[28] subsequently reaction with $Na[BAr^f_4]$ generates the T-shaped boryl system *trans*-$[(Cy_3P)_2Pt\{B(Fc)Br\}]^+[BAr^f_4]^-$. Although the combination of the sterically bulky PCy_3 ligands and the strong *trans*-labilizing effect of the boryl ligand prevent nucleophilic attack at platinum from Lewis bases such as THF and acetonitrile, 4-picoline reacts to form *trans*-$[(Cy_3P)_2Pt\{BFc(4\text{-pic})\}Br]^+[BAr^f_4]^-$ (Scheme 1.40).[73]

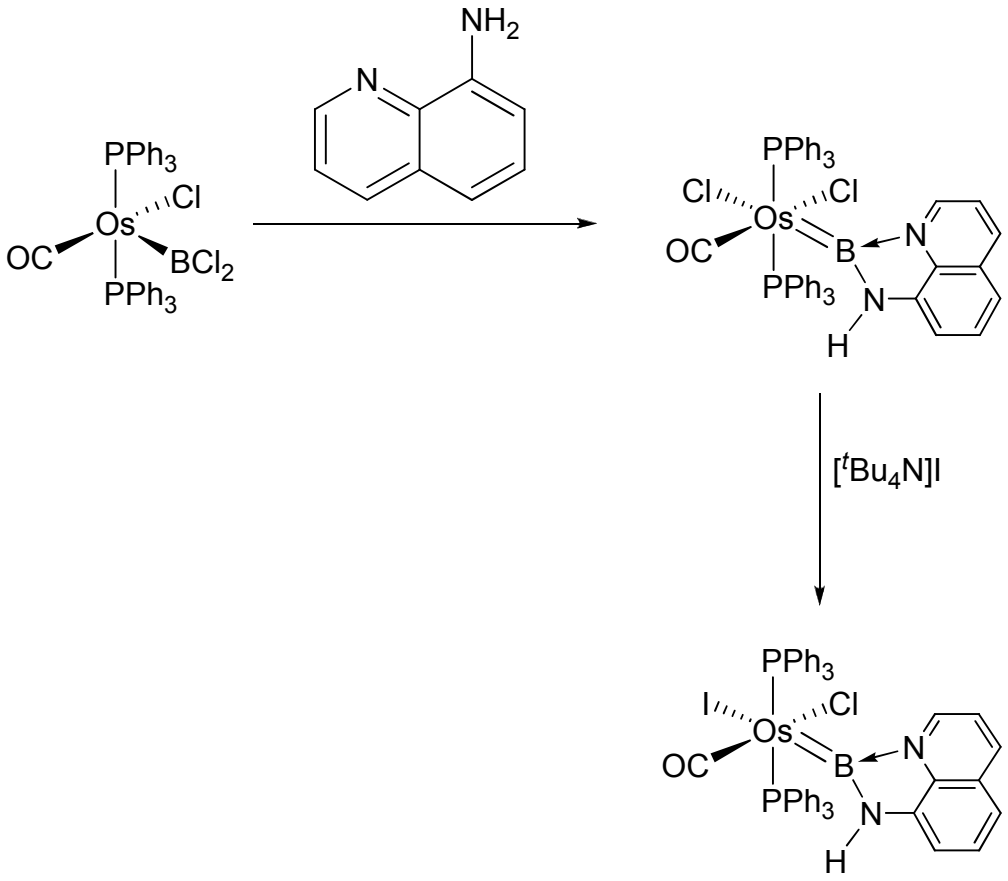


Scheme 1.40 Formation of *trans*-$[(Cy_3P)_2Pt\{BFc(4\text{-pic})\}Br]^+[BAr^f_4]^-$ by halide migration.

The reaction is thought to involve a 1,2-halide shift from boron to platinum, with the driving force being formation of a strong B-N bond and alleviation of the electronic unsaturation around the platinum centre. Such 1,2-shifts find ample precedent in the formation of platinum silylene complexes.[74]

Similar chemistry was exploited by Roper in the formation of the first intramolecularly base-stabilized terminal borylene complex. Reaction of the dichloroboryl $[Os(BCl_2)Cl(CO)(PPh_3)_2]$ with 8-aminoquinolene gives rise to the sparingly soluble complex

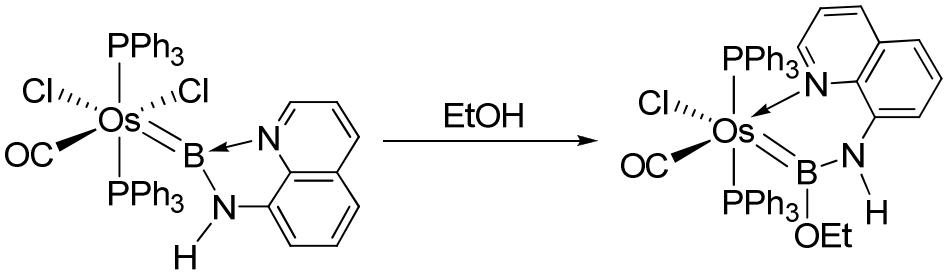
$[Os(BNHC_9H_6N)Cl_2(CO)(PPh_3)_2]$ in 85% yield.[46] Although the complex could not be crystallographically characterized, treatment with $[Bu_4N]I$ afforded the more soluble chloro/iodo complex, $[Os(BNHC_9H_6N)ClI(CO)(PPh_3)_2]$ which did prove amenable to structural studies.



Scheme 1.41 Formation of $[Os(BNHC_9H_6N)ClI(CO)(PPh_3)_2]$.

The high *trans*-influence of the borylene ligand is presumably responsible for the ready substitution by iodide of the *trans* chloride ligand. Reaction of the same boryl precursor with 2-amino*pyridine*, however, gives rise to a mixture of products depending on the regiochemistry of the addition of the nitrogen donors to the boron and osmium centres.[75] In addition to the tethered boryl complex, $[Os\{BCl(NHC_5H_4N)\}Cl(CO)(PPh_3)_2]$ formed by

interaction of the amino function with the boryl ligand, the base-stabilized borylene complex, [Os{BCl(NC$_5$H$_4$NH)}Cl(CO)(PPh$_3$)$_2$] is formed via addition in the reverse sense; further reaction of the B-Cl function with the ethanol solvent then forms the ethoxyborylene, [Os{BOEt(NC$_5$H$_4$NH)}Cl(CO)(PPh$_3$)$_2$] which has been structurally characterized. Better control of regiochemistry can be achieved by the use of the more encumbered 2-methylaminopyridine which generates the borylene system, [Os{BCl(NC$_5$H$_4$NMe)}Cl(CO)(PPh$_3$)$_2$] in 49% isolated yield.

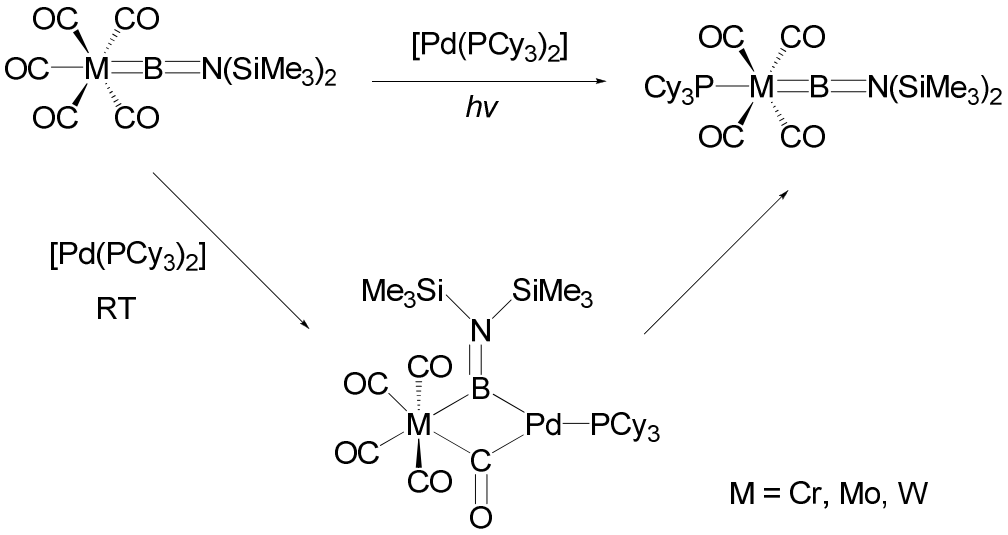


Scheme 1.42 Formation of **[**Os{BOEt(NC$_5$H$_4$NH)}Cl(CO)(PPh$_3$)$_2$].

1.3.2.1.5 Modification of Existing Borylene Systems

In theory modification of an existing metal borylene complex offers an attractive approach for tuning ligand properties. In practice, a relatively small number of systems have been synthesized using this methodology, presumably reflecting the lability of the metal ligand bond under the conditions necessary to bring about substitution of either the metal-bound ligands or the borylene substituent. In order to gain access to terminal borylene complexes containing electronically diverse co-ligands, the reactions of [Pd(PCy$_3$)$_2$] with [(OC)$_5$MBN(SiMe$_3$)$_2$] (M = Cr, Mo, W) were investigated.[76,77] Immediate reaction gave the bridging borylene complexes [(μ-BN(SiMe$_3$)$_2$)(μ-CO){(OC)$_4$M}{Pd(PCy$_3$)}] (M = Cr, W, Mo) at ambient temperature (*vide infra*). The chromium complex, however, is reported to

darken in colour when left at ambient temperature, and is completely converted at 80˚C over a period of 24 h into *trans*-[$(Cy_3P)(OC)_4CrBN(SiMe_3)_2$]. The same compound is also formed after UV irradiation for 4 h, with concomitant formation of palladium black. The tungsten and molybdenum complexes can also be formed by the same route but the reaction is not as clean; irradiation of the aminoborylene precursors [$(OC)_5MBN(SiMe_3)_2$] in the presence of PCy_3, however leads to the formation of *trans*-[$(Cy_3P)(OC)_4MBN(SiMe_3)_2$] after 4 h, by controlled carbonyl substitution.[63]

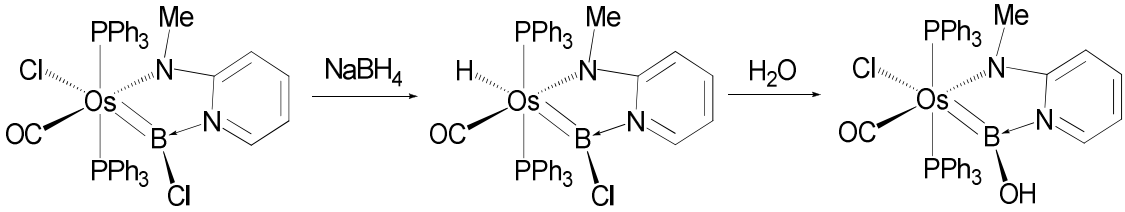


Scheme 1.43 Reactions of [$(OC)_5MBN(SiMe_3)_2$] (M = Cr, Mo, W) with [$Pd(PCy_3)_2$].

It seems likely that the selective substitution of the carbonyl ligand *trans* to the borylene ligand is due not only to the steric bulk of the cyclohexyl and trimethylsilyl substituents but also linked to the higher *trans* influence of the borylene ligand (over CO). The crystal structures of both the molybdenum and tungsten complexes were obtained, revealing M-B bond lengths which are ca. 0.09 Å shorter than the parent pentacarbonyl complex.

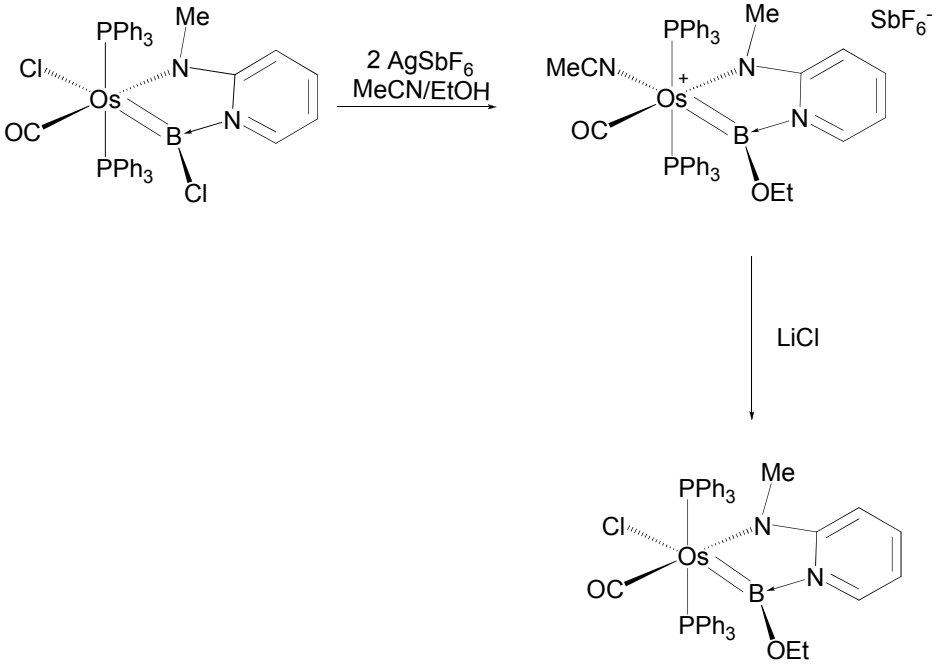
Examples of modification processes occurring at both metal and boron centres have been reported by Roper and co-workers for [$OsB(Cl)(NC_5H_4NMe)Cl(CO)(PPh_3)_2$]. Treatment

with $Na[BH_4]$ leads to reaction at the osmium centre to give the hydride complex $[OsB(Cl)(NC_5H_4NMe)H(CO)(PPh_3)_2]$, which undergoes subsequent hydrolysis to form $[OsB(OH)(NC_5H_4NMe)Cl(CO)(PPh_3)_2]$.



Scheme 1.44 Modification of the tethered borylene $[OsB(Cl)(NC_5H_4NMe)Cl(CO)(PPh_3)_2]$.

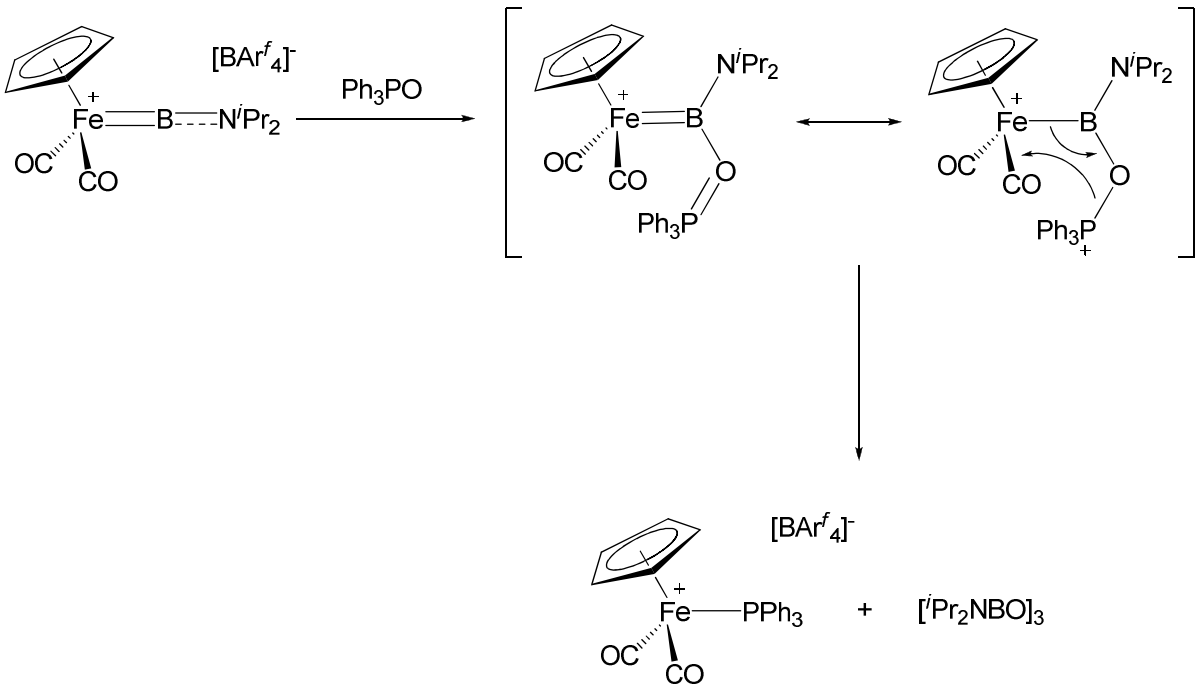
Moreover, ethanolysis of the B-Cl bond in $[OsB(Cl)(NC_5H_4NMe)Cl(CO)(PPh_3)_2]$ occurs under reflux conditions resulting in formation of $[OsB(OEt)(NC_5H_4NMe)Cl(CO)(PPh_3)_2]$. The rate of ethanolysis increases however if the borylene is treated with $Ag[SbF_6]$ to yield $[Os\{B(OEt)(NC_5H_4NMe)\}(CO)(MeCN)(PPh_3)_2]^+[SbF_6]^-$ which reacts further with LiCl to give $[OsB(OEt)(NC_5H_4NMe)Cl(CO)(PPh_3)_2]$.[75]



Scheme 1.45 Ethanolysis of $[OsB(Cl)(NC_5H_4NMe)Cl(CO)(PPh_3)_2]$.

Simple B-coordination of a Lewis base has also been reported in the case of cationic aminoborylene systems. Thus, the reactions of $[CpFe(CO)_2(BNCy_2)]^+[BAr^f_4]^-$ with the nucleophiles 4-picoline and triphenylphosphonium cyclopentadienide results in adduct formation, via coordination of the base at the electrophilic boron centre (Scheme 1.58) (*vide infra*). In the latter case, the major product formed, $[CpFe(CO)_2\{BNCy_2(C_5H_4PPh_3)\}]^+[BAr^f_4]^-$ results from interaction of the electrophilic boron centre with the more sterically accessible cyclopentadienyl 3-carbon and is accompanied by a 1,3-hydride shift. Weaker Lewis bases, such as THF are found to coordinate reversibly.[22] This type of donor/acceptor interaction proves to be an important initial step in much of the further reactivity of cationic terminal borylene complexes, which as a consequence of their heightened electrophilicity display significantly different reaction chemistry than their charge neutral counterparts (*vide infra*).[3n,p]

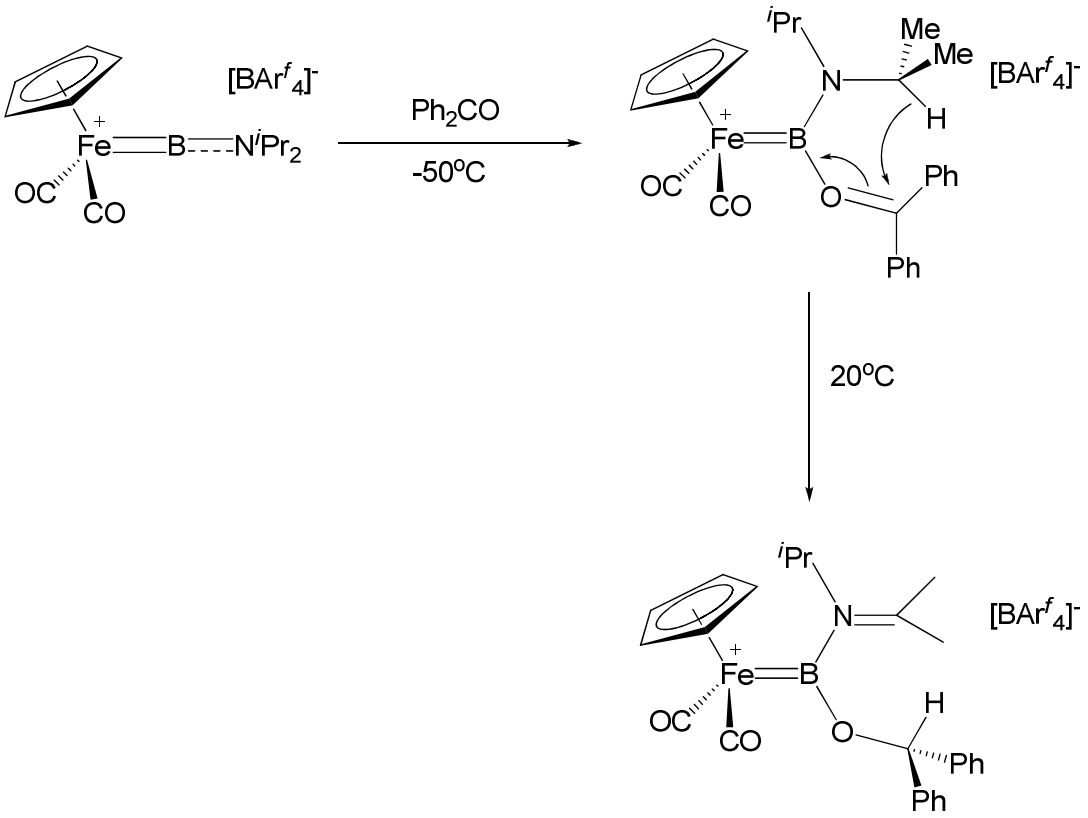
Reactivity of the isopropyl analogue, $[CpFe(CO)_2(BN^iPr_2)]^+[BAr^f_4]^-$ towards Ph_3EX (E = P, X = S, E = As, X = O) has been shown to result in formation of $[CpFe(CO)_2(EPh_3)]^+[BAr^f_4]^-$ and $[^iPr_2NB(\mu\text{-}X)]_n$ (X = S, *n* = 2; X = O, *n* = 3) via metathesis chemistry (*vide infra*).[20] The corresponding reaction with Ph_3PO however, allows some insight into the mechanism of the reaction. Due to the stronger P-O bond, the reaction is significantly slower and reveals the presence of a simple donor/acceptor complex intermediate, $[CpFe(CO)_2\{BN^iPr_2(OPPh_3)\}]^+[BAr^f_4]^-$. This complex was crystallographically characterized and implies that the phosphine oxide coordinates to the boron centre to give an acyclic system in the early stages of the metathesis reaction.



Scheme 1.46 Metathesis reaction of $[CpFe(CO)_2(BN^iPr_2)]^+[BAr^f_4]^-$ with Ph_3PO.

The same cationic terminal borylene reacts with benzophenone via an unusual Meerwein-Ponndorf β-hydride transfer pathway to give the only structurally characterized

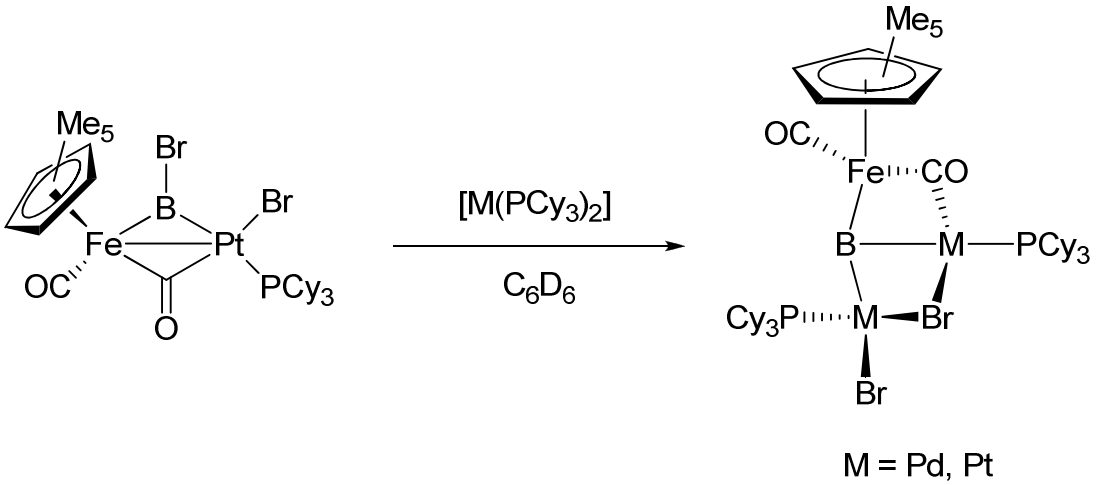
cationic alkoxyborylene complex, $[CpFe(CO)_2\{BOC(H)Ph_2(N^iPrCMe_2)\}]^+[BAr^f_4]^-$, albeit stabilized by coordination of an imine base.[78]



Scheme 1.47 A boron analogue of the Meerwein-Pondorf reaction.

More exotic borylene adducts have been reported by Braunschweig and co-workers; an unprecedented coordination mode for terminal borylenes was described in 2005 with the formation of a metallaborylene stabilized by a transition metal Lewis base of the type $M(PCy_3)$ (M = Pt, Pd). Reaction of the dibromoboryl complex $[Cp^*Fe(CO)_2BBr_2]$ with one equivalent of $[M(PCy_3)_2]$ forms the bridging borylene, $[(\mu\text{-}BBr)(\mu\text{-}CO)\{Cp^*Fe(CO)\}\{Pt(PCy_3)Br\}]$. Addition of a further equivalent of $[M(PCy_3)_2]$ yields the novel metallaborylene complexes $[(Cy_3P)Br_2PtBFe(CO)_2Cp^*M(PCy_3)]$ (M = Pt, Pd), both of

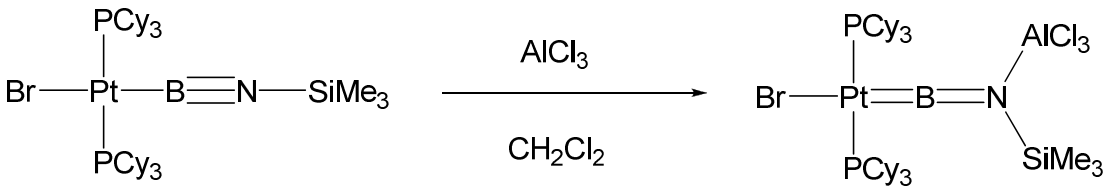
which were structurally characterized, and feature a boron atom coordinated to three transition metals in a pseudo T-shaped geometry (Scheme 1.48).[62]



Scheme 1.48 Reaction of [(μ-BBr)(μ-CO){Cp*Fe(CO)}{(Cy_3P)Pt(Br)}] with [$M(PCy_3)_2$].

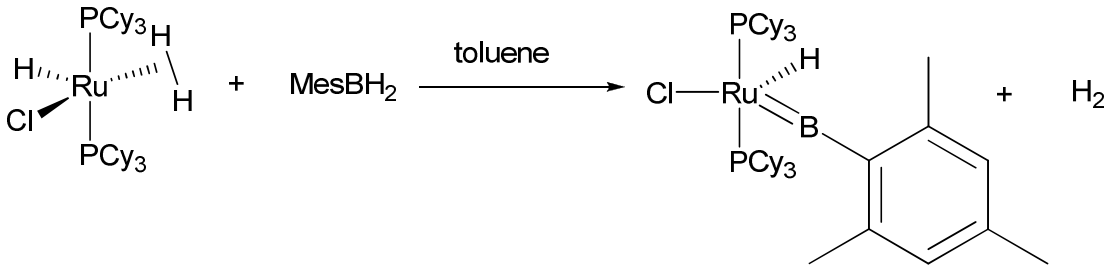
1.3.2.1.6 Miscellaneous Approaches

In 2007, the formation of the first charge neutral platinum borylene complex, [$(Cy_3P)_2$Pt{$BN(SiMe_3)(AlCl_3)$}Br], was reported from the reaction of the Lewis acid, $AlCl_3$ with the iminoboryl system *trans*-[$(Cy_3P)_2$Pt{$BN(SiMe_3)$}Br]. Coordination of the Lewis acid to the nitrogen of the iminoboryl moiety leads to a shortened Pt-B bond and downfield shifted ^{11}B NMR resonance consistent with the formation of a formal Pt=B double bond.[79]



Scheme 1.49 Formation of [$(Cy_3P)_2$Pt{$BN(SiMe_3)(AlCl_3)$}Br].

A novel route to terminal borylene complexes, which is of immense potential versatility and applicability has recently been pursued by Sabo-Etienne and co-workers.[80,81] This methodology uses mesitylborane, $(MesBH_2)_n$, as the boron-containing precursor, in the formation of the ruthenium complex $[RuHCl(BMes)(PCy_3)_2]$ which was isolated as a yellow powder from the reaction with $[RuHCl(H_2)(PCy_3)_2]$.



Scheme 1.50 Synthesis of $[RuHCl(BMes)(PCy_3)_2]$.

1.3.2.2 Spectroscopic and Structural Aspects of Terminal Borylene Complexes

Coordinatively unsaturated terminal borylene complexes typically have ^{11}B NMR resonances that are characteristically downfield shifted with respect to those of corresponding boryl complexes.[3o,p] The charge neutral aminoborylene complexes, $[(OC)_5MBN(SiMe_3)_2]$ (M = Cr, Mo, W)[51,63] and $[CpV(CO)_3BN(SiMe_3)_2]$[66] have ^{11}B NMR shifts of δ_B 87-98, with the more electron rich system $[Cp^*Ir(CO)BN(SiMe_3)_2]$[59] moderately shifted to δ_B 67. Substituting the ancillary carbonyl ligand on the transition metal centre for trialkylphosphine has a minor effect on the ^{11}B NMR shift $[(OC)_4(Cy_3P)MBN(SiMe_3)_2]$ M = Cr, Mo, W δ = 94, 92, 90 ppm respectively).[63] However, substituting the amino group $N(SiMe_3)_2$ on the borylene moiety for the silyl ligand $Si(SiMe_3)_2$ in the chromium complex, $[(OC)_5CrBSi(SiMe_3)_2]$ leads to a significant downfield shift to δ_B 204, reflecting the lack of π-donor stabilization offered by the

silyl ligand.[64] A similar downfield shift is observed for the metallaborylene complexes, $[(OC)_5CrBFe(CO)_2Cp^*]$ (δ_B 205) and $[(OC)_4FeBFe(CO)_2Cp^*]$ (δ_B 191).[65]

A similar trend is observed for the cationic terminal borylene complexes. The mesityl substituted complex, $[Cp^*Fe(CO)_2(BMes)]^+[BAr^f_4]^-$ has a downfield shifted ^{11}B NMR peak (δ_B 145 cf. $[Cp^*Fe(CO)B(Mes)Br]$ δ_B = 113)[34] compared to the π-donor stabilized amino derivatives $[CpM(CO)_2(BNCy_2)]^+[BAr^f_4]^-$ (M = Fe, Ru δ = 93 and 90 respectively).[22,23] Formation of a cationic donor-acceptor adduct by coordination of a substrate at the boron centre results in an upfield shift in the ^{11}B NMR spectrum due to an increase in electron density around the boron centre ($[CpFe(CO)_2\{BN^iPr_2(N^iPrCMe_2)\}]^+[BAr^f_4]^-$ δ_B = 54,[78] $[CpFe(CO)_2\{BN^iPr_2(OPPh_3)\}]^+[BAr^f_4]^-$ δ_B = 49).[20] Cationic metallaborylenes of the type, $[(\mu\text{-}B)\{Mn(CO)_5\}_2]^+[BAr^f_4]^-$ and $[(\mu\text{-}B)\{Cp'Fe(CO)_2\}_2]^+[BAr^f_4]^-$ have downfield shifted resonances of δ_B 225 and 194 respectively, once again reflecting the electronic unsaturation around the boron centre.[71]

Higher coordination numbers at the Lewis acidic boron centre lead to an upfield shift in the ^{11}B NMR spectra, and this is observed for many of the internally stabilized osmium complexes, $[OsB(NHC_9H_6N)ClI(CO)(PPh_3)_2]$ and $[OsB(OEt)(NC_5H_4NH)Cl(CO)(PPh_3)_2]$ (δ_B 52 for both complexes).[46,75] Moreover, complexes of the type, $[(OC)_4Fe(BCp^*)]$ and $[CpFe(CO)_2(BCp^*)]^+[AlCl_4]^-$ have unusually upfield shifted ^{11}B NMR signals compared to other terminal borylene complexes (δ_B -35 and -38 respectively) reminiscent of *nido*-carboranes.[36,50]

To date, there are over 30 crystallographically characterized terminal borylene complexes. For charge neutral complexes, Braunschweig and co-workers have been instrumental in forming and structurally authenticating the majority of these complexes. A

series of complexes featuring the aminoborylene moiety [$BN(SiMe_3)_2$] with a variety of different metals (from group 5, 6 and 9) as well as complexes bearing different ancillary ligands at the metal centre, allows an in-depth structural comparison. Table 1.2 lists the M-B bond length and carbonyl stretching frequencies for these charge neutral complexes.[3p]

Table 1.2 Fe-B bond lengths (Å) and carbonyl stretching frequencies for charge neutral terminal borylene complexes.

Compound	*d*(Fe-B) / Å	υ(CO) / cm^{-1}
$[CpV(CO)_3BN(SiMe_3)_2]$	1.959(6)	1984, 1884, 1842
$[(OC)_5CrBSi(SiMe_3)_2]$	1.878(10)	2066, 2014, 1982, 1952
$[(OC)_5CrBN(SiMe_3)_2]$	1.996(6)	2064, 1981, 1942
$[(OC)_5MoBN(SiMe_3)_2]$	2.152(2)	2073, 1978, 1946
$[(OC)_5WBN(SiMe_3)_2]$	2.151(7)	2075, 1967, 1941
$[(OC)_4(Cy_3P)CrBN(SiMe_3)_2]$	1.915(2)	1898, 1868
$[(OC)_4(Cy_3P)MoBN(SiMe_3)_2]$	2.059(3)	1912, 1894
$[(OC)_4(Cy_3P)WBN(SiMe_3)_2]$	2.058(6)	1903, 1887
$[Cp^*Ir(CO)BN(SiMe_3)_2]$	1.892(3)	1945

The aminoborylene complexes, $[(OC)_5MBN(SiMe_3)_2]$ (M = Cr, Mo, W)[51,63] have all been crystallographically characterized and as such, a direct comparison of complexes differing only at the transition metal centre can be drawn. A common feature of these compounds is the linear geometry of the M-B-N bond. On going down the group 6 metals, the M-B bond length increases from 1.996(6) to 2.151(7) Å for $(OC)_5Cr[BN(SiMe_3)_2]$ and

$(OC)_5W[BN(SiMe_3)_2]$ respectively, due to an increase in the respective covalent radii (1.25 Å versus 1.30 Å for Cr and W respectively).[82]

Substituting the amino substituent $N(SiMe_3)_2$ for $Si(SiMe_3)_3$ results in a shortening in the Cr-B bond from 1.996(6) to 1.878(10) Å, which is as expected as the amino substituent offers π-donor stabilization to the boron centre.[64] The carbonyl stretching frequencies for $[(OC)_5CrBN(SiMe_3)_2]$ however, are only slightly lower than for $[(OC)_5CrBSi(SiMe_3)_2]$ (2064, 1981, 1942 cm^{-1} and 2066, 2014, 1982, 1952 cm^{-1} respectively). Formation of a metallaborylene whereby the boron centre is bound to two transition metals leads to a bond length of 1.975(2) Å which falls between that of the silyl- and aminoborylene systems, consistent with an intermediate bond order.[65]

The development of the halide abstraction methodology by Aldridge and co-workers has allowed access to a range of cationic terminal borylene complexes. Although this area of chemistry is relatively new, a comparative study on structural and computational data for the structurally authenticated compounds (containing variation in the metal, and borylene substituent as well as various base stabilized compounds) has been carried out.[3p]

Table 1.3 Fe-B bond lengths (Å), DFT calculated σ:π contribution to covalent bonding and carbonyl stretching frequencies for cationic terminal borylene complexes.

Compound	*d*(Fe-B) / Å	σ:π	υ(CO) / cm^{-1}
$[Cp^*Fe(CO)_2(BMes)]^+$	1.792(8)	62:38	2055, 2013
$[CpFe(CO)_2(BNCy_2)]^+$	1.859(6)	71:29	2071, 2028
$[CpFe(CO)_2(BCp^*)]^+$	1.977(3)	86:14	2020, 1962
$[CpFe(CO)_2\{BNCy_2(4\text{-pic})\}]^+$	2.049(4)	87:13	2019, 1962
$[CpFe(CO)_2\{BN^iPr_2(N^iPrCMe_2)\}]^+$	2.058(9)	88:12	2007, 1951
$[CpFe(CO)_2\{BN^iPr_2(OPPh_3)\}]^+$	2.057(4)	89:11	2004, 1949
$[CpFe(CO)_2\{BNCy_2(C_5H_4PPh_3)\}]^+$	2.102(5)	90:10	1985, 1927
$[CpRu(CO)_2(BN^iPr_2)]^+$	1.950(8)	*α*	2083, 2038
$[CpRu(CO)_2(BNCy_2)]^+$	1.960(6)	68:32	2022, 1957

[α]Not available

The data reveal that the choice of borylene substituent has a profound effect on the nature of the Fe-B bond. On going from the mesityl substituted borylene,[34] $[Cp^*Fe(CO)_2(BMes)]^+$ to the amino complex,[20,22] $[CpFe(CO)_2(BNCy_2)]^+$ and pentamethylcyclopentadienyl (Cp^*),[36] $[CpFe(CO)_2(BCp^*)]^+$ substituted borylenes we see an increase in the bond length from 1.792(8) to 1.977(3) Å. This is due to the fact that the mesityl substituted borylene features a boron centre benefiting from minimal π donor stabilization and so is the most electrophilic. $[Cp^*Fe(CO)_2(BMes)]^+$ has a bonding situation similar to that reported for Fischer carbenes, comprising B→Fe σ-donor and Fe→B π back-bonding components.[5k] The amino and Cp* substituents however are able to donate π-electron density to the boron centre, and so relieve the electronic unsaturation, leading to reduced π back-

donation from iron, and a longer Fe-B bond. This is further exemplified by looking at the DFT calculated ratios of σ to π contributions to the covalent bonding density for the four compounds. This shows an increasingly σ-based M-B bond as the degree of π donor stabilization from the borylene substituent increase. On going down the series we superficially go from an Fe=B double bond to an Fe-B single bond (donor-acceptor), thereby demonstrating that it is possible to tune the electronics of borylene complexes by appropriate choice of substituent.

The base stabilized cationic terminal borylene complexes are widely accepted as containing a formal M-B single bond implying limited M→B π-interaction. Elongated Fe-B bond lengths and lower carbonyl stretching frequencies support this bonding description ($[CpFe(CO)_2\{BNCy_2(C_5H_4PPh_3)\}]^+$; 2.102(5) Å; 1985, 1927 cm^{-1}; cf. $[CpFe(CO)_2(BNCy_2)]^+$; 1.859(6) Å; 2071, 2028 cm^{-1}).[22] A similar bonding description is also observed for base stabilized osmium complexes.

Another approach to tune the electronic properties of a borylene complex is to vary the transition metal, and recently the cationic ruthenium complexes, $[CpRu(CO)_2(BN^iPr_2)]^+$ and $[CpRu(CO)_2(BNCy_2)]^+$ have been synthesised by the halide abstraction route.[23] The Ru-B bond lengths are longer than for related iron aminoborylene complexes (1.950(8) and 1.960(6) Å for $[CpRu(CO)_2(BN^iPr_2)]^+$ and $[CpRu(CO)_2(BNCy_2)]^+$ respectively, cf. 1.859(6) Å for $[CpFe(CO)_2(BNCy_2)]^+$),[20-22] which is as expected considering the larger covalent radius for ruthenium (1.24 and 1.17 Å for Ru and Fe respectively).[82] However, the M-B bond length decrease on going from the aminoboryl precursor to the aminoborylene is essentially the same for both metal complexes (-9.4 and -8.5% for the iron and ruthenium $BNCy_2$ compounds

respectively). In addition, DFT calculations reveal a similar σ:π contribution to the covalent bond for iron and ruthenium (71:29 and 68:32 for $BNCy_2$ compounds respectively).

Another important structural property of the borylene ligand is its *trans* influence. In the neutral silylborylene, $[(OC)_5CrBSi(SiMe_3)_2]$, for instance, the Cr-CO bond *trans* to the borylene fragment is marginally longer (1.939(10) Å) than the *cis* Cr-CO bonds (mean = 1.894 Å), evidence of greater *trans* influence compared to the carbonyl ligand.[64] Although the *trans* influence in the analogous aminoborylene complex, $[(OC)_5CrBN(SiMe_3)_2]$[57] is less pronounced (*trans* Cr-CO bond = 1.908(6) Å), the fact that *trans* substitution of the carbonyl ligand for PCy_3 is observed is evidence of the *trans* effect of the aminoborylene moiety.[63] That said, it should be noted that borylene ligands have weaker *trans* influences compared to their boryl counterparts, possibly owing to the lower energy and greater s character of the donor orbital in the borylene ligand.

1.3.2.3 Reactivity of Terminal Borylene Complexes

1.3.2.3.1 Borylene Transfer Chemistry

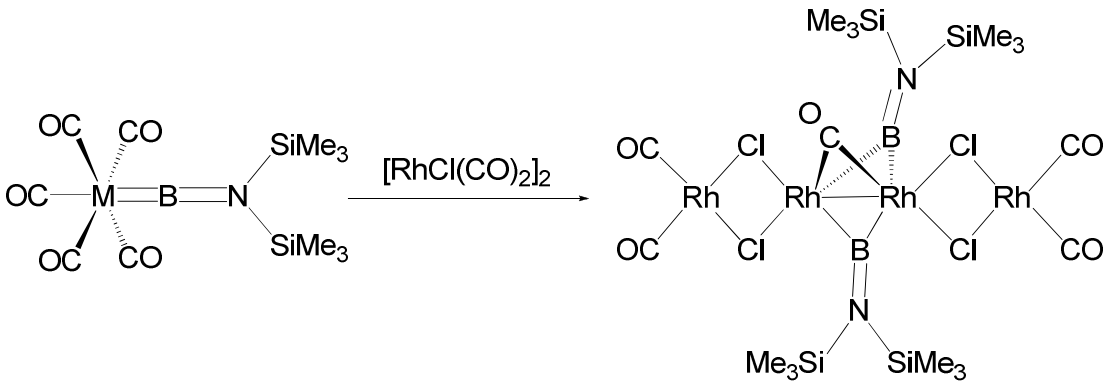
The reactivity of terminal borylene complexes is a relatively new area of research owing to the fact that the first terminal borylene complexes appeared in the literature a decade ago. Broadly speaking the reactivity of these complexes can be categorized into two reaction modes – those involving borylene transfer chemistry, where the borylene fragment moves to a metal or organic complex, and those which proceed via initial coordination of the substrate at the electrophilic boron centre, whereby the borylene fragment is retained within the coordination sphere of the metal. Modes of reactivity have been shown to depend on the nature of the borylene substituent; thus the reactions of the cationic mesityl borylene

complex,[34] $[Cp^*Fe(CO)_2(BMes)]^+[BAr^f_4]^-$ often result in displacement of the borylene fragment, while those of the aminoborylene complexes $[CpFe(CO)_2(BNR_2)]^+[BAr^f_4]^-$ (R = Cy, ^{i}Pr) which feature a π-donor stabilizing amino substituent show a more varied reactivity such as hydride transfer,[78] metathesis[20] and cycloaddition.[22]

Braunschweig and co-workers have reported many examples of borylene transfer chemistry, which have been discussed in the synthesis section. Borylene transfer chemistry proceeds by the transfer of the borylene fragment $[BN(SiMe_3)_2]$ to another organometallic moiety under thermal or photolytic conditions to yield a new terminal or bridged borylene complex. The complexes, $[(OC)_5MBN(SiMe_3)_2]$ (M = Cr, W, Mo),[63] $[Cp(CO)_3VBN(SiMe_3)_2]$[66] and $[(\mu\text{-}BN(SiMe_3)_2)\{CpRe(CO)_2\}_2]$[57] represent examples of complexes formed in this manner. Formation of the first cobalt borylene, $[CpCo(CO)BN(SiMe_3)_2]$ provided support for an associative mechanism for these borylene transfer reactions through the isolation of the intermediate $[(\mu\text{-}BN(SiMe_3)_2)\{CpCo(CO)\}\{W(CO)_5\}]$ (Scheme 1.23).[58]

In addition, the group 9 aminoborylene complexes, $[CpRh(CO)BN(SiMe_3)_2]$ and $[Cp^*Ir(CO)BN(SiMe_3)_2]$ have been synthesized from the molybdenum borylene, $[(OC)_5MoBN(SiMe_3)_2]$ under thermal conditions.[59] It should be noted that both $[CpRh(CO)BN(SiMe_3)_2]$ and $[CpCo(CO)BN(SiMe_3)_2]$ are unstable in solution and eventually decompose to form the corresponding bridging complex, $[(\mu\text{-}BN(SiMe_3)_2)\{CpM(CO)\}_2]$ (*vide supra*). Furthermore, reaction of the borylene complex, $[(OC)_5MBN(SiMe_3)_2]$ (M = Cr, W) with $[RhCl(CO)_2]_2$ at ambient temperature yields the tetranuclear rhodium complex, $[(OC)_2Rh(\mu\text{-}Cl)_2Rh(\mu\text{-}CO)\{\mu\text{-}BN(SiMe_3)_2\}_2Rh(\mu\text{-}Cl)_2Rh(CO)_2]$ – the first example of a bis(borylene) system.[83] The complex features a chain of four rhodium atoms, with the two

internal metal centres bridged by two borylene fragments and a carbonyl ligand. In the solid state the tetramers were reported to aggregate into linear chains.

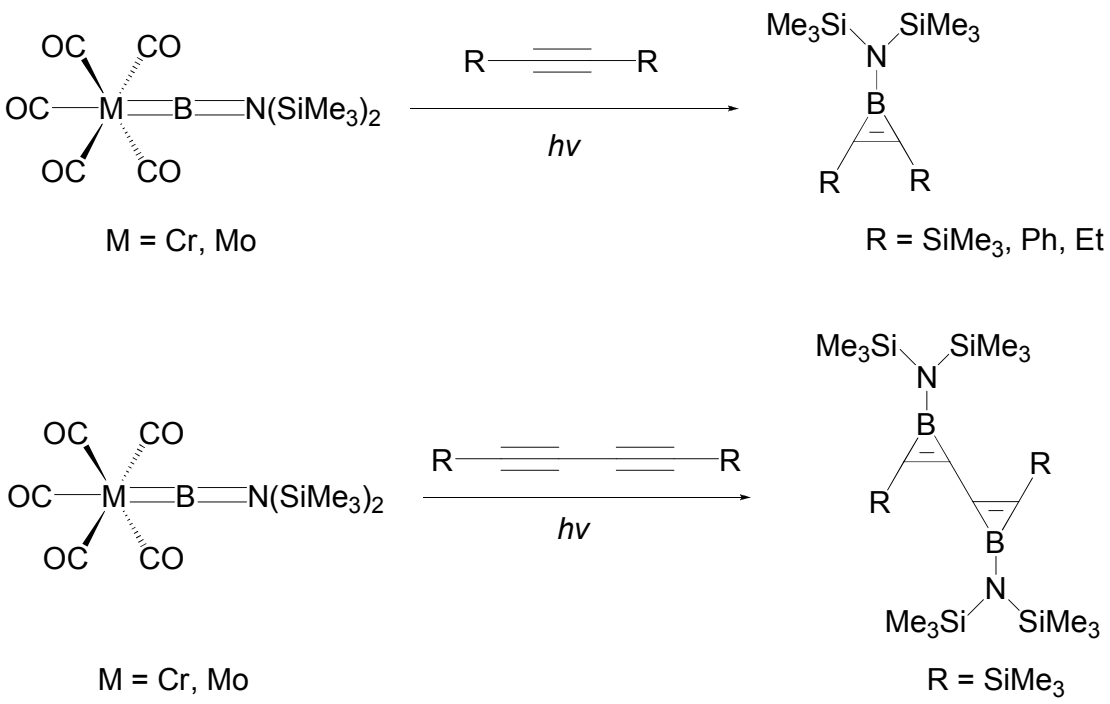


Scheme 1.51 Synthesis of $[(OC)_2Rh(\mu\text{-}Cl)_2Rh(\mu\text{-}CO)\{\mu\text{-}BN(SiMe_3)_2\}_2Rh(\mu\text{-}Cl)_2Rh(CO)_2]$.

To extend transfer of the borylene moiety to late transition metals, under photolytic conditions, the electron-rich but coordinatively unsaturated compounds, $[M'(PCy_3)_2]$ (M' = Pt, Pd) were targeted. However, reaction with $[(OC)_5MBN(SiMe_3)_2]$ forms the heterodinuclear semi-bridging compound, $[(\mu\text{-}BN(SiMe_3)_2)(\mu\text{-}CO)\{(OC)_4M\}\{M'(PCy_3)\}]$ (M/M' = Cr/Pd, W/Pd, Cr/Pt, Mo/Pd, Mo/Pt) at ambient conditions.[63,76,77] The reaction of the tungsten aminoborylene complex, $[(OC)_5WBN(SiMe_3)_2]$ with $[Pt(PCy_3)_2]$ however, forms $[(\mu\text{-}BN(SiMe_3)_2)(\mu\text{-}CO)\{(Cy_3P)(OC)_3W\}\{Pt(PCy_3)\}]$ by substitution of the carbonyl group *trans* to the borylene fragment with PCy_3, a reaction that is also reported when the mono(phosphine) semi-bridging complexes (W/Pd and Cr/Pt) are left for prolonged reaction times. Photolysis or warming of the mono(phosphine) semi-bridging complex leads to formation of the mono-nuclear phosphine complex, *trans*-$[(Cy_3P)(OC)_4M\{BN(SiMe_3)_2\}]$ (M = Cr, Mo). Moreover, an analogous semi-bridged borylene $[(\mu\text{-}B^tBu)(\mu\text{-}CO)\{CpMn(CO)\}\{M'(PCy_3)\}]$ is formed by reaction of $[CpMn(CO)_2(B^tBu)]$ with $M'(PCy_3)_2$ (M' = Pd, Pt). The semi-bridging borylene complexes can also be described as terminal

borylene complexes stabilised by transition metal Lewis base adducts, as there is said to be only a slight change in the M=B bond length on going from the precursor (1.996(6) and 2.084(2) Å for $[(OC)_5CrBN(SiMe_3)_2]$ and $[(\mu\text{-}BN(SiMe_3)_2)(\mu\text{-}CO)\{(OC)_4Cr\}\{Pd(PCy_3)\}]$ and the Si-N-Si plane is almost orthogonal to M-B-M' (Scheme 1.43).

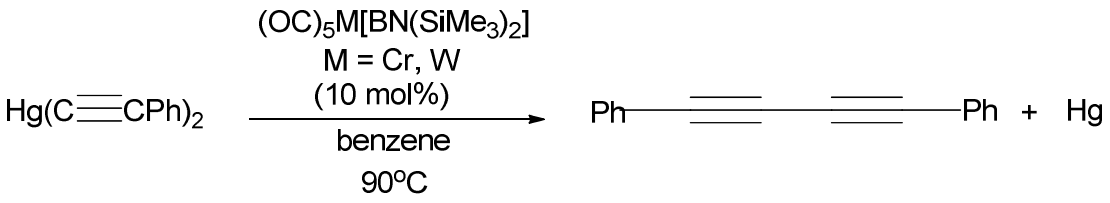
Braunschweig *et al*. have also demonstrated transfer of the borylene fragment to main group elements, and in 2005 reported formation of three membered borirene (boracyclopropene) and diborirene ring systems by irradiation of $[(OC)_5MBN(SiMe_3)_2]$ (M = Cr, W) with the alkynes ($SiMe_3C{\equiv}CSiMe_3$, PhC≡CPh and EtC≡CEt) or the diyne ($SiMe_3C{\equiv}CC{\equiv}CSiMe_3$) via a [2+1] cycloaddition reaction.[84]



Scheme 1.52 Formation of a borirene and diborirene by borylene transfer.

Furthermore, reaction of the metallaborylene, $[(OC)_5CrBFe(CO)_2Cp^*]$ with $SiMe_3C{\equiv}CSiMe_3$, also led to successful transfer of the borylene fragment $[BFe(CO)_2Cp^*]$ and formation of the ferroborirene, $[(\mu\text{-}B)\{Cp^*Fe(CO)_2\}\{SiMe_3C{=}CSiMe_3\}]$ in 35% yield.[85]

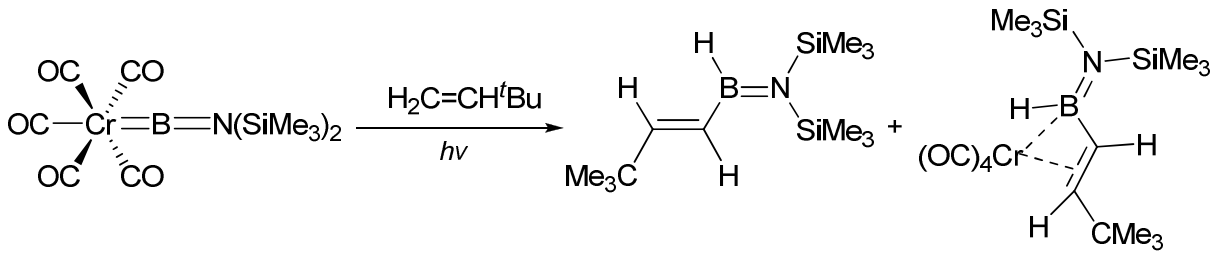
In light of this reactivity, aminoborylene transfer to alkynyl complexes featuring a heavy metal, $Hg(C{\equiv}CR)_2$ (R = Ph, C_6H_5-4-Me, C_6H_4-4-OMe, C_6H_4-4-NMe_2) were attempted. Indeed formation of a diborirene was observed under photolytic conditions, with the reaction proceeding by demercuration of $Hg(C{\equiv}CR)_2$ to form the diyne, $RC{\equiv}CC{\equiv}CR$ followed by transfer of the borylene fragment from $[(OC)_5MBN(SiMe_3)_2]$ (M = Cr, W). However, under thermal conditions the reaction results in formation of the diyne and elemental mercury whilst the aminoborylene remains intact. Repeating the reaction with catalytic amounts of the aminoborylene (10 mol %) also resulted in full conversion to the diyne and mercury, demonstrating for the first time that the borylene can act as a catalyst in the demercuration of bis(alkynyl)mercurials, a process widely used to access conjugated diynes.[86]



Scheme 1.53 Reaction exemplifying the use of "metallaborylene" as a catalyst.

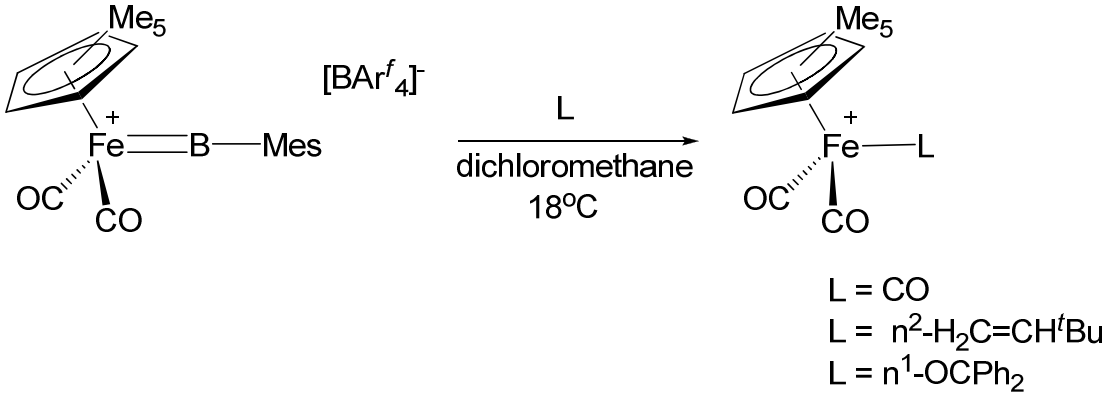
The chromium aminoborylene, $[(OC)_5CrBN(SiMe_3)_2]$ was also irradiated with the olefin, $H_2C{=}CH^tBu$ in the hope of transferring the borylene moiety and forming a saturated three-membered borirene ring. However, the reaction instead proceeded via C-H bond activation to form a mixture of the coordinated vinylaminoborane,

$[(OC)_4Cr(Me_3Si)_2N(H)BC(H)=CH^tBu]$ and the free vinylaminoborane itself $[(Me_3Si)_2N(H)BC(H)=CH^tBu]$.[87]



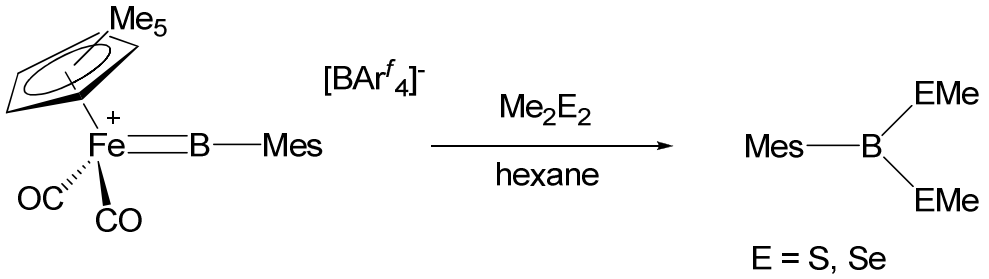
Scheme 1.54 Reaction of $[(OC)_5CrBN(SiMe_3)_2]$ with $H_2C=CH^tBu$.

Insertion of a borylene fragment into a C-H bond has also been reported by Aldridge *et al*. for the reaction of $[Cp^*Fe(CO)_2(BMes)]^+[BAr^f_4]^-$ with substrates such as CO, $H_2C=CH^tBu$ and benzophenone in dichloromethane. This chemistry results in displacement of the borylene fragment and the formation of the cationic complexes, $[Cp^*Fe(CO)L]^+[BAr^f_4]^-$ (L = CO, η^2-$H_2C=CH^tBu$, η^1-$OCPh_2$). The fate of the BMes moiety however, has been shown by kinetic studies to involve insertion into the C-H bond of the dichloromethane solvent, implying that the solvent plays a crucial role in the displacement of the borylene fragment.[35]



Scheme 1.55 Reaction of $[Cp^*Fe(CO)_2(BMes)]^+[BAr^f_4]^-$ by displacement of the borylene fragment.

Furthermore, related reactivity was observed with the dialkyldichalcogenides, Me_2E_2 (E = S, Se) which were used as trapping agents and proceeded by insertion of the BMes moiety into the E-E bond forming the dithio- and diselenoboranes $MesB(EMe)_2$.[35]

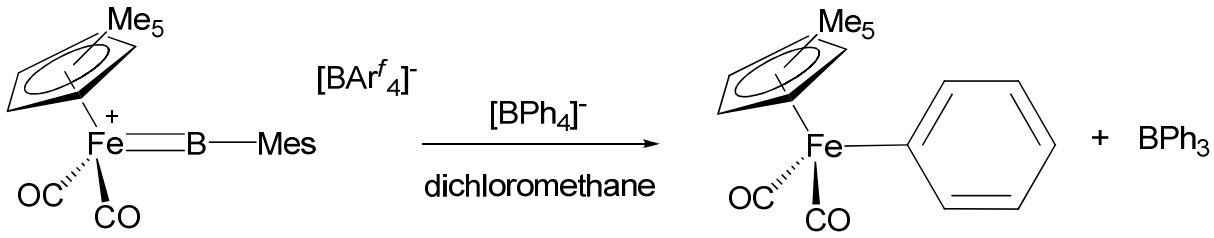


Scheme 1.56 Reaction of $[Cp^*Fe(CO)_2(BMes)]^+[BAr^f_4]^-$ with dialkyldichalcogenides.

1.3.2.3.2 Coordination at Boron

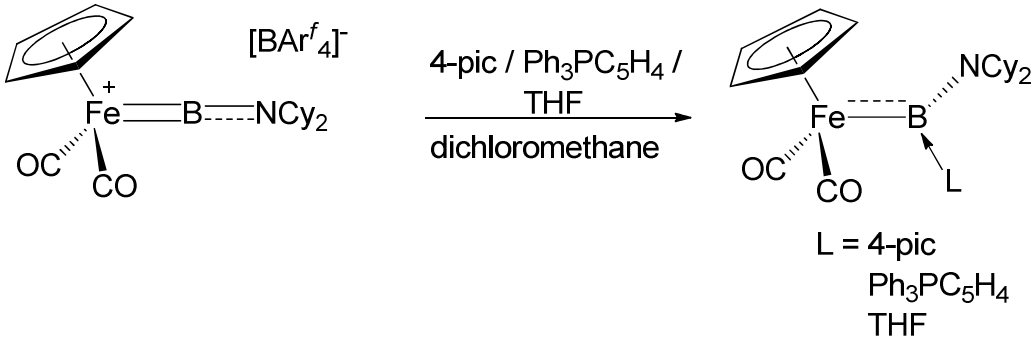
Reactivity of terminal borylene complexes is largely determined by borylene substituent and net charge, and it has been shown, for the cationic class of compounds especially, that reaction proceeds by initial coordination of the substrate at the boron centre. It comes as no surprise, that the electrophilic nature of the boron centre in the cationic terminal borylene, $[Cp^*Fe(CO)_2(BMes)]^+[BAr^f_4]^-$ compound, means that the main mode of reactivity with hard nucleophiles is by charge driven attack at the boron centre. Hence, reaction with suitable halide sources yields the corresponding haloboryl complexes, whereas fluoride abstraction is observed with $[^nBu_4N][BF_4]$ (Scheme 1.9).[35]

By contrast softer nucleophiles such as $[BPh_4]^-$ typically react at the iron centre rather than at boron (in this case forming $[Cp^*Fe(CO)_2Ph]$) possibly due to the high contribution to the LUMO from iron-based orbitals.



Scheme 1.57 Reaction of $[Cp^*Fe(CO)_2(BMes)]^+[BAr^f_4]^-$ with $[BPh_4]^-$.

Simple B-coordination of a Lewis base has also been reported in the case of cationic aminoborylene systems. Thus, the reactions of $[CpFe(CO)_2(BNCy_2)]^+[BAr^f_4]^-$ with the nucleophiles 4-picoline and triphenylphosphonium cyclopentadienide result in adduct formation, via coordination of the base at the electrophilic boron centre (*vide supra*).[22]

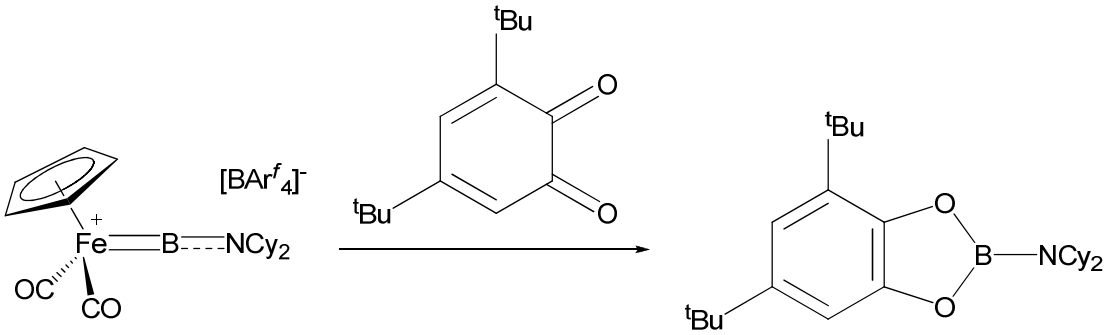


Scheme 1.58 Reaction of $[CpFe(CO)_2(BNCy_2)]^+[BAr^f_4]^-$ with nucleophiles via adduct formation.

Reactivity of the cationic terminal borylene complexes, $[CpFe(CO)_2(BNR_2)]^+[BAr^f_4]^-$ (R = ^{i}Pr, Cy) towards a range of organic substrates has been discussed in the synthesis section. The reactions all proceed with initial coordination of the substrate at the electrophilic boron

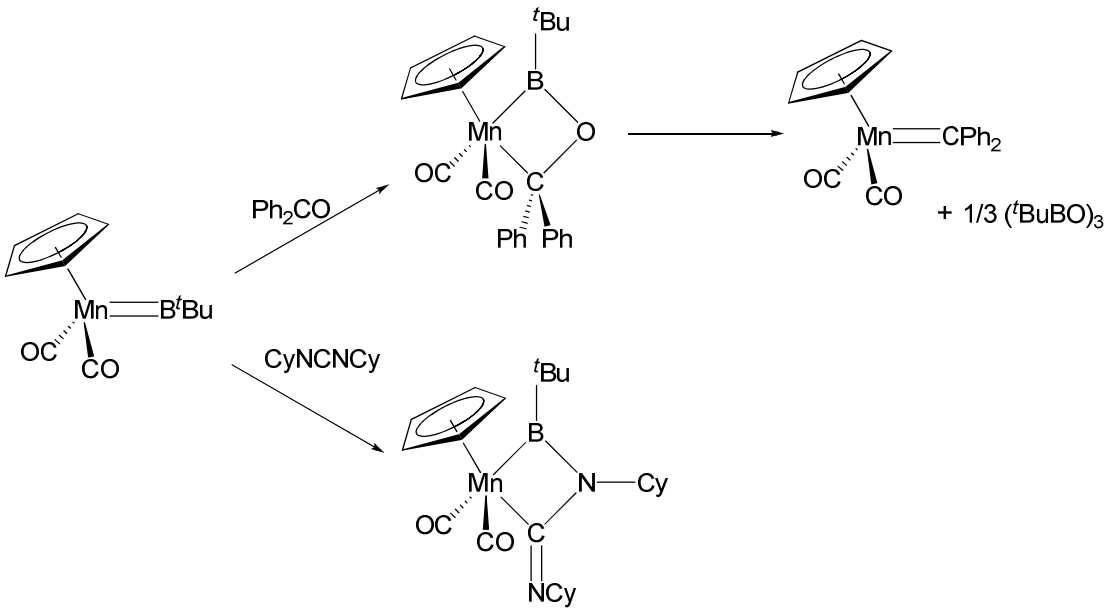
centre and show a range of different activity such as cycloaddition, hydride transfer and metathesis to form base stabilised terminal borylene complexes.[20-22,78]

Reaction of $[CpFe(CO)_2(BNCy_2)]^+[BAr^f_4]^-$ towards 3,5-di-tert-butyl-ortho-benzoquinone, however, proceeds by an unprecedented [4+1] cycloaddition process to form the corresponding catechol derivative (Scheme 1.59).[22]



Scheme 1.59 Reaction of $[CpFe(CO)_2(BNCy_2)]^+[BAr^f_4]^-$ with 3,5-di-tert-butyl-ortho-benzoquinone.

The neutral alkylborylene has also shown to react by metathesis towards the substrates benzophenone and dicyclohexylcarbodiimide. The four-membered cyclic products, $[Cp(CO)_2Mn\{B(^tBu)OC(Ph_2)\}]$ and $[Cp(CO)_2Mn\{B(^tBu)N(Cy)C(NCy)\}]$ are accessed via a [2+2] cycloaddition reaction. In solution however, the benzophenone derived metallacycle was found to undergo a cycloreversion in the opposite sense to form the manganese carbene, $[CpMn(CO)=CPh_2]$ and tri-*tert*-butylboroxine.[88]



Scheme 1.60 Reaction of $[CpMn(CO)_2(B^tBu)]$ via cycloaddition.

Conversely, reaction of the cationic aminoborylene, $[CpFe(CO)_2(BN^iPr_2)]^+[BAr^f_4]^-$ with benzophenone proceeds by initial coordination of the organic substrate at the boron centre to form an imine stabilized alkoxyborylene complex by an intramolecular Meerwein-Ponndorf hydride transfer pathway (Scheme 1.47).[78] The cationic alkoxyborylene, $[CpFe(CO)_2\{BOC(H)Ph_2(N^iPrCMe_2)\}]^+[BAr^f_4]^-$ is formed by the transfer of a β-hydride from the isopropyl group to the coordinated ketone, and it is proposed that the electrophilicity of the carbonyl carbon in the boron bound adduct, $[CpFe(CO)_2\{BOCPh_2(N^iPr_2)\}]^+[BAr^f_4]^-$ is a key factor in facilitating the transfer. In a further mode of reactivity, reaction of the more electrophilic borylene, $[Cp^*Fe(CO)_2(BMes)]^+[BAr^f_4]^-$ with benzophenone results in displacement of the borylene moiety and formation of $[Cp^*Fe(CO)_2(\eta^1\text{-}O{=}CPh_2)][BAr^f_4]^-$.[35] This reactivity once again demonstrates the important role charge and borylene substituent plays in determining patterns of reactivity.

1.4 References for Chapter One

1. (a) R. A. Fischer, J. Weiß, *Angew. Chem. Int. Ed.*, 1999, **38**, 2830. (b) T. M. Trnka, R. H. Grubbs, *Acc. Chem. Res*., 2001, **34**, 18. (c) R. Waterman, P. G. Hayes, T. D. Tilley, *Acc. Chem. Res.*, 2007, **40**, 712.

2. (a) R. T. Baker, D. W. Ovenall, J. C. Calabrese, S. A. Westcott, N. J. Taylor, I. D. Williams, T. B. Marder, *J. Am. Chem. Soc*., 1990, **112**, 9399. (b) J. R. Knorr, J. S. Merola, *Organometallics*, 1990, **9**, 3008.

3. (a) G. Schmid, *Angew. Chem. Int. Ed*., 1970, **9**, 819. (b) G. R. Irvine, G. Lesley, T. B. Marder, N. C. Norman, C. R. Rice, E. G. Robins, W. R. Roper, G. R. Whittell, L. J. Wright, *Chem. Rev*., 1998, **98**, 2685. (c) H. Braunschweig, *Angew. Chem. Int. Ed*., 1998, **37**, 1786. (d) M. R. Smith III, *Prog. Inorg. Chem*., 1999, **48**, 505. (e) B. Wrackmeyer, *Angew. Chem. Int. Ed*., 1999, **38**, 771. (f) H. Braunschweig, M. Colling, *J. Organomet. Chem*., 2000, **614**, 18. (g) H. Braunschweig, M. Colling, *Coord. Chem. Rev*., 2001, **223**, 1. (h) H. Braunschweig, M. Colling, *Eur. J. Inorg. Chem*., 2003, 393. (j) H. Braunschweig, *Adv. Organomet. Chem*. 2004, 51, 163. (i) S. Aldridge, D. L. Coombs, *Coord. Chem. Rev*., 2004, **248**, 535. (j) H. Braunschweig, D. Rais, *Heteroatom Chem*., 2005, **16**, 566. (k) H. Braunschweig, G. R. Whittell, *Chem. Eur. J*., 2005, **11**, 6128. (l) H. Braunschweig, C. Kollann, D. Rais, *Angew. Chem. Int. Ed*., 2006, **45**, 5254. (m) S. Aldridge, D. L. Kays, *Main Group Chem*., 2006, **5**, 223. (n) H. Braunschweig, C. Kollann, F. Seeler, *Contemporary Metal Boron Chemistry I*, eds. T. B. Marder, Z. Lin, Springer, 2008, Vol. 130, p 1. (o) D. L. Kays, S. Aldridge, *Contemporary Metal Boron Chemistry I*, eds. T. B. Marder, Z. Lin, Springer, 2008, Vol. 130, p 29. (p) D. Vidovic, G. A. Pierce, S. Aldridge, *Chem. Comm*., 2009, 1157.

4. (a) Y. Segawa, M. Yamashita, K. Nozaki, *Science*, 2006, **314**, 113. (b) T. B. Marder, *Science*, 2006, **314**, 69. (c) T. Kajiwara, T. Terabayashi, M. Yamashita, K. Nozaki, *Angew. Chem. Int. Ed*., 2008, **47**, 6606. (d) Y. Segawa, Y. Suzuki, M. Yamashita, K. Nozaki, *J. Am. Chem. Soc*., 2008, **130**, 16069.

5. (a) B. E. R. Schilling, R. Hoffmann, D. L. Lichtenberger, *J. Am. Chem. Soc*., 1979, **101**, 585. (b) A. W. Ehlers, E. J. Baerends, F. M. Bickelhaupt, U. Radius, *Chem. Eur. J*., 1998, **4**, 210. (c) U. Radius, F. M. Bickelhaupt, A. W. Ehlers, N. Goldberg, R. Hoffmann, *Inorg. Chem*., 1998, **37**, 1080. (d) C. Boehme, G. Frenking, *Chem. Eur. J*., 1999, **5**, 2184. (e) C. L. B. Macdonald, A. H. Cowley, *J. Am. Chem. Soc*., 1999, **121**, 12113. (f) G. Frenking, N. Fröhlich, *Chem. Rev*., 2000, **100**, 717. (g) J. Uddin, C. Boehme, G. Frenking, *Organometallics*, 2000, **19**, 571. (h) K. T. Giju, F. M. Bickelhaupt, G. Frenking, *Inorg. Chem*., 2000, **39**, 4776. (i)Y. Chen, G. Frenking, *J. Chem. Soc. Dalton. Trans*., 2001, 434. (j) A. A. Dickinson, D. J. Willock, R. J. Calder, S. Aldridge, *Organometallics*, 2002, **21**, 1146. (k) S. Aldridge, A. Rossin, D. L. Coombs, D. J. Willock, *Dalton Trans*., 2004, 2649. (l) J. Zhu, Z. Lin, *Inorg. Chem*. 2005, **44**, 9384. (m) H. F. Bettinger, *Inorg. Chem*., 2007, **46**, 5188. (n) N. D. Coombs, W. Clegg, A. L. Thompson, D. J. Willock, S. Aldridge, *J. Am. Chem. Soc*., 2008, **130**, 5449. (o) U. Flierler, M. Burzler, D. Leusser, J. Henn, H. Ott, H. Braunschweig, D. Stalke, *Angew. Chem. Int. Ed*., 2008, **47**, 4321. (p) K. Götz, M. Kaupp, H. Braunschweig, D. Stalke, *Chem. Eur. J*. 2009, **15**, 623.

6. Z. Lin, *Contemporary Metal Boron Chemistry I*, eds. T. B. Marder, Z. Lin, Springer, 2008, Vol. 130, p 123.

7. H. Nöth, G. Schmid, *Angew. Chem. Int. Ed*., 1963, **2**, 623.

8. J. F. Hartwig, S. Huber, *J. Am. Chem. Soc*., 1993, **115**, 4908.

9. (a) K. M. Waltz, X. He, C. Muhoro, J. F. Hartwig, *J. Am. Chem. Soc*., 1995, **117**, 11357. (b) H. Chen. J. F. Hartwig, *Angew. Chem . Int. Ed*., 1999, **38**, 3391. (c) K. M. Waltz, C. N. Muhoro, J. F. Hartwig, *Organometallics*, 1999, **18**, 3383. (d) C. N. Iverson, M. R. Smith III, *J. Am. Chem. Soc*., 1999, **121**, 7696. (e) H. Chen, S. Schlecht, T. C. Semple, J. F. Hartwig, *Science*, 2000, **287**, 1995. (f) K. M. Waltz, J. F. Hartwig, *J. Am. Chem. Soc*., 2000, **122**, 11358. (g) K. Kawamura, J. F. Hartwig, *J. Am. Chem. Soc*., 2001, **123**, 8422. (h) S. Shimada, A. S. Batsanov, J. A. K. Howard, T. B. Marder, *Angew. Chem. Int. Ed*., 2001, **40**, 2168. (i) J-Y. Cho, M. K. Tse, D. Holmes, R. E. Maleczka Jr, M. R. Smith III, *Science*, 2002, **295**, 305. (j) Y. Kondo, D. Garcia-Cuadrado, J. F. Hartwig, N. K. Boaen, N. L. Wagner, M. A. Hillmyer, *J. Am. Chem. Soc*., 2002, **124**, 1164. (k) T. Ishiyama, J. Takagi, K. Ishida, N. Miyaura, *J. Am. Chem. Soc*., 2002, **124**, 390. (l) R. E. Maleczka Jr, F. Shi, D. Holmes, M. R. Smith III, *J. Am. Chem, Soc*., 2003, **125**, 7792.

10. (a) K. Burgess, M. Ohlmeyer, *Chem. Rev*., 1991, **91**, 1179. (b) I. Beletskaya, A. Pelter, *Tetrahedron*, 1997, **53**, 4957. (c) H. Wadepohl, *Angew. Chem. Int. Ed*., 1997, **36**, 2441. (d) C. M. Crudden, D Edwards, *Eur. J. Org. Chem*., 2003, 4695.

11. (a) T. B. Marder, N. C. Norman, *Top. Catal*. 1998, **5**, 63. (b) H. E. Burks, J. P. Morken, *Chem. Comm*., 2007, 4717. (c) V. Lillo, A. Bonet, E. Fernández, *Dalton Trans*., 2009, 2899. (d) L. Dang, Z. Lin, T. Marder, *Chem. Comm*., 2009, 3987.

12. S. Aldridge, R. J. Calder, R. E. Baghurst, M. E. Light, M. B. Hursthouse, *J. Organomet. Chem*., 2002, **649**, 9.

13. S. Aldridge, R. C. Calder, A. Rossin, A. A. Dickinson, D. J. Willock, C. Jones, D. J. Evans, J. W. Steed, M. E. Light, S. J. Coles, M. B. Hursthouse, *J. Chem. Soc., Dalton*. Trans., 2002, 2020.

14. A. Rossin, S. Aldridge, L-L. Ooi, *Appl. Organometal. Chem*., 2005, **19**, 181.

15. H. Braunschweig, K. Radacki, F. Seeler, G. R. Whittell, *Organometallics*, 2004, **23**, 4178.

16. H. Braunschweig, K. Radacki, F. Seeler, G. R. Whittel, *Organometallics*, 2006, **25**, 4605.

17. D. Vidovic, S. Aldridge, *Angew. Chem. Int. Ed*., 2009, **48**, 3669.

18. H. Braunschweig, C. Kollann, U. Englert, *Eur. J. Inorg. Chem*., 1998, 465.

19. H. Braunschweig, C. Kollann, K. W. Klinkhammer, *Eur. J. Inorg. Chem*., 1999, 1523.

20. D. L. Kays (née Coombs), J. K. Day, L-L. Ooi, S. Aldridge, *Angew. Chem. Int. Ed*., 2005, **44**, 7457.

21. D. L. Kays (née Coombs), A. Rossin, J. K. Day, L-L. Ooi, S. Aldridge, *Dalton Trans*., 2006, 399.

22. S. Aldridge, C. Jones, T. Gans-Eichler, A. Stasch, D. L. Kays (née Coombs), N. D. Coombs, D. J. Willock, *Angew. Chem. Int. Ed*., 2006, **45**, 6118.

23. G. A. Pierce, D. Vidovic, D. L. Kays, N. D. Coombs, A. L. Thompson, D. J. Willock, E. D. Jemmis, S. De, S. Aldridge, *Organometallics*, 2009, **28**, 2947.

24. H. Braunschweig, B. Ganter, M. Koster, T. Wagner, *Chem. Ber*., 1996, **129**, 1099.

25. H. Braunschweig, M. Koster, R. Wang, *Inorg. Chem*., 1999, **38**, 415.

26. H. Braunschweig, M. Koster, *J. Organomet. Chem*., 1999, **588**, 231.

27. H. Braunschweig, C. Kollann, M. Müller, *Eur. J. Inorg. Chem*., 1998, 291.

28. H. Braunschweig, K. Radacki, D. Rais, F. Seeler, *Organometallics*, 2004, **23**, 5545.

29. H. Braunschweig, M. Kraft, S. Schwarz, F. Seeler, S. Stellwag, *Inorg. Chem*., 2006, **45**, 5275.

30. D. L. Coombs, S. Aldridge, C. Jones, *Appl. Organometal. Chem*., 2003, **17**, 356.

31. D. L. Coombs, S. Aldridge, C. Jones, *J. Chem. Soc., Dalton Trans*., 2002, 3851.

32. S. Aldridge, D. L. Coombs, C. Jones, *Chem. Comm*., 2002, 856.

33. D. L. Coombs, S. Aldridge, S. J. Coles, M. B. Hursthouse, *Organometallics*, 2003, **22**, 4213.

34. D. L. Coombs, S. Aldridge, C. Jones, D. J. Willock, *J. Am. Chem. Soc*., 2003, **125**, 6356.

35. D. L. Coombs, S. Aldridge, A. Rossin, C. Jones, D. J. Willock, *Organometallics*, 2004, **23**, 2911.

36. D. Vidovic, M. Findlater, G. Reeske, A. H. Cowley, *Chem. Comm*., 2006, 3786.

37. H. Braunschweig, M. Colling, C. Kollann, U. Englert, *J. Chem. Soc., Dalton. Trans*., 2002, 2289.

38. S. Aldridge, A. Al-Fawaz, R. J. Calder, A. A. Dickinson, D. J. Willock, M. E. Light, M. B. Hursthouse, *Chem. Comm*., 2001, 1846.

39. A. Al-Fawaz, S. Aldridge, D. L. Coombs, A. A. Dickinson, D. J. Willock, L-L. Ooi, M. E. Light, S. J. Coles, M. B. Hursthouse, *Dalton. Trans*., 2004, 4030.

40. T Yasue, Y. Kawano, M. Shimoi, *Chem. Lett*., 2000, **1**, 58.

41. G. J. Irvine, W. R. Roper, L. J. Wright, *Organometallics*, 1997, **16**, 2291.

42. C. E. F. Rickard, W. R. Roper, A. Williamson, L. J. Wright, *Organometallics*, 1998, **17**, 4869.

43. C. E. F. Rickard, W. R. Roper, A. Williamson, L. J. Wright, *Organometallics*, 2000, **19**, 4344.

44. C. E. F. Rickard, W. R. Roper, A. Williamson, L. J. Wright, *Angew. Chem. Int. Ed*., 1999, **38**, 1110.

45. X. He, J. F. Hartwig, *Organometallics*, 1996, **15**, 400.

46. G. J. Irvine, C. E. F. Rickard, W. R. Roper, A. Williamson, L. J. Wright, *Angew. Chem. Int. Ed*., 2000, **39**, 948.

47. (a) P. L. Timms, *J. Am. Chem. Soc*., 1967, **89**, 1629. (b) P. L. Timms, *J. Am. Chem. Soc*., 1968, **90**, 4585.

48. B. Pachaly, R. West, *Angew. Chem. Int. Ed*., 1984, **23**, 454.

49. H. Braunschweig, T. Wagner, *Angew. Chem. Int. Ed*., 1995, **34**, 825.

50. A. H. Cowley, V. Lomeli, A. Voigt, *J. Am. Chem. Soc*., 1998, **120**, 6401.

51. H. Braunschweig, C. Kollann, U. Englert, *Angew. Chem. Int. Ed*., 1998, **37**, 3179.

52. H. Braunschweig, B. Ganter, *J. Organomet. Chem*., 1997, **545**, 163.

53. H. Braunschweig, C. Burschka, M. Burzler, S. Metz, K. Radacki, *Angew. Chem. Int. Ed*., 2006, **45**, 4352.

54. H. Braunschweig, M. Burzler, R. D. Dewhurst, K. Radacki, F. Seeler, *Z. Anorg. Allg. Chem*., 2008, **634**, 1875.

55. M. Shimoi, S. Ikubo, Y. Kawano, K. Katoh, H. Ogino., *J. Am. Chem. Soc*., 1998, **120**, 4222.

56. P. Bissinger, H. Braunschweig, F. Seeler, *Organometallics*, 2007, **26**, 4700.

57. H. Braunschweig, M. Colling, C. Kollann, H. G. Stammler, B. Neumann, *Angew. Chem. Int. Ed*., 2001, **40**, 2298.

58. H. Braunschweig, M. Forster, K. Radacki, F. Seeler, G. R. Whittell, *Angew. Chem. Int. Ed*., 2007, **46**, 5212.

59. H. Braunschweig, M. Forster, T. Kupfer, F. Seeler, *Angew. Chem. Int. Ed*., 2008, **47**, 5981.

60. H. Braunschweig, M. Forster, F. Seeler, *Chem. Eur. J*., 2009, **15**, 469.

61. H. Braunschweig, K. Radacki, D. Rais, F. Seeler, K. Uttinger, *J. Am. Chem. Soc*., 2005, **127**, 1386.

62. H. Braunschweig, K. Radacki, D. Rais, F. Seeler, *Angew. Chem. Int. Ed*., 2006, **45**, 1066.

63. B. Blank, M. Colling-Hendelkens, C. Kollann, K. Radacki, D. Rais, K. Uttinger, G. R. Whittell, H. Braunschweig, *Chem. Eur. J*., 2007, **13**, 4770.

64. H. Braunchweig, M. Colling, C. Kollann, K. Merz, K. Radacki, *Angew. Chem. Int. Ed*., 2001, **40**, 4198.

65. H. Braunschweig, K. Radacki, D. Scheschkewitz, G. R. Whittell, *Angew. Chem. Int. Ed*., 2005, **44**, 1658.

66. H. Braunschweig, M. Colling, C. Hu, K. Radacki, *Angew. Chem. Int. Ed*., 2003, **42**, 205.

67. H. Braunschweig, M. Burzler, T. Kupfer, K. Radacki, F. Seeler, *Angew. Chem. Int. Ed*., 2007, **46**, 7785.

68. S. K. Grumbine, T. D. Tilley, F. P. Arnold, A. L. Rheingold, *J. Am. Chem. Soc*., 1994, **116**, 5495.

69. H. Braunschweig, K. Radacki, K. Uttinger, *Angew. Chem. Int. Ed*., 2007, **46**, 3979.

70. N. R. Bunn, S. Aldridge, D. L. Kays, N. D. Coombs, A. Rossin, D. J. Willock, J. K. Day, C. Jones, L-L. Ooi, *Organometallics*, 2005, **24**, 5891.

71. H. Braunschweig, K. Kraft, T. Kupfer, K. Radacki, F. Seeler, *Angew. Chem. Int. Ed*., 2008, **47**, 4931.

72. H. Braunchweig, M. Burzler, R. D. Dewhurst, K. Radacki, *Angew. Chem. Int. Ed*., 2008, **47**, 5650.

73. H. Braunschweig, K. Radacki, D. Rais, D. Scheschkewitz, *Angew. Chem. Int. Ed*., 2005, **44**, 5651.

74. G. P. Mitchell, T. D. Tilley, *Angew. Chem. Int. Ed*., 1998, **37**, 2524.

75. C. E. F. Rickard, W. R. Roper, A. Williamson, L. J. Wright, *Organometallics*, 2002, **21**, 4862.

76. H. Braunschweig, K. Radacki, D. Rais, K. Uttinger, *Organometallics*, 2006, **25**, 5159.

77. H. Braunschweig, K. Radacki, K. Uttinger, *Eur. J. Inorg. Chem*., 2007, 4350.

78. D. L. Kays (née Coombs), J. K. Day, S. Aldridge, R. W. Harrington, W. Clegg, *Angew. Chem. Int. Ed*., 2006, **45**, 3513.

79. H. Braunschweig, K. Radacki, D. Rais, A. Schneider, F. Seeler, *J. Am. Chem. Soc*., 2007, **129**, 10350.

80. G. Alcaraz, U. Helmstedt, E. Clot, L. Vendier, S. Sabo-Etienne, *J. Am Chem. Soc*., 2008, **130**, 12878.

81. H. Braunschweig, R. D. Dewhurst, *Angew. Chem. Int. Ed*., 2009, **48**, 1893.

82. J. Emsley, *The Elements*; Oxford University Press: Oxford, 1991.

83. H. Braunschweig, M. Forster, K. Radacki, *Angew. Chem. Int. Ed*., 2006, **45**, 2132.

84. H. Braunschweig, R. Herbst, D. Rais, F. Seeler, *Angew. Chem. Int. Ed*., 2005, **44**, 7461.

85. H. Braunschweig, I. Fernández, G. Frenking, K. Radacki, F. Seeler, *Angew. Chem. Int. Ed*., 2007, **46**, 5215.

86. L. Apostolico, H. Braunschweig, A. G. Crawford, T. Herbst, D. Rais, *Chem. Comm*., 2008, 497.

87. H. Braunschweig, R. D. Dewhurst, T. Herbst, K. Radacki, *Angew. Chem. Int. Ed*., 2008, **47**, 5978.

88. H. Braunschweig, M. Burzler, K. Radacki. F. Seeler, *Angew. Chem. Int. Ed*., 2007, **46**, 8071.

Chapter Two

Experimental Techniques

2.1 The Manipulation of Air-Sensitive Compounds

Due to the sensitivity of many of the species investigated towards moisture and/or oxygen, it was essential that their synthesis and manipulation was carried out in an inert environment. The use of both Schlenk and high vacuum line techniques ensured the exclusion of both air and moisture, and a brief discussion of both these techniques is detailed herein.

2.1.1 Inert Atmosphere Techniques

In order to manipulate air sensitive compounds with the exclusion of air, an inert gas such as nitrogen or preferably argon is used. There are two main methods used for the manipulation of air sensitive compounds (i) Schlenk line, a dual manifold system which enables the handling of air-sensitive compounds on the bench top / inside a fume cupboard and (ii) glove box, used for the manipulation, transfer and storage of solids / liquids under an inert atmosphere.[1]

The Schlenk line (Figure 2.1)[2] consists of a dual manifold made of Pyrex glass with several ports. One manifold is connected to an inert gas supply (nitrogen or argon) and the other is connected to a high-vacuum pump with the use of two-way stopcocks providing a means of switching between inert gas and vacuum. To prevent leaks in the system, the stopcocks were lubricated with ‘Dow-Corning High Vacuum’ grease. Glassware was attached to the line using a number of thick-walled tubes, so that several pieces of apparatus could be used simultaneously.

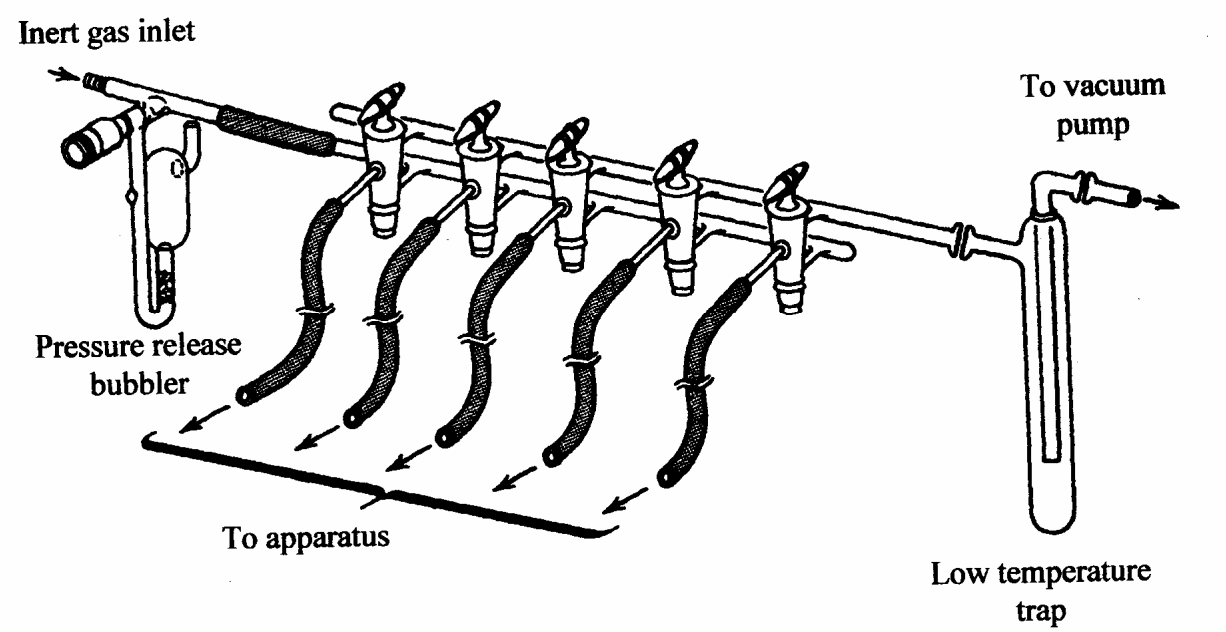


Figure 2.1 A Schlenk line.

Evacuation was achieved using a vacuum pump in conjunction with a liquid nitrogen cooled trap to prevent volatile materials from entering the pump. A pressure of 10^{-1} to 10^{-3} Torr was normally achieved and monitored using a Pirani pressure gauge attached to the vacuum line. The inert gas (usually argon) was fed directly to the apparatus from a cylinder, and a mercury bubbler attached to prevent excessive pressure. Exclusion of oxygen and moisture was achieved by using the 'pump and purge' method whereby the apparatus was evacuated and then purged with inert gas; this method is repeated several times to guarantee an inert atmosphere. Transfer of liquids and solutions between apparatus was achieved using double-ended stainless steel needles (cannulae) or syringes and rubber septa.

The glove box was used to manipulate and store air-sensitive solids in an inert atmosphere. The box consists of a sealed stainless steel container, which can be accessed through a pair of neoprene gloves. Apparatus was loaded into the box via the side port using the 'pump and purge' method. An inert atmosphere was provided by a nitrogen cylinder, which

is recirculated internally through catalyst, molecular sieve and solvent scrubbing columns achieving an atmosphere with oxygen and moisture levels of less than 5 ppm and 10 ppm respectively.[3]

2.1.2 High Vacuum Techniques

The high vacuum line was used for procedures such as vacuum sublimation and removal of trace solvent when the use of mechanical pump on a Schlenk line did not provide an adequate vacuum. The high vacuum apparatus is made of Pyrex glass and incorporates J. Young's stopcocks. Pressures of 10^{-4} mm Hg were achieved by using a combination of mercury diffusion and mechanical pumps, and the pressure was monitored by the use of a Tesla coil which produces a discharge at pressures between 1 and 10^{-3} Torr. As with the Schlenk line, a low temperature cooled trap was also used to prevent contamination of the pump.

2.2 Physical Measurements

2.2.1 NMR Spectroscopy

NMR spectra were measured on the following spectrometers: Bruker AM-400, Jeol 300 Eclipse Plus, Varian 'Mercury' 300, Varity Unity +500 FT-NMR or a Bruker AVII500 with cryoprobe. Deuterated solvents were used for ^{1}H and ^{13}C NMR measurements. ^{11}B, ^{19}F and ^{31}P NMR spectra were referenced against $Et_2O{\cdot}BF_3$, $CFCl_3$ and 85% aqueous H_3PO_4 respectively. Sample preparation typically involved generating an inert atmosphere within a Young's NMR tube using the 'pump and purge' method followed by solution transfer *via* cannula.

2.2.2 Infrared Spectroscopy

Infrared spectra were measured by pressing each compound into a disk with a ten-fold excess of KBr, or as a solution contained within a solution infrared cell. KBr disks of air-sensitive materials were prepared in the glove box, and KBr was dried by heating under high vacuum. Spectra were recorded on a Perkin-Elmer 1600 series FTIR spectrometer or a Nicolet 500 FT-IR spectrometer.

2.2.3 Mass Spectrometry

Mass spectra for neutral complexes were measured by the EPSRC National Mass Spectrometry Service Centre, Swansea University. Spectra of cationic complexes were measured on a Bruker MicroTOF-Q instrument directly linked to a Braun LabMaster glove box at the University of Bath.[4] Perfluorobutylamine (EI) and polyethylenimine (ES) were used as standards for high resolution spectra.

2.2.4 Elemental Analysis

Elemental Analyses were performed by Dr. Stephen Boyer of the London Metropolitan University, and by MEDAC Analytical Services.

2.2.5 X-Ray Crystallography

Data collection was carried out on a Bruker-Nonius APEX II CCD camera diffractometer by Dr. Amber Thompson, Dr. Dave Watkin, Dr Drasko Vidovic and Dr. Delphine LePevelen of the Department of Chemistry, University of Oxford. Prof. Cameron Jones, Dr. Andreas Stasch, Dr. Li-Ling Ooi and Dr. Joanna Day carried out the data collection

at Cardiff University on a similar instrument. The Enraf Nonius Kappa CCD diffractometer was also used by the EPSRC National X-Ray Crystallography Service, at the University of Southampton.

2.2.6 Theoretical Calculations

Theoretical calculations were carried out by Dr. Natalie Coombs and Dr. David J. Willock (Cardiff University) and Miss Susmita De and Prof. Eluvathingal D. Jemmis at the Indian Institute of Science, Bangalore. Calculations carried out in Cardiff University used 'Glyndwr', a Silicon Graphics multiprocessor Origin 2000 machine. A detailed description of the computational methodologies used can be found in the appendix.

2.3 Photolytic Experiments

Photolytic experiments were carried out using a Spectral Energy mercury arc lamp (1 kW) with samples contained within quartz schlenk vessels.

2.4 Purification and Preparation of Essential Solvents and Reagents

Many of the compounds formed had precursors which were readily available and could be used as supplied, a list of sources and procedures for purification is supplied in Table 2.1. Other starting materials however were not commercially available and the syntheses of these compounds are given in this section.

Table 2.1 Sources of chemicals.

Compound	Source	Purity	Procedure
Boron trichloride (1.0M in heptane)	Sigma-Aldrich	*a*	Used as supplied
Dicarbonylcyclopentadienyliron dimer	Sigma-Aldrich	99%	Used as supplied
Dicarbonyl(methylcyclopentadienyl)-iron dimer	*b*	*a*	Used as supplied
Trimethylamine-N-oxide	Sigma-Aldrich	98%	Azeotroped and vacuum sublimed
N,N'-dicyclohexylcarbodiimide	Acros organics	99%	Dried under vacuum
N'N'-diisopropylcarbodiimide	Acros organics	99%	Used as supplied
Sodium tetrafluoroborate	Sigma-Aldrich	98%	Used as supplied
1-Bromo-3,5 bis(trifluoromethyl)benzene	Alfa Aesar	98%	Used as supplied
^{t}BuLi (1.7M in pentane)	Sigma-Aldrich	*a*	Used as supplied
^{n}BuLi (1.6 M in hexane)	Sigma-Aldrich	*a*	Used as supplied
Phenyl isocyanate	Sigma-Aldrich	≥ 98%	Dried over molecular sieves
Cyclohexylisocyanate	Sigma-Aldrich	98%	Dried over molecular sieves
2,6-dimethylphenylisocyanate	Sigma-Aldrich	99%	Dried over molecular sieves
Dicyclohexylamine	Sigma-Aldrich	99%	Dried over molecular sieves
Dibenzylamine	Sigma-Aldrich	97%	Dried over molecular sieves
Diisopropylamine	Sigma-Aldrich	≥ 99.5%	Dried over molecular sieves
Diphenylamine	Sigma-Aldrich	99%	Used as supplied
Triethylamine	Sigma-Aldrich	≥ 99.5%	Dried over potassium mirror
Carbazole	*b*	*a*	Used as supplied
Tris(dimethylamido)borane	Sigma-Aldrich	99%	Degassed
1, 2-dibromoethane	Sigma-Aldrich	99%	Used as supplied
Iodine	Sigma-Aldrich	99.999%	Used as supplied
Ethylenebis(dimethylphosphine)	Sigma-Aldrich	97%	Degassed
Compound	**Source**	**Purity**	**Procedure**
Triphenylphosphine	*c*	*a*	Used as supplied
Trimethyl phosphine	Sigma-Aldrich	97%	Degassed and stored over molecular sieves
Trimethyl phosphite	Sigma-Aldrich	≥99%	Degassed and stored over molecular sieves
Sodium sticks, in mineral oil	Alfa Aesar	99%	Used as supplied
Potassium chunks, in mineral oil	Sigma-Aldrich	99%	Used as supplied
Sodium carbonate anhydrous	Fisher	*a*	Used as supplied
Decolourising charcoal	*d*	*a*	Used as supplied
Mercury	*e*	*a*	Used as supplied
Aluminium trichloride	Sigma-Aldrich	99.9%	Used as supplied
Sodium sulfate	Fisher	*a*	Used as supplied

Solvents			
Toluene	Rathburn Chemicals Ltd	HPLC	Refluxed over sodium followed by distillation/Dried using Braun SPS system, stored over molecular sieves
Hexanes	Rathburn Chemical Ltd	HPLC	Refluxed over potassium followed by distillation/Dried using Braun SPS system, stored over molecular sieves
Dichloromethane	Fisher Scientific	>99%	Refluxed over CaH_2 followed by distillation/Dried using Braun SPS system, stored over molecular sieves
Diethylether	Rathburn Chemical Ltd	HPLC	Refluxed over sodium followed by distillation/Dried using Braun SPS system, stored over molecular sieves
THF	Rathburn Chemical Ltd	HPLC	Refluxed over sodium followed by distillation/Dried using Braun SPS system, stored over molecular sieves
Benzene	Rathburn Chemical Ltd	HPLC	Dried using Braun SPS system, stored over molecular sieves
Compound	**Source**	**Purity**	**Procedure**
Pentane	Rathburn Chemical Ltd	HPLC	Dried using Braun SPS system, stored over molecular sieves
Fluorobenzene	Sigma-Aldrich	99%	Refluxed over CaH_2 followed by distillation, stored over molecular sieves
Deuterated solvents			
Benzene-d_6	Goss	99.6 atom%	Degassed and stored over a potassium mirror
Methylene chloride-d_2	Goss	99.8 atom%	Degassed and stored over flamed-out molecular sieves
Toluene-d_8			Degassed and stored over a potassium mirror
Gases			
Argon	BOC	*a*	Used as supplied
Nitrogen	BOC	*a*	Used as supplied
$^{13}CO_2$	Fluka	99%	Used as supplied

[a]Information not available. Courtesy of [b]Dr N. D. Coombs, [c]Dr D. L. Kays, [d]Prof C. Jones, Cardiff University, and Mr C. Botham, [e]University of Oxford respectively.

Two different methods were employed in order to dry the solvents and ensure they were free of moisture and air. Distillation was used in Cardiff University whereas the Braun SPS system was used in the University of Oxford.

2.4.1 Preparation of Precursors

2.4.1.1 Preparation of Transition Metal Anions

Preparation of Na[CpFe(CO)$_2$]

[CpFe(CO)$_2$]$_2$ (10.377 g, 29.3 mmol) in THF (120 cm^3) was added via cannula to a sodium amalgam (2 g of sodium in 40 cm^3 Hg) and allowed to stir for 24 h. Filtration and removal of volatiles by reduced pressure yielded Na[CpFe(CO)$_2$]. The yellow solid was washed with hot toluene (3 x 50 cm^3) and boiling hexane (1 x 50 cm^3) and dried under high vacuum.[5]

Preparation of Na[Cp'Fe(CO)$_2$]

In an analogous method employed for Na[CpFe(CO)$_2$], [Cp'Fe(CO)$_2$]$_2$ was dissolved in THF and reacted with sodium amalgam at room temperature for 48 h. After filtration and removal of the solvent in *vacuo*, the solid was washed with hot toluene and boiling hexane.[6]

2.4.1.2 Preparation of Na[B{3,5-(CF$_3$)$_2$C$_6$H$_3$}$_4$]

Na[B{3,5-(CF$_3$)$_2$C$_6$H$_3$}$_4$] was synthesized according to the procedure by Reger *et al.*[7] A three-necked flask fitted with a reflux condenser and a dropping funnel was charged with Mg (1.0 g, 41.7 mmol), NaBF$_4$ (0.7 g, 6.4 mmol) and diethyl ether (150 cm^3). Dibromoethane (0.5 cm^3, 5.7 mmol) was added and the flask was heated for a few minutes to initiate the Grignard reaction. A solution of 3,5-bis(trifluoromethyl)bromobenzene (5.9 cm^3, 34.2 mmol) in diethyl

ether (50 cm^3) was added over a period of 30 min. The reaction was subsequently refluxed for 30 min and then stirred at room temperature overnight. The reaction mixture was added to Na_2CO_3 (16 g, 151 mmol) in water and stirred for 30 min. The solution was then filtered, the organic layer separated and the aqueous layer washed with copious amounts of diethyl ether. The combined diethyl ether layers were dried over sodium sulfate and treated with decolourising charcoal. Filtration and removal of volatiles under reduced pressure yielded an oily solid that was dissolved in benzene (200 cm^3) and azeotroped to remove traces of water. The solution was concentrated to *ca*. 40 cm^3 and then filtered from the solid product. The solid was washed with hexanes and dried under high vacuum for 12 h to yield the product in a 49 % yield. The purity of the product was verified by ^1H, ^{11}B and ^{19}F NMR spectroscopy and compared to data reported in the literature.[7]

2.4.1.3 Preparation of $[CpFe(CO)_2(BNR_2)]^+[BAr^f_4]^-$ (R = ^{i}Pr / Cy / Me)

Preparation of $^iPr_2NBCl_2$

$^iPr_2NBCl_2$ was prepared by minor modification of the synthesis published by Gerrard *et al.*[8] $^iPr_2NH$ (3 cm^3, 21 mmol) in dichloromethane (20 cm^3) was added to a solution of BCl_3 (1.1 equiv., 1.0 M in heptane) at –80˚C over 15 min. The mixture was stirred for 1 h at –80˚C and then the volatiles were removed in *vacuo*. The resulting white solid was dissolved in benzene (40 cm^3) and Et_3N (11.3 cm^3, 81 mmol) added. The reaction mixture was stirred for 24 h and judged to be complete by ^{11}B NMR spectroscopy. Filtration and vacuum transfer at 0˚C afforded the product as an oil in 55% yield, which was dissolved in diethyl ether to form a stock solution. The purity of $^iPr_2NBCl_2$ was confirmed by both ^1H and ^{11}B NMR spectroscopy, by comparison with the literature.[8]

Preparation of Cy_2NBCl_2

Cy_2NBCl_2 was prepared in an analogous reaction employed for $^{i}Pr_2NBCl_2$. Cy_2NH (8cm^3, 40 mmol) in dichloromethane (20 cm^3) was added to a solution of BCl_3 (1.1 eq, 1.0 M in heptane) at –80˚C over 15 min. The mixture was stirred for 1 h at –80˚C and the solvent was removed under reduced pressure. The residue was then dissolved in benzene (40 cm^3) and Et_3N (5 cm^3, 36 mmol) added; the reaction was then stirred for 24 h. Filtration, extraction into hexanes and removal of solvent under *vacuo* afforded Cy_2NBCl_2 as a white solid in a 54% yield (as confirmed by ^{1}H and ^{11}B NMR spectroscopy).[8]

Preparation of Me_2NBCl_2

Me_2NBCl_2 was synthesized by minor modification of the method reported by Banister *et al*.[9] A solution of tris(dimethylamino)borane (3.6 cm^3, 20.6 mmol) in toluene was reacted with BCl_3 (2 eq) and allowed to stir for 24 h. The reaction was judged to be complete by ^{11}B NMR spectroscopy and stored as a toluene stock solution (1.03 M) at –30˚C.[9]

Preparation of $[CpFe(CO)_2B(N^{i}Pr_2)Cl]$

$[CpFe(CO)_2B(N^{i}Pr_2)Cl]$ was prepared by the method reported by Aldridge *et al*.[10] Reaction of $^{i}Pr_2NBCl_2$ (23.7 cm^3, 5.50 mmol) and $Na[CpFe(CO)_2]$ (1.1 eq) in toluene for 24 h, followed by extraction into hexanes, filtration, concentration and storage at –30˚C yielded an oily brown solid in a 49% yield. Both ^{1}H and ^{11}B NMR spectroscopy were in agreement with those reported in the literature.[10]

Preparation of [CpFe(CO)$_2$B(NCy$_2$)Cl]

[CpFe(CO)$_2$B(NCy$_2$)Cl] was prepared by minor modification of the synthesis published by Aldridge *et al.*[11] A mixture of Cy$_2$NBCl$_2$ (1.00 g, 4.03 mmol) and Na[CpFe(CO)$_2$] (1.1 eq) in diethyl ether (40 cm^3) was stirred for 12 h. Extraction into pentane (50 cm^3), filtration, concentration and storage at –30˚C yielded the product as a brown solid in a 52% yield, as determined by comparison of ^{1}H and ^{11}B NMR spectroscopy with those reported in the literature.[11]

Preparation of [CpFe(CO)$_2$B(NMe$_2$)Cl]

Prepared in a similar method to the synthesis reported by Braunschweig *et al.*[12] A mixture of Me$_2$NBCl$_2$ (1.00 g, 7.95 mmol) and Na[CpFe(CO)$_2$] (1.1 eq) in diethyl ether (40 cm^3) was stirred for 12 h. Extraction into pentane (50 cm^3), filtration, concentration and storage at –30˚C yielded the product as a brown solid in a 39% yield. The purity of the compound was assessed by ^{1}H and ^{11}B NMR, which was compared to data reported in the literature.[12]

Preparation of [CpFe(CO)$_2$(BNR$_2$)]$^+$[BAr$^f_4$]$^-$ (R = ^{i}Pr, Cy, Me)

The formation of [CpFe(CO)$_2$(BNR$_2$)]$^+$[BAr$^f_4$]$^-$ was formed by minor modification of the procedure published by Aldridge *et al.*[10,11,13] and was always carried out in situ. A mixture of [CpFe(CO)$_2$B(NR$_2$)Cl] and Na[BAr$^f_4$] (1.1 eq) in dichloromethane was sonicated for 20 min. and judged to be complete by ^{11}B NMR spectroscopy. Filtration yielded the cationic borylene, which was subsequently used for further chemistry.

2.5 References for Chapter Two

1. R. J. Errington, *Advanced Practical Inorganic and Metalorganic Chemistry*, Blackie Academic & Professional, an imprint of Chapman & Hall, 1997.
2. D. F. Shriver, M. A. Drezdzon, *The Manipulation of Air-Sensitive Compounds*, 2nd edn., Wiley-Interscience, New York, 1986.
3. Saffron Scientific Equipment Ltd., glove box operation manual.
4. A. T. Lubben, J. S. McIndoe, A. S. Weller, *Organometallics*, 2008, **27**, 3303.
5. R. B, King, K. H. Pannell, *Inorg. Chem*., 1968, **7**, 1510.
6. W. Clegg, N. A. Compton, R. J. Errington, N. C. Norman, *J. Chem. Soc.*, *Dalton Trans*., 1988, 1671.
7. D. L. Reger, T. D. Wright, C. A. Little, J. J. S. Lamba, M. D. Smith, *Inorg. Chem*., 2001, **40**, 3810.
8. W. Gerrard, H. R. Hudson, E. F. Mooney, *J. Chem. Soc.*, 1960, 5168.
9. A. J. Banister, N. N. Greenwood, B. P. Straughan, J. Walker, *J. Chem. Soc*., 1964, 995.
10. D. L. Kays (née Coombs), J. K. Day, L-L. Ooi, S. Aldridge, *Angew. Chem. Int. Ed*., 2005, **44**, 7457.
11. S. Aldridge, C. Jones, T. Gans-Eichler, A. Stasch, D. L. Kays (née Coombs), N. D. Coombs, D. J. Willock, *Angew. Chem. Int. Ed*., 2006, **45**, 6118.
12. H. Braunschweig, C. Kollann, U. Englert, *Eur. J. Inorg. Chem*., 1998, 465.
13. D. L. Coombs, S. Aldridge, A. Rossin, C. Jones, D. J. Willock, *Organometallics*, 2004, **23**, 2911.

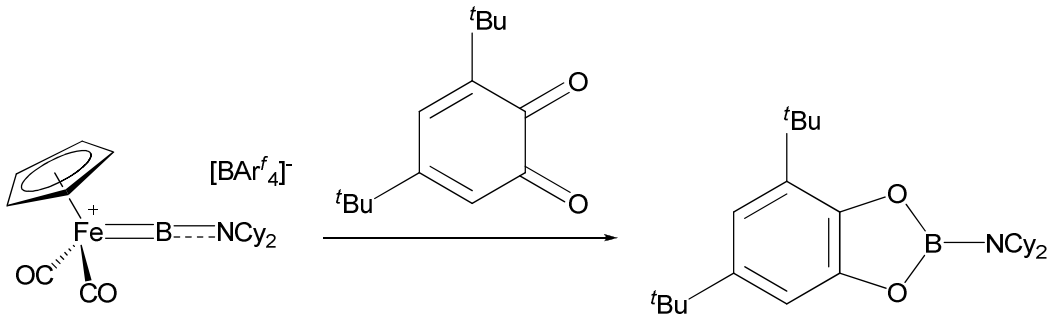
Chapter Three

Insertion Reactions of Carbodiimide with Two-Coordinate Aminoborylene Complexes

3.1 Introduction

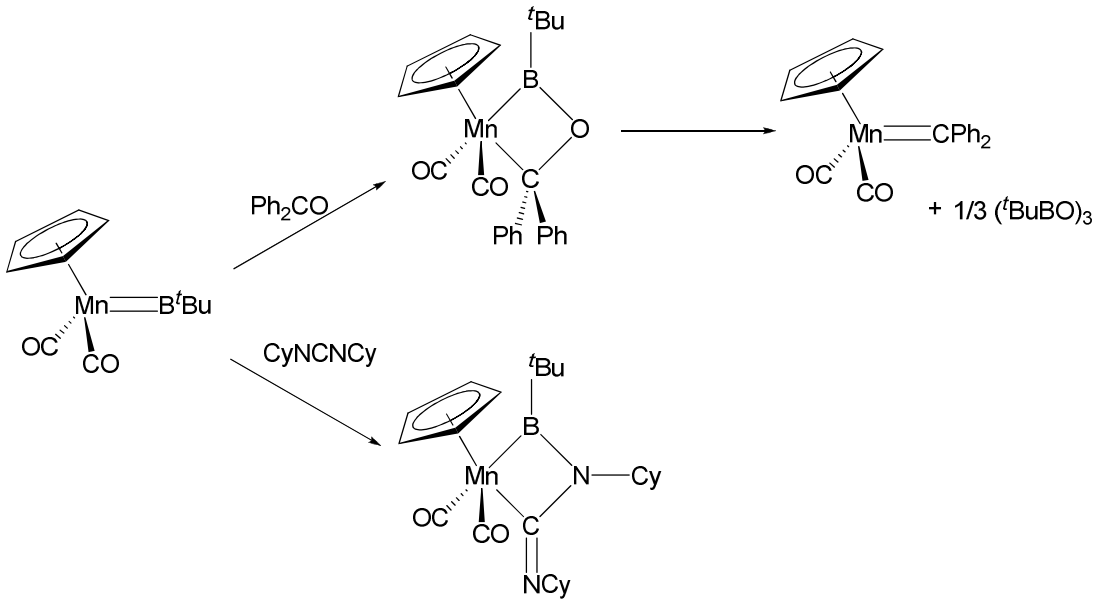
The reactivity of terminal borylene complexes[1] is a relatively new area of study compared to related, multiply bonded systems such as carbenes and silylenes which have been thoroughly investigated and exploited, for example in alkene metathesis.[2] Furthermore, the reactivity of *cationic* terminal borylene complexes is even less well understood. Thus far, patterns of reactivity have been shown to vary depending on the nature of the boron bound substituent; the poorly π-donor stabilized mesitylborylene complex, $[Cp^*Fe(CO)_2(BMes)]^+[BAr^f_4]^-$ for instance, is characterized by overwhelming electrophilicity, and thus reactions proceed by either addition at boron or displacement of the mesitylborylene fragment.[3] The chemistries of the BN vinylidene analogues, $[CpFe(CO)_2(BNR_2)]^+[BAr^f_4]^-$ however, while still reflecting the presence of a Lewis acidic boron centre, show a more varied reactivity including cycloaddition[4], metathesis[5] and reduction processes[6] which are more characteristic of M=E multiple bonds. A feature that seems common to the reactivity of cationic aminoborylene complexes with polar substrates is initial coordination of the substrate at the electrophilic boron centre.[4-6]

Both Aldridge[4] and Braunchweig[7] have reported reaction of borylene complexes via cycloaddition reactions. The reaction of $[CpFe(CO)_2(BNCy_2)]^+[BAr^f_4]^-$ with 3,5-di-*tert*-butyl-ortho-benzoquinone yields the corresponding catechol derivative via a net [4+1] cycloaddition reaction (Scheme 3.1).[4]



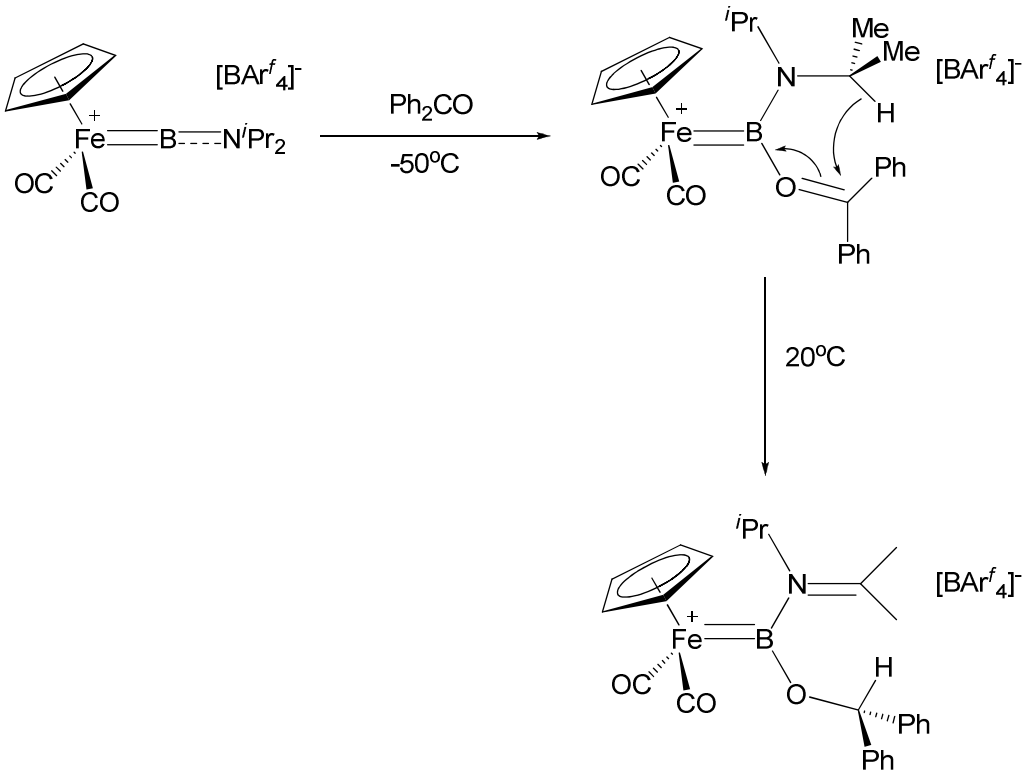
Scheme 3.1 Reaction of $[CpFe(CO)_2(BNCy_2)]^+[BAr^f_4]^-$ via [4+1] cycloaddition.

Reaction of the neutral alkylborylene, $CpMn(CO)_2B^tBu$ with benzophenone and dicyclohexylcarbodiimide forms the four-membered cyclic products, $Cp(CO)_2Mn\{B(^tBu)OC(Ph_2)\}$ and $Cp(CO)_2Mn\{B(^tBu)N(Cy)C(NCy)\}$ respectively, via a [2+2] cycloaddition reaction (Scheme 3.2).[7] In solution however, the benzophenone derived metallacycle undergoes cycloreversion to form the manganese carbene, $[CpMn(CO)CPh_2]$ and tri-*tert*-butylboroxine.



Scheme 3.2 Reaction of $[CpMn(CO)_2(B^tBu)]$ via cycloaddition.

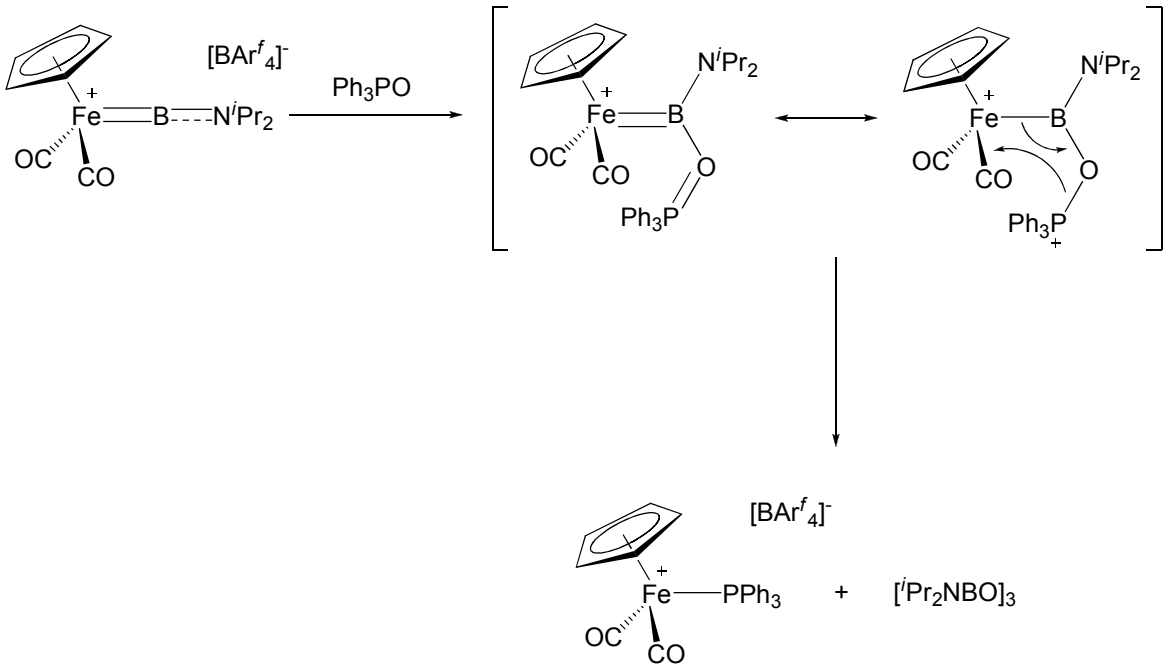
Conversely, reaction of the aminoborylene, $[CpFe(CO)_2(BN^iPr_2)]^+[BAr^f_4]^-$ with benzophenone proceeds by initial coordination of the organic substrate at the boron centre. The final product is an imine stabilized alkoxyborylene complex formed by an unprecedented intramolecular Meerwein-Ponndorf hydride transfer pathway (Scheme 3.3).[6] Interestingly, reaction of the electrophilic borylene, $[Cp^*Fe(CO)_2(BMes)]^+[BAr^f_4]^-$ with benzophenone[3b] results in displacement of the borylene moiety and formation of $[Cp^*Fe(CO)_2(\eta^1\text{-}O{=}CPh_2)][BAr^f_4]^-$.



Scheme 3.3 Meerwein-Ponndorf β-hydride transfer.

By comparison, the same aminoborylene complex, $[CpFe(CO)_2(BN^iPr_2)]^+[BAr^f_4]^-$ was reacted with Ph_3EX (E = P, X = S; E = As, X = O) generating $[CpFe(CO)_2(EPh_3)]^+[BAr^f_4]^-$ and $[^iPr_2NB(\mu\text{-}X)]_n$ (X = S, *n* = 2; X = O, *n* = 3) by the first reported example of M=B

metathesis chemistry (Scheme 3.4).[5] Reaction with Ph_3PO decreases the rate of reaction and allows access to the intermediate, $[CpFe(CO)_2\{BN^iPr_2(OPPh_3)]^+[BAr^f_4]^-$ which was structurally characterized. Thus the intermediate in this reaction pathway is shown to be a cyclic donor/acceptor species, rather than a metallacycle, found for M=C/C=C metathesis.[2b,c]



Scheme 3.4 Reaction of $[CpFe(CO)_2(BN^iPr)]^+[BAr^f_4]^-$ via a net metathesis process.

Computational studies carried out by Jemmis *et al*.[8] analysed the two different reaction pathways (i.e. metathesis and hydride transfer) and observed that substrates, E=X that are polar and have low-lying σ* molecular orbitals are more likely to react via the metathesis route. The calculations also revealed that substrates having low-energy π* molecular orbitals can react via either metathesis or β-hydride reaction, depending on the stability of the respective products, which is determined by the strength of both the Fe-E and B-X bonds.

3.1.1 Aims of the Present Research

With a view to further investigate the reactivity of cationic terminal borylene complexes, $[CpFe(CO)_2(BNR_2)]^+[BAr^f_4]^-$ (R = ^{i}Pr, Cy) was reacted with a family of unsaturated hetero-allene substrates: CO_2, isocyanates, RNCO (R = Ph, Cy, 2,6-Xyl) and carbodiimides, RNCNR (R = Cy, ^{i}Pr). Modifying the sterics and electronic structure by sequentially replacing the O groups for NR was expected to lead to systematic variation in the pattern of reactivity.

3.2 Experimental

Attempted reaction of $[CpFe(CO)_2(BNCy_2)]^+[BAr^f_4]^-$ with CO_2

To a solution of $[CpFe(CO)_2(BNCy_2)]^+[BAr^f_4]^-$ (0.15 g, 0.12 mmol) in dichloromethane/fluorobenzene in an NMR tube, was introduced $^{13}CO_2$ at -80˚C. After gradual warming to room temperature the reaction mixture was monitored by ^{11}B and ^{13}C NMR. No reaction was observed at room temperature, however, heating the reaction to 55˚C and/or photolysing for several days resulted in a peak at δ_B = -7 ppm. A control reaction without CO_2 however, also resulted in formation of a peak at -7 ppm indicating decomposition of the borylene complex by reaction with the solvent or the anion.

Synthesis of $[CpFe(CO)_2(CNPh)]^+[BAr^f_4]^-$ (**3.1**)

A mixture of $[CpFe(CO)_2(BNCy_2)]^+[BAr^f_4]^-$ (0.305 g, 0.25 mmol) and PhNCO (5 equiv.) in dichloromethane was stirred for 48 h at room temperature after which time the reaction was judged to be complete by ^{11}B NMR spectroscopy. Removal of volatiles under reduced pressure, extraction of the residue into fluorobenzene, layering with hexanes and storage at

–30˚C led to the formation of crystals of **3.1** suitable for X-ray diffraction. Yield: 0.116 g, 41%. ^{1}H NMR (300 MHz, CD_2Cl_2) δ 5.49 (s, 5H, Cp), 7.10-7.52 (overlapping m, 5H, Ph), 7.54 (s, 4H, *para*-H of $BAr^{f}_{4}^{-}$), 7.73 (s, 8H, *ortho*-H of $BAr^{f}_{4}^{-}$). ^{13}C NMR (75 MHz, CD_2Cl_2) δ 87.7 (Cp), 117.9 (*para*-C of $BAr^{f}_{4}^{-}$), 125.0 (q, $^{1}J_{CF}$ = 273 Hz, CF_3 of $BAr^{f}_{4}^{-}$), 125.6 (*ortho*-CH of Ph), 126.9 (*para*-CH of Ph), 129.3 (q, $^{2}J_{CF}$ = 38 Hz, *meta*-C of $BAr^{f}_{4}^{-}$), 130.5 (*meta*-CH of $BAr^{f}_{4}^{-}$) 132.2 (*ortho*-C of $BAr^{f}_{4}^{-}$), 135.3 (*ipso*-C of $BAr^{f}_{4}^{-}$), 162.2 (q, $^{1}J_{CB}$ = 55 Hz, *ipso*-C of $BAr^{f}_{4}^{-}$), 205.6 (CO). ^{11}B NMR (96 MHz, CD_2Cl_2) δ -9 ($BAr^{f}_{4}^{-}$). ^{19}F NMR (283 MHz, CD_2Cl_2) δ -62.7 (CF_3). IR (CD_2Cl_2 soln, cm^{-1}) υ 2197 (CN), 2087, 2052 (CO) MS (positive ion electrospray) m/z (%) 280.0 (80) M^+, 252.0 (47.4) $(M\text{-}CO)^+$, 224.0 (100) $(M\text{-}2CO)^+$; exact mass (calc. for M^+) m/z 280.0055, (obs.) 280.0023. Crystallographic data: $C_{46}H_{22}BF_{24}FeNO_2 \cdot 0.5(C_6H_5F)$, M_r 1191.36, orthorhombic, space group Pbca, a = 17.9155(2), b = 16.2092(3), c = 33.7381(5) Å, V= 9797.4(3) $Å^3$, Z = 8, ρ_{calcd} = 1.615 Mg m^{-3}, T = 150(2) K, λ = 0.71073 Å. 57876 reflections collected, 11086 independent [R(int) = 0.0786], which were used in all calculations. R_1 = 0.0657, wR_2 = 0.1599 for observed unique reflections [$F^2 > 2\sigma(F^2)$] and R_1 = 0.1229, wR_2 = 0.1883 for all unique reflections. Max./min. residual electron densities 1.001/-1.233 e $Å^{-3}$.

Synthesis of $[CpFe(CO)_2C(NCy)_2BNR_2]^+[BAr^{f}_{4}]^-$ (R = ^{i}Pr, Cy) (**3.5**)

(i) Variable temperature NMR studies. To a solution of $[CpFe(CO)_2(BN^{i}Pr_2)]^+[BAr^{f}_{4}]^-$ (0.104 g, 0.09 mmol) in CD_2Cl_2 (1.5 cm^3) at -80°C was added a solution of dicyclohexylcarbodiimide (2 equiv.) in CD_2Cl_2 (1.0 cm^3). Warming to -50°C led to complete conversion to a single species, giving rise to a broad ^{11}B NMR resonance at 71 ppm (fwhm ca.

900 Hz). Further warming to -30 and 20°C led to sequential formation of a second intermediate (δ_B 25 ppm, fwhm 430 Hz) and the final product (δ_B 3 ppm, fwhm 12 Hz).

(ii) Isolation of the intermediate $[CpFe(CO)_2C(NCy)_2BNCy_2]^+[BAr^f_4]^-$. By carrying out the reaction in a carefully controlled fashion, i.e. by titrating a stock solution of dicyclohexylcarbodiimide into that of the borylene (with ^{11}B NMR monitoring), it proved possible to isolate single crystals of the second intermediate species **3.5** i.e. that giving rise to the ^{11}B NMR signal at δ_B 25 ppm. Crystals suitable for X-ray diffraction were obtained by filtration of the reaction mixture, concentration (to ca. 5cm^3), layering with hexanes and storage at -30°C. Isolated yield: 24 % (ca. 0.01g scale). ^1H NMR (400 MHz, CD_2Cl_2) d 1.02-1.77 (m, 40H, CH_2 of Cy), 3.26 (m, 2H, CH of Cy), 3.42 (m, 2H, CH of Cy), 4.99 (s, 5H, Cp), 7.46 (s, 4H, *para*-H of $BAr^f_4^-$), 7.63 (s, 8H, *ortho*-H of $BAr^f_4^-$). ^{13}C NMR (76MHz, CD_2Cl_2), d 25.1, 25.2 (4-CH_2 of Cy), 25.9, 27.1 (3-CH_2 of Cy), 33.1, 35.4 (2-CH_2 of Cy), 58.1, 58.7 (CH of Cy), 86.3 (Cp), 117.5 (*para*-CH of $BAr^f_4^-$), 124.7 (q,$^1J_{CF}$ = 274 Hz, CF_3 of $BAr^f_4^-$), 129.0 ($^2J_{CF}$ = 32 Hz, *meta*-C of $BAr^f_4^-$), 134.9 (*ortho*-CH of $BAr^f_4^-$), 161.9 (q, $^1J_{CB}$ = 50 Hz *ipso*-C of $BAr^f_4^-$), 209.6 (CO), 251.5 (metalla-amidinate quaternary). ^{11}B NMR (96MHz, CD_2Cl_2) δ 27 (br, fwhm 430 Hz), -8 ($BAr^f_4^-$). ^{19}F NMR (283 MHz, CD_2Cl_2) δ -62.7 (CF_3). IR (CD_2Cl_2 soln, cm^{-1}) υ 2049, 2003 (CO). MS (positive ion electrospray) m/z (%) 518.1 (weak) M-CO$^+$, correct isotope pattern, (negative ion electrospray) 863.1 (100%) $BAr^f_4^-$. Crystallographic data: $C_{67}H_{68}B_2F_{24}FeN_3O_2$, M_r 1480.71, monoclinic, *P*2(1)/*c*, *a* = 19.098(5), *b* = 18.691(5), *c* = 23.105(5) Å, ß = 112.450(5), *V* = 7623(3) Å3, *Z* = 4, ρ_{calcd} = 1.290 Mg m^{-3}, *T* = 150(2) K, λ = 0.71069 Å. 20582 reflections collected, 13257 independent [*R*(int) = 0.0342], which were used in all calculations. R_1 = 0.0687, wR_2 = 0.1711 for observed unique reflections [F^2 >

$2\sigma(F^2)$] and R_1 = 0.1026, wR_2 = 0.1858 for all unique reflections. Max. and min. residual electron densities 0.525 and -0.304 e Å^{-3}.

Synthesis of [CpFe(CO)$_2$C(NCy)$_2$B(NCy)$_2$CNCy$_2$]$^+$[BAr$^f_4$]$^-$ (**3.6**)

A mixture of [CpFe(CO)$_2$(BNCy$_2$)]$^+$[BAr$^f_4$]$^-$ (0.092 g, 0.07 mmol) and dicyclohexylcarbodiimide (2 equiv.) in dichloromethane (3 cm^3) was stirred for 4 h at room temperature, after which time the reaction was judged to be complete by ^{11}B NMR spectroscopy. Layering with hexanes and storage at –30˚C led to the formation of colourless crystals of **3.6** suitable for X-ray diffraction. Isolated yield: 0.088 g, 65 %. ^{1}H NMR (400 MHz, CD_2Cl_2) δ 1.03-1.93 (m, 60H, CH_2 of Cy), 3.07 (m, 2H, CH of NCy_2), 3.37 (m, 2H, CH of NCy), 3.44 (m, 2H, CH of NCy), 4.99 (s, 5H, Cp), 7.48 (s, 4H, *para*-H of BAr$^f_4$$^-$), 7.65 (s, 8H, *ortho*-H of BAr$^f_4$$^-$). ^{13}C NMR (76 MHz, CD_2Cl_2) δ 25.3, 25.4, 25.5 (4-CH_2 of Cy), 25.5, 25.9, 26.9 (3-CH_2 of Cy), 31.4, 33.9, 34.9 (2-CH_2 of Cy), 55.8 (CH of NCy_2), 56.9, 60.0 (CH of NCy), 86.1 (Cp), 117.6 (*para*-CH of BAr$^f_4$$^-$), 124.6 (q, $^1J_{CF}$ = 274 Hz, CF_3 of BAr$^f_4$$^-$), 129.0 ($^2J_{CF}$ = 32 Hz, *meta*-C of BAr$^f_4$$^-$), 134.8 (*ortho*-CH of BAr$^f_4$$^-$), 161.8 (q, $^1J_{CB}$ = 52 Hz *ipso*-C of BAr$^f_4$$^-$), 167.1 (guanidinate quaternary), 211.9 (CO), 224.0 (metalla-amidinate quaternary). ^{11}B NMR (96 MHz, CD_2Cl_2) δ 2 (s, fwhm ca. 21 Hz, cation), -8 (BAr$^f_4$$^-$). ^{19}F NMR (283 MHz, CD_2Cl_2) δ -62.8 (CF_3). IR (CD_2Cl_2 soln, cm^{-1}) υ 2040, 1992 (CO). MS (positive ion electrospray) m/z (%) 780.5 (10) M$^+$, correct isotope pattern; (negative ion electrospray): 863.1 (100) BAr$^f_4$$^-$; exact mass (calc. for M$^+$ ^{54}Fe isotopomer) m/z 778.5091, (obs.) 778.5101. *Crystallographic data*: $C_{77}H_{83}B_2F_{24}FeN_5O_2$, M_r 1644.0, triclinic, p-1, *a* = 13.416(5), *b* = 13.451(5), *c* = 22.291(5) Å, α = 87.61(5), β = 82.33(5), γ = 89.49(5)°, *V* = 3983 (2) Å^3, *Z* = 2, ρ_{calcd} = 1.371 Mg m^{-3}, *T* = 150(2) K, λ = 0.71069 Å. 25618 reflections collected, 13912

independent [*R*(int) = 0.0409], which were used in all calculations. R_1 = 0.0884, wR_2 = 0.1946 for observed unique reflections [$F^2 > 2\sigma(F^2)$] and R_1 = 0.1098, wR_2 = 0.2050 for all unique reflections. Max. and min. residual electron densities 0.826 and -0.365 e Å^{-3}.

Synthesis of [CpFe(CO)$_2$C(NCy)$_2$B(NCy)$_2$CN^{i}Pr$_2$]$^+$[BAr$^f_4$]$^-$ (**3.7**)

3.7 was prepared from the reaction of [CpFe(CO)$_2$(BN^{i}Pr$_2$)]$^+$ [BAr$^f_4$]$^-$ and dicyclohexylcarbodiimide (2 equiv.) by a method analogous to that used for **3.6**. Yield: 0.053 g, 37 %. ^{1}H NMR (400 MHz, CD_2Cl_2) δ 1.32 (d, $^3J_{HH}$ = 7 Hz, 12H, CH_3 of ^{i}Pr), 1.00-1.92 (m, 40H, CH_2 of NCy), 3.09 (m, 2H, CH of NCy), 3.38 (m, 2H, CH of NCy), 3.90 (sept, $^3J_{HH}$ = 7 Hz, 12H, CH_3 of ^{i}Pr), 4.98 (s, 5H, Cp), 7.48 (s, 4H, *para*-H of BAr$^f_4$$^-$), 7.64 (s, 8H, *ortho*-H of BAr$^f_4$$^-$). ^{13}C NMR (76 MHz, CD_2Cl_2) δ 22.4 (CH_3 of ^{i}Pr), 25.3 (2 overlapping signals, 4-CH_2 of NCy), 25.4, 25.9 (3-CH_2 of NCy), 31.1, 34.9 (2-CH_2 of NCy), 50.6 (CH of ^{i}Pr), 53.8, 54.2 (CH of NCy), 86.1 (Cp), 117.5 (*para*-CH of BAr$^f_4$$^-$), 124.6 (q, $^1J_{CF}$ = 274 Hz, CF_3 of BAr$^f_4$$^-$), 128.9 ($^2J_{CF}$ = 34 Hz, *meta*-C of BAr$^f_4$$^-$, 134.8 (*ortho*-CH of BAr$^f_4$$^-$), 161.8 (q, $^1J_{CB}$ = 50 Hz, *ipso*-C of BAr$^f_4$$^-$), 167.1 (guanidinate quaternary), 211.8 (CO), 244.0 (metalla-amidinate quaternary), ^{11}B NMR (96 MHz, CD_2Cl_2), δ 3 (s, fwhm ca. 12 Hz, cation), -8 (BAr$^f_4$$^-$), ^{19}F NMR (283 MHz, CD_2Cl_2) δ –62.8 (CF_3), IR (CD_2Cl_2 soln, cm^{-1}) υ 2040, 1993 (CO), MS (positive ion electrospray) m/z (%) 700.4 (55) M$^+$, correct isotope pattern, (negative ion electrospray) m/z 863.1 (100) BAr$^f_4$$^-$; exact mass (calc. for M$^+$, ^{54}Fe isotopomer) 697.4502, (obs.) 697.4494. Crystallographic data: $C_{71}H_{75}B_2F_{24}FeN_5O_2$, M_r = 1563.83, monoclinic, space group P2(1)/n, a = 12.973(5), b = 27.190(5), c = 21.590(5) Å, β = 105.219(5)˚, V = 7348 Å^3, Z = 4, ρ_{calcd} = 1.414 Mg m^{-3}, T = 150(2) K, λ = 0.71069 Å, 28224 reflections collected, 14381 independent [R(int) = 0.0292], which were used in all calculations. R_1 = 0.0419, wR_2 = 0.1046

for observed unique reflections [$F^2 > 2\sigma(F^2)$] and $R_1 = 0.0564$, $wR_2 = 0.1120$ for all unique reflections. Max./min. residual electron densities 0.312 and -0.422 e $Å^{-3}$.

3.3 Results and Discussion

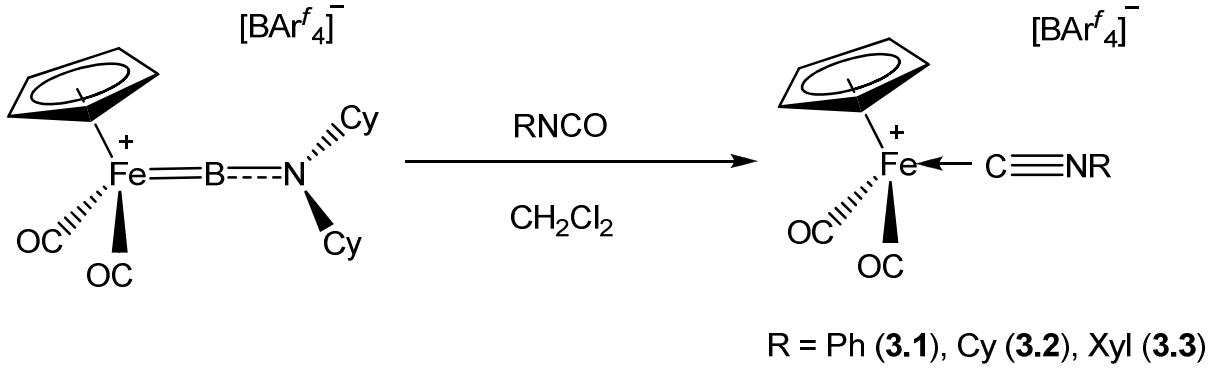
3.3.1 Reaction of $[CpFe(CO)_2(BNCy_2)]^+[BAr^f_4]^-$ with CO_2

The reaction of $[CpFe(CO)_2(BNCy_2)]^+[BAr^f_4]^-$ with ^{13}C labelled CO_2 in dichloromethane or fluorobenzene was carried out under ambient conditions and monitored by ^{11}B NMR. Unfortunately, the aminoborylene complex appeared to be unreactive towards CO_2. Photolysing and/or heating the reaction to 55˚C resulted in formation of a peak at -7 ppm which was attributed to decomposition of the borylene by reaction with the solvent or anion as heating the aminoborylene, as a control reaction without CO_2 also resulted in a peak at -7 ppm in the ^{11}B NMR spectrum.

Previous studies of the reactivity of aminoborylenes with organic substrates such as $Ph_3E{=}X$ (E = P, As, X = S, O)[5] and $Ph_2C{=}O$[6] show that the initial step is coordination of the substrate at the boron centre. Therefore, replacing one of the oxygen atoms on CO_2 for the more basic NR group would hopefully lead to coordination at the borylene by the nitrogen lone pair, and so the corresponding reactions with the isocyanates CyNCO, PhNCO and 2,6-XylNCO were investigated.

3.3.2 Oxygen Atom Abstraction

The cationic terminal borylene, $[CpFe(CO)_2(BNCy_2)]^+[BAr^f_4]^-$ was reacted with the isocyanates CyNCO, PhNCO and 2,6-XylNCO in order to investigate how replacing the O atom for an NR group might affect the reactivity.



Scheme 3.5 Reaction of $[CpFe(CO)_2(BNCy_2)]^+[BAr^f_4]^-$ with RNCO (R = Cy, Ph, Xyl).

Reaction of $[CpFe(CO)_2(BNCy_2)]^+[BAr^f_4]^-$ with five equivalents of PhNCO in dichloromethane was monitored by ^{11}B NMR spectroscopy and showed complete conversion from δ_B 90 ppm for the aminoborylene through to a green solution giving rise to a signal at δ_B 25 ppm and finally to a red solution with δ_B 6 ppm after 48 h (Scheme 3.5).[9] Removal of volatiles under *vacuo*, extraction into fluorobenzene, layering with hexanes and storage at –30˚C led to the isolation of $[CpFe(CO)_2(CNPh)]^+[BAr^f_4]^-$, **3.1** as the major organometallic product in 41 % yield. Both ^1H and ^{13}C NMR spectroscopies were consistent with formation of the isonitrile complex and confirmed the presence of Cp, Ph and the $BAr^f_4^-$ fragments. The IR spectrum also supported the proposed formulation with stretching frequencies for CN (2197 cm^{-1}) as well as CO (2087, 2052 cm^{-1}). Crystals suitable for X-ray diffraction were obtained (as the fluorobenzene hemi-solvate) from a fluorobenzene/hexane layering stored at -30˚C. The solid state structure is shown in Figure 3.1 and a list of selected bond lengths and angles given in Table 3.1.

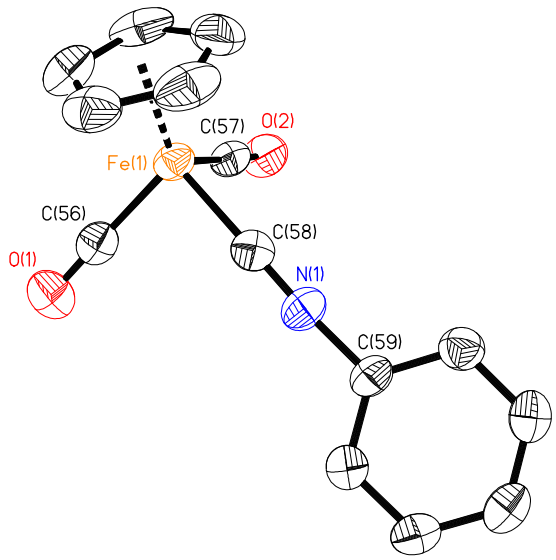


Figure 3.1 The molecular structure of the cationic component of $[CpFe(CO)_2(CNPh)]^+[BAr^f_4]^-$ (**3.1**). Solvent molecule and hydrogen atoms omitted for clarity. Ellipsoids set at the 50% probability level.

Table 3.1 Selected bond lengths [Å] and angles [°] for **3.1**.

Fe1-C58	1.851(4)	Fe1-C56	1.794(4)
N1-C58	1.158(5)	Fe1-C57	1.796(5)
N1-C59	1.400(5)		
N1-C58-Fe1	175.6(3)	C58-N1-C59	174.5(4)

The solid state structure of **3.1** shows the half sandwich geometry expected at the iron centre, with the coordination sphere being completed by two carbonyl ligands and the isonitrile CNPh moiety. Although the cation, $[CpFe(CO)_2(CNPh)]^+$ has previously been reported by Fehlhammer[10] as the $[PF_6]^-$ salt, no crystal structure was obtained. The carbonyl stretching frequencies in both reports are in good agreement (υ 2197 (CN), 2087, 2052 (CO) for **3.1**, 2194 (CN), 2081, 2038 (CO) for $[CpFe(CO)_2(CNPh)]^+[PF_6]^-$). The $[CpFe(CO)_2C{\equiv}N]$ moiety can be compared to structures that have previously been reported. The Fe-C distance for **3.1** is 1.851(4) Å which is very similar to the bond length reported by Nakazawa[11] for $[CpFe(CO)_2(CNSiMe_3)]^+[OTf]^-$ (1.862(4) Å) but slightly shorter than the Fe-C bond reported by Darensbourg *et al.*[12] for $[CpFe(CO)_2C{\equiv}N]$ (1.933(4) Å). The C≡N bond length is 1.158(5) Å which is also comparable to the distance for $[CpFe(CO)_2(CNSiMe_3)]^+[OTf]^-$ (1.157(6) Å).[11] The average Fe-CO bond distance (1.795(5) Å) in **3.1** is shorter than the Fe-CN bond distance (1.851(4) Å), reflecting the better π-acceptor capabilities of CO compared to CN. Both the Fe-C-N and C-N-C*ipso* arrangements are near linear at 175.6(3)˚ and 174.5(4)˚ respectively, which is as expected.

In situ monitoring of the reaction was carried out by positive-ion ESI-MS in order to gain an understanding of the reaction mechanism. Reacting the aminoborylene complex, $[CpFe(CO)_2(BNCy_2)]^+[BAr^f_4]^-$ with PhNCO showed the formation of $[CpFe(CO)_2(CNPh)]^+[BAr^f_4]^-$ at *m/z* = 280.0 but also revealed the presence of small amounts of $[CpFe(CO)_3]^+$ corresponding to a peak at *m/z* = 205.0. During the course of the reaction, a peak at *m/z* = 606 was observed which, together with the isotopic profile and accurate mass is consistent with a cationic species formed from the borylene plus two molecules of PhNCO. Fragmentation studies of this cation by MS/MS yields both $[CpFe(CO)_2(CNPh)]^+$ and

$[CpFe(CO)_3]^+$. Mechanistic details are discussed later in the chapter in conjunction with computational studies.

The reactions of $[CpFe(CO)_2(BNCy_2)]^+[BAr^f_4]^-$ with CyNCO and 2,6-XylNCO were also investigated; each resulted in a single major product giving rise to a ^{11}B NMR signal at ~6ppm. ESI-MS analysis of the reaction mixture also indicates formation of the isonitrile products $[CpFe(CO)_2(CNR)]^+[BAr^f_4]^-$ (R = Cy **3.2**, Xyl **3.3**) in each case, together with smaller amounts of the tricarbonyl complex.

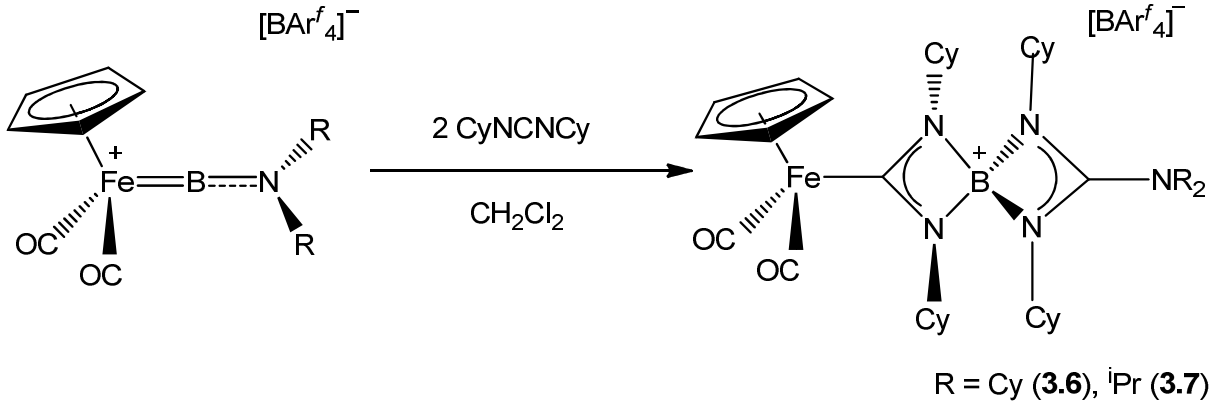
Both ESI/MS and the crystal structure supports an overall reaction mechanism which proceeds via net oxygen abstraction from the isocyanate. However, in order to gain an in-depth understanding of the reaction mechanism, computational studies have been carried out and are discussed at the end of the chapter.

3.3.3 Insertion of Dicyclohexylcarbodiimide into Aminoborylene Complexes

It was hoped that substituting the second oxygen atom of the isocyanate by a bulkier NR group would hopefully offer sufficient stability so that intermediate species could be isolated. Therefore reactions of the aminoborylenes $[CpFe(CO)_2(BNR_2)]^+[BAr^f_4]^-$ (R = ^{i}Pr, Cy) with the sterically demanding dicyclohexylcarbodiimide, CyNCNCy were attempted.

The reaction of the aminoborylene complexes $[CpFe(CO)_2(BNR_2)]^+[BAr^f_4]^-$ (R = Cy, ^{i}Pr) with two or more equivalents of dicyclohexylcarbodiimide in dichloromethane resulted in complete conversion to the spirocyclic complexes, $[CpFe(CO)_2C(NCy)_2B(NCy)_2CNR_2]^+[BAr^f_4]^-$ (**3.6**: R = Cy, **3.7**: R = ^{i}Pr) after 4 h.[13] The sharp upfield shifted ^{11}B NMR chemical signal at ca. 3 ppm implies a highly symmetrical four-coordinate boron centre featuring no metal-boron bonds.[1j] Multinuclear NMR spectroscopies

(^{1}H, ^{13}C, ^{19}F) are consistent with formation of the double insertion products (Scheme 3.6). The ^{13}C NMR spectrum for **3.6** shows peaks for the CH_2 and CH groups of the three respective Cy groups (two NCy groups and one NCy_2 group) and the ^{1}H and ^{13}C NMR spectra for **3.7** account for both the ^{i}Pr and NCy groups. The guanidinate and metalla-amidinate quaternary carbons are also represented in the ^{13}C NMR spectrum (167.1, 224.0 ppm respectively for **3.6**; 167.1, 244.0 ppm respectively for **3.7**). Positive electrospray mass spectrometry also shows the presence of M^{+} for both **3.6** (*m/z* = 780.5) and **3.7** (*m/z* = 700.4) further supporting the formation of the double insertion products.



Scheme 3.6 Synthetic route to complexes **3.6** and **3.7**.

Colourless crystals suitable for X-ray diffraction were isolated in 65% and 37% yield (**3.6** and **3.7**, respectively) by layering with hexanes and storage at -30ºC. The crystal structures are shown in Figures 3.2 and 3.3 and the relevant bond lengths and angles are listed in Table 3.2 and 3.3 respectively.

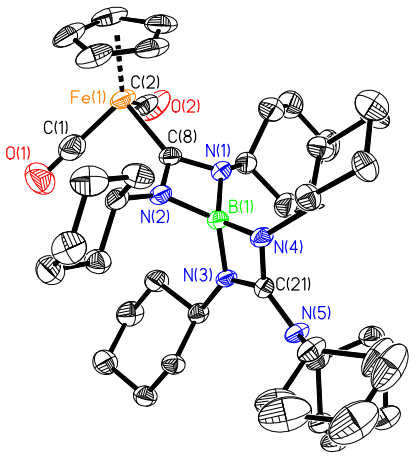


Figure 3.2 The molecular structure of the cationic component of $[CpFe(CO)_2C(NCy)_2B(NCy)_2CNCy_2]^+[BAr^f_4]^-$ (**3.6**). Solvent molecule and hydrogen atoms omitted for clarity. Ellipsoids set at the 50% probability level.

Table 3.2 Selected bond lengths [Å] and angles [°] for **3.6**.

Fe1-C8	1.96(2)	B1-N3	1.55(3)
C8-N1	1.37(3)	B1-N4	1.56(3)
C8-N2	1.35(3)	N3-C21	1.34(3)
B1-N1	1.56(3)	N4-C21	1.37(3)
B1-N2	1.54(1)	N5-C21	1.35(3)

N1-C8-N2	99.0(2)	N3-B1-N4	84.1(17)
N1-B1-N2	83.8(17)	N3-C21-N4	100.4(19)

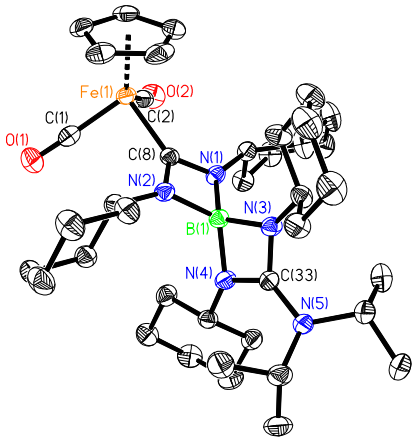


Figure 3.3 The molecular structure of the cationic component of $[CpFe(CO)_2C(NCy)_2B(NCy)_2CN^iPr_2]^+[BAr^f_4]^-$ (**3.7**). Solvent molecule and hydrogen atoms omitted for clarity. Ellipsoids set at the 50% probability level.

Table 3.3 Selected bond lengths [Å] and angles [°] for **3.7**.

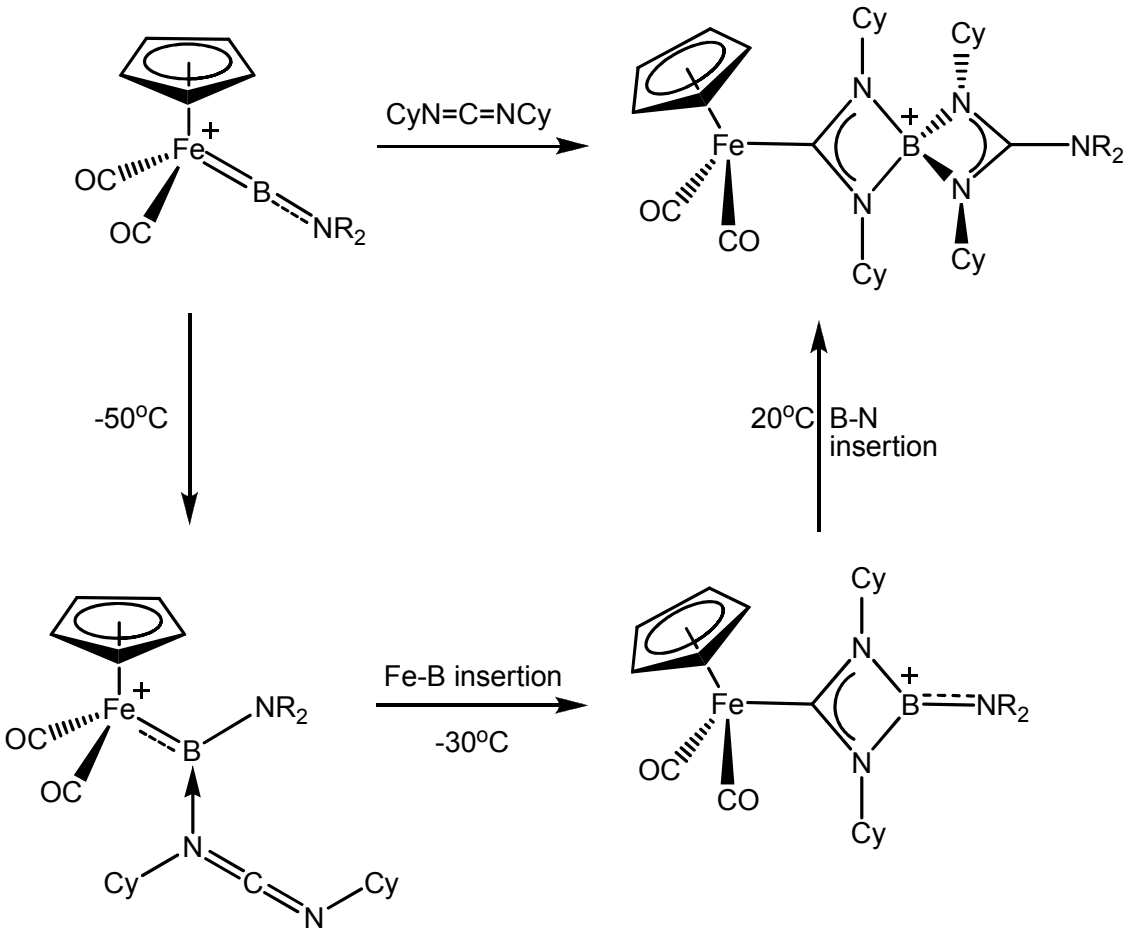
Fe1-C8	1.948(2)	B1-N3	1.564(2)
C8-N1	1.354(2)	B1-N4	1.560(2)
C8-N2	1.356(2)	N3-C33	1.350(2)
B1-N1	1.550(2)	N4-C33	1.344(2)
B1-N2	1.552(2)	N5-C33	1.366(2)
N1-C8-N2	98.8(1)	N3-B1-N4	83.2(1)
N1-B1-N2	83.1(1)	N3-C33-N4	100.8(1)

The molecular structures for **3.6** and **3.7** illustrate the presence of both guanidinate and metallamidinate rings with a four-coordinate, tetrahedral cationic boronium centre. The boronium centre is stabilized by two formally anionic nitrogen substituents, whilst the other two coordination sites are occupied by neutral nitrogen substituents.[14] The guanidinate ring is very similar to other boron guanidinate complexes reported.[13a,15-17] In $Me_2NC(NPh)_2B(CF_3)_2$, for example, the exocyclic C-N bond is short at 1.315(3) Å, reflecting a significant C-N π bond.[15] The π-interaction results in a planar guanidinate ring with a small torsion angle of 13.0˚ between the ring plane and the exocyclic NMe_2 substituent. In **3.6** and **3.7** however, the bulkier amino substituents (Cy and ^{i}Pr) enforce a non-coplanar alignment which results in a diminished π-bonding interaction and subsequently a C-N bond of 1.35(3) Å and 1.366(2) Å for **3.6** and **3.7** respectively. A similar effect was observed in the guanidinate boron dihalides, $Ph_2NC(NMes)_2BCl_2$ and $Ph_2NC(NDipp)_2BCl_2$ (C-N bond 1.342(2) Å and 1.353(6) Å respectively).[17] Moreover, the average C-N bond distances for both complexes (1.36(3) Å for **3.6** and 1.347(2) Å for **3.7**) are intermediate between those of typical C=N double bonds and C-N single bonds (av. C=N bond = 1.21 Å, C-N bond 1.46 Å)[18] further highlighting the delocalization in the guanidinate ring. The average B-N bond distances of 1.56(3) Å and 1.562(2) Å (**3.6** and **3.7** respectively) are also similar to those found in other guanidinate rings (1.554(3) Å for $Me_2NC(NPh)_2B(CF_3)_2$,[15] 1.564(3) Å for $Ph_2NC(NMes)_2BCl_2$.[17] The N-B-N bite angle for both complexes was also found to be in the range expected for guanidinate rings (84.1(17)˚ and 83.2(1)˚ for **3.6** and **3.7** respectively).

The $\{CpFe(CO)_2C(NCy)_2B\}$ unit is an example of a metalla-amidinate ring, and also contains a fairly short M-C(sp^2) distance (1.96(2) Å and 1.948(2) Å for **3.6** and **3.7** respectively). By means of comparison, the first reported example of such a system,

$[CpMo(CO)_3C(NPh)_2Mo(CO)_2Cp]$ was described as containing a Mo-C(sp^2) single bond and has a Mo-C distance of 2.283(3) Å (bearing in mind the covalent radii for Mo and Fe is 1.45 Å and 1.25 Å respectively).[19] The Fe-C(sp^2) distance falls in the range reported previously for compounds of the type $[CpFe(CO)_2$-CH=CHR], such as $[CpFe(CO)_2$Fe-CH=CH-CH=CHBr] (1.971(3) Å).[20] However, DFT calculations carried out on **3.5** suggest contribution from the carbenoid resonance form is small (*vide infra*).[13]

In order to investigate the likely mechanism of the reaction, *in situ* VT NMR experiments were carried out over a temperature range of –80ºC to 20ºC.



Scheme 3.7 Mechanistic route to the synthesis of **3.6** and **3.7**.

These experiments revealed the presence of two intermediates; the first appearing at –50ºC and giving rise to a resonance at δ_B 71 ppm was assigned as the boron-bound carbodiimide adduct, $[CpFe(CO)_2B(NR_2)(CyNCNCy)]^+[BAr^f_4]^-$, (**3.4**) arising from coordination of CyNCNCy at the boron centre. An upfield shift from δ_B 92 to δ_B 71 is as expected for the formation of a donor/acceptor bond between a cationic borylene and compounds containing the C=NR function.[6] The two imine adducts, $[CpFe(CO)_2\{B(X)(^iPrN{=}CMe_2)]^+[BAr^f_4]^-$ (X = $OC(H)Ph_2$ and N^iPr_2), formed from the reaction of $[CpFe(CO)_2(BN^iPr_2)]^+[BAr^f_4]^-$ with Ph_2CO / $^iPrN{=}CMe_2$, respectively, have shifts of δ_B 64 and δ_B 54 ppm.[6] Cowley *et al.*[21] have also demonstrated that the reaction of $PhBCl_2$ with dicyclohexylcarbodiimide, which forms the amidinate $[PhC\{NCy\}_2BCl_2]$ by an insertion reaction, initially proceeds via the donor-acceptor adduct, $PhBCl_2{\cdot}$CyNCNCy which was crystallographically characterized. Unfortunately, the donor/acceptor adduct, **3.4** was very labile and attempts to isolate it were unsuccessful.

The second intermediate appearing at -30ºC gives rise to a broad resonance at δ_B 25, which implies a three-coordinate boron centre with the absence of any metal-boron bonds.[1j,k] Spectroscopic data also supports the proposed mono(insertion) product, $[CpFe(CO)_2C(NCy)_2BNR_2]^+[BAr^f_4]^-$, **3.5** with peaks in the ^1H and ^{13}C NMR spectra accounting for the NCy_2, NCy, Cp and $[BAr^f_4]^-$ fragments. Furthermore, the ^{13}C NMR spectrum contains peaks corresponding to CO (209.6 ppm) and the metalla-amidinate quaternary carbon (251.5 ppm) (*vide infra*). The positive ion electrospray also supports formation of **3.5**, with a peak at 518.1 corresponding to $(M\text{-}CO)^+$. However, the fact that significant amounts of the double insertion product are formed at –20˚C indicated that isolation of the single insertion product would be challenging.

Titration of a sub-stoichiometric amount of dicyclohexylcarbodiimide into $[CpFe(CO)_2(BNCy_2)]^+[BAr^f_4]^-$ in dichloromethane yielded the single insertion product, **3.5**, free from the double-insertion product, **3.6**. **3.5** was subsequently crystallised by layering with hexanes and storage at –30˚C. The crystal structure is shown in Figure 3.4 and the relevant bond lengths and angles are listed in Table 3.4.

The solid state structure confirmed the formation of the mono(insertion) product $[CpFe(CO)_2C(NCy)_2BNCy_2]^+[BAr^f_4]^-$, which features a three-coordinate cationic borenium centre stabilized by two formally anionic nitrogen donors and one neutral nitrogen substituent.[14] The $\{CpFe(CO)_2C(NCy)_2\}$ metalla-amidinate ring is similar to the analogous ring in the double insertion product (**3.6**), containing a short Fe-C bond length of 1.938(3) Å (cf. 1.96(2) Å for **3.6**). The four-membered ring is also similar to that found in $[CpFe(CO)_2(CS_2)Zr\{(2\text{-}FC_6H_4)NSiMe_2\}_3CH]$ reported by Gade *et al.*[22] which also features a short Fe-C bond length of 1.934(11) Å ascribed to partial carbenoid character (Fe=C). This is further supported by the ^{13}C NMR signal of the metalla-amidinate carbon reported by Gade (334.0 ppm). This represents a significant downfield shift, as quaternary amidinate and guanidinate carbon atoms typically resonate in the region 160-170 ppm.[15,17] The ^{13}C NMR shift for the metalla-amidinate carbon in **3.5** also resonates at a downfield shift of 251.5 ppm, indicating partial carbenoid character. However, DFT calculations were carried out to determine the bonding density for the metalla-amidinate Fe-C bond in **3.5** and the calculations reveal a σ/π breakdown of 85:15[13a] which compared to the model system, $[CpFe(CO)_2(=CH_2)]^+$ which has a 64:36 σ/π ratio,[23a] suggests that the contribution from the carbenoid resonance form is small.

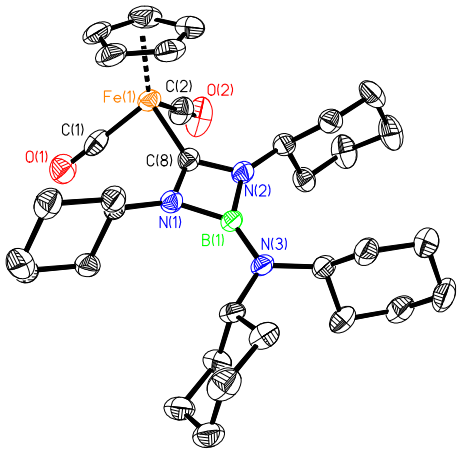


Figure 3.4 The molecular structure of the cationic component of $[CpFe(CO)_2C(NCy)_2BNCy_2]^+[BAr^f{}_4]^-$ (**3.5**). Solvent molecule and hydrogen atoms omitted for clarity. Ellipsoids set at the 50% probability level.

Table 3.4 Selected bond lengths [Å] and angles [°] for **3.5**.

Fe1-C8	1.938(3)	B1-N1	1.506(4)
C8-N1	1.358(4)	B1-N2	1.492(4)
C8-N2	1.357(4)	B1-N3	1.371(4)
N1-C8-N2	98.3(2)	N1-B1-N2	86.5(2)

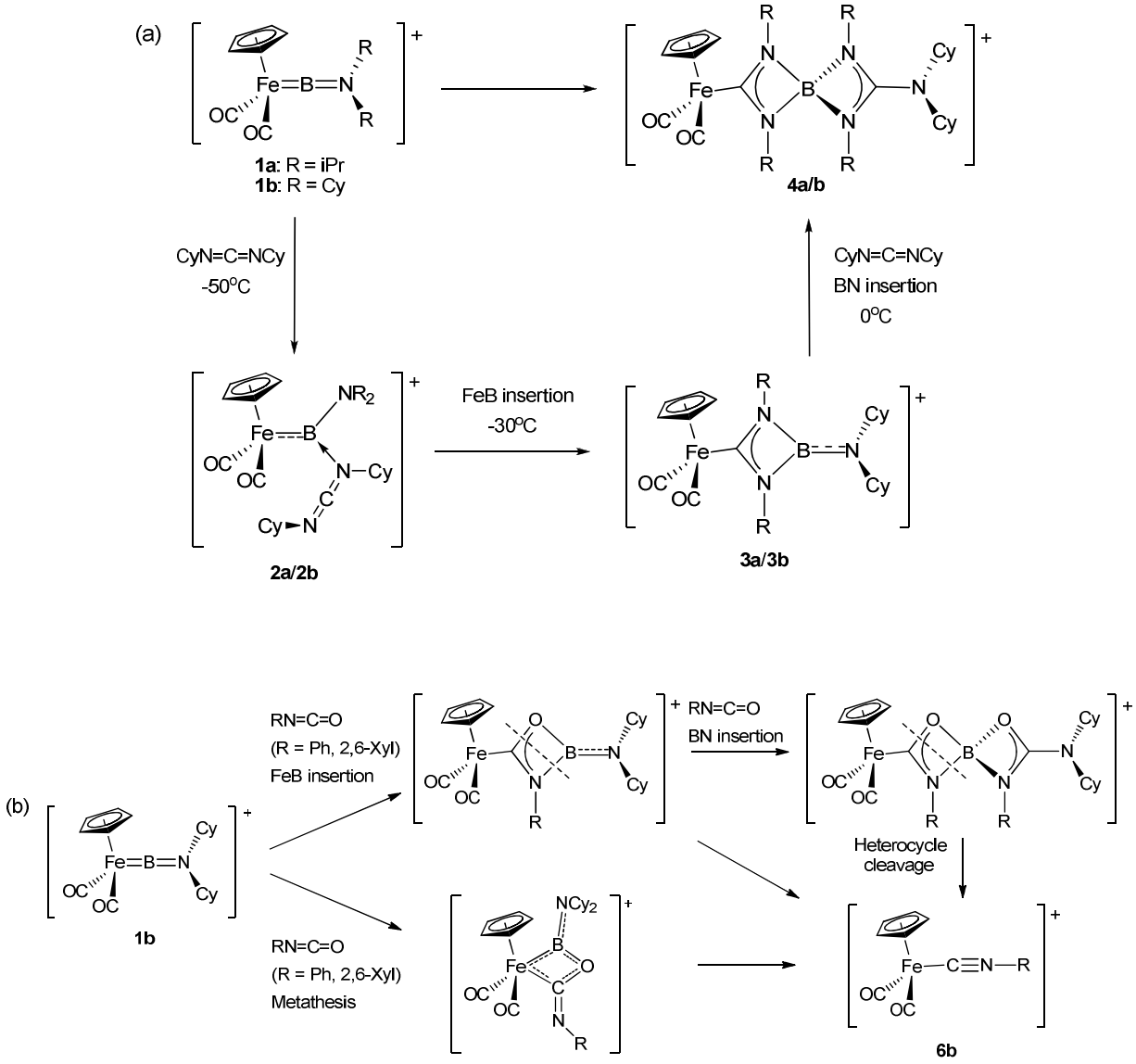
As expected, **3.5** was found to be very labile and reacted further in the presence of excess carbodiimide, even at -20ºC, to form **3.6**. The insertion of carbodiimides into a B=N bond of strongly electrophilic boranes has previously been reported;[24] Burgër and co-workers reported the reaction of $(CF_3)_2BNMe_2$ with RNCNR (R = Ph, Cy) to proceed by a [2+2] cycloaddition reaction,[15] whilst Cowley *et al*. demonstrated that insertion of carbodiimides, CyNCNCy into the B=N bonds of the boranes, $PhBCl_2$ and $(Me_3Si)_2NBCl_2$ proceeds by initial formation of a donor-acceptor adduct.[16,17,21]

Formation of the donor/acceptor complex, $[CpFe(CO)_2B(NR_2)(CyNCNCy)]^+[BAr^f_4]^-$, **3.4** implies that a mechanism is operating whereby the substrate coordinates to the ligand (boron) followed by migration of the metal. This mechanism is different to classical organometallic insertion reactions, where coordination of the substrate to the metal takes place, followed by migration of the ligand. Gade and co-workers have also reported on this type of cooperative reactivity between linked Lewis acidic centres for insertion of unsaturated polar substrates such as CS_2, phenyl isocyanate and phenyl isothiocyanate into the Zr-Fe bond in $[HC\{SiMe_2NR\}_3Zr\text{-}FeCo(CO)_2]$.[22] Their study revealed that the polar substrate initially coordinates to the zirconium centre, which increases its coordination number and leads to polarization and subsequent dissociation of the Zr-Fe bond. The nucleophilic transition metal, Fe, then attacks the electrophilic carbon atom of the substrate to complete insertion of the substrate between the two metal centres. Therefore in the reaction of the aminoborylenes with carbodiimides, it is likely that coordination of the carbodiimide at the electrophilic boron centre polarizes the carbodiimide substrate, activating it for nucleophilic attack by iron. To further investigate the mechanism, computational studies have been carried out and an in-

depth discussion is given to investigate the different mechanisms observed for reaction of the aminoborylene with carbodiimides and isocyanates.[25]

3.3.4 Computational Studies of the Reaction of the Model Aminoborylene $[CpFe(CO)_2(BNMe_2)]^+[BAr^f_4]^-$ with Heteroallenes

After the unprecedented results from the reactions of the aminoborylenes $[CpFe(CO)_2(BNR)]^+[BAr^f_4]^-$ (R = ^{i}Pr, Cy) with both isocyanates and carbodiimides, it was decided to carry out computational studies in order to gain an understanding of the likely reaction mechanisms.[25] Reactions of the NCy_2 aminoborylene complex with isocyanates formed the isonitrile complexes, **3.1, 3.2** and **3.3** via a net oxygen abstraction (or overall metathesis) process (Scheme 3.5). Dicyclohexylcarbodiimide on the other hand yielded a bis(insertion) product, **3.6** and **3.7**, where one equivalent of carbodiimide is inserted into each of the Fe=B and B=N bonds (Scheme 3.6 and 3.7). Although experimental results provided an outline mechanism, there were still many unanswered questions that needed addressing. **3.1** for instance, could have been formed by cleavage of the 4-membered heterocyclic rings formed by an insertion reaction, analogous to the intermediate formed with carbodiimides (**3.5**). Alternatively, **3.1** could have been formed by a single metathesis step (Scheme 3.8). Computational studies would hopefully provide a mechanistic understanding as to how and why the two organic substrates react differently towards the aminoborylene, and in addition, why the aminoborylene reacts differently towards heteroallenes as compared to other polar molecules (P=O/P=S metathesis,[5] C=O hydride transfer, C=N coordination at B).[6]



Scheme 3.8 Potential mechanisms for the reaction of the aminoborylene complexes with heteroallenes: (a) insertion of CyNCNCy and (b) oxygen abstraction from isocyanates, RNCO (R = Ph, Cy, Xyl).

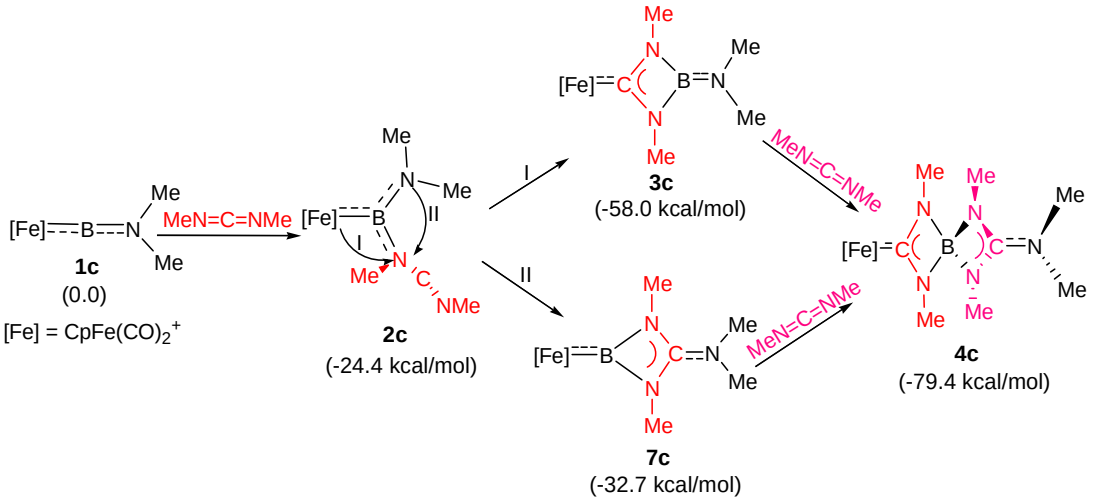
The calculated structures corresponding to various starting materials, intermediates and final products have been numbered 1a, 2b, 4c etc. to differentiate them from the experimentally realized compounds **3.1**, **3.2** etc. For simplicity, the bulky Cy and ^{i}Pr groups

on the aminoborylenes, the Cy group on the carbodiimides and the Ph, Cy and 2,6-Xyl groups on the isocyanates were substituted for Me groups. Thus, while compounds featuring N^iPr_2 and NCy_2 substituents are given labels 'a' and 'b' respectively, species obtained from the reactions of the model borylene, $[CpFe(CO)_2(BNMe_2)]^+[BAr^f_4]^-$ (**1c**) with the MeNCNMe will be given the suffix 'c'. In the case of the isocyanate reaction, attack of the substrate, MeNCO can proceed either by oxygen attack or nitrogen attack, and therefore the study compounds and their intermediates will be given the suffix 'd' and 'e' respectively.

In the following section an in-depth discussion of the mechanism of insertion of MeNCNMe into the Fe=B and B=N bond of the model aminoborylene complex, $[CpFe(CO)_2(BNMe_2)]^+[BAr^f_4]^-$, **1c**, will first be detailed, and then the more complex oxygen abstraction reaction with isocyanates will be discussed.

3.3.4.1 Computational Studies of the Insertion of Carbodiimides, MeNCNMe into $[CpFe(CO)_2(BNMe_2)]^+[BAr^f_4]^-$

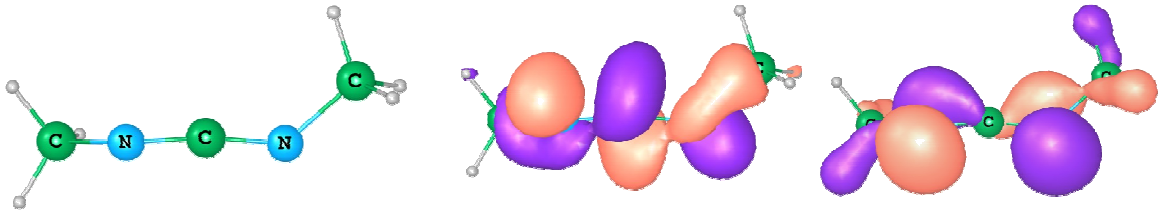
VT NMR experiments simply reveal an unusual mode of reactivity for insertion of the carbodiimide into the cationic terminal aminoborylene complexes $[CpFe(CO)_2(BNCy_2)]^+[BAr^f_4]^-$, with initial attack of the carbodiimide at the electrophilic boron centre being followed by migration of the metal fragment rather than the more classical insertion mechanism of attack at the metal centre and migration of the ligand.[13] The reaction of the cationic aminoborylenes $[CpFe(CO)_2(BNR_2)]^+[BAr^f_4]^-$ with various organic substrates has typically been shown to proceed via initial coordination of the substrate to the electrophilic boron centre and so an in-depth analysis of the energetics of this coordination process was warranted.[4-6]



Scheme 3.9 Schematic representation of the two possible pathways for formation of the model double insertion product **4c**

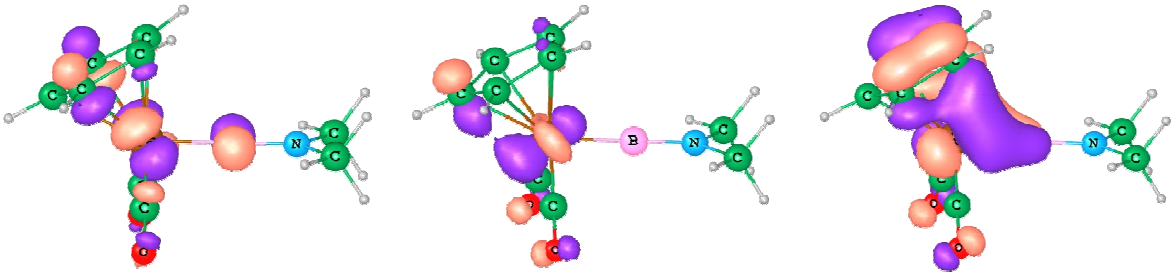
3.3.4.1.1 Insertion of the First Equivalent of MeNCNMe

The first step in the reaction of the model borylene complex, $[CpFe(CO)_2(BNMe_2)]^+[BAr^f_4]^-$, **1c** with one equivalent of carbodiimide, MeNCNMe, is formation of the donor/acceptor complex, **2c**, (Scheme 3.9) which was calculated to be exothermic by 24.4 kcal/mol due to the donation of one of the nitrogen-centred lone pairs of the carbodiimide (HOMO, Figure 3.5) to the LUMO, mainly located on the boron atom (Figure 3.6 and 3.7). Formation of the donor/acceptor adduct, **2c** from **1c** was preceded by the transition state, **1c-2c** which is only 5.2 kcal/mol higher in energy than the reactants themselves, which is consistent with the high reactivity of the borylene towards nucleophilic attack.



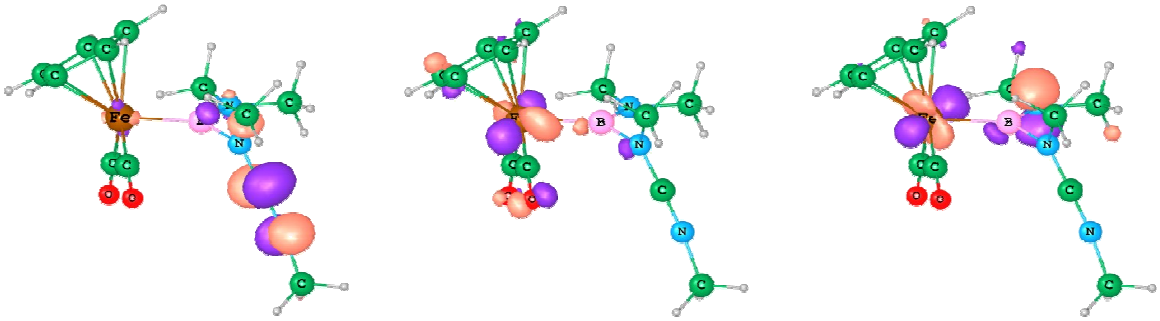
MeNCNMe | LUMO (0.0333) | HOMO (-0.2362)

Figure 3.5 Important molecular orbitals of the model carbodiimide, MeNCNMe



LUMO (-0.2209) | HOMO (-0.4147) | HOMO-2 (-0.4274)

Figure 3.6 Important molecular orbitals of the model iron borylene complex, $[CpFe(CO)_2(BNMe_2)]^+[BAr^f_4]^-$ (**1c**)

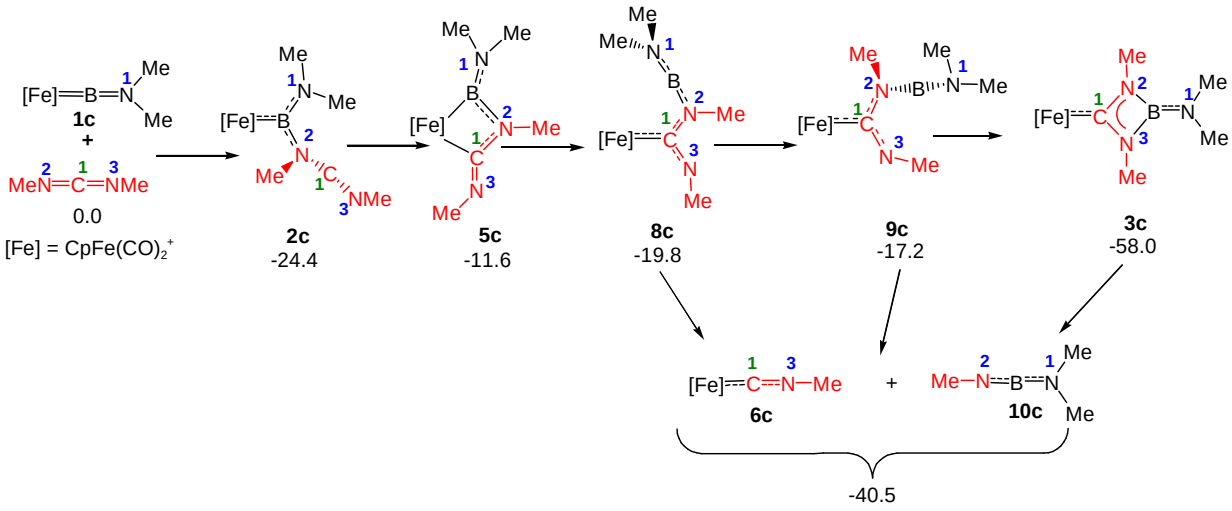


LUMO (-0.1789) | HOMO (-0.3590) | HOMO-2 (-0.3745)

Figure 3.7 Important molecular orbitals of the intermediate donor/acceptor adduct **2c**

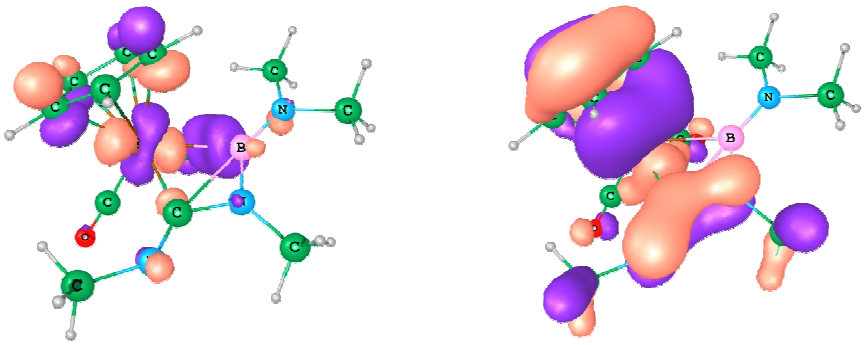
In the model acyclic intermediate, **2c** the plane of the MeNCNMe fragment is perpendicular to the $FeBNMe_2$ unit and so one of two mechanisms can occur (Scheme 3.9). Either the carbodiimide can insert into the Fe=B bond to form **3c** (pathway I) or into the B=N bond to form **7c** (pathway II). Calculations reveal that Fe=B insertion to form **3c** is more thermodynamically favourable, with an energy of –58.0 kcal/mol, versus **7c**, formed by B=N insertion and which has an energy of –32.7 kcal/mol compared to the adduct **2c**.

Analysis of relevant orbital interactions further supports the notion that insertion into the Fe=B bond is also likely to be kinetically favoured over insertion into the B=N bond. Fe=B insertion requires interaction of the HOMO (which is mainly iron d-orbital in character) with the LUMO which is a C-N π^* orbital (Figure 3.7). B=N insertion however, requires interaction between the LUMO and the HOMO-2 which is a lone pair on the nitrogen. The iron-centred HOMO (–0.3590 a.u) is likely to be a better donor than the deeper lying HOMO-2 (-0.3745 a.u) resulting in a better orbital interaction for Fe=B insertion. Electrostatic factors can also be used to rationalise the regiochemistry of the insertion reaction. The negative charge on iron (-0.998) is much greater than that on nitrogen (-0.136); attack of the iron centre at the C-N π^* orbital would therefore be expected to be more favourable than attack by the nitrogen lone pair. In effect, the nitrogen lone pair is already being utilized in the formation of the B-N π bond and is therefore less available for the formation of further bonds. Due to the strong support for insertion of the first equivalent of carbodiimide into the Fe=B bond (and not the B=N bond) further computational studies were only carried out for Fe=B insertion (Scheme 3.10).



Scheme 3.10 Mechanism of insertion of one molecule of MeNCNMe into the Fe=B bond of **1c**

The next step in the formation of the single insertion product, **3c** is in the formation of a four-membered metallacyclic intermediate **5c** by the interaction of the HOMO of **2c** (mainly localized on iron) with the LUMO (C-N3 π*) antibonding molecular orbital (Figure 3.7).



LUMO (-0.2310) HOMO-5 (-0.4336)

Figure 3.9 Fe-B antibonding and C-N π molecular orbitals of the metallacycle **5c**

This results in a lengthening of the C-N3 bond from 1.179 Å (in **2c**) to 1.261 Å (in **5c**). The methyl substituents on N1 and N2 also no longer lie in the same plane (dihedral angle N1BN2C = 20.1˚C) presumably to avoid steric interaction between the methyl groups on N1 and N2 and the bonding pair-lone pair repulsive interaction between the N2-Me and the N3 lone pair. This intermediate **5c** was found to be 12.8 kcal/mol less stable than **2c** (Scheme 3.10). A similar metallacyclic complex was isolated and structurally characterized in the reaction of $[CpMn(CO)_2(B^tBu)]$ with CyNCNCy thus providing precedent for this type of structure.[7]

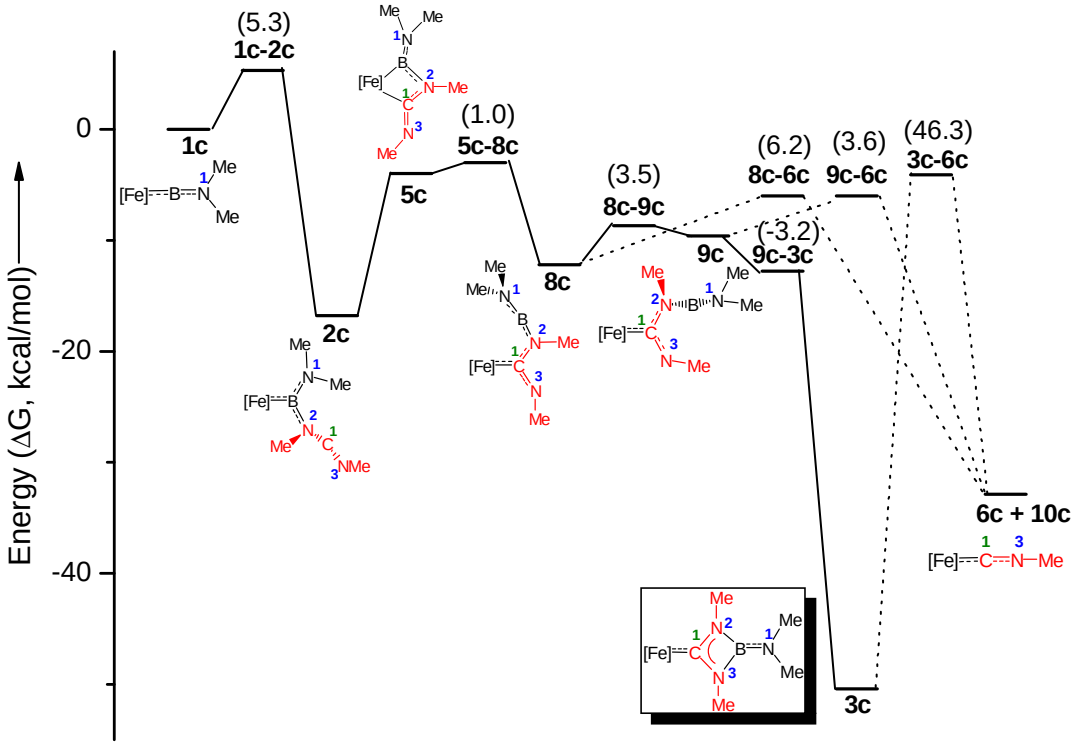
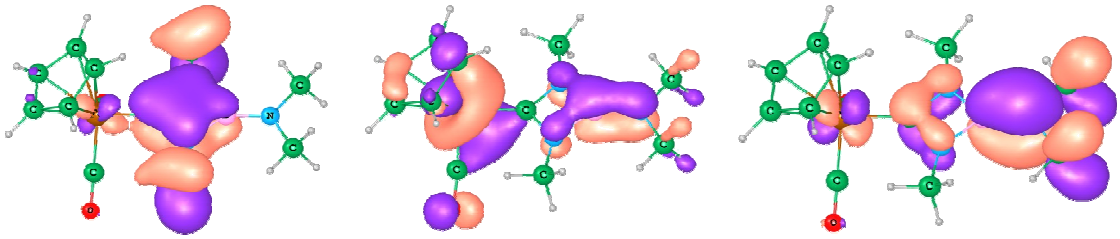


Figure 3.10 Potential energy diagram for insertion of one molecule of MeNCNMe into the Fe=B bond of **1c**. The dotted line indicates formation of the dissociated products.

The cyclic intermediate **5c** can undergo cleavage of the Fe-B bond to form a second acyclic intermediate **8c** which is more stable than **5c** by 8.2 kcal/mol; this process has an energy barrier of 1.0 kcal/mol (Figure 3.10, Scheme 3.10). Metallacycle cleavage can occur via two ways, by Fe-B bond breakage (ca. 85.5 kcal/mol) which is the most favourable or by C-N bond cleavage (179.5 kcal/mol).[25] In addition, the LUMO of **5c** is the Fe-B σ* orbital (Figure 3.9), and donation of the C-N π electron density, from the HOMO-5 to the Fe-B σ* orbital results in Fe-B bond weakening and breakage to form **8c**. This leads to a subsequent elongation in the C1-N2 bond from 1.401 Å to 1.503 Å. Furthermore, facile rotation about the C1-N2 bond (energy barrier = 3.5 kcal/mol) brings N3 closer to B1 (3.570 to 3.272 Å) and results in the formation of the intermediate **9c** albeit energetically uphill (by 2.6 kcal/mol). Once again, the C-N2 bond is elongated (to 1.604 Å in **9c** from 1.401 Å in **5c**) and dissociation of the bond to yield the metathesis products **6c** and **10c** (the products of the reaction with isocyanates) is conceivable. Computational studies show that the energy barrier for formation of **6c** and **10c** from **8c** and **9c** are 6.2 and 3.6 kcal/mol respectively and the reactions are exothermic with energies of 20.7 and 23.3 kcal/mol. Alternatively **9c** can undergo cyclization to form **3c** by donation of the lone pair at N3 into the B-N2 π* orbital, resulting in elongation of both the C3-N3 (1.393 Å) and B-N2 (1.510 Å) bonds. Formation of **3c** is exothermic by 40.8 kcal/mol with an energy barrier of –3.2 kcal/mol and provides good evidence that this cyclization pathway is more likely to be followed than the competing dissociation to give **6c** and **10c**. Experimentally this was the pathway observed. Once formed, dissociation to form the metathesis products **6c** and **10c** is again unlikely due to a very high energy barrier (46.4 kcal/mol) and the fact that the reaction would be endothermic (17.5 kcal/mol). The stability of **3c** can also be attributed to π delocalisation in the 4-membered ring,

with the exocyclic B-N1 π-orbital also being delocalised into the 4-membered ring resulting in a marginally longer B-N1 linkage (1.373 Å) (cf. B-N1 in model borylene complex **1c**, 1.355 Å) (Figure 3.11). The presence of three strong B-N bonds (92.7 kcal/mol) and one C-N bond (179.5 kcal/mol) also contributes to the high stability of **3c**.



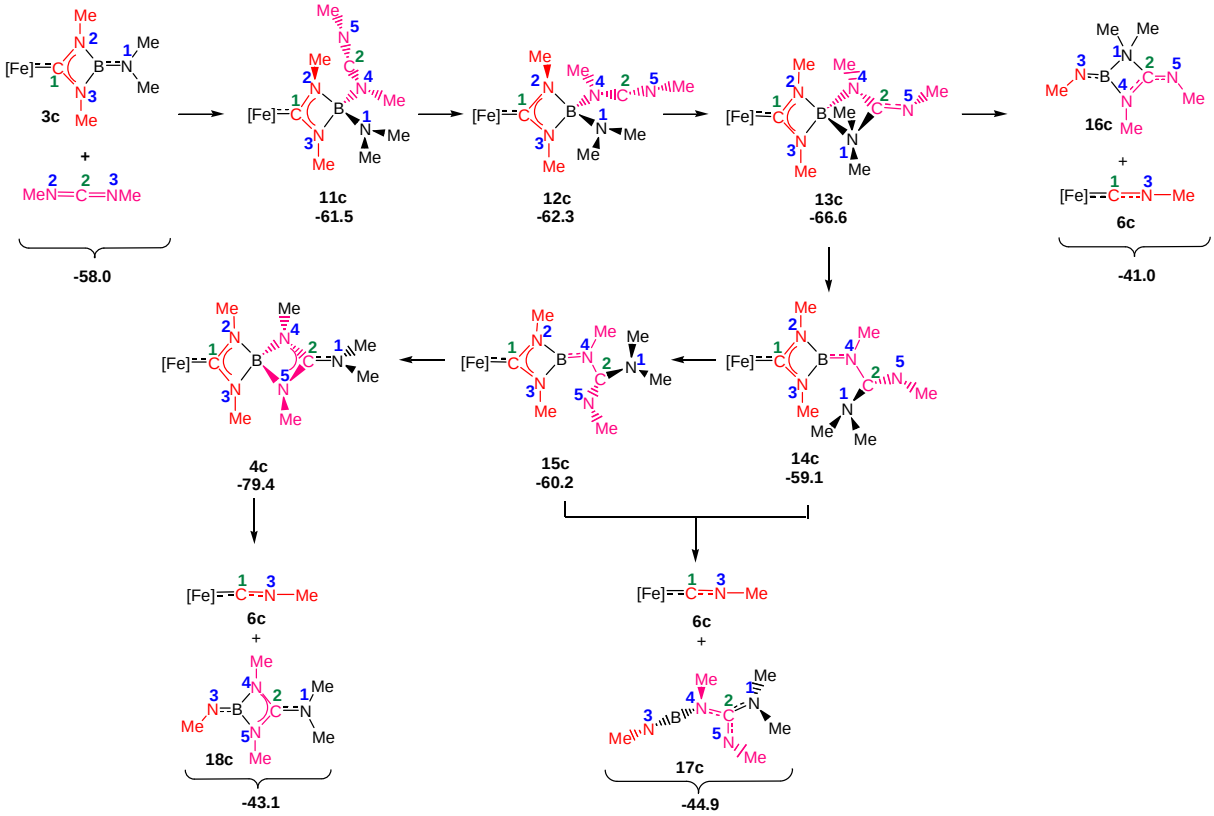
HOMO-9 (-0.4987) HOMO-4 (-0.4275) HOMO-1 (-0.3857)

Figure 3.11 Important molecular orbitals of the mono(insertion) product **3c**

3.3.4.1.2 Insertion of the Second Equivalent of MeNCNMe

Reaction of **3c** with a second equivalent of carbodiimide by insertion into the B=N bond was observed experimentally for the corresponding cyclohexyl system even at –20˚C. Mirroring the first insertion step, a nitrogen lone pair from the second equivalent of carbodiimide can attack the electrophilic boron centre to form intermediate **11c** (cf. **2c**). Formation of **11c** is exothermic by 3.5 kcal/mol and has a barrier to formation of only 1.7 kcal/mol (Scheme 3.11, Figure 3.12). Subsequent rotation about the B-N4 bond brings C2 closer to N1 (*d*(C2-N1) reduced from 3.639 Å to 2.767 Å) allowing the formation of **12c** (which has a similar energy to **11c**, differing by only 0.8 kcal/mol). Interaction of the lone pair at N1 with the LUMO of the carbodiimide fragment (mainly located at C2) then results in formation of the bicyclic intermediate **13c**. The ring-closure process is exothermic by 4.3 kcal/mol and the second 4-membered ring is planar and perpendicular to the first. An

alternative mechanism for the formation of **13c** from **3c** is a [2+2] cycloaddition process which has been reported by Bürger and co-workers for insertion of dicyclohexylcarbodiimide into a B=N bond.[15] This would involve interaction between B-N1 π and C-N4 π* but no transition state corresponding to this process could be located, possibly due to the delocalisation of the B-N1 π bond into the existing 4-membered ring.



Scheme 3.11 Mechanism of the insertion of a second molecule of MeNCNMe into the B=N bond of **3c**.

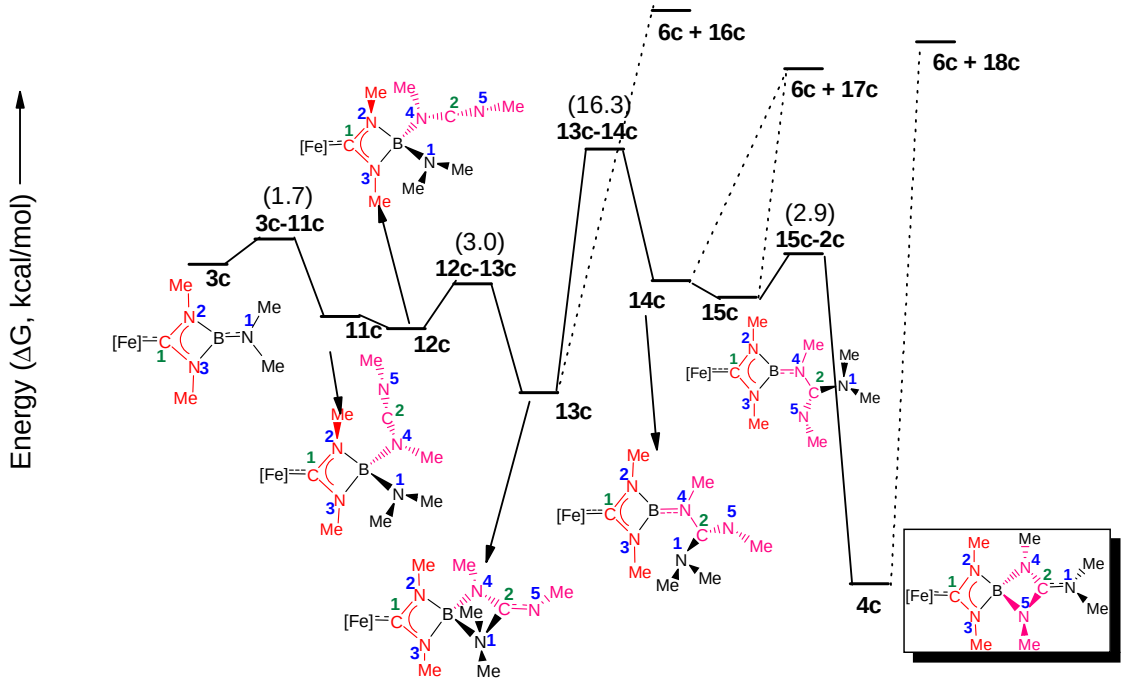


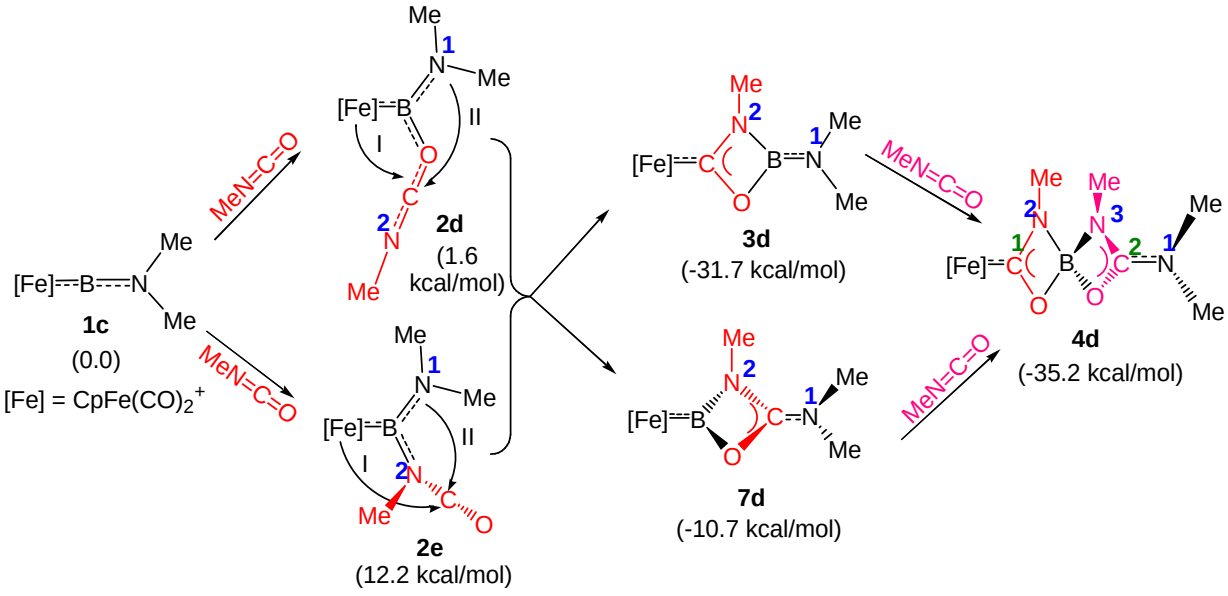
Figure 3.12 Potential energy diagram for the insertion of a second molecule of MeNCNMe into the B=N bond of the intermediate **3c**.

The final steps in the formation of the double insertion product, **4c** occur via intermediates **14c** and **15c**. Breakage of the B-N1 bond in **13c** is endothermic (7.5 kcal/mol) with a corresponding energy barrier of 16.3 kcal/mol and results in **14c**. Subsequent rotation about the C2-N4 bond forms **15c**, which is 1.1 kcal/mol lower in energy. The intermediates **14c** and **15c** are both structurally similar to **3c** with the Me group of **3c** formally being replaced with $C(NMe)NMe_2$. Further rotation about the C2-N4 bond then brings N5 closer to the B atom so that donation of the lone pair of electrons from the nitrogen to the p-orbital at boron can take place resulting in **4c**, the final bis(insertion) product. The final step is exothermic by 19.2 kcal/mol (Scheme 3.11). One other mechanistic alternative is that any of the intermediates **13c, 14c, 15c** and **4c** could undergo breakage of the C1-N2 and B-N3 bonds to form the isonitrile complex **6c** and the boron-containing compounds **16c, 17c** and **18c**.

However, all of these dissociation products are significantly higher in energy than their precursors, presumably due to the high B-N and C-N bond dissociation energies. Consistent with this, only the bis(insertion) product $[CpFe(CO)_2C(NCy)_2B(NCy)_2NR_2]^+[BAr^f_4]^-$ is observed in experimental studies with no trace of the dissociation products, $[CpFe(CO)_2(CNCy)]^+$ being detected.[13]

3.3.4.2 Computational Studies of the Reaction of the Isocyanate, MeNCO with $[CpFe(CO)_2(BNMe_2)]^+[BAr^f_4]^-$

The experimental reactions of the aminoborylene complex $[CpFe(CO)_2(BNCy)_2]^+[BAr^f_4]^-$ with isocyanates, RNCO (R = Ph, Cy, 2,6-Xyl) have been shown to yield the corresponding isonitrile complexes, $[CpFe(CO)_2CNR]^+[BAr^f_4]^-$ **3.1**, **3.2** and **3.3**, in contrast to the reaction bis(insertion) products, **3.6** and **3.7** obtained with carbodiimides.

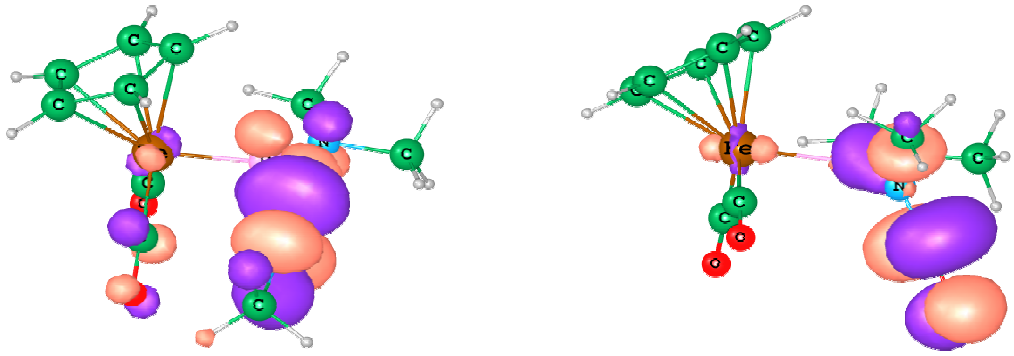


Scheme 3.12 Schematic representation of the two possible pathways for formation of the model double insertion product **4d**

The main difference between carbodiimides and isocyanate nucleophiles is the fact that the latter can attack the electrophilic boron centre of **1c** via O-attack or N-attack; the reaction can then proceed by insertion into either the Fe=B bond or the B=N bond (Scheme 3.12). As with the carbodiimide reaction however, Fe=B insertion is thermodynamically more favourable (by 21.0 kcal/mol) than B=N insertion. In addition, the increased availability of the HOMO (mainly iron d-orbital) compared to the deeper lying HOMO-2 (a nitrogen lone pair) in the donor/acceptor adduct **2d** (as in **2c**) implies a greater *rate* of formation for the Fe=B insertion product. Therefore, computational studies have analysed both the oxygen and nitrogen attack pathways but only for insertion into the Fe=B bond.

3.3.4.2.1 Insertion of the First Equivalent of MeNCO

Formation of the donor/acceptor adduct by either O-attack or N-attack, requires interaction between the lone pair of electrons at oxygen (**2d**) or nitrogen (**2e**) with the LUMO of **1c**, largely located on the boron atom (Figure 3.13). The energy change on formation of the N-bound isomer, **2e** is endothermic at +12.2 kcal/mol with an energy barrier of 18.2 kcal/mol, possibly due to the steric bulk at nitrogen. The methyl group in **2e** lies in a plane perpendicular to Fe, B and N1 and so creates more of a hindrance for the lone pair on nitrogen to attack the boron centre, compared to oxygen, **2d** which is able to lie in the same plane as Fe, B and N1 and results in a smaller energy change of only +1.6 kcal/mol and an energy barrier of 3.0 kcal/mol. Mulliken population analysis also supports the idea that O-attack is more facile than N-attack as O is more negatively charged (-2.262) than N (-0.005).



LUMO+4
(-0.1476)

LUMO
(-0.2387)

Figure 3.13 The LUMO+4 of the acyclic intermediate **2d** and the LUMO of **2e**

The next step is the formation of the metallacyclic four-membered ring intermediates, **5d /5e** via the donation of electron density from the HOMO into the LUMO+4 (-0.1476 a.u.) or LUMO (-0.2387 a.u.) of the intermediates **2d** or **2e** respectively, which are both antibonding in character and mainly located on C1 of the NCO fragment (Scheme 3.13/3.14, Figure 3.13). Formation of **5e** is more favourable, being exothermic (by 9.3 kcal/mol) compared to the endothermic formation of **5d** (14.9 kcal/mol). The LUMO+4 (on **2d**) is so high lying that interaction with the HOMO of the iron borylene complex makes **5d** less stable and results in an elongation of the C1-O bond from 1.241 Å in **2d** to 1.468 Å, compared to the less pronounced lengthening in **2e** (1.264 Å to 1.382 Å in **5e**).

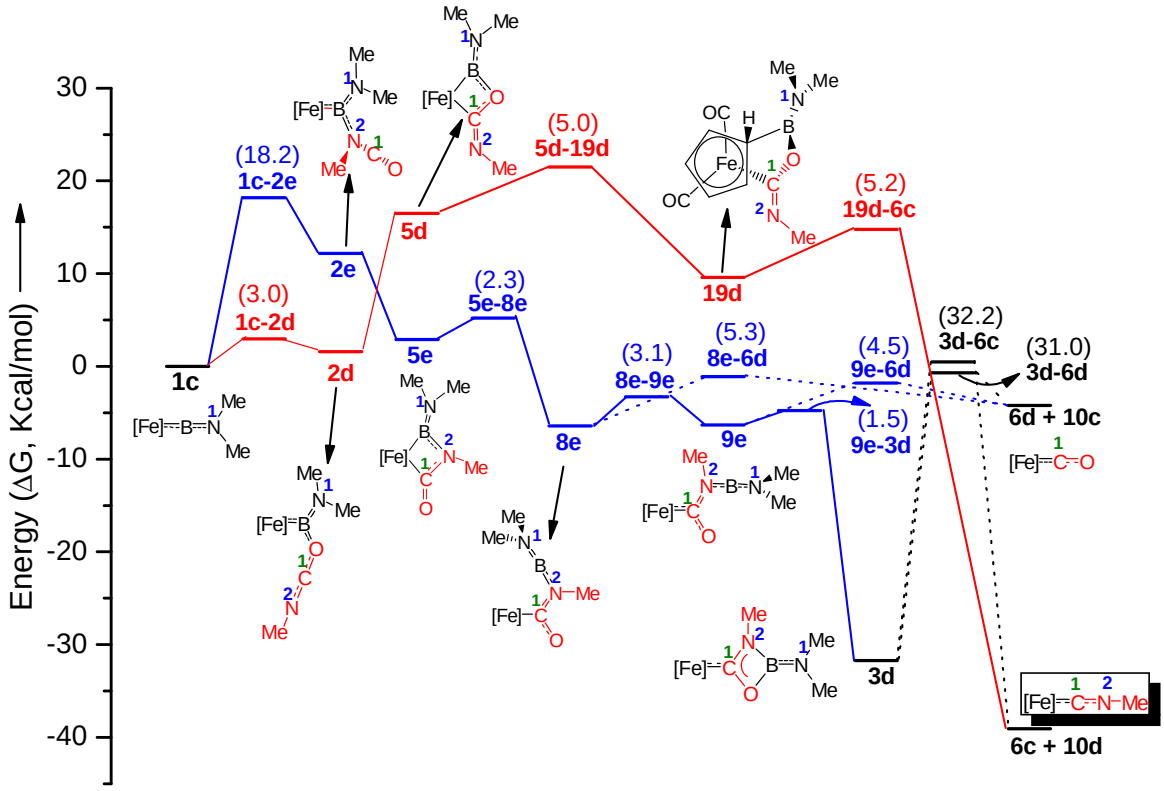
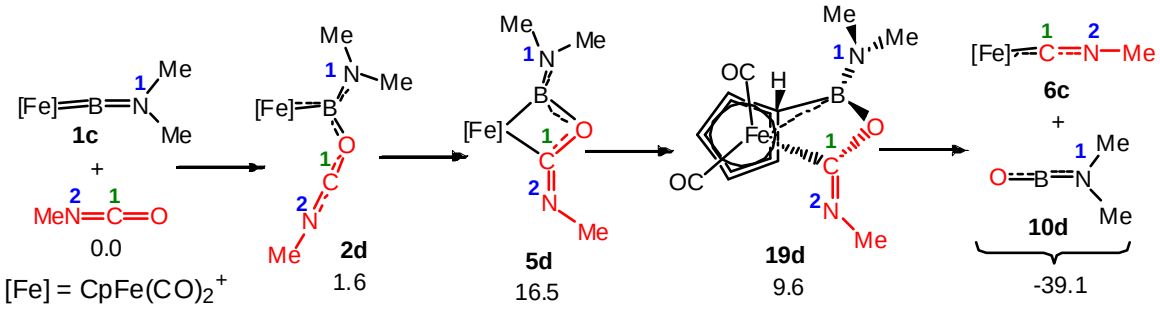
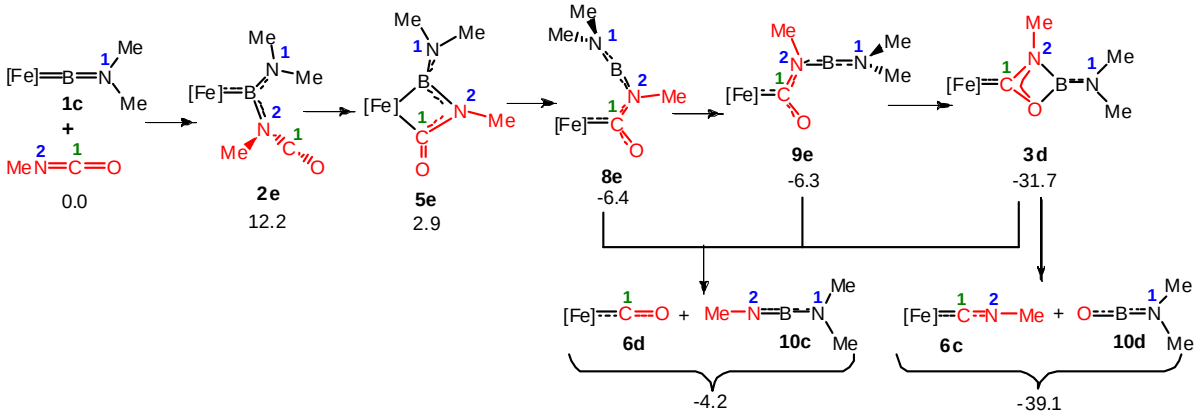


Figure 3.14 Potential energy diagram for the reaction of one equivalent of MeNCO into the Fe=B bond of **1c**.

Following the oxygen attack pathway we see that rearrangement of **5d** to **19d** is exothermic by 6.9 kcal/mol with a concomitant energy barrier of 5.0 kcal/mol (Scheme 3.13, Figure 3.14). The intermediate formed has an unusual structure in that the boron atom forms a bond with one of the carbon atoms on the Cp ring [*d*(B-C) = 1.690 Å][26] and the Fe-B distance is elongated to 2.644 Å which is outside the sum of the covalent radii of iron and boron (ca. 2.05 Å).[27] The intermediate **19d** dissociates in a highly exothermic reaction (48.7 kcal/mol) with an energy barrier of 5.2 kcal/mol to form the metathesis products **6c** and **10d** by cleavage of the C(Cp)-B and C1-O bonds.



Scheme 3.13 Mechanism for the insertion of one equivalent of MeNCO into the Fe=B bond of **1c** via the oxygen attack pathway.

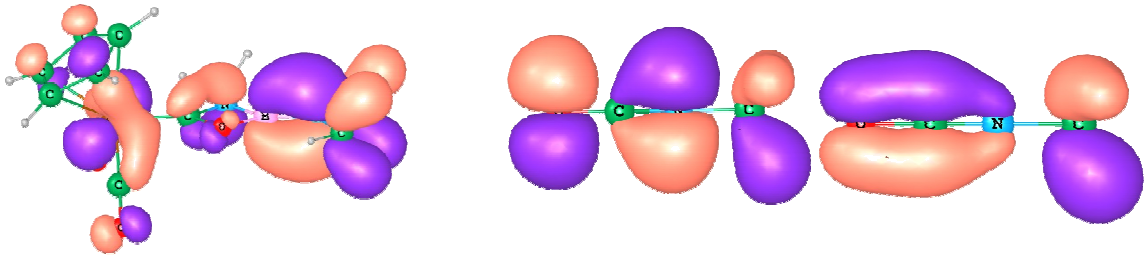


Scheme 3.14 Mechanism for the insertion of one equivalent of MeNCO into the Fe=B bond of **1c** via the nitrogen attack pathway.

The intermediate **5e** on the other hand (Scheme 3.14), rearranges to form the acyclic intermediate **8e**, which is similar to the intermediate formed in the carbodiimide reaction (**8c**). **8e** is formed by breaking the Fe-B bond in **5e** which is an exothermic process (9.3 kcal/mol) with an energy barrier of 3.3 kcal/mol. Rotation about the C-N2 bond in **8e** forms another intermediate **9e**, which cyclizes to the four-membered ring **3d** by donation of the lone pair of electrons on oxygen to boron. The energy change for this cyclization is 1.5 kcal/mol with

formation of an additional donor/acceptor bond being exothermic by 25.4 kcal/mol. As with the carbodiimide reaction, both intermediates **8e** and **9e** can dissociate to form the metathesis products **6d** and **10c** by scission of the C-N2 bond. However, this transformation is found to be endothermic by 2.2 kcal/mol and therefore thermodynamically unfavourable. The mono(insertion) product, **3d** can also undergo dissociation at both the C1-N2 and O-B bonds to form **6d** and **10c**. However, this process is also endothermic (27.5 kcal/mol) with an energy barrier of 31.0 kcal/mol. Dissociation of the bonds C1-O and B-N2 to form **6c** and **10d**, however, is exothermic by 7.4 kcal/mol, but the energy barrier is very high at 32.2 kcal/mol. It is likely that formation of the stronger B-O bond in **10d** (192.6 kcal/mol) plays a major role in stabilizing the dissociation products formation in comparison to **3d** (Scheme 3.13).

(a) (b)



HOMO (-0.4209) HOMO (-0.2834) HOMO-2 (-0.4254)

Figure 3.15 a) The HOMO of the cyclic intermediate **3d**. b) The HOMO and HOMO-2 of MeNCO.

To summarize, reaction of the borylene with isocyanates via O-attack leads exclusively to the metathesis product **6c**. On the other hand N-attack leads to the formation of the single insertion product, **3d**, which could dissociate to form **6c** only be overcoming a significant energy barrier and an endothermic reaction profile. Formation of the

donor/acceptor adduct via O-attack, **2d** is kinetically more favourable with an energy barrier of 3.0 kcal/mol versus N-attack, **2e** (18.2 kcal/mol) due, in part, to the steric bulk around nitrogen compared to oxygen. The computational data are consistent with the experimental analysis in that reaction of the aminoborylene complex, $[CpFe(CO)_2(BNCy_2)]^+[BAr^f_4]^-$ with RNCO (R = Ph, Cy, 2,6-Xyl) forms the isonitrile product, $[CpFe(CO)_2(CNR)]^+[BAr^f_4]^-$, **3.1, 3.2** and **3.3** as the major product. The ESI-MS results however, reveal the presence of small quantities of $[CpFe(CO)_3]^+$ (**6d**) which implies that the N-attack pathway is also active, since formation of **6d** by O-attack is kinetically unfavourable.

The kinetics of the initial O-attack/N-attack give further evidence for the products obtained for the reactions of the aminoborylene with PhNCO and 2,6-XylNCO. The two methyl groups in the ortho positions of the 2,6-XylNCO sterically hinder the approach of the lone pair of electrons on the nitrogen to the boron centre in N-attack compared to O-attack. Hence O-attack is more favourable and so the isonitrile product **3.3** is obtained, which agrees with the ESI-MS experimental results. PhNCO on the other hand, is less sterically bulky and so attack by either O or N is feasible and thus **6c** is formed as the major product (O-attack) but **6d** is also obtained as a minor product (N-attack). This is also in agreement with experimental results.

The energy barriers for the initial O-attack/N-attack have also been calculated for the reaction with PhNCO and 2,6-XylNCO. For PhNCO, O-attack (4.7 kcal/mol) was found to be more favourable than N-attack (18.3 kcal/mol); these figures are comparable to those found for the model system, MeNCO. The energy barrier for N-attack in the case of 2,6-XylNCO was significantly higher at 23.9 kcal/mol (compared to PhNCO) owing to the extra steric bulk around the isocyanate nitrogen afforded by the two methyl groups. The O-attack pathway

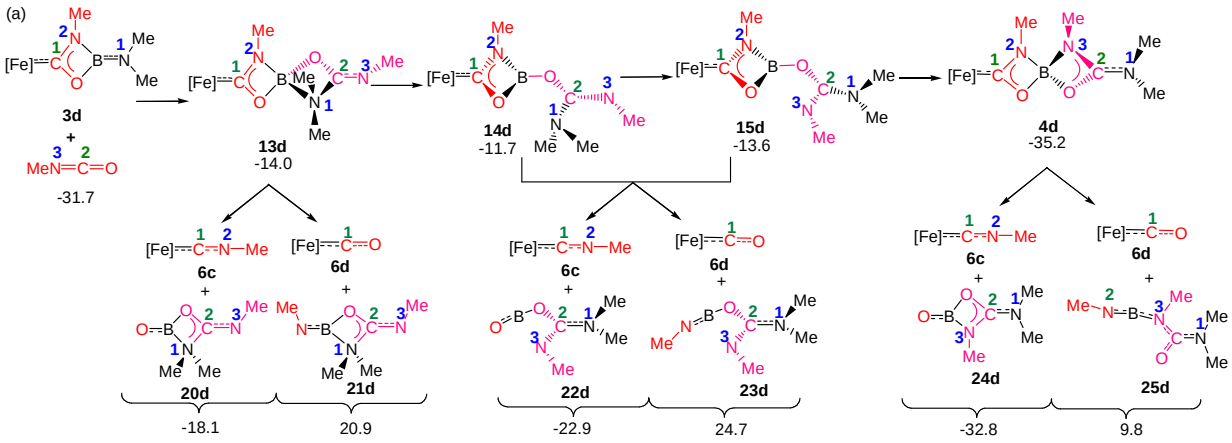
barrier (4.4 kcal/mol) however, remained virtually unchanged in energetic terms. The studies show that the N-attack pathway leads to the insertion reaction, whereas, the O-attack pathway leads to a metathesis reaction and the results agree with an earlier study reported by Jemmis *et al*. which revealed that substrates having more polar bonds (contain a low-lying σ* molecular orbital) prefer boron metathesis type reactions, compared to substrates containing less polar bonds.[8]

3.3.4.2.2 Insertion of the Second Equivalent of MeNCO

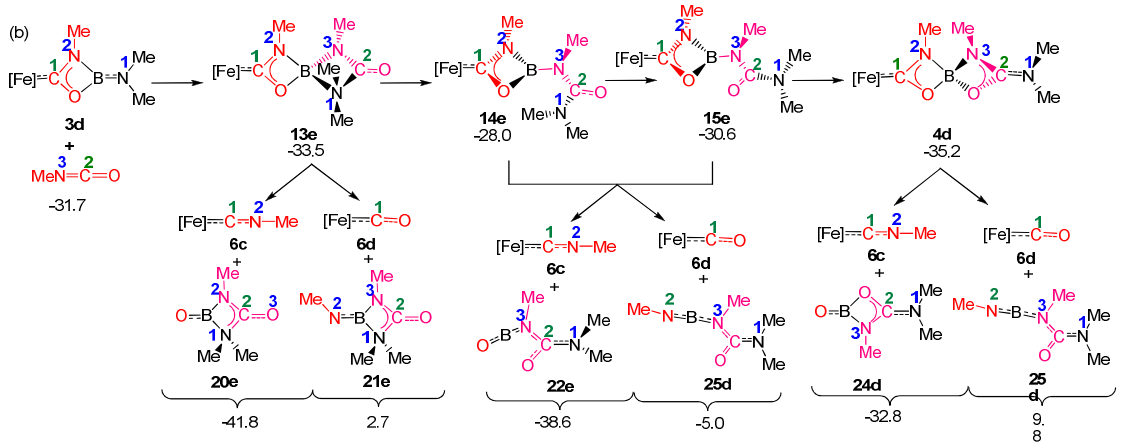
As previously discussed, the mono(insertion) product, **3d** has a high energy barrier for dissociation into either **6c** or **6d**, and therefore in the presence of excess isocyanate, **3d** can react further by other pathways. As with the first insertion process, there are two ways in which this can occur, via O-attack (**13d**) (Scheme 3.15) or N-attack (**13e**) at boron (Scheme 3.16).

The formation of the bicyclic intermediate **13d** or **13e** takes place via a [2+2] cycloaddition reaction between the B-N π orbital of **3d** (HOMO) and the C2-N (HOMO) or C2-O (HOMO-2) π orbital of the isocyanate. There is an increase in the B-N1 bond length from 1.363 Å to 1.630 Å (**13d**) or 1.621 Å (**13e**) reflecting a reduction in the B-N multiple bonding character. As with the first insertion process, the energy barriers for the formation of both the B-O (23.8 kcal/mol) and B-N (20.5 kcal/mol) are comparable; however, **13d** is less stable than the corresponding intermediate **13e** by 19.5 kcal/mol (Figure 3.16). Once again, there are two possible ways in which **13d**/**13e** can dissociate, either by scission of the C1-O and B-N2 bonds to form **6c**, or by breakage of the C1-N2 and B-O bonds to give **6d**. In each case, formation of **6c** is the most energetically favourable, with formation of **6d** being

endothermic. From a thermodynamic perspective, the bond enthalpies for the C-N (179.5 kcal/mol) and B-O (192.6 kcal/mol) bonds are greater than that for the summation of the C-O (256.3 kcal/mol) and B-N (92.7 kcal/mol) bonds by 23 kcal/mol.[25] Therefore breakage of the C1-O and B-N2 bonds seems more likely, resulting in formation of the isonitrile complex product **6c** rather than **6d**. Despite this, it is worth noting that the energy barriers to the formation of the isonitrile are not insignificant, indicating that **13d**/**13e** may be present in solution for a marked lifetime. This result is consistent with results from the ESI-MS analysis for the reaction of borylene with PhNCO, where a species was identified corresponding to the borylene complex with two equivalents of isocyanate.



Scheme 3.15 Mechanism of the insertion of a second molecule of MeNCO into the B=N bond of **3d** via the oxygen attack pathway.



Scheme 3.16 Mechanism of the insertion of a second molecule of MeNCO into the B=N bond of **3d** via the nitrogen attack pathway.

An alternative route for the formation of the bis(insertion) product from the bicyclic intermediates **13d**/**13e** is via the acyclic O-bound intermediates **14d** and **14d** or the more stable N-bound species **14e** and **15e**. Formation of **14d** from **13d** by cleavage of the B-N1 bond is endothermic by 13.5 kcal/mol and formation of **14e** from **13e** is 20.8 kcal/mol. Despite this, **14e** was found to be more stable that **14d** by 14.4 kcal/mol. Subsequent formation of the more stable intermediates, **15d** and **15e** occurs by rotation about the C2-O or C2-N3 bonds respectively. Here too, **15d** and **15e** can also dissociate to form **6c** (and **2d** and **22e**) by breakage of C1-O and N2-B or C1-N2 and O-B. The isonitrile, **6c** formed by scission of C1-O and N2-B is more stable than the preceding intermediate. Breakage of C1-N2 and O-B however, leads to formation of the carbonyl complex **6d** which is an endothermic process (38.3 and 23.0 kcal/mol for **15d** and **15e** respectively). The analogous bis(insertion) product **4d**, which was formed in the carbodiimide reaction, can also be accessed from **15d** and **15e** by an exothermic process (22.6 and 4.6 kcal/mol respectively).

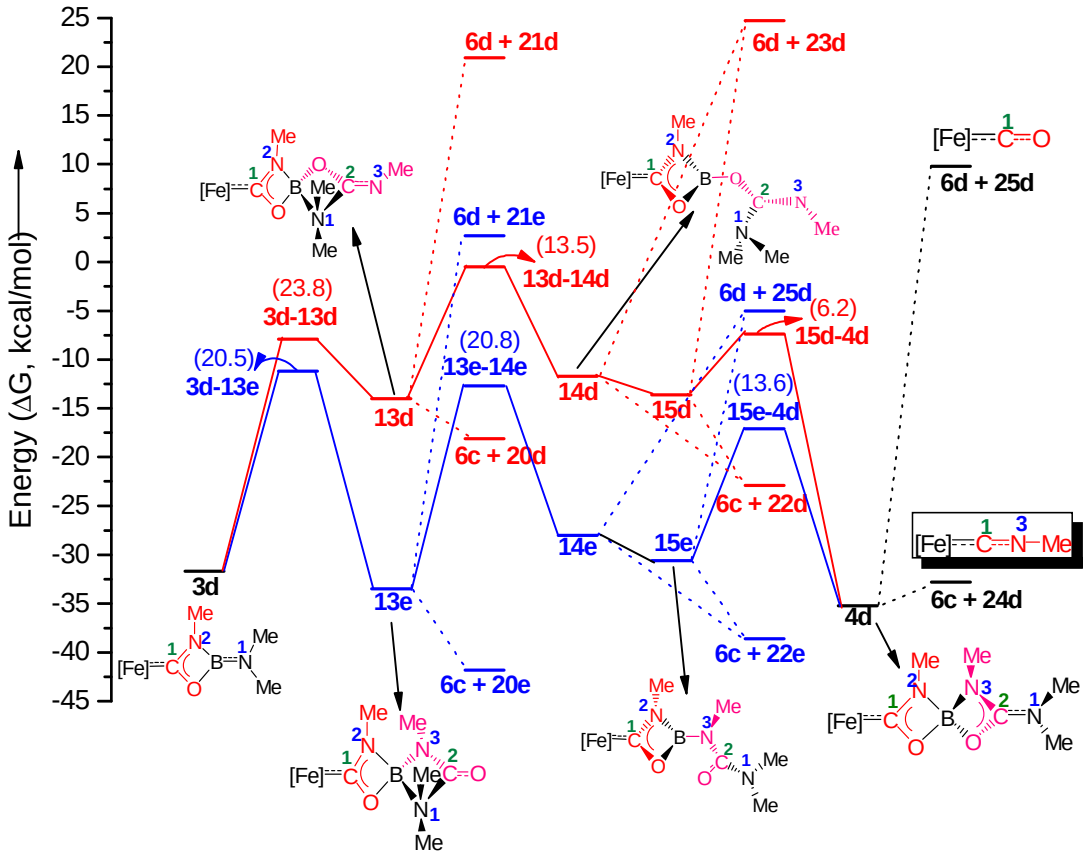


Figure 3.16 Potential energy diagram for the reaction of MeNCO into the B=N bond of the complex **3d**.

Thus, while the conversions of **13d**/**13e** into **14d**/**14e** are endothermic reactions, the alternative dissociation pathways for **13d**/**13e** to form **6c** are exothermic. Hence, formation of the isonitrile complex, **6c** is thermodynamically favourable which is consistent with the experimentally observed product distribution.

The four membered ring in the intermediates **13d** and **13e** (BOC2N1 and BN3C2N1) are devoid of delocalisation over all four atoms in the ring due to the tetra coordination at N1. They are both therefore less stable than the final spirocyclic product **4d**, in which both rings are delocalised over the three atoms N, C and O. However, the energies of both **13e** and **4d** are

very close (1.7 kcal/mol). There is also a possibility that **4d** can dissociate to form **6c** or **6d**. **4d** was found to be more stable than the dissociated products **6c** and **24d** by 2.4 kcal/mol and than **6d** and **25d** by 45.4 kcal/mol, thus it is unlikely that formation of the metathesis products occurs via this route as this would be energetically uphill. The ESI-MS experiments are consistent with an intermediate containing one equivalent of borylene and two equivalents of isocyanate, which is then converted into the isonitrile complex. Given that the energetic calculations for the dissociation of **4d** show this process to be endothermic, the ESI-MS peak is unlikely to be due to **4d** and is most likely due to intermediates **13d** and **13e**, which also have a mass consistent with the assimilation of two isocyanate molecules by the borylene.

3.4 Conclusions and Suggestions for Further Research

The reaction of aminoborylenes $[CpFe(CO)_2(BNR_2)]^+[BAr^f_4]^-$ (R = Cy, ^{i}Pr) with heteroallenes such as isocyanates and carbodiimides have been investigated. Reactions with dicyclohexylcarbodiimide (CyNCNCy) results in the first examples of insertion into a M=B bond and yields the spirocyclic boronium complexes, $[CpFe(CO)_2C(NCy_2)B(NCy_2)CNCy_2]^+[BAr^f_4]^-$ (**3.6**) and $[CpFe(CO)_2C(NCy_2)B(NCy_2)CN^iPr_2]^+[BAr^f_4]^-$ (**3.7**) by assimilating two equivalents of the substrate, one into each of the Fe=B and B=N bonds.[13] Low temperature NMR experiments were instrumental in understanding the reaction mechanism, and both the donor/acceptor adduct $[CpFe(CO)_2(B(NR_2)(CyNCNCy)]^+$, **3.4** and the mono(insertion) complex, $[CpFe(CO)_2C(NCy_2)BNR_2]^+$, **3.5** were identified as intermediates, with the latter being crystallographically characterized. Isocyanates, RNCO (R = Ph, Cy, 2,6-Xyl) on the other hand react to form the corresponding isonitrile complexes, $[CpFe(CO)_2(CNR)]^+$ (**3.1**, **3.2** and

3.3) via a net oxygen abstraction process.[9] Both carbodiimides and isocyanates appear to pre-coordinate at the boron centre, which is possibly why these aminoborylene complexes are unreactive towards the more weakly nucleophilic CO_2 molecule. Both substrates also showed preference for initial insertion into the Fe=B bond rather than the B=N bond of the aminoborylene complex (25.3 kcal/mol and 21.0 kcal/mol more stable for insertion of carbodiimide and isocyanate into the Fe=B bond rather than the B=N bond respectively).

A detailed computational analysis was carried out in an attempt to explain the different reaction pathways taking place.[25] The study reveals that formation of the bis(insertion) products, **3.6** and **3.7**, rather than the related isonitrile complex $[CpFe(CO)_2(CNR)]^+$ (R = Cy, ^{i}Pr) is the most kinetically and thermodynamically favourable process for CyNCNCy. The reaction proceeds by initial coordination of the carbodiimide substrate at the electrophilic boron centre, followed by migration of the metal fragment in a cooperative reaction.[22] The nucleophilic transition metal fragment thus attacks the electrophilic carbon atom of the carbodiimide substrate (which has been polarised on coordination) thereby leading to insertion of the substrate between the metal and boron centres. This mechanism is different to classical insertion reactions, in which coordination of the substrate at the metal takes place followed by migration of the ligand.

In comparison, the reaction with isocyanates could viably proceed via metathesis or insertion, a factor arising from the potential for the substrate to attack through oxygen or nitrogen. Initial coordination through oxygen was found to be the most kinetically favourable, and resulted in the metathesis product, $[CpFe(CO)_2(CNR)]^+$. Insertion chemistry however, was found to be feasible if the isocyanate attacked through the nitrogen donor. Further reaction of the mono(insertion) species with excess isocyanate to form the bis(insertion)

product however, seems unlikely, due to a number of competing, low energy reaction pathways which ultimately yield $[CpFe(CO)_2(CNR)]^+$.

An interesting possibility for further research would be to adjust the electronics of the aminoborylene complex accordingly in order to increase the likelihood of initial insertion into the B=N bond rather than the Fe=B bond. The strength of the B=N bond compared to the Fe=B bond is a major factor in the preference for Fe=B attack, so increasing the strength of the Fe=B bond would be vital. One option would be to substitute the carbonyl ligands on the transition metal iron centre, for trialkyl phosphine groups. Trialkyl phosphines are good σ-donors but poor π-acceptors which would result in an increase in electron density on iron which could in turn be back-bonded to the boron centre, strengthening the Fe=B bond. I have recently formed mono- and bis(phosphine) substituted aminoborylene complexes and these results are discussed in Chapter Five.[9] An alternative option would be to substitute the BNR_2 group for BPR_2 resulting in a weaker B=X bond (X = P, N) thus promoting insertion into the B=X bond rather than the Fe=B bond.

3.5 References for Chapter Three

1. (a) H. Braunschweig, M. Colling, *Coord. Chem. Rev*., 2001, **223**, 1. (b) H. Braunschweig, M. Colling, *Eur. J. Inorg. Chem*., 2003, 393. (c) H. Braunschweig, *Adv. Organomet. Chem*. 2004, **51**, 163. (d) S. Aldridge, D. L. Coombs, *Coord. Chem. Rev*., 2004, **248**, 535. (e) H. Braunschweig, D. Rais, *Heteroatom Chem*., 2005, **16**, 566. (f) H. Braunschweig, G. R. Whittell, *Chem. Eur. J*., 2005, **11**, 6128. (g) H. Braunschweig, C. Kollann, D. Rais, *Angew. Chem. Int. Ed*., 2006, **45**, 5254. (h) S. Aldridge, D. L. Kays, *Main Group Chem*., 2006, **5**, 223. (i) H. Braunschweig, C. Kollann, F. Seeler, *Contemporary Metal Boron Chemistry I*, eds. T. B. Marder, Z. Lin, Springer, 2008, Vol. 130, p 1. (j) D. L. Kays, S. Aldridge, *Contemporary Metal Boron Chemistry I*, eds. T. B. Marder, Z. Lin, Springer, 2008, Vol. 130, p 29. (k) D. Vidovic G. A. Pierce, S. Aldridge, *Chem. Comm*., 2009, 1157.
2. (a) G. P. Mitchell, T. D. Tilley, *J. Am. Chem. Soc*., 1997, **119**, 11236. (b) R. R. Schrock, *J. Chem. Soc., Dalton Trans*., 2001, 2541. (c) T. M. Trnka, R. H. Grubbs, *Acc. Chem. Res*., 2001, **34**, 18.
3. (a) D. L. Coombs, S. Aldridge, C. Jones, D. J. Willock, *J. Am. Chem. Soc*., 2003, **125**, 6356. (b) D. L. Coombs, S. Aldridge, A. Rossin, C. Jones, D. J. Willock, *Organometallics*, 2004, **23**, 2911.
4. S. Aldridge, C. Jones, T. Gans-Eichler, A. Stasch, D. L. Kays (née Coombs), N. D. Coombs, D. J. Willock, *Angew. Chem. Int. Ed*., 2006, **45**, 6118.
5. D. L. Kays (née Coombs), J. K. Day, L. –L. Ooi, S. Aldridge, *Angew. Chem. Int. Ed*., 2005, **44**, 7457.

6. D. L. Kays, J. K. Day, S. Aldridge, R. W. Harrington, W. Clegg, *Angew. Chem. Int. Ed*., 2006, **45**, 3513.

7. H. Braunschweig, M. Burzler, K. Radacki, *Angew. Chem. Int. Ed*., 2007, **46**, 8071.

8. S. De, P. Parameswaran, E. D. Jemmis, *Inorg. Chem*., 2007, **46**, 6091.

9. G. A. Pierce, D. Vidovic, D. L. Kays, N. D. Coombs, A. L. Thompson, D. J. Willock, E. D. Jemmis, S. De, S. Aldridge, *Organometallics*, 2009, **28**, 2947.

10. W. P. Fehlhammer, A. Mayr, *J. Organomet. Chem*., 1980, **191**, 153.

11. H. Nakazawa, M. Itazaki, M. Owaribe, *Acta. Cryst*., 2005, **61**, 1073.

12. D. J. Darensbourg, W-Z. Lee, J. C. Yarbrough, *Inorg. Chem*., 2001, **40**, 6533.

13. (a) G. A. Pierce, N. D. Coombs, D. J. Willock, J. K. Day, A. Stasch, S. Aldridge, *Dalton Trans*., 2007, 4405. (b) G. A. Pierce, S. Aldridge, C. Jones, T. Gans-Eichler, A. Stasch, N. D. Coombs, D. J. Willock, *Angew. Chem. Int. Ed*., 2007, **46**, 2043.

14. W. E. Piers, S. C. Bourke, K. D. Conroy, *Angew. Chem. Int. Ed*., 2005, **44**, 5016.

15. (a) D. J. Brauer, S. Buchheim-Spiegel, H. Burger, R. Gielen, G. Pawelke, J. Rothe, *Organometallics*, 1997, **16**, 5321. (b) A. Ansorge, D. J. Brauer, H. Burger, F. Dorrenbach, T. Hagen, G. Pawelke, W. Weuter, *J. Organomet. Chem*., 1991, **407**, 283.

16. M. Findlater, N. J. Hill, A. H. Cowley, *Polyhedron*, 2006, **25**, 983.

17. M. Findlater, N. J. Hill, A. H. Cowley, *Dalton Trans*., 2008, 4419.

18. D. R. Lide, *CRC Handbook of Chemistry and Physics*, 86th eds., Taylor & Francis group, LLC., 2005.

19. H. Brunner, W. Meler, J. Wachter, I.Bernal, E. Raabe, *J. Organomet. Chem*., 1989, **362**, 95.

20. R. Ferede, M. Noble, A. W. Cordes, N. T. Allison, *J. Organomet. Chem*., 1988, **339**, 1.

21. N. J. Hill, J. A. Moore, M. Findlater, A. H. Cowley, *Chem. Comm*., 2005, 5462.

22. L. H. Gade, H. Memmler, U. Kauper, A. Schneider, S. Fabre, I. Bezougli, M. Lutz, C. Galka, I. J. Scowen, M. McPartlin, *Chem. Eur. J*., 2000, **6**, 692.

23. (a) A. Dickinson, D. J. Willock, R. J. Calder, S. Aldridge, *Organometallics*, 2002, **21**, 1146. (b) S. Aldridge, A. Rossin, D. L. Coombs, D. J. Willock, *Dalton Trans*., 2004, 2649.

24. R. Jefferson, M. F. Lappert, B. Prokai, B. P. Tilley, *J. Chem. Soc. A*., 1966, 1584.

25. S. De, G. A. Pierce, Drasko Vidovic, D. L. Kays, N. D. Coombs, E. D. Jemmis, S. Aldridge, *Organometallics*, 2009, **28**, 2961.

26. S. Aldridge, D. L. Kays (née Coombs), A. Al-Fawaz, K. M. Jones, P. N. Horton, M. B. Hursthouse, R. W. Harrington, W. Clegg, *Chem. Comm*., 2006, 2578.

27. J. Emsley, *The Elements*, Oxford University Press: Oxford, 1991.

Chapter Four

Synthesis and Reactivity of Three-Coordinate Amino Boranes and Boryls Towards Dicyclohexylcarbodiimide

4.1 Introduction

Formation of the first N-heterocyclic carbene (NHC) ligands bound to a metal, reported by both Wanzlick[1] and Öfele[2] in 1968 led to an extensive investigation into the structure, coordination modes and reactivity[3] - aspects which are now well understood, with the first stable, crystalline example reported by Arduengo[4] and co-workers in 1991. The ligands have since found a variety of important industrial applications as selective catalysts owing to their strong metal-ligand bonds.[3] One advantage of these ligands is that they are very good σ-donors but poor π-acceptors, and because of this they are often thought of as phosphine mimics. Their reactivity and mode of coordination can also be tuned by appropriate choice of nitrogen substituents, which makes them especially attractive. Since their discovery, there has been an interest in forming N-heterocyclic carbene analogues featuring other main group metal centres other than carbon.

Five- and six-membered N-heterocyclic carbene analogues featuring group 13 metal centres have received sustained interest over the past decade.[5] The long-sought anionic boron N-heterocyclic carbene analogue, boryllithium was synthesized and structurally characterized in 2006 by Yamashita *et al*. and the nucleophilic properties of the complex have been investigated.[6]

In 2004, the first four-membered N-heterocyclic carbene was synthesized by Grubbs and co-workers,[7] and since then, focus has turned to the development of analogous group 13

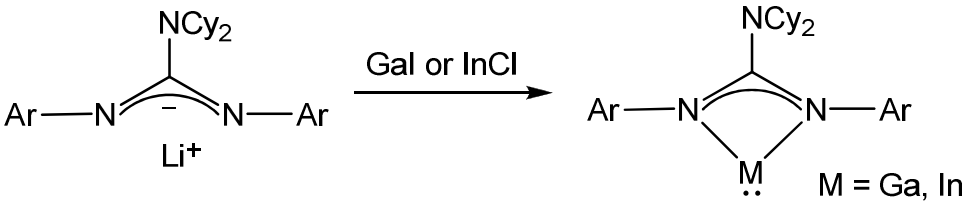
M(I) systems.[8] Complexes containing Ga, In and Tl have been reported but to date, no charge neutral complexes featuring boron have surfaced.

Group 13 N-heterocyclic carbene analogues have found use in a variety of industrial applications; gallium N-heterocyclic carbene analogues for instance have been used as precursors for nitride materials,[9] whilst the aluminium derivatives have been used as active catalysts for olefin polymerization.[10] There have been many studies interested in the structure of these group 13 N-heterocyclic carbene analogues and in understanding their relationship with transition metals in the hope of mimicking the reactivity of N-heterocyclic carbene ligands.[5-10]

One of the inherent challenges associated with formation of these four-membered NHC analogues is in the stabilization of the donor centre from nucleophilic attack. In five- and six-membered N-heterocyclic carbene analogues, the donor centre is sterically protected by bulky nitrogen substituents. In four-membered rings however, this stabilization is not as effective due to the reduced bite-angle of the N-donor-N bond, which in turn leads to a more strained geometry. However, the open donor centres in these compact four-membered rings make them very attractive ligands.[8a]

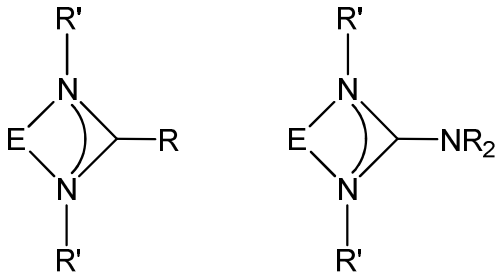
Theoretical studies have been carried out on models of group 13 N-heterocyclic carbene analogues.[5,11] The group 13 metal centre has a lone pair (HOMO) which may be donated to the transition metal centre by σ-donation. In addition, the group 13 metal centre has an empty p-orbital (LUMO), which can participate in π-back donation from the transition metal. The HOMO-LUMO gap for this interaction has been calculated to be large at ca. 60 kcal mol^{-1}, but smaller than for related six-membered heterocycles (ca. 100 kcal mol^{-1}).[8b]

The main synthetic route to these group 13 N-heterocyclic carbene analogues has been via the reaction of amidinate or guanidinate salts with M(I) halides. In 2006 Jones and co-workers reported formation of the first four-membered group 13 metal(I) N-heterocyclic carbene analogues by this route (Scheme 4.1).[8a]



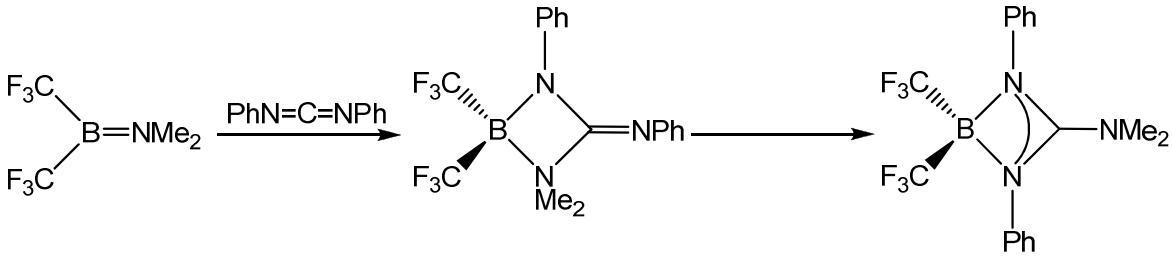
Scheme 4.1 Synthesis of the first four-membered group 13 N-heterocyclic carbene analogues via salt elimination.

The advantage of using amidinate or guanidinate salts is that their steric and metal-binding properties can be tuned by appropriate choice of the nitrogen substituent.[11] It is important for the amidinate/guanidinate used to feature sufficiently bulky nitrogen substituents in order to increase the N-C-N angle (by steric repulsion between the bulky N-substituents and the C-R/CNR backbone) and thereby project the nitrogen σ-donor orbitals towards the electron deficient group 13 metal, favouring chelation.



Scheme 4.2 Amidinate and guanidinate ligands.

The synthesis, structure and reactivity of four-membered amidinate complexes containing boron is an area of research that is receiving increasing attention.[12,13] Cowley *et al*.[13] for example, have synthesized a range of these complexes either by the salt elimination reaction between an amidinate salt and BX_3,[13a] or by insertion of a carbodiimide into B-aryl bonds;[13c] in 2007 they extended this series to include binuclear amidinate complexes.[12d] At the time this research was instituted, however, there was only one crystallographically characterized example of a boron guanidinate in the literature. $Me_2NC(NPh)_2B(CF_3)_2$ was reported by Brauer and co-workers[14] to be formed via a [2+2] cycloaddition reaction of the borane, $Me_2NB(CF_3)_2$ and diphenylcarbodiimide (Scheme 4.3). Since this work was begun only two additional examples have been structurally authenticated, namely $Ph_2NC(NMes)_2BCl_2$ and $Ph_2NC(NDipp)_2BCl_2$.[13e]



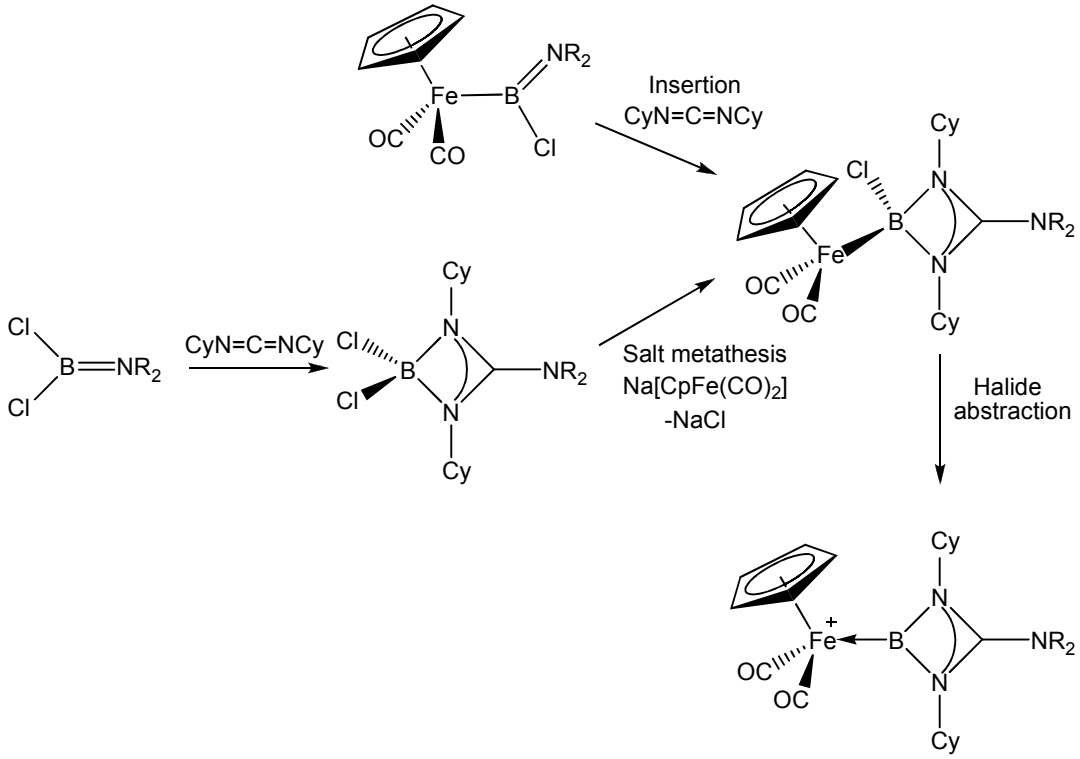
Scheme 4.3 Synthesis of the guanidinate complex, $Me_2NC(NPh)_2B(CF_3)_2$ via [2+2] cycloaddition of PhN=C=NPh.

4.1.1 Aims of the Present Research

Reaction of the cationic aminoborylene, $[CpFe(CO)_2(BNCy_2)]^+[BAr^f_4]^-$ with dicyclohexylcarbodiimide (reported in Chapter Three) proceeds by insertion of the substrate into the Fe=B bond to form the guanidinate complex, $[CpFe(CO)_2C(NCy)_2BNCy_2]^+[BAr^f_4]^-$, and then into the B=N bond to form a spirocyclic four-coordinate boronium complex,

$[CpFe(CO)_2C(NCy)_2B(NCy)_2NCy_2]^+[BAr^f_4]^-$, containing both guanidinate and metalla-amidinate rings.[15]

It was decided to react the aminoboryl complexes, $[CpFe(CO)_2B(NR_2)Cl]$ (R = Cy, ^{i}Pr) and the aminoboranes, R_2NBCl_2 (R = Cy, ^{i}Pr) with dicyclohexylcarbodiimide in the hope of developing synthetic routes to guanidinate(boron) complexes (Scheme 4.5).[13,14] Reaction of the aminoboryl complex with dicyclohexylcarbodiimide offers a route to the synthesis of the guanidinate complex, $[CpFe(CO)_2B\{(NCy)_2CNCy_2\}Cl]$ by insertion into the B=N bond. Halide abstraction could then be used to form the cationic N-heterocyclic carbene analogue, $[CpFe(CO)_2B(NCy)_2CNCy_2]^+ [BAr^f_4]^-$ (Scheme 4.4).[11] An alternative route would be insertion of the substrate into the B=N bond of the aminoborane, a reaction that has precedent in the literature.[14,16] Subsequent salt metathesis, using the nucleophilic reagent, $Na[CpFe(CO)_2]$, would hopefully yield the desired four-coordinate guanidinate complex. It would be especially interesting, given the reaction of the two-coordinate cationic aminoborylene with dicyclohexylcarbodiimide, to see how three-coordinate aminoboryl and aminoborane complexes behave towards the heteroallene, and how the reactivity varies with different substituents at the boron centre.[15]



Scheme 4.4 Potential route to four-membered cationic N-heterocyclic carbene analogues.

4.2 Experimental

*Synthesis of [$Cy_2NC(NCy)_2BCl_2$] (**4.1**) via the reaction of dicyclohexylcarbodiimide with the aminoboryl complex [$CpFe(CO)_2B(NCy_2)Cl$]*

To a solution of [$CpFe(CO)_2B(NCy_2)Cl$] (0.03 g, 0.08 mmol) in deuterated toluene was added a solution of CyNCNCy (2.1 equiv.) also in deuterated toluene (2 cm^3) and the reaction mixture heated at 65˚C for 336 h. The reaction was monitored by ^{11}B NMR and judged to be complete by the disappearance of the peak at δ_B 58 and formation of $Cy_2NC(NCy)_2BCl_2$ (δ_B 4). Yield of **4.1**: 0.02 g, 49%. ^1H NMR (300 MHz, C_6D_6) δ 0.65–2.31 (overlapping m, 40H, CH_2 of Cy), 3.14 (overlapping m, 4H, CH of Cy). ^{13}C NMR (76 MHz, C_6D_6) δ 24.2, 24.4 (4-CH_2 of Cy), 25.1, 25.5 (3-CH_2 of Cy), 30.6, 32.3 (2- CH_2 of Cy), 54.9, 58.2 (CH of Cy), 160.9

(guanidinate quaternary). ^{11}B NMR (96 MHz, $C_6D_5CD_3$) δ 4 (s, fwhm ca. 19 Hz). IR (benzene soln, cm^{-1}) υ(CN) 1618. MS (electron ionization) m/z (%) 467 (weak) M^+, 432 (72) $(M-Cl)^+$; exact mass (calc. for M^+) m/z 466.3036, (obs.) 466.3033. Elemental analysis (calc. for $C_{25}H_{44}BCl_2N_3$) C 64.11, H 9.47, N 8.97, (obs.) C 63.88, H 9.28, N 8.78.

*Synthesis of (**4.1**) via the reaction of dicyclohexylcarbodiimide with the aminoborane, Cy_2NBCl_2*

To a solution of Cy_2NBCl_2 (0.20 g, 0.8 mmol) in toluene (10 cm^3) was added a solution of CyNCNCy (0.20 g, 1.0 mmol) also in toluene (10 cm^3). The reaction mixture was heated at 50˚C and progress monitored by ^{11}B NMR spectroscopy. After 36 h, the reaction was judged to be complete by quantitative conversion of the signal at δ_B 29 due to Cy_2NBCl_2 to that at δ_B 4 characteristic of **4.1**. The reaction mixture was filtered, layered with hexanes and cooled to −30˚C yielding crystals suitable for X-ray diffraction. Yield of crystalline product: 0.22 g, 58%. For spectroscopic data see the above method.

*Synthesis of [^{i}Pr$_2$NC(NCy)$_2$BCl$_2$] (**4.2**) via the reaction of dicyclohexylcarbodiimide with the aminoboryl complex [CpFe(CO)$_2$B(N^{i}Pr$_2$)Cl]*

The synthesis of **4.2** was carried out in a similar manner to that of **4.1** via the reaction of the aminoboryl complex [$CpFe(CO)_2B(N^iPr_2)Cl$] with CyNCNCy in deuterated toluene at 65˚C. Yield: 0.01 g, 31%. ^{1}H NMR (300 MHz, CD_2Cl_2) δ 0.86 – 1.79 (m, 32H, CH_2 of Cy and CH_3 of ^{i}Pr), 2.29 (q, $^3J_{HH}$= 8 Hz, 2H, CH of Cy), 3.22 (m, 2H, CH of ^{i}Pr). ^{13}C NMR (76 MHz, C_6D_6) δ 22.4 (CH_3 of ^{i}Pr), 25.3 (4-CH_2 of NCy), 25.5 (3-CH_2 of NCy), 33.2 (2-CH_2 of NCy), 53.1 (CH of Cy), 176.2 (guanidinate quaternary). ^{11}B NMR (96 MHz, $C_6D_5CD_3$) δ 5 (s, fwhm

ca. 11 Hz). IR (benzene soln, cm^{-1}) υ (CN) 1650. MS (electron ionization) m/z (%) 387 (weak) M^+, 344 (25) $(M\text{-}^i Pr)^+$, 309 (100) $(M\text{-}^i Pr\text{-}Cl)^+$. Elemental analysis: (calc. for $C_{19}H_{36}BCl_2N_3$) C 58.78, H 9.35, N 10.82; (obs.) C 58.72, H 9.11, N 10.46.

*Synthesis of [$^i Pr_2NC(NCy)_2BCl_2$](**4.2**) via salt elimination*

4.2 was formed by minor modification of the literature preparation reported by Qi *et al*.[17] To a solution of $^i Pr_2NH$ (1.23 cm^3, 15.00 mmol) in diethyl ether (10 cm^3) was added dropwise a solution of ^{n}BuLi (9.38 cm^3 of a 1.6 M solution in hexanes, 1 equiv.) at -30°C. The reaction mixture was allowed to stir for 1 h, cooled to -80°C and CyNCNCy (3.16 g, 15.3 mmol) in diethyl ether (20 cm^3) added. Slow warming to room temperature and stirring for 12 h was followed by the addition of water and the removal of volatiles in *vacuo*. The residue was then dissolved in water (20 cm^3), extracted repeatedly with dichloromethane (3 x 30 cm^3) and the combined extracts dried over $MgSO_4$. Filtration, removal of solvent under reduced pressure and recrystallization from hot hexanes yielded $^i Pr_2NC(NCy)(NHCy)$ as a white crystalline solid which was used in subsequent chemistry without further purification (isolated yield: 1.26 g, 27 %).

To a solution of $^i Pr_2NC(NCy)(NHCy)$ (1.26 g, 4.08 mmol) in diethyl ether (20 cm^3) was added ^{n}BuLi (2.55 cm^3 of a 1.6 M solution in hexanes, 4.08 mmol) at -30°C. The reaction mixture was stirred for 1 h, cooled to -80°C and added dropwise to a solution of BCl_3 (4.08 cm^3, 4.08 mmol) in diethyl ether (40 cm^3). After warming to room temperature and stirring for 12 h, volatiles were removed under reduced pressure and the residue extracted with hexanes, concentrated (to ca. 20 cm^3) and cooled to -30°C to yield **4.2** as a white microcrystalline solid. Isolated yield (for second step): 0.477 g, 30 %. For spectroscopic data see the above method.

*Synthesis of [CpFe(CO)$_2$B(NPh$_2$)Cl] (**4.3**)*

4.3 was synthesized by a similar method to that reported by Aldridge *et al.*[18c] A solution of Ph_2NBCl_2 (0.77 g, 3.09 mmol) in diethyl ether (20 cm^3) was added to a suspension of Na[CpFe(CO)$_2$] (0.62 g, 3.09 mmol) in diethyl ether (20 cm^3) and the mixture stirred for 12 h. Volatiles were removed under reduced pressure and the residue extracted into hexanes, concentrated (to *ca.* 5 cm^3) and cooled to −30°C. **4.3** was then obtained as a colourless microcrystalline solid which was washed with cold hexane (2 × 30 cm^3). Crystals suitable for X-ray diffraction were obtained by recrystallization from a hexanes–toluene mixture (ca. 50:1). Yield of crystalline product: 0.62 g, 51%. ^{1}H NMR (300 MHz, CD_2Cl_2) δ 4.67 (s, 5H, Cp), 6.85–7.23 (m, 10H, Ph). ^{13}C NMR (76 MHz, CD_2Cl_2) δ 84.1 (Cp), 125.1, 126.2 (*ortho*-C of Ph), 126.6, 127.8 (*para*-C of Ph), 128.1, 128.5 (*meta*-C of Ph), 146.4, 149.2 (*ipso*-C of Ph), 213.7 (CO). ^{11}B NMR (96 MHz, CD_2Cl_2) δ 61 (b, fwhm ca. 210 Hz). IR (CD_2Cl_2 soln, cm^{-1}) υ(CO) 2011, 1951. MS (electron ionization) m/z (%) 363 (weak) $(M-CO)^+$, 335 (26) $(M-2CO)^+$, 169 (100) $(Ph_2N)^+$; exact mass (calc.) *m*/*z* 363.0290, (obs.) 363.0285.

*Synthesis of [CpFe(CO)$_2$B(NBz$_2$)Cl] (**4.4**)*

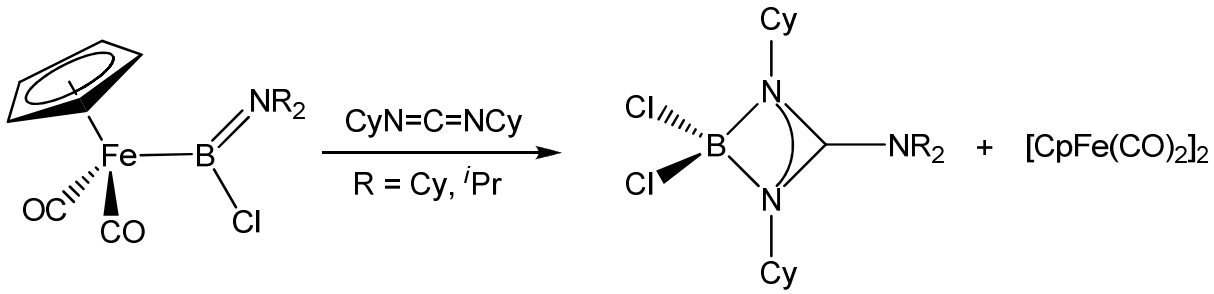
4.4 was synthesized by a similar method reported by Aldridge *et al.*[18c] A solution of Bz_2NBCl_2 (0.40 g, 1.43 mmol) in diethyl ether (20 cm^3) was added to a suspension of Na[CpFe(CO)$_2$] (0.29 g, 1.44 mmol) in diethyl ether (20 cm^3) and the mixture stirred for 12 h. Volatiles were removed in *vacuo* and the residue extracted into hexanes, concentrated (to ca. 5 cm^3) and cooled to -30°C, yielding crystals suitable for X-ray diffraction. Yield of crystalline product: 0.063 g, 11%. ^{1}H NMR (300 MHz, CD_2Cl_2) δ 4.25 (s, 5H, Cp), 4.68 (s, 2H, CH_2Ph), 4.87 (s, 2H, CH_2Ph), 7.13 – 7.47 (m, 10H, CH_2Ph). ^{13}C NMR (76 MHz, CD_2Cl_2), δ 51.8

(CH_2), 55.0 (CH_2), 83.4 (Cp), 126.1 (*ortho*-C of Ph), 126.3 (*ortho*-C of Ph), 126.8 (*para*-C of Ph), 127.7 (*meta*-C of Ph), 127.8 (*meta*-C of Ph), 137.9 (*ipso*-C of Ph), 138.3 (*ipso*-C of Ph), 214.4 (CO). ^{11}B NMR (96 MHz, CD_2Cl_2) δ 58 (b, fwhm ca. 377 Hz). IR (CD_2Cl_2 soln, cm^{-1}) ν (CO) 1996, 1933. MS (electron ionization) m/z (%) 419 (weak) M^+, 362 (100) $(M-2CO)^+$; exact mass (calc. for M^+) m/z 419.0541, (obs.) 419.0544.

4.3 Results and Discussion

4.3.1 Reactions of Carbodiimide with Aminoboryl Complexes

Reaction of the aminoboryl complexes [$CpFe(CO)_2B(NR_2)Cl$] (R = Cy, ^{i}Pr) with CyNCNCy in toluene at 65˚C, somewhat surprisingly yields the corresponding guanidinate complexes $R_2NC(NCy)_2BCl_2$ (R = Cy **4.1**, ^{i}Pr **4.2**), as judged by the disappearance of the peak at δ_B 58 in the ^{11}B NMR spectrum, corresponding to the aminoboryl starting material, and formation of a complex with a resonance of δ_B 4-5 (complete conversion after ca. 336 h).



Scheme 4.5 Formation of $R_2NC(NCy)_2BCl_2$ (R = Cy **4.1**, ^{i}Pr **4.2**)

The ^{11}B NMR signal indicates formation of a four-coordinate boron centre with no metal-boron bonds.[19,15a] Both complexes, **4.1** and **4.2**, were also characterized by multinuclear NMR spectroscopy (^{1}H, ^{11}B, ^{13}C), IR spectroscopy and mass spectrometry, all of which were in accord with formation of guanidinate complexes featuring four-coordinate boron

centres.[13,14] Quaternary amidinate and guanidinate carbon atoms typically resonate in the region 160-170 ppm; the guanidinate quaternary carbon for the complex, $Me_2NC(NPh)_2B(CF_3)_2$, reported by Brauer and co-workers[14] gives rise to a signal at δ_C 160.3 for example, and the resonances for the guanidinate quaternary carbons for both **4.1** and **4.2** were found to be in the same region (δ_C 169.9 **4.1**, δ_C 176.2 **4.2**). In addition to the formation of the guanidinate functional groups revealed by NMR spectroscopy, IR spectroscopy revealed the presence of the organometallic product $[CpFe(CO)_2]_2$, which has a highly diagnostic carbonyl stretching frequency at ca. 1770 cm^{-1} for the bridging carbonyls and 1960 cm^{-1} for the terminal carbonyl ligands (1783, 1953 cm^{-1} and 1773, 1955 cm^{-1} for the reactions forming **4.1** and **4.2** respectively).[20]

The structures of both **4.1** and **4.2** were also confirmed by single crystal X-ray diffraction and the molecular structures are shown in Figure **4.1** and **4.2** respectively. Both **4.1** and **4.2** are the first structurally characterized examples of (guanidinate)boron dihalide complexes. Since this work was instituted Cowley and co-workers have reported the formation and full characterization of a further two (guanidinate)boron dihalide compounds.[13e] Relevant bond lengths and angles for both compounds are given in Tables **4.1** and **4.2**, respectively.

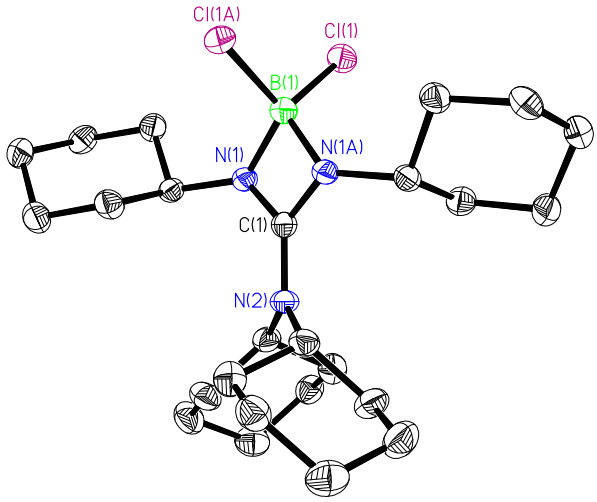


Figure 4.1 Molecular structure of $Cy_2NC(NCy)_2BCl_2$ (**4.1**). Solvent molecule and hydrogen atoms omitted for clarity. Ellipsoids set at the 50% probability level.

Table 4.1 Selected bond lengths [Å] and angles [°] for **4.1**

B(1)-Cl(1)	1.854(2)	B(1)-Cl(1')	1.854(2)
B(1)-N(1)	1.554(3)	B(1)-N(1')	1.553(3)
C(1)-N(1)	1.354(2)	C(1)-N(1')	1.354(2)
C(1)-N(2)	1.348(3)		

N(1)-B(1)-N(1')	84.4(2)	N(1)-C(1)-N(1')	100.9(2)
Cl(1)-B(1)-Cl(1')	108.8(2)		

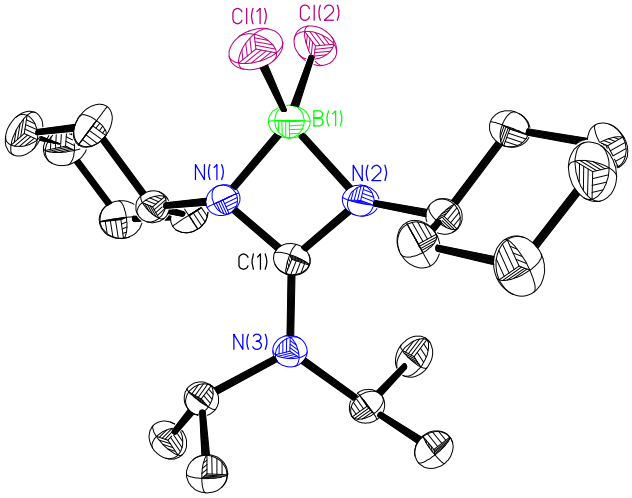


Figure 4.2 Molecular structure of $^{i}Pr_2NC(NCy)_2BCl_2$ (**4.2**). Solvent molecule and hydrogen atoms omitted for clarity. Ellipsoids set at the 50% probability level.

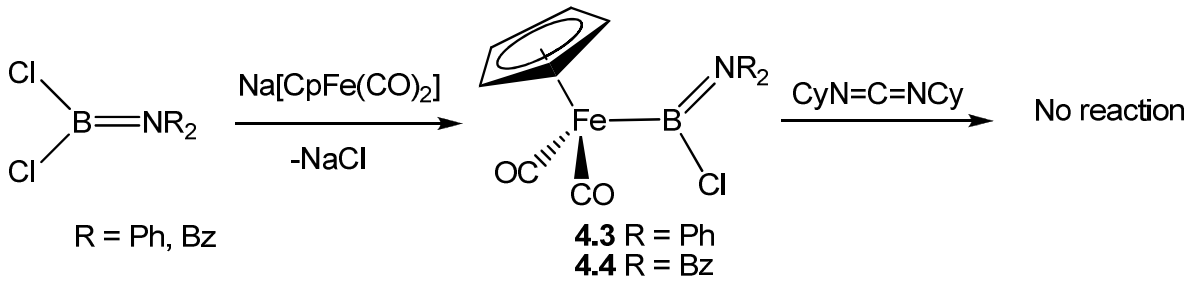
Table 4.2 Selected bond lengths [Å] and angles [°] for **4.2**

B(1)-Cl(1)	1.852(3)	B(1)-Cl(2)	1.853(3)
B(1)-N(1)	1.554(4)	B(1)-N(2)	1.554(4)
C(1)-N(1)	1.356(3)	C(1)-N(2)	1.350(3)
C(1)-N(3)	1.349(3)		

N(1)-B(1)-N(2)	84.4(2)	N(1)-C(1)-N(2)	100.5(2)
Cl(1)-B(1)-Cl(2)	109.1(1)		

The guanidinate rings in both **4.1** and **4.2** are very similar to other boron guanidinate complexes,[13,14] each featuring the expected four-membered BN_2C heterocycle and exocyclic NR_2 moiety (R = Cy, ^{i}Pr). In the related complex, $[Me_2NC(NPh)_2B(CF_3)_2]$, reported by Brauer *et al.*[14a] the C-N bond is short at 1.315(3) Å, which indicates partial double bond character. This π-interaction results in a planar guanidinate ring with a small torsion angle (13.0˚) between the ring plane and the exocyclic NMe_2 substituent. In **4.1** and **4.2** however, the bulkier amino substituents (Cy and ^{i}Pr) enforce a non-coplanar alignment (torsion angles of 28.3 and 30.4˚ for **4.1** and **4.2** respectively) which results in a diminished π-bonding interaction and subsequently longer C-N bonds (1.348(3) and 1.349(3) Å for **4.1** and **4.2** respectively). A similar effect has also been observed in the guanidinate boron dihalides, $[Ph_2NC(NMes)_2BCl_2]$ and $[Ph_2NC(NDipp)_2BCl_2]$ (C-N bond 1.342(2) Å and 1.353(6) Å respectively).[13e] Futhermore, the mean C-N bond distances (within the guanidinate ring) for both complexes are intermediate between those of typical C=N double bonds and C-N single bonds (av. C=N bond = 1.21 Å, C-N bond 1.46 Å)[21] (1.354(2) Å for **4.1**, 1.353(3) Å for **4.2**), and are comparable to those reported by Cowley for $[Ph_2NC(NMes)_2BCl_2]$ and $[Ph_2NC(NDipp)_2BCl_2]$ (1.350(3) and 1.351(6) Å, respectively) which serves to further highlight the delocalization in the guanidinate rings.[13e] The average B-N bond distances for both complexes are 1.554(3) and 1.554(4) Å (for **4.1** and **4.2**, respectively) and are also typical of a four-coordinate boron atom bound to a three-coordinate nitrogen centre (cf. 1.554(3) Å for $[Me_2NC(NPh)_2B(CF_3)_2]$; 1.564(3) Å for $[Ph_2NC(NMes)_2BCl_2]$).[13e,14a] The N-B-N bite angle for both complexes was 84.4(2)˚ which is in the range expected for guanidinate boron dihalide rings (cf. 83.69(14)˚ for $[Ph_2NC(NMes)_2BCl_2]$, 83.4(3)˚ for $[Ph_2NC(NDipp)_2BCl_2]$).

Formation of **4.1** and **4.2** from the interaction of $[CpFe(CO)_2B(NR_2)Cl]$ with CyNCNCy indicates that the reaction pathway involves insertion into the B=N bond at some stage. The forcing conditions employed in the reaction (i.e. heating to 65˚C over a period of 336 h) may however, have led to decomposition of the putative direct insertion product, $[CpFe(CO)_2B\{(NCy)_2CNR_2\}Cl]$, which is likely to be sterically congested at boron. Compounds were therefore targeted which might allow insertion of carbodiimides under milder conditions. Therefore, boryl compounds containing a weaker B=N bond were targeted. One way of weakening the B=N bond is to employ aryl substituents,[22] since the lone pair on nitrogen could conceivably be delocalized into the aromatic system, thereby weakening the B=N π bond. Diaryl substituents were therefore chosen and the complex $[CpFe(CO)_2B(NPh_2)Cl]$ **4.3** (together with $[CpFe(CO)_2B(NBz_2)Cl]$ **4.4** for comparison) was formed by the standard salt elimination route from the corresponding borane, R_2NBCl_2 (R = Ph, Bz) to $Na[CpFe(CO)_2]$ in diethyl ether (Scheme 4.7).[18c] Volatiles were removed under reduced pressure and single crystals suitable for X-ray diffraction of $[CpFe(CO)_2B(NPh_2)Cl]$ (**4.3**) and $[CpFe(CO)_2B(NBz_2)Cl]$ (**4.4**) were isolated by cooling saturated solutions of the complexes in hexanes to -30˚C.



Scheme 4.6 Synthesis of novel aminoboryl complexes $[CpFe(CO)_2B(NR_2)Cl]$ (R = Ph **4.3**, Bz **4.4**), and attempted reaction with dicyclohexylcarbodiimide.

Spectroscopic data support the formulation proposed with the presence of Cp and amino substituents; Ph and Bz, being confirmed by ^{1}H and ^{13}C NMR. The ^{11}B NMR resonance of δ_B 61 for **4.3** and δ_B 58 for **4.4** is typical of an aminoboryl complex (cf. $[CpFe(CO)_2B(NCy_2)Cl]$[18c] δ_B 55, $[CpFe(CO)_2B(N^iPr_2)Cl]$[18a] δ_B 55, $[CpFe(CO)_2B(NMe_2)Cl]$ δ_B 56).[23] Mass spectrometry also indicates formation of **4.3** and **4.4** with the molecular ion being observed in each case, as well as peaks corresponding to loss of one or both carbonyl ligands.

The spectroscopic data for both complexes **4.3** and **4.4** were confirmed by the results of single crystal X-ray diffraction experiments and are illustrated in Figures **4.3** and **4.4** respectively. Relevant bond lengths and angles are also given in Tables **4.3** and **4.4**, respectively.

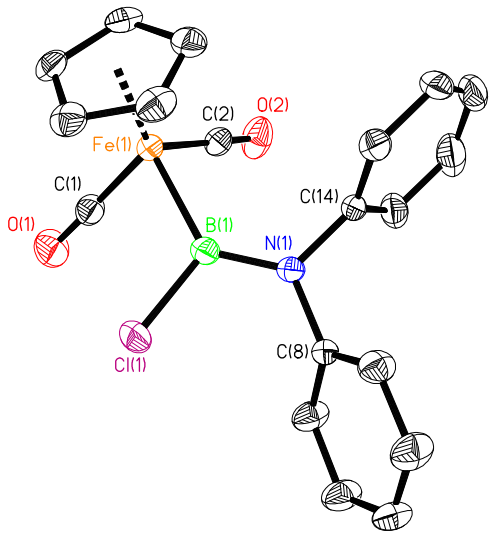


Figure 4.3 Molecular structure of $[CpFe(CO)_2B(NPh_2)Cl]$ (**4.3**). Solvent molecule and hydrogen atoms omitted for clarity. Ellipsoids set at the 50% probability level.

Table 4.3 Selected bond lengths [Å] and angles [°] for **4.3**.

Fe(1)-B(1)	2.022(3)	B(1)-N(1)	1.412(3)
B(1)-Cl(1)	1.824(3)		

Fe(1)-B(1)-Cl(1)	116.2(1)	Fe(1)-B(1)-N(1)	130.2(2)
N(1)-B(1)-Cl(1)	113.5(2)	B(1)-N(1)-C(8)	124.7(2)
B(1)-N(1)-C(14)	122.3(2)	C(8)-N(1)-C(14)	113.0(2)

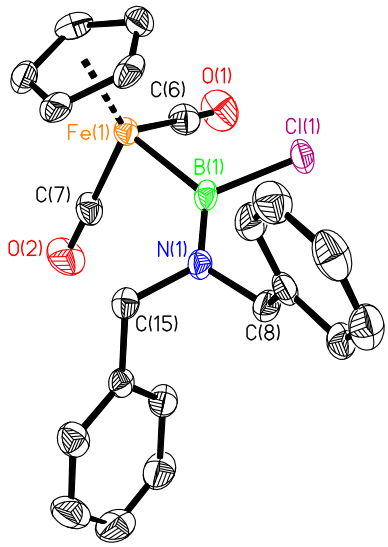


Figure 4.4 Molecular structure of $[CpFe(CO)_2B(NBz_2)Cl]$ (**4.4**). Solvent molecule and hydrogen atoms omitted for clarity. Ellipsoids set at the 50% probability level.

Table 4.4 Selected bond lengths [Å] and angles [°] for **4.4**.

Fe(1)-B(1)	2.036(4)	B(1)-N(1)	1.394(5)
B(1)-Cl(1)	1.837(4)		
Fe(1)-B(1)-Cl(1)	115.4(2)	Fe(1)-B(1)-N(1)	130.3(3)
N(1)-B(1)-Cl(1)	114.2(3)	B(1)-N(1)-C(8)	124.2(3)
B(1)-N(1)-C1(5)	123.9(3)	C(8)-N(1)-C1(5)	111.7(3)

The structures of the chloroboryl complexes display the expected half sandwich geometry at the iron centre, with the coordination sphere completed by two carbonyl ligands and the aminoboryl ligand. The Fe-B distances (2.022(3) and 2.036(4) Å for **4.3** and **4.4** respectively) are similar to related *dialkyl*amino boryl complexes, $[CpFe(CO)_2B(NR_2)Cl]$ (R = ^{i}Pr, Cy 2.054(4) and 2.053(3) Å respectively).[18] The B-N distances of 1.412(3) and 1.394(5) Å respectively (**4.3**, **4.4**) are also comparable to the analogous amino derivatives (1.389(5) and 1.396(4) Å for $[CpFe(CO)_2B(N^{i}Pr_2)Cl]$ and $[CpFe(CO)_2B(NCy_2)Cl]$ respectively).[18] The fact that there is no significant lengthening of the B-N bond in **4.3** conceivably reflects the relative orientations of the boryl and phenyl planes. The two phenyl substituents are oriented at angles of 79.8 and 67.6˚ with respect to the plane defined by the boryl ligand (defined by B(1), Cl(1) and N(1)), presumably due to the steric interaction of the bulky aromatic rings thus minimizing the N-C π overlap (88.8 and 85.6˚ for the orientation of the phenyl rings in **4.4** with respect to the boryl ligand B(1), Cl(1) and N(1)). Formation of an aminoboryl complex featuring the bulky, rigid carbazolyl substituent was also attempted, and although the ^{11}B NMR of the reaction mixture in diethyl ether indicated synthesis of $[CpFe(CO)_2B(NC_{12}H_8)Cl]$, ($\delta_B$ = 56) the complex could not be isolated.

Unfortunately, both **4.3** and **4.4** were unreactive towards carbodiimide, even at relatively forcing conditions of 60˚C over 120 h.

In 2006, Jones *et al.*[11] reported the first example of formation of the gallium, aluminium and indium amidinate complexes; $[CpFe(CO)_2E(X)(amid)]$ (amid = ^{t}BuC(NR$_2$), R = Cy, ^{i}Pr) by a salt elimination reaction between $Na[CpFe(CO)_2]$ and the analogous four-membered amidinate dihalide, $[EX_2(amid)]$. With this in mind, complexes **4.1** and **4.2** were reacted with the same nucleophilic organometallic anion $Na[CpFe(CO)_2]$, in an effort to

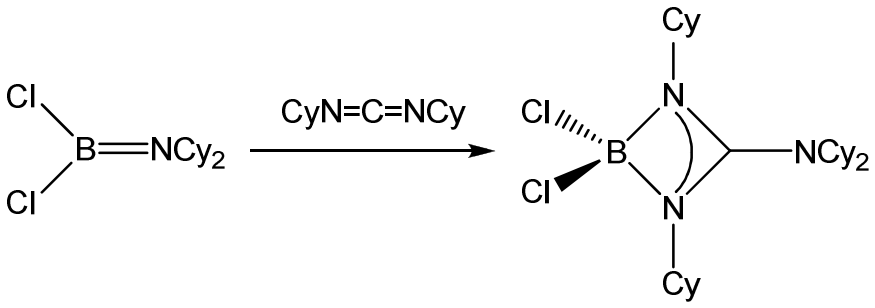
displace one of the halide substituents by the transition metal fragment. The reaction however proved unsuccessful. The steric bulk of the dicyclohexyl nitrogen substituents could possibly be prohibiting nucleophilic attack. Reaction of a related complex, an intramolecular base-stabilised boron dihalide, 6-[(trimethylsilyl)amido]-2-picolyl boron dibromide, with the same nucleophilic reagent, $Na[CpFe(CO)_2]$ has also been reported to be similarly unsuccessful despite attempts to vary the reaction conditions - stoichiometry, solvent, temperature and reaction time.[24] The fact that substitution of a chloride from a four-coordinate gallium centre is possible but does not occur with a four-coordinate boron centre could be due to boron being smaller than gallium and thus more sterically crowded when four-coordinate. Moreover, substitution at a three-coordinate boron centre is possible due to its electrophilicity, whereas the Lewis acidity of the boron centre in a four-coordinate complex would be reduced and so less likely to be susceptible to nucleophilic attack.

4.3.2 Rational Synthetic Routes to Guanidinate Complexes, 4.1 and 4.2

Reaction of the aminoboryl complexes, $[CpFe(CO)_2B(NR_2)Cl]$ (R = Cy, ^{i}Pr) with dicyclohexylcarbodiimide resulted in formation of the guanidinates $[R_2NC(NCy)_2BCl_2]$ (R = Cy, ^{i}Pr) **4.1** and **4.2**. Given these observations it was decided to attempt the more rational synthesis of the same guanidinate complexes either by insertion of the heteroallene into the B=N bond of a simple aminoborane or by salt elimination chemistry. A computational study of the formation of four-membered guanidinate and amidinate rings by insertion of related carbodiimides into Al-N and Al-alkyl bonds respectively was reported by Barry and co-workers in 2005.[25] The proposed mechanism proceeded by initial coordination of a carbodiimide lone pair to the aluminium centre, forming an adduct, followed by migration of

one of the aluminium bound ligands to the carbon of the carbodiimide and finally coordination of the remaining carbodiimide nitrogen donor at aluminium forming the final insertion product. Pre-coordination of the heteroallene to the Lewis acidic metal centre is thus thought to be a key step in the insertion mechanism. Furthermore Gambarotta[26] has proposed that initial coordination of the substrate provides a close geometric proximity for the migrating group and also enhanced polarization of the inserting molecule. Cowley *et al.*[13b] successfully isolated an example of such a donor-acceptor adduct in 2005, by coordination of dicyclohexylcarbodiimide to the electrophilic boron centre in $PhBCl_2$; this adduct was shown to be an intermediate in the formation of the amidinate, $[PhC(NCy)_2BCl_2]$, a complex which unfortunately could not be structurally characterized.

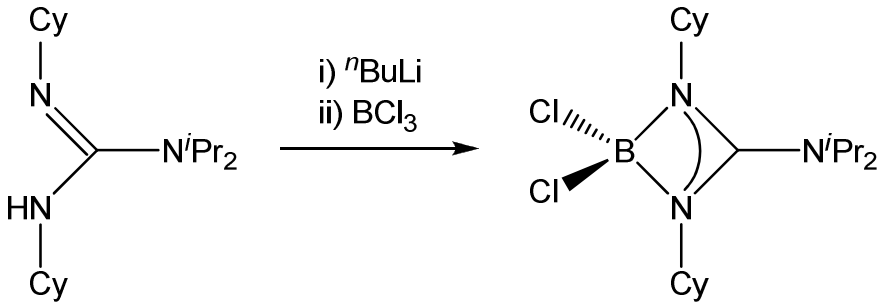
The aminoborane, Cy_2NBCl_2, and dicyclohexylcarbodiimide were heated at 50˚C in toluene for 36 h resulting in formation of the guanidinate complex $[Cy_2NC(NCy_2)_2BCl_2]$, **4.1** as judged by an upfield shift in the ^{11}B NMR from δ_B 28 to δ_B 4. The product was isolated in a 58% yield by cooling a toluene/hexane layering to -30˚C. The only other reported example of insertion into the B-N bond of an aminoboron dihalide resulting in the formation of $[(Me_3Si)_2NC\{NCy\}_2]BCl_2$ from $(Me_3Si)_2NBCl_2$ proceeded under ambient conditions in a hexane/diethyl ether solvent mixture, and resulted in a somewhat higher yield (89%).[13c]



Scheme 4.7 Preparation of **4.1** by carbodiimide insertion.

4.1 was spectroscopically and crystallographically analysed; data was in good agreement with that collected for the same complex from the reaction of $[CpFe(CO)_2B(NCy_2)Cl]$ with CyNCNCy.

An alternative route to guanidinate complexes of this sort is by salt elimination between a halide substrate and a lithium guanidinate, a route which has been widely reported for the synthesis of many such complexes of the heavier group 13 elements.[5,6,8] In order to investigate the use of such chemistry in boron guanidinate chemistry the reaction was carried out between the isopropyl guanidine, $[^{i}Pr_2NC(NCy)(NHCy)]$, and butyllithium, followed by boron trichloride.[17] $[^{i}Pr_2NC(NCy)_2BCl_2]$, **4.2** was isolated from a saturated solution in hexanes and stored at -30˚C. Yields of **4.2** (second step) by this metathesis route appear to be somewhat lower than by the insertion methodology (30% for **4.2**, cf. 58% for **4.1**), probably due to the reaction requiring more manipulation. Cowley *et al*.[13c] have also reported lower yields for formation of amidinates/guanidinates via salt elimination versus insertion.



Scheme 4.8 Preparation of **4.2** by salt eliminaltion.

The ^{11}B NMR shift for **4.2** (δ_B 5) is very similar to that recorded for **4.1**, and is characteristic of a four-coordinate boron centre. Once again, the spectroscopic data collected for this reaction corresponded to that for the same guanidinate formed by reaction of dicyclohexyl carbodiimide with the aminoboryl complex, $[CpFe(CO)_2B(N^{i}Pr_2)Cl]$.

4.3 Conclusions and Suggestions for Further Research

The reactivity of aminoboryl complexes, $[CpFe(CO)_2B(NR_2)Cl]$ (R = Cy, ^{i}Pr) towards dicyclohexylcarbodiimide has been investigated. Although the isolation of products resulting from insertion into the BN bond suggests the intermediacy of the putative complex, $[CpFe(CO)_2B(Cl)(NCy)_2CNR_2]$, the forcing conditions employed (65˚C) led to the formation of the simple guanidinate complexes, $[Cy_2NC(NCy)_2BCl_2]$ **4.1** and $[^{i}Pr_2NC(NCy)_2BCl_2]$ **4.2**. The complexes are the first structurally authenticated examples of boron guanidinate complexes featuring dihalide substituents.

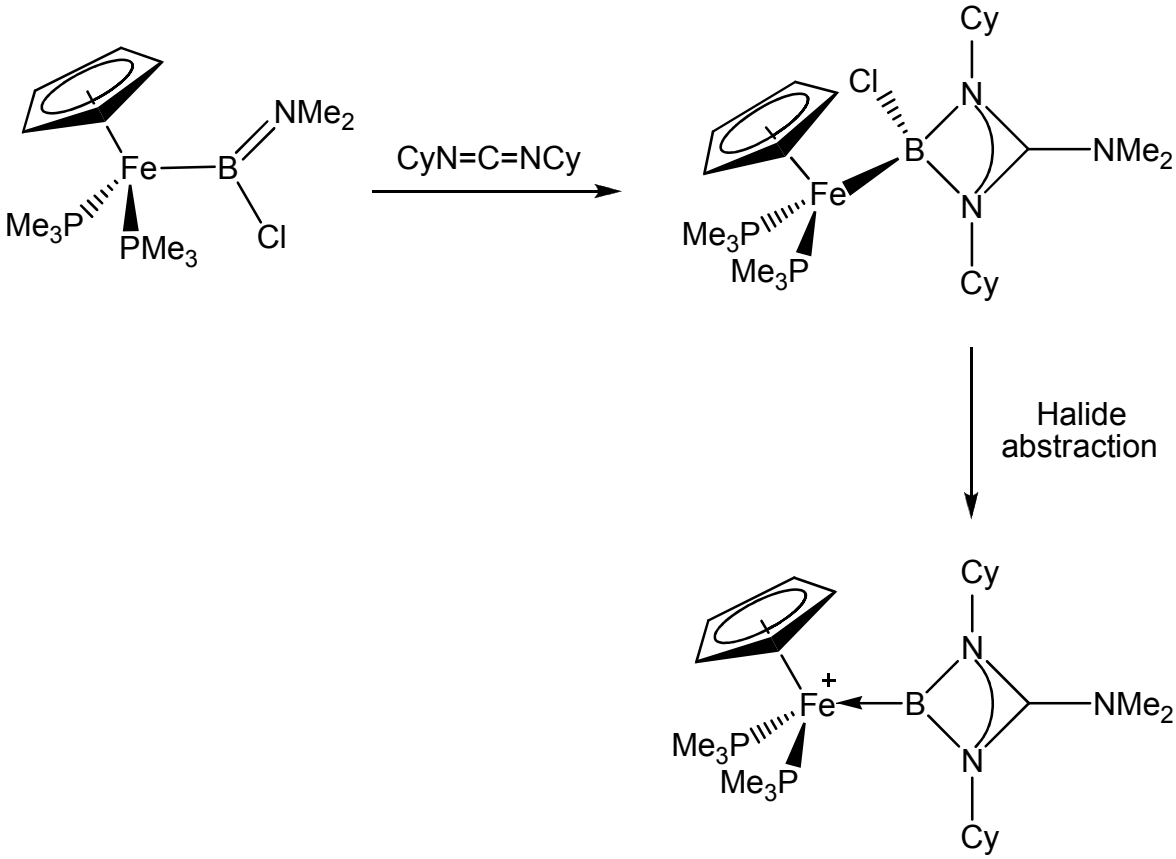
In order to access the desired complex, $[CpFe(CO)_2B(Cl)(NCy)_2CNR_2]$ and avoid such forcing conditions, aminoboryl complexes featuring aryl substituents and consequently weaker BN π-interactions were pursued. Formation of the novel complexes, $[CpFe(CO)_2B(NPh_2)Cl]$ **4.3** and $[CpFe(CO)_2B(NBz)_2Cl]$ **4.4** was achieved via a simple salt elimination route from the analogous aminodichloro boranes, and both were crystallographically characterized. Unfortunately, further reactivity with the carbodiimide was unsuccessful.

Investigation into the formation of **4.1** and **4.2** directly from the respective aminoboranes, however was successful. The cyclohexyl derivative **4.1** was formed by insertion of dicyclohexylcarbodiimide into the B=N bond of the aminoborane, Cy_2NBCl_2. **4.2**, on the other hand, was obtained by a salt elimination route utilizing the reaction of the guanidine, $[^{i}Pr_2NC(NCy)(NHCy)]$ with BCl_3. The metathesis reaction resulted in a lower yield of the guanidinate, probably due to the increased manipulation required. Further reaction of the guanidinate **4.1** and **4.2** by salt elimination to obtain $[CpFe(CO)_2B(Cl)(NCy)_2CNR_2]$

however was unsuccessful, possibly owing to steric factors and reduced electrophilicity at the four-coordinate boron centre.

Reaction of dicyclohexylcarbodiimide with three-coordinate aminoboryl complexes and aminboranes has proved to be much more difficult than reaction with two-coordinate cationic aminoborylene complexes. Whereas the latter react by insertion into the Fe=B bond initially, reactions with aminoboryl complexes and aminoboranes proceed by insertion into the B=N bond, requiring more forcing conditions. Insertion of the carbodiimide molecule into the B=N bond in cationic terminal borylene complexes only occurs once insertion into the Fe=B bond had taken place and was much more facile (Chapter Three).[15]

Further work to form the elusive boron N-heterocyclic carbene analogue could concentrate on modifying the electronic structure of the aminoboryl system. Substituting the carbonyl ligands for σ-donating trialkyl phosphine groups would result in an increase in electron density at the transition metal, and by implication a stronger Fe-B π back-bonding component. Both the mono- and bis(substituted) phosphine analogues have been formed (see Chapter Five).[27] Substitution of one of the carbonyl ligands for a phosphine results in a decrease in the Fe-B bond from 2.053(3) Å for $[CpFe(CO)_2B(NCy_2)Cl]$ to 2.023(2) Å for $[CpFe(CO)(PMe_3)B(NCy_2)Cl]$. Substituting the second carbonyl ligand for a phosphine would be expected to reduce the Fe-B bond length further, increasing its strength, whilst weakening the B-N bond, and would therefore offer a better chance for insertion into the B=N bond under milder conditions.



Scheme 4.9 Potential route to four-membered cationic N-heterocyclic carbene analogues.

4.4 References for Chapter Four

1. (a) H. W. Wanzlick, *Angew. Chem. Int. Ed*., 1962, **1**, 75. (b) H. W. Wanzlick, H. J. Schönherr, *Angew. Chem. Int. Ed*., 1968, **7**, 141.

2. K. Öfele, *J. Organomet. Chem*., 1968, **12**, 42.

3. (a) D. Bourissou, O. Guerret, F. P. Gabai, G Bertrand, *Chem. Rev*., 2000, **100**, 39. (b) W. A. Herrmann, *Angew. Chem. Int. Ed*., 2002, **41**, 1291. (c) C. M. Crudden, D. P. Allen, *Coord. Chem. Rev*., 2004, **248**, 2247. (d) R. H. Crabtree, *J. Organomet. Chem*., 2005, **690**, 5451. (e) P. L. Arnold, S. Pearson, *Coord. Chem. Rev*., 2007, **251**, 596. (f) F. E. Hahn, M. C. Jahnke, *Angew. Chem. Int. Ed*., 2008, **47**, 3122.

4. (a) A. J. Arduengo III, R. L. Harlow, M. Kline, *J. Am. Chem. Soc*., 1991, **113**, 361. (b) A. J. Arduengo III, M. Kline, J. C. Calabrese, F. Davidson, *J. Am. Chem. Soc*., 1991, **113**, 9704.

5. (a) A. Sundermann, M. Reiher, W. W. Schoeller, *Eur. J. Inorg. Chem*., 1998, 305 (b) N. Metzler-Nolte, *New. J. Chem*., 1998, 793. (c) E. S. Schmidt, A. Jockisch, H. Schmidbaur, *J. Am. Chem. Soc*., 1999, **121**, 9758. (d) N. J. Hardman, B. E. Eichler, P. P. Power, *Chem. Comm*., 2000, 1991. (e) C. Cui, H. Roesky, H.-G. Schmidt, M. Noltemeyer, H. Hao, F. Cimpoesu, *Angew. Chem. Int. Ed*., 2000, **39**, 4274. (f) R. J. Baker, R. D. Farley, C. Jones, M. Kloth, D. M. Murphy, *J. Chem. Soc., Dalton. Trans*., 2002, 3844. (g) M. Reiher, A. Sundermann, *Eur. J. Inorg. Chem*., 2002, **7**, 1854. (h) H. W. Roesky, *Inorg. Chem*., 2004, **43**, 7284. (i) M. S. Hill, P. B. Hitchcock, *Chem. Comm*., 2004, 1818. (j) M. S. Hill, P. B. Hitchcock, R. Pongtavornpinyo, *Dalton. Trans*., 2005, 273. (j) R. J. Baker, C. Jones, *Coord. Chem. Rev*., 2005, **249**, 1857. (k)

S. Aldridge, R. J. Baker, N. D. Coombs, C. Jones, R. P. Rose, A. Rossin, D. J. Willock, *Dalton Trans*., 2006, 3313.

6. (a) Y. Segawa, M. Yamashita, K. Nozaki, *Science*, 2006, **314**, 113. (b) M. Yamashita, Y. Suzuki, Y. Segawa, K. Nozaki, *J. Am. Chem. Soc*., 2007, **129**, 9570. (c) Y. Segawa, M. Yamashita, K. Nozaki, *Angew. Chem. Int. Ed*., 2007, **46**, 6710.

7. E. Despagnet-Ayoub, R. H. Grubbs, *J. Am. Chem. Soc*., 2004, **126**, 10198.

8. (a) C. Jones, P. C. Junk, J. A. Platts, A. Stasch, *J. Am. Chem. Soc*., 2006, **128**, 2206. (b) S. P. Green, C. Jones, A. Stasch, *Inorg. Chem*., 2007, **46**, 11.

9. J. Barker, N. C. Blacker, P. R. Phillips, N. W. Alcock, W. Errington, M. G. H. Wallbridge, *J. Chem. Soc., Dalton Trans*., 1996, 431.

10. (a) R. Duchateau, A. Meetsma, J. H. Teuben, *Chem. Comm*., 1996, 223. (b) M. P. Coles, D. C. Swenson, R. F. Jordan, *Organometallics*, 1997, **16**, 5183. (c) M. P. Coles, D. C. Swenson, R. F. Jordan, *Organometallics*, 1998, **17**, 4042. (d) S. Dagorne, R. F. Jordan, *Organometallics*, 1999, **18**, 4619. (e) S. Dagorne, I. A. Guzei, M. P. Coles, R. F. Jordan, *J. Am. Chem. Soc*., 2000, **122**, 274. (f) G. Talarico, P. H. M. Budzelaar, *Organometallics*, 2000, **19**, 5691.

11. (a) C. Jones, S. Aldridge, T. Gans-Eichler, *Dalton Trans*., 2006, 5357. (b) P. Junk, M. L. Cole, *Chem. Comm*., 2007, 1579.

12. (a) C. Ergezinger, F. Weller, K. Dehnicke, *Z. Naturforsch., B: Chem. Sci*., 1988, **43**, 1621. (b) P. Blais, T. Chivers, A. Downward, M. Parvez, *Can. J. Chem*., 2000, **78**, 10, (c) M. R. Terry, L. A. Mercando, C. Kelly, G. L. Geoffroy, P. Nombel, N. Lugen, R. Mathieu, R. L. Ostrander, B. E. Owens-Whitmire, A. L. Rheingold, *Organometallics*, 1994, **13**, 843.

13. (a) N. J. Hill, M. Finslater, A. H. Cowley, *Dalton Trans*., 2005, 3229. (b) N. J. Hill, J. A. Moore, M. Findlater, A. H. Cowley, *Chem. Comm*., 2005, 5462. (c) M. Findlater, N. J. Hill, A. H. Cowley, *Polyhedron*, 2006, **25**, 983. (d) Z. Lu, N. J. Hill, M. Findlater, A. H. Cowley, *Inorganica Chimica Acta*, 2007, 1316. (e) M. Findlater, N. J. Hill, A. H. Cowley, *Dalton. Trans*., 2008, 4419.

14. (a) D. J. Brauer, S. Buchheim-Spiegel, H. Bürger, R. Gielen, G. Pawelke, Jürgen Rothe, *Organometallics*, 1997, **16**, 5321. (b) A. Ansorge, D. J. Brauer, H. Bürger, F. Dörrenbach, T. Hagen, G. Pawelke, W. Weuter, *J. Organomet. Chem*., 1991, **407**, 283.

15. (a) G. A. Pierce, S. Aldridge, C. Jones, T. Gans-Eichler, A. Stasch, N. D. Coombs, D. J. Willock, *Angew. Chem. Int. Ed*., 2007, **46**, 2043. (b) G. A. Pierce, N. D. Coombs, D. J. Willock, J. K. Day, A. Stasch, S. Aldridge, *Dalton Trans*., 2007, 4405.

16. R. Jefferson, M. F. Lappert, B. Prokai, B. P. Tilley, *J. Chem. Soc*. 1966, 1584.

17. C. Jing-Lei, Y. Ying-Ming, L. Yun-Jie, Z. Li-Ying, Z. Yong, S, Qi, *J. Organomet. Chem*., 2004, 1019.

18. (a) D. L. Kays (née Coombs), J. K. Day, L-L. Ooi, S. Aldridge, *Angew Chem. Int. Ed*., 2005, **44**, 7457. (b) D. L. Kays (née Coombs), J. K. Day, S. Aldridge, R. W. Harrington, W. Clegg, *Angew. Chem. Int. Ed*., 2006, **45**, 3513. (c) S. Aldridge, C. Jones, T. Gans-Eichler, A. Stasch, D. L. Kays (née Coombs), N. D. Coombs, D. J. Willock, *Angew. Chem. Int. Ed*., 2006, **45**, 6118.

19. (a) D. L. Kays, S. Aldridge, *Contemporary Metal Boron Chemistry I*, eds. T. B. Marder, Z. Lin, Springer, 2008, Vol. 130, p 29. (b) D. Vidovic G. A. Pierce, S. Aldridge, *Chem. Comm*., 2009, 1157.

20. R. D. Fischer, A. Vogler, *J. Organomet. Chem*., 1967, **7**, 135.

21. D. R. Lide, *Handbook of Chemistry and Physics*, 86th eds., Taylor & Francis group, LLC., 2005.

22. G. J. Bullen, N. H. Clark, *J. Chem. Soc*., 1970, 992.

23. H. Braunschweig, C. Kollann, U. Englert, *Eur. J. Inorg. Chem*., 1998, 465.

24. (a) S. Aldridge, R. J. Calder, D. L. Coombs, C. Jones, J. W. Steed, S. Coles, M. B. Hursthouse, *New. J. Chem*., 2002, **26**, 677. (b) D. L. Coombs, PhD Thesis, Cardiff University, 2003.

25. C. N. Rowley, G. A. DiLabio, S. T. Barry, *Inorg. Chem*., 2005, **44**, 1983.

26. S. Gambarotta, S. Strologo, C. Floriani, A. Chiesi-Villa, C. Guastini, *Inorg. Chem*., 1985, **24**, 654.

27. G. A. Pierce, D. Vidovic, D. L. Kays, N. D. Coombs, A. L. Thompson, D. J. Willock, E. D. Jemmis, S. De, S. Aldridge, *Organometallics*, 2009, **28**, 2947.

Chapter Five

Studies of Ligand Variation in Cationic Terminal Borylene Complexes

5.1 Introduction

The development of different synthetic methodologies which generate terminal borylene complexes has allowed access to a range of complexes featuring different metals, borylene substituents and charges.[1] An instructive comparison of electronic structure and bonding can therefore be gained by the systematic variation of these factors. A comparison of a series of cationic iron containing terminal borylene complexes featuring various boron-bound substituents has been reported by Aldridge and co-workers.[1j] Analysis of structural, spectroscopic and computational data for $[Cp^*Fe(CO)_2(BMes)]^+$,[2] $[CpFe(CO)_2(BNCy_2)]^+$ (each isolated as the $[BAr^f_4]^-$ salt)[3] and $[CpFe(CO)_2(BCp^*)]^+$ (isolated by Cowley *et al*., as the $[AlCl_4]^-$ salt)[4] is presented in Table 5.1.

Table 5.1 Comparison of Fe-B bond lengths and σ:π bonding contributions for cationic terminal borylene complexes with varying borylene substituents.

	d(Fe-B) / Å	σ:π	
$[Cp^*Fe(CO)_2(BMes)]^+$	1.792(8)	62:38	M=B double bond
$[CpFe(CO)_2(BNCy_2)]^+$	1.859(6)	71:29	
$[CpFe(CO)_2(BCp^*)]^+$	1.977(3)	86:14	M-B single bond

Progressing from the highly electrophilic mesityl substituted borylene, to the amino and pentamethylcyclopentadienyl (Cp*) substituted complexes we see an increase in the FeB

bond length from 1.792(8) to 1.977(3) Å. The mesityl substituted borylene features a boron centre benefiting from minimal π-donor stabilization, and is consistent with a bonding model analogous to that operating for Fischer carbenes[5] and silylenes,[6] i.e. comprising of B→Fe donor and Fe→B back-bonding components. The amino and Cp* substituents however are able to donate electron density to the boron centre via a π-interaction and so relieve the electronic unsaturation. Consequently the boron centre is less electron deficient and engages in markedly less π-back bonding with the metal centre. This is further exemplified by looking at the DFT calculated ratio of σ to π contributions to the covalent bonding density for the three compounds; the calculated π component of the FeB bond is found to decrease as the π-donor capabilities of the borylene substituent increases. On going down the series there is a change from an Fe=B double bond to an Fe-B single bond and that it is therefore possible to tune the electronics of the borylene by appropriate choice of substituent.

Furthermore, the nature of the boron-bound substituent not only has a profound effect on the electronic structure of the complex, but also on the mode of reactivity. Whilst $[Cp^*Fe(CO)_2(BMes)]^+$ is characterized by its electrophilic boron centre and dominated by reactions such as addition at the boron centre or displacement of the borylene fragment,[2] the aminoborylene complexes, $[CpFe(CO)_2(BNR_2)]^+$ (R = Cy, ^{i}Pr) show a more varied pattern of reactivity such as cycloaddition, metathesis, insertion and reduction, possibly due to the milder electrophilicity of the boron centre.[3,7]

Another way in which to tune the electronic structure and reactivity of cationic borylenes is by varying the transition metal, and this has recently been reported by Aldridge *et al*. using ruthenium.[7e] The ruthenium aminoboryl precursor, $[CpRu(CO)_2B(NCy_2)Cl]$ was formed by a salt elimination route, analogous to that employed for the closely related iron

system,[3] and was subsequently reacted via halide abstraction to form the first crystallographically characterized cationic ruthenium borylene complex, $[CpRu(CO)_2(BNCy_2)]^+[BAr^f_4]^-$. As expected on the basis of the respective covalent radii (Fe = 1.17 Å vs. Ru = 1.24 Å),[8] the M=B distance in the ruthenium borylene is longer than that for the iron borylene (1.960(6) Å for $[CpRu(CO)_2(BNCy_2)]^+[BAr^f_4]^-$, 1.859(6) Å for $[CpFe(CO)_2(BNCy_2)]^+[BAr^f_4]^-$),[3] however the percentage shortening of the metal-boron bond on going from the aminoboryl precursor to the aminoborylene complex is similar for both iron and ruthenium systems at ~ 10%.[7e]

5.1.1 Aims of the Present Research

Whilst the electronic structure of the cationic terminal borylene complex, $[L_nMBX]^+$ has already been investigated by systematic variation in both the borylene substituent and the transition metal, it was decided to probe variation in the ancillary ligands at the metal centre. Modifying the Cp substituent to Cp' would be expected to have relatively minor effects on electronic structure of the aminoborylene linkage; replacing the π-acidic carbonyl ligands with phosphines, however, could conceivably have a more pronounced effect. Trialkyl phosphines are very good σ donors but relatively poor π acceptors, so replacing the carbonyl ligands with phosphines means that more electron density would be available at the metal centre to participate in π back-bonding to the boron centre, resulting in a shortening of the Fe=B bond. In addition, this might allow a probe of multiple bonding character in the complex by calculating a barrier to rotation about the M=B bond by NMR methods.

In contrast to the less electrophilic charge neutral aminoborylene complexes, $[(OC)_5MBN(SiMe_3)_2]$ (M = Cr, W, Mo), which undergo carbonyl substitution to give *trans*-

$[(Cy_3P)(OC)_4MBN(SiMe_3)_2]$ on irradiation with PCy_3,[9] it is not possible to replace the carbonyl ligands of a cationic aminoborylene complex due to the increased electrophilicity at the boron centre. Related reactions with 4-picoline, for instance, lead to formation of the boron-bound adduct, $[CpFe(CO)_2\{B(NCy_2)(4\text{-pic})\}]^+[BAr^f_4]^-$.[3] Therefore, in order to displace the ancillary carbonyl ligands for phosphines, substitution must occur at an earlier stage in the synthetic pathway, i.e. at the aminoboryl precursor.

5.2 Experimental

Synthesis of $[Cp'Fe(CO)_2(BN^iPr_2)]^+[BAr^f_4]^-$ (**5.1**)

A solution of $[Cp'Fe(CO)_2B(N^iPr_2)Cl]$ (0.10 g, 0.30 mmol) in dichloromethane (~ 20 cm^3) was added to a suspension of $Na[BAr^f_4]$ (1.1 equiv). The reaction was sonicated for 20 min after which the reaction was judged to be complete by ^{11}B and ^{31}P NMR spectroscopy. Filtration, layering with hexanes and storage at -30˚C led to formation of crystals suitable for X-ray diffraction. Isolated yield: 0.06 g, 18%. ^1H NMR (400 MHz, CD_2Cl_2) δ 1.43 (d, $^3J_{HH}$ = 7 Hz, 12H, CH_3 of ^{i}Pr), 2.06 (s, 3H, Me of Cp'), 3.38 (sept, $^3J_{HH}$ = 7 Hz, 2H, CH of ^{i}Pr), 5.17 (t, $^3J_{HH}$ = 2 Hz, 2H, CH of Cp'), 5.27 (t, $^3J_{HH}$ = 2 Hz, 2H, CH of Cp'), 7.64 (s, 4H, *para*-H of $BAr^f_4^-$), 7.73 (s, 8H, *ortho*-H of $BAr^f_4^-$). ^{13}C NMR (126 MHz, CD_2Cl_2) δ 12.4 (CH_3 on Cp'), 24.8 (CH_3 of ^{i}Pr), 51.5 (CH of ^{i}Pr), 85.4 (CH of Cp'), 87.6 (CH of Cp'), 108.5 (C on Cp'), 117.9 (*para*-C of $BAr^f_4^-$), 125.1 (q, $^1J_{CF}$ = 273 Hz, CF_3 of $BAr^f_4^-$), 129.3 (q, $^2J_{CF}$ = 31 Hz, *meta*-C of $BAr^f_4^-$), 135.2 (*ortho*-CH of $BAr^f_4^-$), 162.2 (q, $^1J_{CB}$ = 50 Hz, *ipso*-C of $BAr^f_4^-$), 206.5 (CO). ^{11}B NMR (96 MHz, CD_2Cl_2) δ 94 (br, fwhm ca.439 Hz). ^{19}F NMR (283 MHz, CD_2Cl_2) δ -62.7 (CF_3). IR (CD_2Cl_2 soln, cm^{-1}) υ 2065, 2023 (CO). MS (positive ion electrospray) m/z (%) 302 (13) M^+; exact mass (calc. for M^+) m/z 302.1, (obs.) 302.0. Elemental analysis (calc.) C 47.42, H 2.85,

N 1.20; (obs.) C 47.44, H 2.82, N 1.34. Crystallographic data: $C_{46}H_{33}B_2F_{24}FeNO_2$, Mr 1165.20, monoclinic, space group P2(1)/n, a = 17.000(5) , b = 13.633(5), c = 21.041(5) Å, β = 97.303(5)°, V= 4837(3) $Å^3$, Z = 4, ρ_{calcd} = 1.600 Mgm^{-3}, T = 150(2) K, λ = 0.71069 Å. 17588 reflections collected, 9402 independent [R(int) = 0.0419], which were used in all calculations. R_1 = 0.0482, wR_2 = 0.0856 for observed unique reflections [$F_2>2\sigma(F_2)$] and R_1 = 0.0819, wR_2 = 0.0955 for all unique reflections. Max./min. residual electron densities 0.254/-0.359 $eÅ^{-3}$.

Synthesis of [CpFe(CO)(PMe$_3$)B(NCy$_2$)Cl] (**5.2**)

A mixture of [$CpFe(CO)_2B(NCy_2)Cl$] (0.20 g, 0.5 mmol) and PMe_3 (2 equiv.) in toluene was photolysed for 6 h with stirring, and the reaction monitored by both ^{11}B and ^{31}P NMR spectroscopy. After removal of the volatiles under reduced pressure, and extraction into pentane (ca. 30 cm^3), storage at –80˚C led to the formation of red crystals (of the pentane hemi-solvate) suitable for X-ray diffraction. Yield: 0.07 g, 33%. ^1H NMR (300 MHz, C_6D_6) δ 0.93-2.18 (overlapping m, 20H, CH_2 of Cy), 1.14 (d, $^2J_{HP}$ = 9 Hz, 9H, PMe_3), 2.10, 2.97 (m, 2H, CH of Cy), 4.26 (s, 5H, Cp). ^{13}C NMR (126 MHz, C_6D_6) δ 20.8 (d, $^1J_{CP}$ = 30 Hz, PMe_3), 26.5, 26.6, 26.7, 26.8, 28.1, 28.2, 33.1, 33.9, 34.6, 34.7 (CH_2 of NCy_2) 59.2, 65.1 (CH of NCy_2), 82.2 (Cp), 220.2 (d, $^2J_{CP}$ = 38 Hz, CO). ^{11}B NMR (96 MHz, C_6D_6) δ 62 (br, fwhm ca. 500 Hz). ^{31}P NMR (122 MHz, C_6D_6) δ 41.5. IR (C_6D_6 soln, cm^{-1}) υ 1890 (CO). MS (electron ionisation), m/z (%) 451 (4) M^+, 423.1 (19) $(M\text{-}CO)^+$, 389.2 (25) $(M\text{-}CO\text{-}Cl)^+$; exact mass (calc. for M^+, ^{56}Fe, ^{10}B isotopomer) m/z 450.1696, (obs.) 450.1697. Crystallographic data: $C_{21}H_{36}BClFeNOP\cdot 1/2(C_5H_{12})$, Mr 487.68, monoclinic, space group P2(1)/n, a = 13.75620(10), b = 12.30200(10), c = 15.96190(10) Å, β = 93.8710(4)°, V= 2695.05(3) $Å^3$, Z = 4, ρ_{calcd} = 1.202 Mgm^{-3}, T = 150 K, λ = 0.71073 Å. 51592 reflections collected, 6134 independent [R(int) = 0.039], which were used in all calculations. R_1 = 0.0430, wR_2 = 0.1068 for observed

unique reflections [$F_2>2\sigma(F_2)$] and R_1 = 0.0541, wR_2 = 0.1123 for all unique reflections. Max./min. residual electron densities 0.62/-0.49 eÅ^{-3}.

Synthesis of [CpFe(CO)(PMe$_3$)$_2$]$^+$Cl$^-$ (**5.3**)

[CpFe(CO)(PMe$_3$)$_2$]$^+$Cl$^-$ was formed as a by-product from the reaction of [CpFe(CO)$_2$B(NCy$_2$)Cl] with PMe$_3$ (2 equiv.) in toluene under photolytic conditions. Due to the cationic nature of **5.3**, it precipitates during the reaction as a yellow crystalline solid. Yield: 0.12 g, 72%. ^{1}H NMR (300 MHz, CD_2Cl_2) δ 4.56 (s, 10H, Cp), 1.45 (d, 18H, $^1J_{CP}$ = 10 Hz, PMe$_3$). ^{13}C NMR (75 MHz, CD_2Cl_2) δ 24.2 (t, $^1J_{CP}$ = 16 Hz, PMe$_3$), 83.2 (Cp), 215.3 (d, J_{CP} = 28 Hz, CO), ^{31}P NMR (121 MHz, CD_2Cl_2) δ 28.6. IR (CD_2Cl_2 soln, cm^{-1}) υ 1949 (CO). MS (positive ion electrospray) m/z 301.2 (100) $(M)^+$, correct isotope pattern; (negative ion electrospray) 863.3 (100) $BAr^f{}_4^-$; exact mass (calc. for M^+ ^{54}Fe isotopomer) 299.0615, (obs.) 299.0610. Crystallographic data $C_{12}H_{23}FeOP_2\cdot(CH_2Cl_2\cdot Cl)$, Mr 421.49, monoclinic, space group C 2/c, a = 31.4550(6), b = 7.9830(2), c = 18.2228(4) Å, β = 124.6365(11)°, V= 3764.89(15) Å^3, Z = 8, p_{calcd} = 1.487 Mgm^{-3}, T = 150 K, λ = 0.71073 Å. 23231 reflections collected, 4259 independent [R(int) = 0.073], which were used in all calculations. R_1 = 0.0429, wR_2 = 0.0789 for observed unique reflections [$F_2>2\sigma(F_2)$] and R_1 = 0.0753, wR_2 = 0.0894 for all unique reflections. Max./min. residual electron densities 1.48/-1.31 eÅ^{-3}.

Synthesis of [(μ-BNCy$_2$)(μ-CO){CpFe(CO)}$_2$] (**5.4**)

A mixture of Cy_2NBCl_2 (0.2 g, 0.81 mmol) and Na[CpFe(CO)$_2$] (2.5 equiv.) in toluene was heated to 55˚C and stirred for 72 h, and judged to be complete by the formation of a peak at δ_B 101 and the disappearance of the signal (at δ_B 28) due to the starting material. The volatiles

were removed under reduced pressure and the residue extracted into hexane. A red solid was isolated after cooling a saturated hexane solution to -30˚C. Yield: 0.1 g, 24%. ^{1}H NMR (300 MHz, C_6D_6) δ 0.86-1.93 (m, 20H, CH_2 of Cy), 3.95 (m, 2H, CH of Cy), 4.24 (s, 5H, Cp).^{13}C NMR (75 MHz, C_6D_6) 26.0, 27.2, 35.1 (CH_2 of Cy), 63.2 (CH of Cy), 88.4 (Cp), 213.4 (CO), 275.3 (μ-CO). ^{11}B NMR (96 MHz, C_6D_6) δ 101 (br, fwhm ca. 671 Hz). IR (C_6D_6 soln, cm^{-1}) υ (CO) 1997, 1954, (μ-CO) 1781. MS (electron ionisation) m/z (%) 517.0 (weak) M^+, 489.3 (weak) $(M\text{-}CO)^+$, 461.3 (weak) $(M\text{-}2CO)^+$; exact mass (calc. for M^+ ^{56}Fe and ^{10}B isotopomer) m/z 516.1205, (obs.), 516.1203.

Synthesis of [CpFe(CO)(PPh$_3$)B(NCy$_2$)Cl] (**5.5**)

Irradiation of a mixture of [$CpFe(CO)_2B(NCy_2)Cl$] (0.10 g, 0.2 mmol) and PPh_3 (2 equiv.) in toluene (ca. 40 cm^3) was judged to be complete after 6 h by ^{11}B and ^{31}P NMR spectroscopy. Volatiles were removed in *vacuo* and the residue subsequently extracted into pentane. The solution was placed at -30˚C and a yellow-orange solid precipitated. Yield: 0.10 g, 63%. ^{1}H NMR (300MHz, $C_6D_5CD_3$) δ 0.84-2.68 (m, 20H, CH_2 of Cy), 2.68 (overlapping m, 2H, CH of Cy), 4.34 (s, 5H, Cp), 6.72-7.87 (m, 15H, Ph). ^{13}C NMR (75 MHz, $C_6D_5CD_3$) δ 26.0, 26.2 (2 overlapping signals), 27.2, 27.7, 27.8, 32.5, 33.4, 33.7, 34.0 (CH_2 of NCy_2), 59.1, 64.4 (CH of NCy_2), 83.3 (Cp), 129.4 (d, $^{3}J_{CP}$ = 10 Hz, *meta*-CH of Ph), 131.9 (*para*-CH of Ph), 132.8 (d, $^{2}J_{CP}$ = 10 Hz, *ortho*–CH of Ph), 133.8 (d, $^{1}J_{CP}$ = 52 Hz, *ipso*-C of Ph), 221.3 (d, $^{2}J_{CP}$ = 35 Hz, CO). ^{11}B NMR (96 MHz, $C_6D_5CD_3$) δ 61 (br, fwhm ca. 722 Hz). ^{31}P NMR (121 MHz, $C_6D_5CD_3$) δ 82.0. IR (C_6D_6 soln, cm^{-1}) υ 1901 (CO). MS (electron ionisation) m/z (%) 637.1 (weak) M^+, 609.1 (10) $(M\text{-}CO)^+$, 262 (100) PPh_3; exact mass (calc. for M^+, ^{56}Fe and ^{10}B isotopomer) m/z 608.2217, (obs.) 608.2217.

Synthesis of $[CpFe(CO)(PMe_3)(BNCy_2)]^+$ $[BAr^f{}_4]^-$ (**5.8**)

A solution of $[CpFe(CO)(PMe_3)B(NCy_2)Cl]$ (0.17 g, 0.37 mmol) in dichloromethane (2 cm^3) was added to a suspension of $Na[BAr^f{}_4]$ (1.1 equiv.). The reaction was sonicated for 20 min after which the reaction was judged to be complete by ^{11}B NMR and ^{31}P NMR spectroscopy. Layering with hexane and storage at -30˚C led to the formation of crystals suitable for X-ray diffraction. Isolated yield: 0.13 g, 27%. ^1H NMR (300 MHz, CD_2Cl_2) δ 1.02-2.18 (overlapping m, 20H, CH_2 of Cy), 1.61 (d, $^2J_{HP}$=12 Hz, 9H, PMe_3), 2.89 (m, 2H, CH of Cy), 4.95 (d, $^3J_{HP}$= 2 Hz, 5H, Cp), 7.57 (s, 4H, *para*-H of $BAr^f{}_4^-$), 7.73 (s, 8H, *ortho*-H of $BAr^f{}_4^-$). ^{13}C NMR (76 MHz, CD_2Cl_2) δ 22.7 (d, $^1J_{CP}$ = 36 Hz, PMe_3), 25.3, 26.3, 26.4, 36.6 (2 overlapping signals) (CH_2 of NCy_2), 57.5 (CH of NCy_2), 84.8 (Cp), 117.8 (*para*-C of $BAr^f{}_4^-$), 124.9 (q, $^1J_{CF}$ = 276 Hz, CF_3 of $BAr^f{}_4^-$), 129.2 (q, $^2J_{CF}$ = 31 Hz, *meta*-C of $BAr^f{}_4^-$), 135.1 (*ortho*-CH of $BAr^f{}_4^-$), 162.1 (q, $^1J_{CB}$ = 50 Hz, *ipso*-C of $BAr^f{}_4^-$), 270.7 (CO). ^{11}B NMR (96 MHz, CD_2Cl_2) δ 93 (br, fwhm ca. 728 Hz). ^{19}F NMR (283 MHz, CD_2Cl_2) δ -62.8 (CF_3). ^{31}P NMR (121 MHz, CD_2Cl_2) δ 31.7. IR (CD_2Cl_2 soln, cm^{-1}) υ 1981 (CO). MS (positive ion electrospray) m/z (%) 416 (100) M^+; exact mass (calc. for M^+) m/z 416.1975, (obs.) 416.1991. Elemental analysis (calc.) C 49.76, H 3.78, N 1.09; (obs.) C 49.81, H 3.85, N 1.02. Crystallographic data: $C_{53}H_{48}B_2F_{24}FeNOP\cdot(CH_2Cl_2)$, Mr 1364.30, monoclinic, space group C 2/c, a = 17.48100(10) , b = 18.27830(10), c = 37.2971(3) Å, β = 96.0302(3)°, V= 11851.34(13) $Å^3$, Z = 8, p_{calcd} = 1.529 Mgm^{-3}, T = 150 K, λ = 0.71073 Å. 63388 reflections collected, 13462 independent [R(int) = 0.053], which were used in all calculations. R_1 = 0.0636, wR_2 = 0.1516 for observed unique reflections [$F_2>2\sigma(F_2)$] and R_1 = 0.1025, wR_2 = 0.1711 for all unique reflections. Max./min. residual electron densities 0.92/-0.70 $eÅ^{-3}$.

Synthesis of [CpFe(CO)(PPh$_3$)(BNCy$_2$)]$^+$[BAr$^f_4$]$^-$ (**5.9**)

A solution of [CpFe(CO)(PPh$_3$)B(NCy$_2$)Cl] (0.10 g, 0.16 mmol) in dichloromethane was added to a suspension of Na[BAr$^f_4$] (1.1 equiv.). The reaction was sonicated for 20 min after which the reaction was judged to be complete by ^{11}B NMR and ^{31}P NMR spectroscopy. Layering with hexane and storage at -30˚C led to the isolation of **5.9** as a pale yellow microcrystalline solid. Yield 0.04 g, 18%. ^{1}H NMR (300 MHz, CD_2Cl_2) δ 0.87-2.24 (m, 20H, CH_2 of Cy), 2.87 (m, 2H, CH of Cy), 5.01 (d, $^3J_{PH}$ = 1 Hz, 5H, Cp), 7.32-7.62 (m, 15H, Ph), 7.63 (s, 4H, *para*-H of BAr$^f_4$$^-$), 7.80 (s, 8H, o*rtho*-H of BAr$^f_4$$^-$). ^{13}C NMR (75 MHz, CD_2Cl_2) δ 24.7, 25.9, 26.0, 35.3, 36.0 (CH_2 of NCy_2), 56.1 (CH of NCy_2), 86.7 (Cp), 118.8 (*para*-C of BAr$^f_4$$^-$), 126.0 (q, $^1J_{CF}$ = 275 Hz, CF_3 of BAr$^f_4$$^-$), 129.4 (d, $^2J_{CP}$ = 10 Hz, *ortho*-C of Ph), 130.3 (q, $^2J_{CF}$ = 34 Hz, *meta*-C of BAr$^f_4$$^-$), 131.9 (*para*-C of Ph), 132.8 (d, $^3J_{CP}$ = 10 Hz, *meta*-C of Ph), 133.8 (d, $^1J_{CP}$ = 52 Hz, *ipso*-C of Ph), 136.3 (*ortho*-CH of BAr$^f_4$$^-$), 163.6 (q, $^1J_{CB}$ = 50 Hz, *ipso*-C of BAr$^f_4$$^-$), 270.3 (CO). ^{11}B NMR (96 MHz, CD_2Cl_2) δ 92 (br, fwhm ca.1193 Hz). ^{19}F NMR (283 MHz, CD_2Cl_2) δ -62.8 (CF_3). ^{31}P NMR (121 MHz, CD_2Cl_2) δ 68.0. IR (CD_2Cl_2 soln, cm^{-1}) υ 1988 (CO). MS (positive ion electrospray) m/z (%) 602 (100) M$^+$; exact mass (calc.) 602.2448, (obs.) 602.2430.

Synthesis of meso-[{CpFe(CO)(BNCy$_2$)}$_2$(μ-dmpe)]$^{2+}$[BAr$^f_4$]$_2^-$ (**5.11**)

A mixture of [CpFe(CO)$_2$B(NCy$_2$)Cl] (0.15 g, 0.37 mmol) and dmpe (1 equiv.) in toluene was photolysed for 36 h with stirring, after which the reaction was judged to be complete by ^{11}B NMR (disappearance of starting material δ_B 58 and appearance of broad signal at δ_B 63). Volatiles were removed under reduced pressure and the residue extracted into pentane (ca. 50 cm^3). Unfortunately, attempted crystallization led to the formation of an oily residue

containing an intractable mixture of products. While a single broad ^{11}B resonance at δ_B 63 was observed, a number of ^{31}P signals were found at δ_P ca. 55. Presumably this reflects, at least in part, the formation of diastereomeric dinuclear boryl complexes of the type *rac/meso*-[{CpFe(CO)B(NCy_2)Cl}$_2$(μ-dmpe)]. Given the greater ease of separation likely for the more crystalline cationic borylene complexes, halide abstraction was carried out on the mixture with the aim of separating the resulting products by fractional crystallization. A solution of [{CpFe(CO)B(NCy_2)Cl}$_2$(μ-dmpe)] (0.12 g, 0.25 mmol) in dichloromethane was added to a suspension of Na[BAr^f_4] (1.1 equiv.) and allowed to stir for 1 h. The solvent was removed under reduced pressure and the residue extracted into fluorobenzene, layering with hexanes and storage at –30˚C led to the formation of crystals suitable for X-ray diffraction. Yield: 0.02 g, 19%. ^1H NMR (300 MHz, CD_2Cl_2) δ 0.76-2.18 (overlapping m, 44H, CH_2 of Cy and CH_2 of dmpe), 1.55, 1.59 (d, $^2J_{HP}$ = 12 Hz, 12H, PMe_2), 2.96 (m, 4H, CH of Cy), 4.97 (s, 10H, Cp), 7.61 (s, 8H, *para*-H of $BAr^f_4^-$), 7.78 (s, 16H, *ortho*-H of $BAr^f_4^-$). ^{13}C NMR (75 MHz, CD_2Cl_2) δ 18.8, 20.2 (br, PMe_3), 24.9 (d, $^1J_{CP}$ = 49 Hz, PCH_2), 24.3, 26.3, 31.0, 31.1, 36.7 (CH_2 of NCy_2), 57.7 (CH of NCy_2), 84.9 (Cp), 117.9 (*para*-C of $BAr^f_4^-$), 125.0 (q, $^1J_{CF}$ = 276 Hz, CF_3 of $BAr^f_4^-$), 129.3 ($^2J_{CF}$ = 27 Hz, *meta*-C of $BAr^f_4^-$), 135.3 (*ortho*-CH of $BAr^f_4^-$), 162.2 (q, $^1J_{CB}$ = 50 Hz, *ipso*-C of $BAr^f_4^-$), 212.4 (CO). ^{11}B NMR (96 MHz, CD_2Cl_2) δ 91 (br, fwhm ca.2400 Hz). ^{19}F NMR (283 MHz, CD_2Cl_2) δ -62.7 (CF_3). ^{31}P NMR (121 MHz, CD_2Cl_2) δ 45.7 (d, $^3J_{PP}$ = 15 Hz). IR (CD_2Cl_2 soln, cm^{-1}) υ 1979 (CO). MS (positive ion electrospray) m/z (%) 415 (100) M^{2+}; exact mass (calc. for M^{2+}) 415.1901, (obs.) 415.1891. Crystallographic data: $C_{53.5}H_{48}B_2ClF_{24}FeNOP$, Mr 1380.82, triclinic, space group P-1, a = 2.6073(1), b = 19.6463(2), c = 26.4427(4) Å, α = 70.5296(5), β = 87.0531(5), γ = 78.5273(5)°, V= 6050.80(12) $Å^3$, Z = 4, p_{calcd} = 1.450 Mgm^{-3}, T = 150 K, λ = 0.71073 Å. 81455 reflections collected, 26654

independent [R(int) = 0.064]. R_1 = 0.0847, wR_2 = 0.0883 for observed unique reflections [$F_2>2\sigma(F_2)$] and R_1 = 0.1261, wR_2 = 0.1257 for all unique reflections. Max./min. residual electron densities 1.97/-1.20 eÅ^{-3}.

Synthesis of [CpFe(PMe$_3$)$_2$B(NMe$_2$)Cl] (**5.13**)

A solution of [CpFe(CO)$_2$B(NMe$_2$)Cl] (0.20 g, 0.78 mmol) and PMe$_3$ (>2 equiv.) in toluene was irradiated for ~ 100 h. The reaction was monitored by ^{11}B and ^{31}P NMR spectroscopies and shows systematic formation of the mono(substituted) complex, **5.12** (δ_B 62, δ_P 41) and subsequently the bis(substituted) complex, **5.13** (δ_B 67, δ_P 42). Attempts to isolate **5.13** by extracting into pentane resulted in the formation of **5.14** (*vide infra*).

Synthesis of [CpFe(dmpe)B(NMe$_2$)Cl] (**5.16**)

A solution of [CpFe(CO)$_2$B(NMe$_2$)Cl] (0.20 g, 0.78 mmol) and dmpe (>2 equiv.) in toluene was irradiated for ~ 100 h. The reaction was monitored by ^{11}B and ^{31}P NMR spectroscopy and shows systematic formation of the mono(substituted) complex, **5.15** (δ_B 62, δ_P 53) and then the bis(substituted) complex, **5.16** (δ_B 66, δ_P 75). Attempts to isolate **5.16** by extraction into pentane resulted in the formation of **5.17**.

Synthesis of [CpFe(PMe$_3$)$_2$(BNMe$_2$)]$^+$Cl$^-$ (**5.14**)

5.14 was synthesized by washing **5.13** with pentane and extracting the resulting residue into dichloromethane (20 cm^3). ^{1}H NMR (300 MHz, CD_2Cl_2) δ 1.26 (s, 18H, PMe$_3$), 2.63 (s, 6H, Me), 4.44 (s, 5H, Cp). ^{13}C NMR (126 MHz, CD_2Cl_2) δ 25.7-26.3 (m, PMe$_3$), 35.7 (m, NMe$_2$),

82.8 (Cp). ^{11}B NMR (96 MHz, CD_2Cl_2) δ 91 (br, fwhm ca.498 Hz). ^{31}P NMR (121 MHz, CD_2Cl_2) δ 32.5.

Synthesis of [CpFe(dmpe)(BNMe$_2$)]$^+$Cl$^-$ (**5.17**)

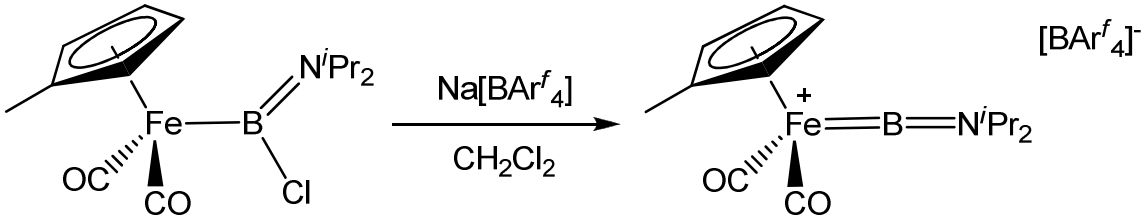
5.17 was synthesized by washing **5.16** with pentane and extracting the resulting residue into dichloromethane (20 cm^3). ^{1}H NMR (300 MHz, CD_2Cl_2) δ 1.52-1.64 (m, 12H, PMe_2), 1.77-2.09 (m, 4H, PCH_2), 2.75 (s, 6H, NMe_2), 4.65 (s, 5H, Cp). ^{13}C NMR (126 MHz, CD_2Cl_2) δ 21.7 (m, PMe), 24.7 (dd, $^1J_{CP}$ = 21.4 Hz, $^4J_{CP}$ = 20.2 Hz, PMe), 31.1 (q, $^1J_{CP}$ = 21 Hz, PCH_2), 34.5 (NMe_2), 80.4 (Cp). ^{11}B NMR (96 MHz, CD_2Cl_2) δ 88 (br, fwhm ca.337 Hz). ^{31}P NMR (121 MHz, CD_2Cl_2) δ 79. MS (positive ion electrospray) m/z (%) 326 (100) M^+; exact mass (calc. for M^+) 326.1049, (obs.) 326.1058.

5.3 Results and Discussion

5.3.1 Synthesis of [Cp'Fe(CO)$_2$(BN^{i}Pr$_2$)]$^+$[BAr$^f_4$]$^-$

The cationic aminoborylene, $[CpFe(CO)_2(BN^iPr_2)]^+$ has never been structurally characterized, despite numerous attempts and it was therefore decided to subtly modify the complex, by substituting hydrogen on the Cp ring for a methyl group which would hopefully lead to crystallisation. The aminoboryl complex, $[Cp'Fe(CO)_2B(N^iPr_2)Cl]$ (synthesized originally by Dr. D. L. Kays) was extracted into dichloromethane and added to a solution of $Na[BAr^f_4]$; the reaction was monitored by ^{11}B NMR and judged to be complete by conversion of the aminoboryl resonance (δ_B 56) to that due to the cationic aminoborylene, $[Cp'Fe(CO)_2(BN^iPr_2)]^+$ (**5.1** at δ_B 93). The novel cationic aminoborylene was fully spectroscopically characterized, and the data was in good agreement with the analogous but

not structurally characterized complex, $[CpFe(CO)_2(BN^iPr_2)]^+[BAr^f_4]^-$.[5] The ^{11}B NMR resonance for **5.1** is δ_B 93 which is almost identical to the shifts for $[CpFe(CO)_2(BN^iPr_2)]^+$ (94) and $[CpFe(CO)_2(BNCy_2)]^+$ (93).[4] The carbonyl stretching frequencies are also comparable (υ = 2065, 2023 cm^{-1} for **5.1**, 2070, 2028 cm^{-1} for $[CpFe(CO)_2(BN^iPr_2)]^+$).



Scheme 5.1 Synthesis of $[Cp'Fe(CO)_2(BN^iPr_2)]^+[BAr^f_4]^-$ by halide abstraction.

Crystals suitable for X-ray diffraction were obtained from a dichloromethane/hexane layering stored at -30˚C. The molecular structure is given in Figure 5.1 and a table of key bond lengths and angles listed in Table 5.2.

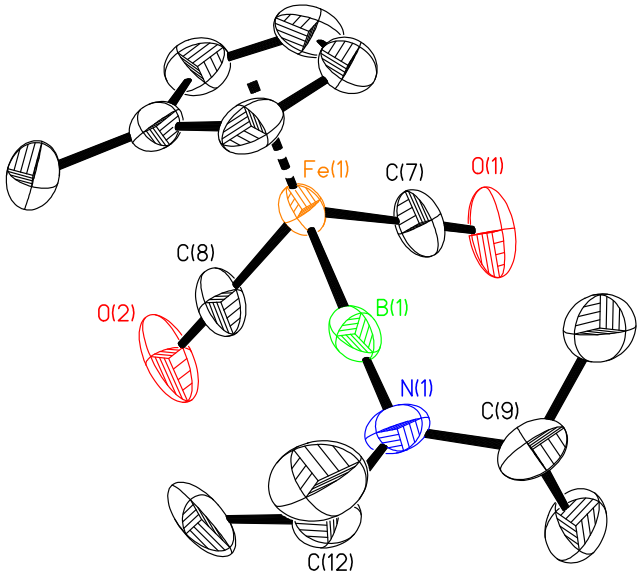


Figure 5.2 Molecular structure of $[Cp'Fe(CO)_2(BN^iPr_2)]^+[BAr^f_4]^-$ (**5.1**). Solvent molecule and hydrogen atoms omitted for clarity. Ellipsoids set at the 50% probability level.

Table 5.2 Selected bond lengths [Å] and angles [°] for **5.1**

Fe(1)-B(1)	1.835(3)	B(1)-N(1)	1.334(3)
C(7)-O(1)	1.143(3)	C(8)-O(2)	1.139(3)
Fe(1)-B(1)-N(1)	179.0(2)	CT-Cp-Fe(1)-N(1)-C(9)	95.2

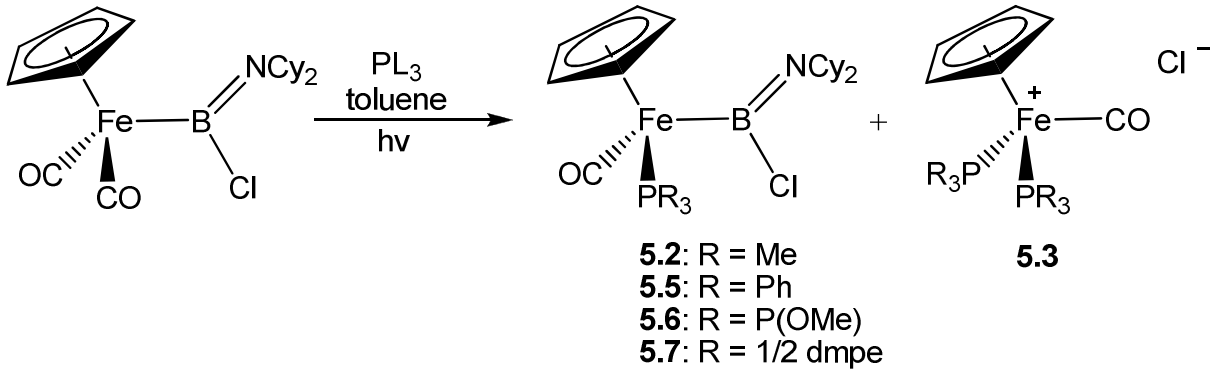
Unfortunately, the analogous complex, $[CpFe(CO)_2(BN^iPr_2)]^+[BAr^f_4]^-$ is an oil and therefore no crystallographic data is available. However, it is possible to compare the data to various other cationic aminoborylene complexes such as $[CpFe(CO)_2(BNCy_2)]^+$ and $[CpRu(CO)_2(BN^iPr_2)]^+$.[4,7e] **5.1** features the linear Fe-B-N framework (179.0(2)˚) common to all cationic aminoborylene complexes. The Fe-B bond, 1.835(3) Å is very similar to that found in $[CpFe(CO)_2(BNCy_2)]^+$ 1.859(6) Å (within experimental error), but significantly longer than the mesityl substituted borylene complex $[CpFe(CO)_2(BMes)]^+$ which has the shortest Fe-B bond of all the cationic borylene complexes (1.792(8) Å).[2] The ruthenium complex, $[CpRu(CO)_2(BN^iPr_2)]^+$ has a longer Ru-B bond however (1.950(8) Å), as expected due to the increased covalent radii of Ru versus Fe (1.17 and 1.24 Å for Fe and Ru respectively).[8] The B-N bond length 1.334(3) Å is also found to be in agreement with the dicyclohexyl aminoborylene complex, $[CpFe(CO)_2(BNCy_2)]^+$ (1.324(7) Å). The carbonyl stretching frequencies (2065, 2023 cm^{-1}) are almost identical to those reported for $[CpFe(CO)_2(BNCy_2)]^+$ (2071, 2028 cm^{-1}) and are consistent with a similar electronic structure. Furthermore, DFT calculations have been carried out on **5.1** and reveal σ and π contributions to the covalent bond of 70:30 which is as expected for the cationic aminoborylene complexes (cf. $[CpFe(CO)_2(BNCy_2)]^+$ 71:29, $[CpRu(CO)_2(BNCy_2]^+$ 68:32).

Variation of the Cp ring by substituting hydrogen for a methyl group clearly has no great effect on the electronic structure of the aminoborylene system, as supported by structural and computational analysis. However, the subtle change in the structure ensured crystallization of an isopropyl substituted cationic terminal borylene. With a view to examining the broader effects of ligand substitution pattern it was therefore decided to

investigate varying the carbonyl ligands to see what effect this might have on the cationic aminoborylene complexes.

5.3.2 Mono(Substitution) of Carbonyl Ligands for Phosphines

Reaction of the aminoboryl complex [CpFe(CO)$_2$B(NCy$_2$)Cl] with PMe$_3$ (2 equiv.) in toluene for 6 h under photolytic conditions led to formation of the mono(phosphine) complex, [CpFe(CO)(PMe$_3$)B(NCy$_2$)Cl] (**5.2**) in 33% yield.[7e] ^{11}B NMR spectroscopy showed a downfield shift from δ_B 58 for [CpFe(CO)$_2$B(NCy$_2$)Cl] to δ_B 61 for **5.2** which is consistent with data reported by Hartwig and co-workers for a similar catecholboryl complex,[10] (52 ppm to 58 ppm for [CpFe(CO)$_2$Bcat] and [CpFe(CO)(PMe$_3$)Bcat] respectively). ^{31}P NMR data are also in accord with those reported for [CpFe(CO)(PMe$_3$)Bcat] (δ_P 39.2 cf. δ_P 41.5 ppm for **5.2**). The ^{13}C NMR spectra are interesting in that they reveal the presence of twelve peaks corresponding to the twelve inequivalent cyclohexyl carbons, attributed to slow rotation about the BN bond, and to the diastereotopic inequivalence of both cyclohexyl rings due to the chiral metal centre.



Scheme 5.2 Synthesis of the mono(phosphine) amino boryl, [CpFe(CO)(PR$_3$)B(NCy$_2$)Cl].

Single crystals of the hemi-solvate suitable for X-ray diffraction were obtained from a saturated pentane solution at -30˚C. The crystal structure is shown in Figure 5.2 and key bond lengths and angles are listed in Table 5.3.

In order to observe the effect of replacing the π-acidic carbonyl group for the σ-donating phosphine it is instructive to compare the structure of **5.2** with its dicarbonyl analogue, $[CpFe(CO)_2B(NCy_2)Cl]$.[4] This substitution process reduces the Fe-B bond distance from 2.053(3) Å to 2.023(2) Å. Despite its greater bulk (cf. CO), trimethylphosphine is a better σ-donor resulting in increased Fe to B back donation. However, it is worth noting that although modification of the boryl substituents can exert some influence on the extent of Fe-B π-bonding, the boron based acceptor orbital has been calculated to typically lie too high in energy with respect to the corresponding filled metal d-orbital to participate in π-back bonding to any great extent.[11] To further highlight this, the Cp centroid-Fe-B-Cl torsion angle for **5.2** was calculated to be near perpendicular (78.0˚), indicating little or no π interaction of the formally vacant boron p-orbital with the HOMO of the metal fragment; the HOMO-2 (perpendicular to the HOMO) can also participate in π-interaction, but to a lesser extent due to its markedly lower energy.[11] Interestingly, the B=N bond length is the same (within experimental error) being 1.396(4) Å for the dicarbonyl precursor and 1.406(3) Å for **5.2**.

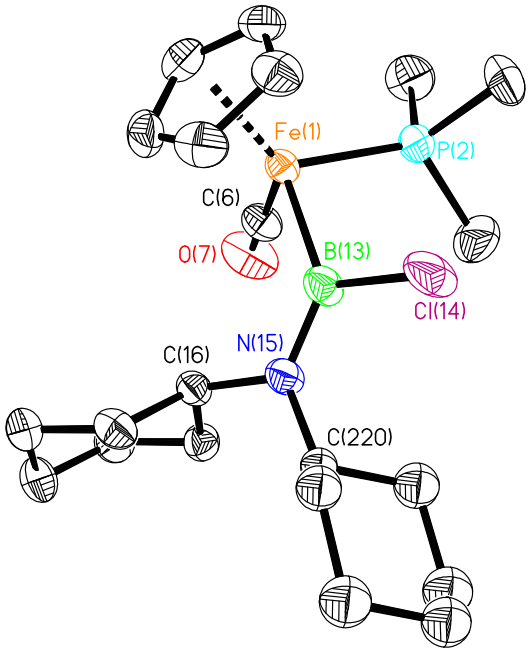


Figure 5.2 The molecular structure of [CpFe(CO)(PMe_3)B(NCy_2)Cl] (**5.2**). Solvent molecule and hydrogen atoms omitted for clarity. Ellipsoids set at the 50% probability level.

Table 5.3 Selected bond lengths [Å] and angles [°] for **5.2**

Fe(1)-B(13)	2.023(2)	Fe(1)-P(2)	2.1645(6)
Fe(1)-C(6)	1.711(2)	B(13)-N(15)	1.406(3)
B(13)-Cl(14)	1.870(2)	C(6)-O(7)	1.169(3)

Fe(1)-B(13)-N(15)	130.95(15)	Fe(1)-B(13)-Cl(14)	114.79(12)
Cl(14)-B(13)-N(15)	114.04(15)		

The Fe-C bond for **5.2**, at 1.711(2) Å is shorter than the average Fe-C bond length in [CpFe(CO)$_2$B(NCy$_2$)Cl] (1.743(3) Å),[4] as expected due to the increased π back donation into the remaining carbonyl ligand. The carbonyl stretching frequency of 1890 cm^{-1} is lower than those for the dicarbonyl derivative (2000, 1939 cm^{-1}), which is as expected for an increase in π back-bonding.

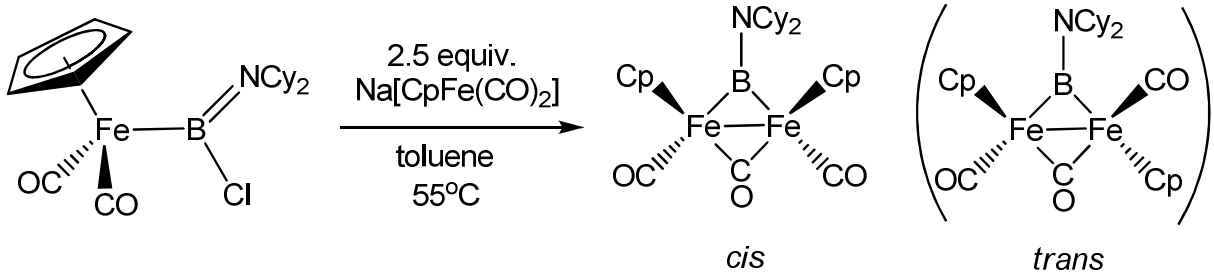
Hartwig reports formation of the bis(phosphine) compound, [CpFe(PMe$_3$)$_2$Bcat] in 52% yield by irradiation of the mono(substituted) complex, [CpFe(CO)(PMe$_3$)Bcat] with excess PMe$_3$ in pentane.[10] However, reacting **5.2** with excess PMe$_3$ under conditions of prolonged photolysis, does not lead to displacement of the second carbonyl substituent; rather [CpFe(CO)(PMe$_3$)$_2$]$^+$Cl$^-$, **5.3** is formed by extrusion of the borylene fragment.[12] This organometallic product was isolated as a yellow solid and its structure confirmed by X-ray crystallography. Although spectroscopic data for this compound have been reported in several papers no crystallographic data has yet been reported. The crystal structure is discussed at greater length later in this chapter. Although no definitive information concerning the nature of the boron-containing species accompanying the formation of **5.3** could be obtained, previous studies of the reactivity of [CpFe(CO)$_2$(BMes)]$^+$[BAr$^f_4$]$^-$ with various organic substrates were consistent with borylene insertion into the C-H bonds of the solvent.[2b]

The fact that both the mono(substituted) complexes, [CpFe(CO)(PMe$_3$)B(NCy$_2$)Cl] and [CpFe(CO)(PMe$_3$)Bcat] are formed, but the bis(phosphine) complex can only be formed for the Bcat complex, [CpFe(PMe$_3$)$_2$Bcat],[10] indicates that reactivity may be influenced by steric and electronic properties. A factor inhibiting substitution of the second carbonyl ligand, may be the strong binding of the remaining carbonyl group. A comparison of the IR measured carbonyl stretching frequencies for the mono(substituted) complexes,

[CpFe(CO)(PMe_3)B(NCy_2)Cl] (1890 cm^{-1}) and [CpFe(CO)(PMe_3)Bcat] (1927 cm^{-1}), is consistent with a greater degree of back-bonding from iron resulting in a stronger Fe-CO bond for **5.2**. As the phosphine donor is the same in both complexes, the stronger binding of the CO in **5.2** compared to [CpFe(CO)(PMe_3)Bcat] must be due to the weaker π-acceptor properties of the B(NCy_2)Cl ligand versus Bcat, a fact supported by comparison of the carbonyl stretching frequencies for both parent dicarbonyl complexes (2024, 1971 cm^{-1} for [CpFe($CO)_2$Bcat] and 2001, 1943 cm^{-1} for [CpFe($CO)_2$B(NCy_2)Cl] respectively). Another factor in the impaired substitution chemistry for **5.2** could be the steric bulk of the dicyclohexyl groups on the borylene substituent B(NCy_2)Cl compared to Bcat. In order to try to displace the second carbonyl ligand, different phosphine ligands were attempted and the reaction solvent was also varied.

Hartwig *et al*. reported irradiation of [CpFe($CO)_2$Bcat] to form [CpFe($PMe_3)_2$Bcat] took place in pentane.[10] Therefore, attempts were made at carrying out photolysis of [CpFe($CO)_2$B(NCy_2)Cl] in pentane rather than toluene, to see if varying the solvent had any significant influence on displacing the second carbonyl ligand. Irradiation in pentane however led to a growth of an ^{11}B NMR resonance at δ_B 101; the implied solubility in pentane leads to the conclusion that the species giving rise to this resonance is charge neutral. The complex was tentatively formulated as the bridging borylene complex [(μ-BNCy_2)(μ-CO){CpFe(CO)}$_2$], **5.4** on the basis of the downfield shift in the ^{11}B NMR to δ_B ~100, a resonance typical of bridging borylene complexes.[1d] In order to gain further evidence that this was indeed the complex formed, the bridging borylene was synthesized by a second route in a similar manner to that reported by Braunschweig and co-workers for the trimethylsilyl-substituted analogue, [(μ-B$N(SiMe_3)_2$)(μ-CO){CpFe(CO)}$_2$] (i.e. salt metathesis).[13a]

Cy_2NBCl_2 was reacted with 2.5 equiv. $Na[CpFe(CO)_2]$ in toluene at 55˚C, in order to force the reaction through from $[CpFe(CO)_2B(NCy_2)Cl]$ to the bridged complex (Scheme 5.3). **5.4** precipitated as a red crystalline solid from a saturated hexane solution at -30˚C. Multinuclear NMR (^1H, ^{11}B, ^{13}C), IR spectroscopy and mass spectrometry all confirmed formation of the bridged borylene, which can be compared to a related compound reported by Braunschweig, $[(\mu\text{-}BNMe_2)(\mu\text{-}CO)\{CpFe(CO)\}_2]$.[13b] The highly deshielded ^{11}B NMR shift of δ_B 101 is in accord with the dimethyl analogue (δ_B 103.5). ^{13}C NMR (δ_C 275.3) and the carbonyl stretching frequency (1781 cm^{-1}) for the bridging carbonyl ligand are also in agreement with data obtained for similar bridging aminoborylene complexes; ($[(\mu\text{-}BNMe_2)(\mu\text{-}CO)\{CpFe(CO)\}_2]$ δ_C 275.8, υ 1776 cm^{-1}, $[(\mu\text{-}BNMe_2)(\mu\text{-}CO)\{Cp'Fe(CO)\}_2]$ δ_C 277.0, υ 1778 cm^{-1},[13b] $[(\mu\text{-}BN(SiMe_3)_2)(\mu\text{-}CO)\{CpFe(CO)\}_2]$ δ_C 276.6, υ 1770 cm^{-1}, $[(\mu\text{-}BN(SiMe_3)_2)(\mu\text{-}CO)\{Cp^*Fe(CO)\}_2]$ δ_C 279.3, υ 1770 cm^{-1}).[13a] The complex, $[(\mu\text{-}BNCy_2)(\mu\text{-}CO)\{CpFe(CO)\}_2]$ can, however, exist as one of two isomers i.e. *cis* or *trans* (Scheme 5.3).



Scheme 5.3 Synthesis of the bridged borylene **5.4** and its *cis* and *trans* isomers.

The structurally characterized complexes reported by Braunschweig each give rise to two carbonyl stretching frequencies, one for the bridging carbonyl (~1770 cm^{-1}) and one corresponding to the asymmetric stretching vibration of the terminal carbonyls (1920-1950

cm^{-1}). The IR spectra of [(μ-$BNCy_2$)(μ-CO){$CpFe(CO)\}_2$] however, shows *three* carbonyl stretching frequencies: one for the bridging carbonyl ligand (1781 cm^{-1}), together with the anti-symmetric stretching vibration of the terminal carbonyls (1954 cm^{-1}) and the corresponding symmetric stretching mode (1997 cm^{-1}). Such data are more consistent with a formulation as the *cis* isomer.

Ogino *et al.* reported formation of the gallylene bridged complex, [(μ-GaMes)(μ-CO){$CpFe(CO)\}_2$], which exist as an equilibrium mixture of *cis* and *trans* isomers.[14] The IR spectrum of the *cis* isomer has three carbonyl stretching frequencies at 1942, 1905 and 1751 cm^{-1} consistent with the shifts observed for **5.4**. In addition, the ^{13}C NMR spectrum of **5.4** reveals the presence of broad signals at δ_C 63.2 and δ_C 35.1 corresponding to the CH and adjacent CH_2 groups of the cyclohexyl substituents respectively. Variable temperature NMR experiments were carried out to ascertain if this broadening was due to a fluxional process. On cooling to -30˚C the broad signal at δ_C 63.2 split into two signals (δ_C 68.0 and 56.9) corresponding to the CH groups on each cyclohexyl ring, and the peak at δ_C 35.1 splits into two signals (δ_C 37.4 and 34.6) corresponding to two inequivalent CH_2 groups (adjacent to CH) on the cyclohexyl rings (Figure 5.3). Coalescence of the respective peaks was achieved at -5˚C and the rate constant at coalescence is thereby calculated to be 1858.4 s^{-1} ($\Delta\upsilon_o$ = 837.1 Hz).[15] The Eyring equation can then be used to determine the barrier to rotation as 48.6 kJ mol^{-1}.[16]

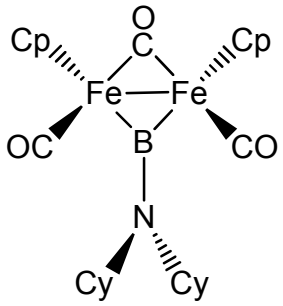


Figure 5.3 The *cis* isomer of **5.4**, illustrating the inequivalent cyclohexyl groups

A solid state structure of **5.4** would confirm formation of the *cis*-isomer, however, various attempts at crystallising the complex, by varying the solvent (hexane, pentane, toluene, octane) were unsuccessful. The Cp' analogue [(μ-$BNCy_2$)(μ-CO){Cp'Fe(CO)}$_2$] was also targeted (δ_B 101), in the hope that this might prove easier to crystallise, however, unfortunately no crystals suitable for X-ray diffraction were obtained.

Returning to phosphine substitution chemistry, the reaction of the aminoboryl complex, [$CpFe(CO)_2B(NCy_2)Cl$] was also carried out with the weaker σ-donor PPh_3 under photolytic conditions in toluene and the mono(substituted) complex, [$CpFe(CO)(PPh_3)B(NCy_2)Cl$], **5.5** synthesized in 60% yield. PPh_3 has a cone angle of 145˚ which is significantly greater than that of PMe_3 (118˚) and so only the mono(substituted) complex is expected to be formed.[17] Multinuclear spectroscopy, IR spectroscopy and mass spectrometry were all consistent with the formation of **5.5**, however, no crystals suitable for X-ray diffraction could be obtained. A similar upfield shift (δ_B 58 to δ_B 61) was observed as for the formation of **5.2**. The weaker σ-donating properties of triphenylphosphine compared to trimethylphosphine are reflected in the carbonyl stretching frequencies, which were higher for **5.5** (1901 cm^{-1} cf. 1890 cm^{-1} for **5.2**).

In order to promote displacement of the second carbonyl ligand it was decided to try the π-acceptor trimethylphosphite. Formation of the corresponding mono(phosphite) complex would hopefully reduce the degree of π back-bonding to the remaining carbonyl ligand and hopefully make it easier to displace. Trimethylphosphite was reacted with $[CpFe(CO)_2B(NCy_2)Cl]$ in toluene under photolytic conditions and once again despite a smaller cone angle than PMe_3 (107˚ versus 118˚)[18] and prolonged photolysis, it seems that only the mono(substituted) complex was formed, ($[CpFe(CO)\{P(OMe)_3\}B(NCy_2)Cl]$, **5.6**, as indicated by ^{11}B and ^{31}P NMR signals at δ_B 61, δ_P 193). Unfortunately, attempts to isolate **5.6** by cooling a pentane extraction to -30˚C did not lead to any tractable products.

An attractive alternative to photolytic carbonyl substitution is to use trimethylamine N-oxide as an oxidant.[19-21] The reagent works by attacking the carbonyl carbon, oxidising it to form CO_2, which is evolved thereby replacing the carbon monoxide ligand either with trimethylamine or an additional added ligand. Brown and co-workers have demonstrated that decarbonylation using trimethylamine N-oxide is generally restricted to carbonyls with stretching frequencies > ~2000 cm^{-1}; lower carbonyl stretching frequencies would result in a stronger metal-carbonyl bond and harsher reaction conditions would be required to remove the carbonyl.[20] They reported reaction of $[PhMn(CO)_5]$ and $[CpM(CO)_3X]$ (M = Mo, W, X = halide) with triphenylphoshine in the presence of trimethylamine N-oxide proceeds by coordination of the oxidant to the carbonyl which loses CO_2, with subsequent complexation of the phosphine at the metal centre. Davies *et al.* also carried out the reaction of $[CpFe(CO)_3]^+[PF_6]^-$ with PPh_3 or $P(OMe)_3$ in the presence of Me_3NO.[21] The carbonyl stretching frequencies of $[CpFe(CO)_2B(NCy_2)Cl]$ are 2000 and 1939 cm^{-1} and so it was decided to attempt the decarbonylation reaction via this route. The reaction was carried out in

the presence of $P(OMe)_3$ as this phosphite has the smallest cone angle (107˚ versus 118˚ for PMe_3), and is less likely to be oxidised. Thus the phosphite, Me_3NO and $[CpFe(CO)_2B(NCy)_2Cl]$ were mixed in dichloromethane, but the reaction was unsuccessful, and the ^{11}B NMR indicated decomposition of the $[CpFe(CO)_2B(NCy_2)Cl]$ complex with the major signal at δ_B 19 being attributed to a boron coordinated to three oxygen atoms.

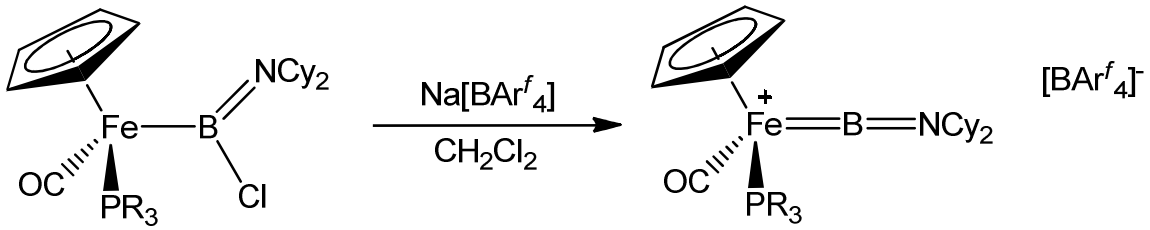
Ueno and co-workers have reported substitution of both carbonyl ligands of the gallyl complex $[Cp^*Fe(CO)_2GaCl_2]$ by using the chelating phosphine dmpe, $(Me_2PCH_2CH_2PMe_2)$ in toluene under photolytic conditions.[22] The reaction proceeds by coordination of one of the phosphine donors to the electrophilic gallium centre; irradiation then displaces one carbonyl and the free phosphine donor coordinates at the iron centre. Further photolysis then substitutes the remaining carbonyl and $[Cp^*Fe(dmpe)GaCl_2]$ is formed. Mimicking this methodology, the boryl complex $[CpFe(CO)_2B(NCy_2)Cl]$ was also reacted with the chelating phosphine, dmpe leading to a downfield shift in the ^{11}B NMR spectrum to δ_B 61 ppm and a peak at δ_P 52 in the ^{31}P NMR.[7e] Ueno reports a ^{31}P NMR shift of 69 ppm for the chelating dmpe in $[Cp^*Fe(dmpe)GaCl_2]$, and although resonances at δ_P ~80 were observed, they were never in tractable amounts. No attempt was made to isolate the highly soluble boryl complex, however further reaction by halide abstraction yielded the bridged species, *meso*-$[\{CpFe(CO)(B(NCy_2)\}_2(\mu\text{-dmpe})]^{2+}$ (*vide infra*) indicating that the boryl species formed is $[\{CpFe(CO)B(NCy_2)Cl\}_2(\mu\text{-dmpe})]$ **5.7**.

As varying the trialkylphosphine groups had little or no effect on displacing the second carbonyl, it is likely that the higher steric demands of the $B(NCy_2)Cl$ substituent (cf. the Bcat ligand) probably inhibits attack of the second phosphine. Reactivity of $[Cp^*Fe(CO)_2GaI_2]_2$, for instance, with the chelating ligand dppe ($PPh_2CH_2CH_2PPh_2$) led to formation of the

disubstituted complex, [Cp*Fe(dppe)GaI_2] which was crystallographically characterized.[23] In comparison, $GaI(\mu\text{-}I)_2$ is a much smaller fragment than the sterically demanding $B(NCy_2)Cl$ ligand, and therefore it was decided to substitute the dicyclohexyl substituents for the much smaller dimethyl substituents; this work is discussed towards the end of this chapter.

5.3.3 Synthesis of Mono(Substituted) Cationic Borylene Complexes

The boryl complexes, [CpFe(CO)(PMe_3)$B(NCy_2)$Cl], [CpFe(CO)(PPh_3)$B(NCy_2)$Cl], [CpFe(CO){$P(OMe)_3$}$B(NCy_2)$Cl] and [{CpFe(CO)$B(NCy_2)$Cl}$_2$(μ-dmpe)] were all subsequently reacted with Na[BAr^f_4] in order to form the corresponding cationic aminoborylene complexes by halide abstraction (Scheme 5.4).



5.2: $PR_3 = PMe_3$
5.5: $PR_3 = PPh_3$
5.6: $PR_3 = P(OMe)_3$
5.7: PR_3 = 1/2 dmpe

5.8: $PR_3 = PMe_3$
5.9: $PR_3 = PPh_3$
5.10: $PR_3 = P(OMe)_3$
5.11: PR_3 = 1/2 dmpe

Scheme 5.4 Synthesis of $[CpFe(CO)(PR_3)(B(NCy_2)]^+[BAr^f_4]^-$

Reaction of **5.2** with Na[BAr^f_4] in dichloromethane led to isolation of the cationic terminal aminoborylene complex, $[CpFe(CO)(PMe_3)(BNCy_2)]^+[BAr^f_4]^-$ in 27% yield.[7e] Formation of **5.8** results in a downfield ^{11}B NMR shift to δ_B 93, as expected for cationic terminal borylene complexes.[1] The carbonyl stretching frequency is blue shifted to 1981 cm^{-1} compared to the boryl precursor **5.2** (1890 cm^{-1}) as expected for the formation of a cationic

complex. This can be compared to the analogous dicarbonyl substituted aminoboryl and aminoborylene complexes (2000, 1939 cm^{-1} and 2071, 2028 cm^{-1}, respectively). Compared to the dicarbonyl analogue, $[CpFe(CO)_2(BNCy_2)]^+[BAr^f_4]^-$ however, the carbonyl stretching frequency for **5.8** is red shifted (1981 vs. 2071, 2028 cm^{-1}) due to an increase in back donation to the single π-acceptor carbonyl ligand.[4] Unlike the ^{13}C NMR spectra for the corresponding boryl complex, **5.2** which contained twelve peaks for each diastereotopic carbon in the cyclohexyl rings, the spectra for **5.8**, at room temperature, reveal the presence of only six peaks. These spectra indicate rapid rotation about the M-B-N axis on the NMR timescale which results in both the cyclohexyl rings becoming equivalent. In order to gain a further understanding of the electronic structure of the Fe-B bond, a variable temperature NMR experiment was carried out from 20˚C to -80˚C, focussing on the resonances for the CH of the Cy substituent. At room temperature, this peak is a singlet (at δ_C 55), and to calculate the barrier to rotation about the double bond, this peak would need to coalesce at lower temperature. Unfortunately, no splitting was observed, even at -80˚C, although the observed line broadening (1.82 Hz on going from 20˚C to –80˚C) could be used to obtain an estimate of the upper limit to the barrier to rotation using the line broadening analysis reported by Brookhart.[16] A better estimate can be obtained, however, from the corresponding ruthenium complex $[CpRu(CO)(PMe_3)(BNCy_2)]^+[BAr^f_4]^-$ (synthesized by Dr. D. Vidovic) for which the line broadening is more pronounced at 4.1 Hz.[7e] An estimate of the chemical shift difference (υ_A-υ_X) in the slow exchange limit is obtained for the two CH groups by comparing to the two methyl resonances in the compound $[CpRe(NO)(PPh_3)(=C=CMe_2)]^+$ ($\Delta\delta_C$ = 3.7 ppm = 465 Hz) reported by Gladysz *et al*.[24] Using the fast exchange approximation $k = (\upsilon_A-\upsilon_X)^2/2\Delta W$ the rate constant was calculated to be 2.60 x 10^4 s^{-1} (5.95 x 10^4 s^{-1} for **5.8**). Using the Eyring

equation the energy for the barrier to rotation is calculated at ≤ 30.3 kJ mol^{-1} (28.9 kJ mol^{-1} for **5.8**).

Crystals of **5.8** (Figure 5.4) were obtained from a hexane layering of a solution in dichloromethane and storage at -30˚C and a table of relevant bond lengths and angles determined by X-ray diffraction are given in Table 5.4

The solid state structure of **5.8** features the linear Fe-B-N framework (∠Fe-B-N = 177.7(3)˚) common to terminal borylene complexes (cf. 178.8(5)˚ for $[CpFe(CO)_2(BNCy_2)]^+[BAr^f_4]^-$).[4] The Fe-B bond length, 1.821(4) Å, however, is shorter than the analogous carbonyl complex (1.859(6) Å) presumably due to the increased Fe to B π back bonding. The percentage decrease in the Fe-B bond length on going from the mono(substituted) boryl complex, **5.2** to the mono(substituted) borylene **5.8** is -10%, which is very similar to the change observed on going from the dicarbonyl ligated boryl complex to the borylene (-9.4%).[7e] The torsion angle Cp centroid-Fe(1)-N(14)-C(15) was calculated to be 92.2˚, which is therefore consistent with π-interaction between the HOMO of the $[CpFe(CO)_2]^+$ fragment and one of two empty p-orbitals at boron. The boron centre is of course stabilized by π-interaction from the amine (NCy_2) into the other perpendicular B p-orbital. Such π back donation results in a reduction in the Fe-B bond length. The Fe-CO bond length is 1.743(4) Å which is shorter than the average bond length for the dicarbonyl derivative, indicative of the increased π-back-bonding from the metal centre to the π-acid carbonyl ligand.

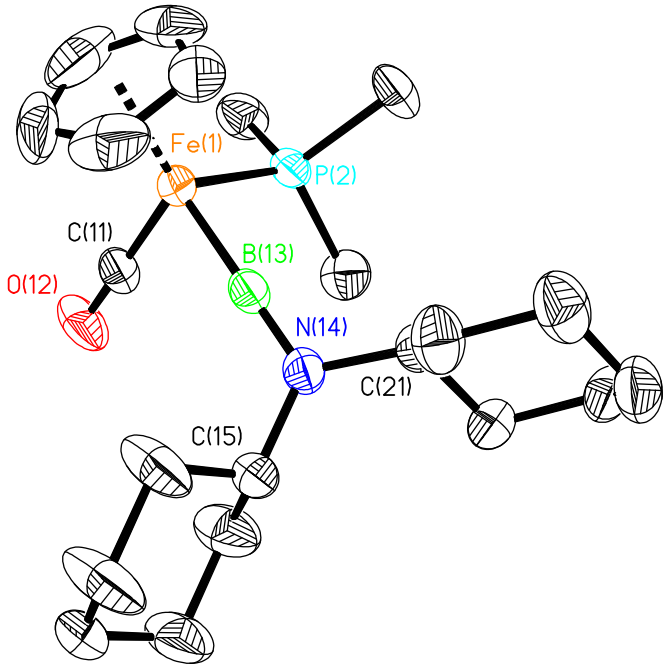


Figure 5.4 The molecular structure of $[CpFe(CO)(PMe_3)(B(NCy_2)]^+[BAr^f_4]^-\cdot CH_2Cl_2$ (**5.8**). Solvent molecule and hydrogen atoms omitted for clarity. Ellipsoids set at the 50% probability level.

Table 5.4 Selected bond lengths [Å] and angles [°] for **5.8**.

Fe(1)-B(13)	1.821(4)	B(13)-N(14)	1.347(5)
Fe(1)-P(2)	2.1804(10)	Fe(1)-C(11)	1.743(4)
Fe(1)-B(13)-N(14)	177.7(3)	P(2)-Fe(1)-C(11)	89.45(12)
C(15)-N(14)-C(21)	120.0(3)	CT-Cp-Fe(1)-N(14)-C(15)	92.2

The crystal structure of **5.8** can be compared to that of the cationic by-product formed during photolysis of $[CpFe(CO)_2B(NCy_2)Cl]$ with PMe_3, i.e. $[CpFe(CO)(PMe_3)_2]^+$, **5.3** where the borylene fragment ($BNCy_2$) is replaced by the poor π-acceptor, PMe_3. **5.3** would therefore be expected to have a stronger, shorter Fe-CO bond (and a longer, weaker C-O bond) than **5.8**. Comparison of the bond lengths however, reveal that they are actually equal within experimental error (Fe-CO for **5.3** is 1.736(3) Å, for 1.743(4) Å for **5.8**, C-O bond is 1.156(4) Å for **5.3**, 1.140(4) Å for **5.8**). Comparison of the carbonyl stretching frequency however, reveal more π-back-bonding to the carbonyl ligand in **5.3** (1949 cm^{-1}) compared to **5.8** (1981 cm^{-1}) as expected. The molecular structure of **5.3** is given in Figure 5.5 and a list of relevant bond lengths and angles given in Table 5.5.

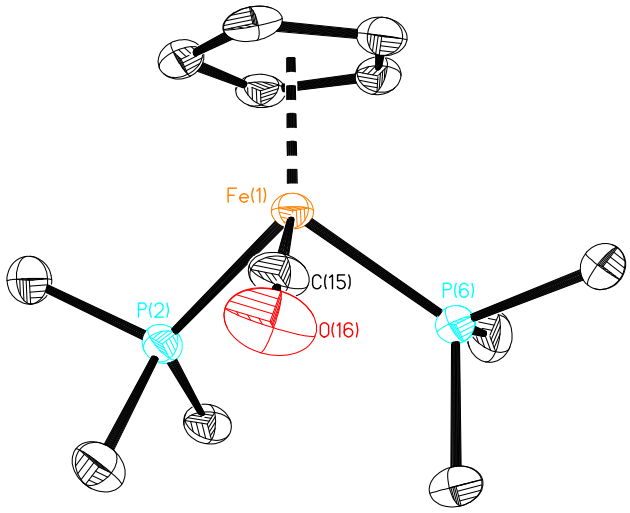


Figure 5.5 Molecular structure of $[CpFe(CO)(PMe_3)_2]^+Cl^-$ (**5.3**). Solvent molecule and hydrogen atoms omitted for clarity. Ellipsoids set at the 50% probability level.

Table 5.5 Selected bond lengths [Å] and angles [°] for **5.3**.

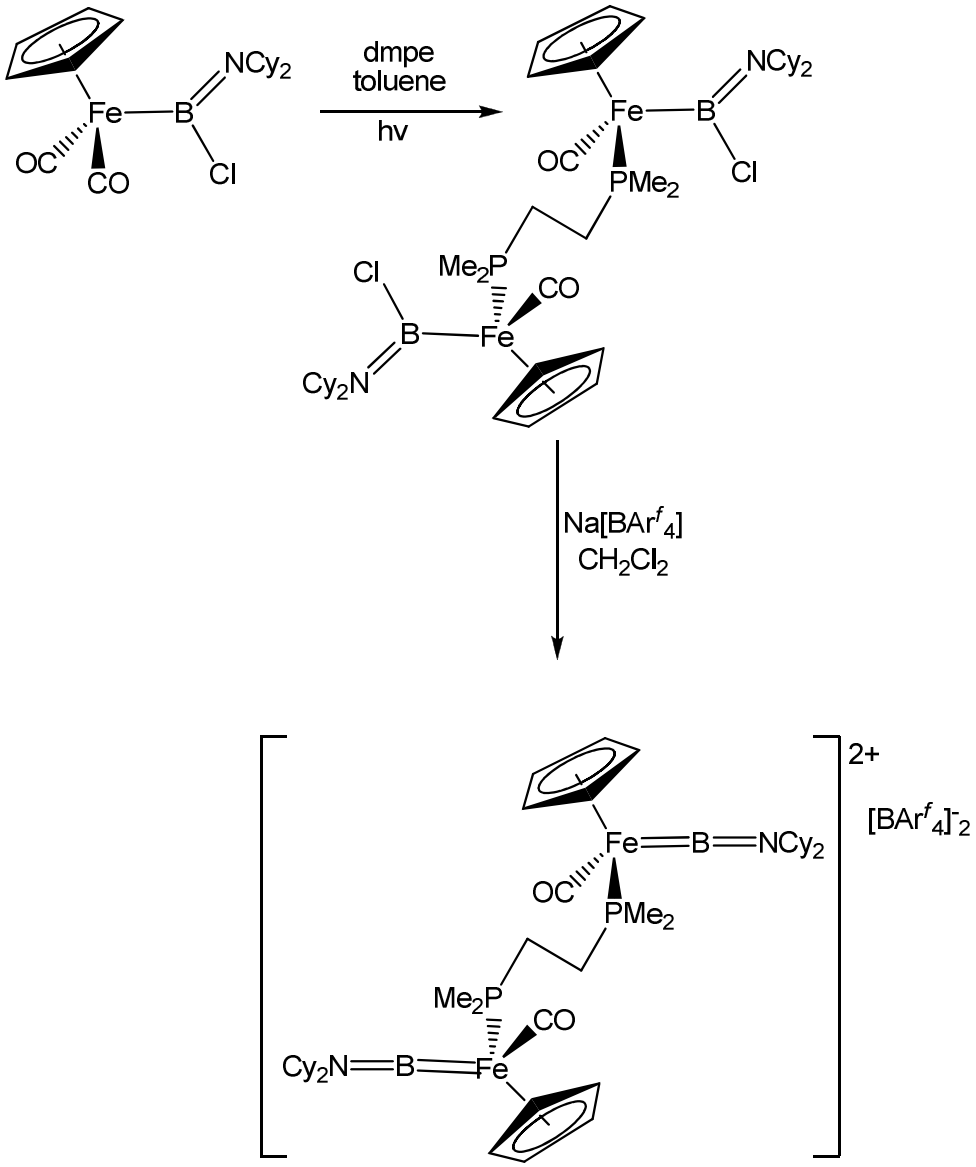
Fe(1)-P(2)	2.2244(9)	Fe(1)-P(6)	2.2042(9)
Fe(1)-C(15)	1.736(3)	C(15)-O(16)	1.156(4)
P(2)-Fe(1)-C(15)	91.96(10)	P(6)-Fe(1)-C(15)	90.33

The reaction of [CpFe(CO)(PPh_3)B(NCy_2)Cl], **5.5** with Na[BAr^f_4] in dichloromethane was monitored by both ^{11}B and ^{31}P NMR and indicated formation of the mono(substituted) cationic terminal borylene [CpFe(CO)(PPh_3)($BNCy_2$)]$^+$[BAr^f_4]$^-$ (**5.9**) (δ_B 92 and δ_P 68). Spectroscopic data (multinuclear NMR and IR spectroscopy) along with electrospray mass spectrometry (m/z 602) support formation of **5.9**. The carbonyl stretching frequency for **5.9** is 1988 cm^{-1}, which is higher than that for **5.8** (1981 cm^{-1}), as expected owing to the weaker σ-donor capabilities of PPh_3 compared to PMe_3. Unfortunately, no crystal structure could be isolated from various layerings such as dichloromethane/hexane and fluorobenzene/hexane, but spectroscopic data and comparison with those obtained for structurally characterized **5.8** provide convincing evidence for this formula.

Reaction of [CpFe(CO){$P(OMe)_3$}B(NCy_2)Cl], **5.6** by halide abstraction also gives evidence for the formation of the analogous borylene, [CpFe(CO){$P(OMe)_3$}($BNCy_2$)]$^+$, **5.10** from (δ_B 90, δ_P 193). However, layering with hexane and storage at -30˚C failed to provide any crystals suitable for X-ray diffraction.

As was briefly mentioned earlier in the chapter, photolysis of [$CpFe(CO)_2B(NCy_2)Cl$] with dmpe yielded the dinuclear species; [{CpFe(CO)B(NCy_2)Cl}$_2$(μ-dmpe)], which was identified by subsequent reaction with Na[BAr^f_4] in dichloromethane to form the dicationic dinuclear borylene species, [{CpFe(CO)($BNCy_2$)}$_2$(μ-dmpe)]$^{2+}$[BAr^f_4]$^-_2$ (**5.11**) in 19% yield (Scheme 5.5). As the compound contains two chiral iron centres, it has the possibility of existing as either the *rac* or *meso* diastereoisomers. Multinuclear NMR spectroscopies cannot distinguish between the two isomers, however, if both diastereoisomers existed in solution,

there should be two sets of peaks in the spectra. However, only one peak exists for the Cp in the ^{1}H and ^{13}C NMR spectra and only one peak is observed in the ^{31}P NMR, indicating the presence of only one diastereoisomer (which was subsequently shown by crystallography to be the *meso* form). It is likely that both the *rac* and *meso* boryl diastereoisomers are formed but when the cationic borylene is formed only one diastereoisomer – *meso*, is crystallised. Redissolving the *meso* diastereoisomer in CD_2Cl_2, however, shows the presence of only one diasteroisomer in the ^{1}H and ^{13}C NMR spectra and hence the rate of epimerization must be very slow.



Scheme 5.5 Synthesis of $[\{CpFe(CO)(BNCy_2)\}_2(\mu\text{-dmpe})]^{2+}[BAr^f_4]^-_2$.

Single crystals of **5.11** suitable for X-ray diffraction were isolated by layering the solution with fluorobenzene, and storage at -30˚C. The solid state structure is shown in Figure 5.6 and Table 5.6 shows a list of relevant bond lengths and angles.

5.11 crystallised with two independent centrosymmetric dications, four anions and a molecule of dichloromethane. The molecular structure confirms the compound is in the *meso* form. As the cations are essentially identical, only one will be discussed. Also, only one half

of the dication will be discussed; in addition each half of each cation is related to the other by a centre of inversion. The complex features an approximately linear geometry around the Fe-B-N framework expected for cationic terminal borylene complexes (171.2(5)˚) but is slightly more distorted compared to the analogous complexes $[CpFe(CO)(PMe_3)(BNCy_2)]^+$, **5.8** (177.7(3)˚) and $[CpFe(CO)_2(BNCy_2)]^+$ (178.8(5)˚) possibly due to the bridging dmpe ligand, or more likely, the packing effects in the solid state. The Fe-B length of 1.830(7) Å is the same as that reported for **5.8** (1.821(4) Å) (within experimental error); the B-N bond, 1.342(8) Å is also in agreement with the B-N bond for **5.8** (1.347(5) Å). Once again, as with the **5.8**, the Fe-CO bond (1.760(7) Å) is shorter than for the dicarbonyl complex, due to a increased π back-bonding.

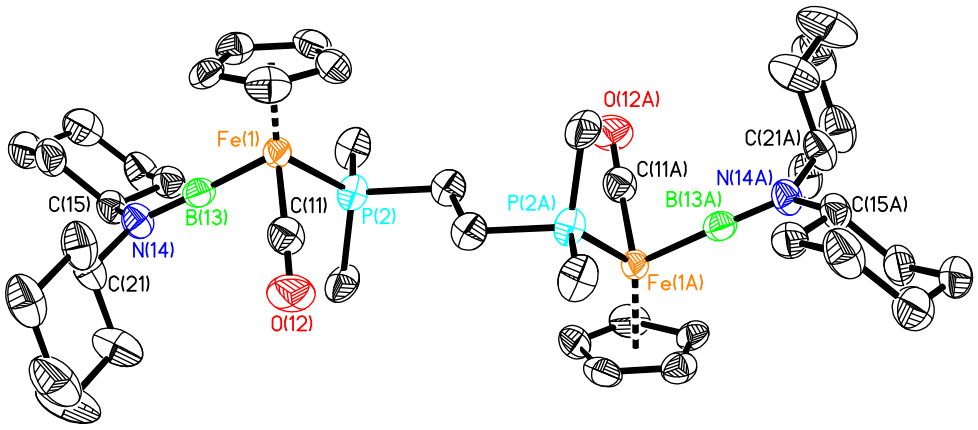


Figure 5.6 Molecular structure of $[\{CpFe(CO)(BNCy_2)\}_2(\mu\text{-dmpe})]^{2+}[BAr^f_4]^-_2\cdot 1/2CH_2Cl_2$ (**5.11**). Solvent molecule and hydrogen atoms omitted for clarity. Ellipsoids set at the 50% probability level.

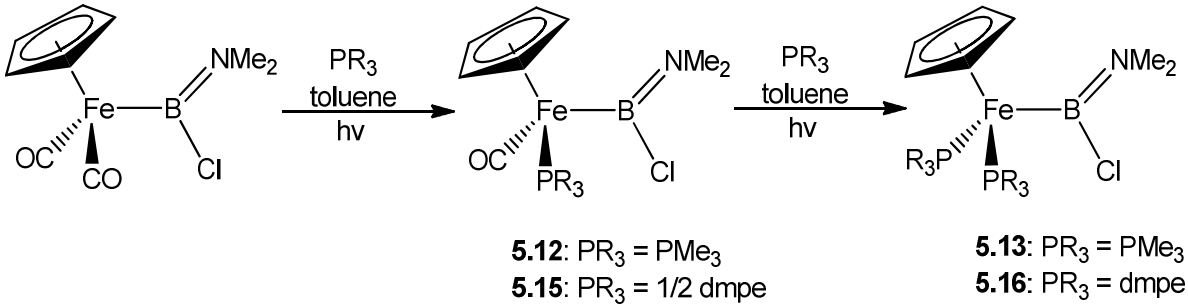
Table 5.6 Selected bond lengths [Å] and angles [°] for **5.11**

Fe(1)-B(13)	1.830(7)	B(13)-N(14)	1.342(8)
Fe(1)-P(2)	2.169(2)	Fe(1)-C(11)	1.760(7)
Fe(1)-B(13)-N(14)	171.2(5)	P(2)-Fe(1)-C(11)	89.3(2)
C(15)-N(14)-C(21)	115.1(4)	CT-Cp-Fe(1)-N(14)-C(21)	95.5

5.3.4 Substitution of Both Carbonyls for Phosphines

Ultimately, a primary aim of the research was to displace the second carbonyl ligand with a less π acidic ligand in order to see what effect having two σ-donors rather than two π-acceptors on the metal would have on the Fe-B bond. Numerous attempts at displacing the second carbonyl on [CpFe(CO)(PMe_3)B(NCy_2)Cl] by using various phosphine ligands and varying the reaction solvent were unsuccessful, apparently due to the steric bulk of the B(NCy_2)Cl ligand. Replacing the cyclohexyl groups on the amine with smaller methyl groups would hopefully facilitate displacement of the second carbonyl.

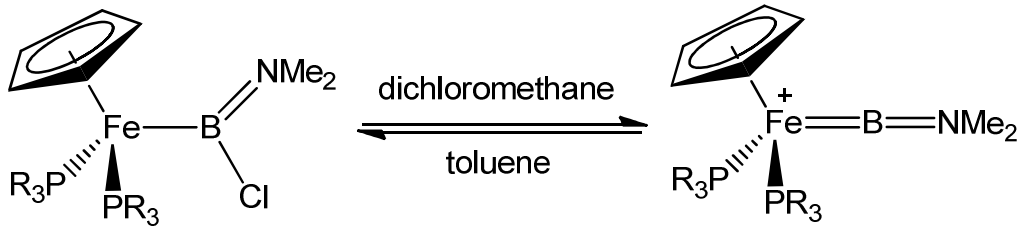
Irradiation of [CpFe$(CO)_2$B(NMe_2)Cl] with PMe_3 (2 equiv.) in toluene was monitored by both ^{11}B and ^{31}P NMR, and after 6 h led to conversion of [CpFe$(CO)_2$B(NMe_2)Cl] (δ_B 56) to a species giving rise to resonances at δ_B 62 and δ_P 41 (cf. δ_B 62, δ_P 41.5 for [CpFe(CO)(PMe_3)B(NCy_2)Cl]) indicating formation of the mono(phosphine) complex, [CpFe(CO)(PMe_3)B(NMe_2)Cl], **5.12**. However, there was also a peak at δ_B 62, indicating formation of the bis(phosphine) complex. A similar systematic downfield shift was reported by Hartwig for the formation of the bis(phosphine) complexes (δ_B 58 for [CpFe(CO)(PMe_3)Bcat], δ_B 60 for [CpFe$(PMe_3)_2$Bcat]).[10] The reaction was therefore photolysed further until all the mono(phosphine) complex was converted to the bis(phosphine) complex, [CpFe$(PMe_3)_2$B(NMe_2)Cl] (**5.13**) (δ_B 67, δ_P 42) (Scheme 5.6).



Scheme 5.6 Synthesis of the bis(substituted) phosphine aminoboryl complexes.

In order to crystallise the bis(phosphine) boryl substituted complex, **5.13** the volatiles were removed under reduced pressure and the residue extracted into pentane. However, ^{11}B NMR spectra of the pentane extract did not contain any of the boryl complex. The residue was subsequently extracted into dichloromethane and revealed the presence of a peak at δ_B 91 in the ^{11}B NMR spectrum and at δ_P 30 in the ^{31}P NMR spectrum (consistent with $[CpFe(CO)(PMe_3)(BNCy_2)]^+[BAr^f_4]^-$ δ_B 92, δ_P 32), implying formation of the cationic terminal aminoborylene $[CpFe(PMe_3)_2(BNMe_2)]^+Cl^-$, **5.14**. Both ^1H and ^{13}C NMR spectra support the formation of **5.14** with peaks corresponding to Cp and PMe_3 ligands and equivalent amino methyl substituents. Unfortunately, attempts to undertake electrospray mass spectrometry on this solution were unsuccessful, possibly due to **5.14** being too reactive to moisture/air.

Similar solvent dependency was observed by Tilley in 2004 for the osmium silyl complex, $[Cp^*Os(PMe_3)_2Si(^iPr_2)OTf]$.[25] In deuterated benzene, ^{29}Si NMR indicated formation of the silyl complex, however in the more polar solvent deuterated dichloromethane, the ^{29}Si NMR was significantly downfield shifted, supporting dissociation of triflate and synthesis of the silylene complex, $[Cp^*Os(PMe_3)_2(Si^iPr_2)]^+[OTf]^-$ (Scheme 5.7).



5.13: $PR_3 = Me_3$
5.16: PR_3 = 1/2 dmpe

5.14: $PR_3 = PMe_3$
5.17: PR_3 = 1/2 dmpe

Scheme 5.7 Spontaneous formation of the cationic aminoborylene, $[CpFe(PR_3)_2(BNMe_2)]^+Cl^-$.

Despite many attempts to obtain a molecular structure of **5.14** by layering with dichloromethane/hexane or fluorobenzene/hexane, no crystals suitable for X-ray diffraction were isolated. **5.14** was also reacted with $Na[BAr^f_4]$ and $AlCl_3$ in the hope that varying the counter-ion might result in crystals suitable for diffraction. Despite crystals of the $[CpFe(PMe_3)_2(BNMe_2)]^+[BAr^f_4]^-$ being obtained and data being collected there were problems with disorder about the three-legged piano stool structure involving the single $BNMe_2$ and two PMe_3 ligands.

Reaction of the aminoboryl, $[CpFe(CO)_2B(NMe_2)Cl]$ with the chelating ligand dmpe also leads to a systematic shift in the ^{11}B NMR from δ_B 56 for $[CpFe(CO)_2B(NMe_2)Cl]$ to δ_B 62 (δ_P 53) for the mono(substituted) system (**5.15**) to δ_B 66 (δ_P 75) for $[CpFe(dmpe)B(NMe_2)Cl]$ (**5.16**). Once again, the dried reaction mixture was washed with pentane (the ^{11}B NMR of which revealed no Fe-B containing species and then extracted into dichloromethane yielding the cationic aminoborylene, $[CpFe(dmpe)(BNMe_2)]^+Cl^-$ (**5.17**) (δ_B 88 and δ_P 75). Both ^1H and ^{13}C NMR spectra confirm formation of **5.17** with peaks for Cp, PMe_2, PCH_2 and equivalent NMe groups identified. The ESI-MS further supports formation of **5.17** with a peak at *m/z* 326 corresponding to M^+ (accurate mass 326.1049). As with compound **5.14**, crystallization was attempted by layering dichloromethane/hexane and fluorobenzene/hexane, but to no avail. **5.17** was also reacted with $AlCl_3$ and $Na[BAr^f_4]$ in order to obtain crystals suitable for X-ray diffraction, but once again this was unsuccessful. Interestingly, crystals were obtained of the paramagnetic complex, $[\{\eta^5\text{-}C_5H_4B(NMe_2)Cl\}Fe(dmpe)Cl]^+[AlCl_4]^-$ formed by Cp C-H activation (Figure 5.7), a phenomenon that has precedence in the literature for similar complexes.[26]

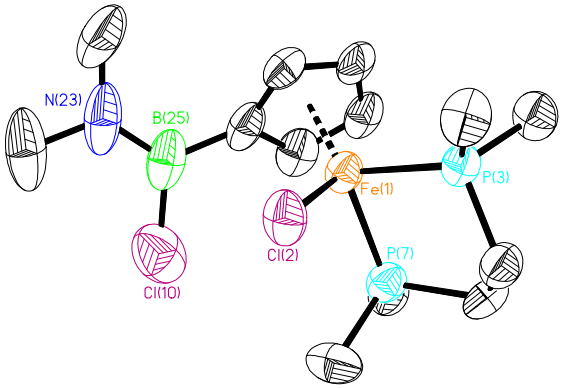


Figure 5.7 Molecular structure of $[\{\eta^5\text{-}C_5H_4B(NMe_2)Cl\}Fe(dmpe)Cl]^+[AlCl_4]^-$. Solvent molecule and hydrogen atoms omitted for clarity. Ellipsoids set at the 50% probability level.

Although I was unable to crystallize **5.17** to obtain definitive structural data, recent work by David Addy in the Aldridge group has resulted in formation and structural characterization of $[CpFe(dmpe)(BNMe_2)]^+[BPh_4]^-$ (Figure 5.8) via the methods described above, providing conclusive evidence of the formation of the bis(substituted) borylene complex.

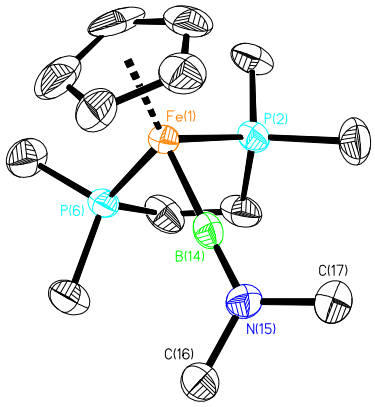


Figure 5.8 Molecular structure of the cationic component of $[CpFe(dmpe)(BNMe_2)]^+[BPh_4]^-$ (**5.17**). Solvent molecule and hydrogen atoms omitted for clarity. Ellipsoids set at the 50% probability level.

5.4 Conclusions and Suggestions for Further Research

Formation of a new cationic terminal borylene complex, $[Cp'Fe(CO)_2(BN^iPr_2)]^+[BAr^f_4]^-$ featuring a methyl-substituted Cp ring is reported. This represents the first isopropyl substituted aminoborylene complex to be structurally characterized. Attention was subsequently directed towards substituting the π-acceptor carbonyl ligands for trialkylphosphines. Irradiation of the aminoboryl complex, $[CpFe(CO)_2B(NCy_2)Cl]$ in the presence of trialkylphosphines, PR_3 (PR_3 = PMe_3, PPh_3, $P(OMe)_3$, ½ dmpe) yields the mono(phosphine) complexes, $[CpFe(CO)(PR_3)B(NCy_2)Cl]$ (PR_3 = PMe_3 **5.2**, PPh_3 **5.5**, $P(OMe)_3$ **5.6**, ½ dmpe **5.7**) by a simple carbonyl substitution process. Replacement of the second carbonyl is prohibited by the steric bulk of the dicyclohexylamino substituent, and instead $[CpFe(CO)(PR_3)_2]^+Cl^-$ is formed by extrusion of the borylene fragment.

Formation of the bridging borylene complex, $[(\mu\text{-}BNCy_2)(\mu\text{-}CO)\{CpFe(CO)_2\}_2]$ (**5.4**) was reported by the reaction of the aminoboryl $[CpFe(CO)_2B(NCy_2)Cl]$ with excess $Na[CpFe(CO)_2]$. Unfortunately, crystals could not be obtained.

Reaction of the mono(phosphine) complexes, **5.2**, **5.5**, **5.6**, **5.7** with $Na[BAr^f_4]$ by halide abstraction leads to the corresponding cationic aminoborylene complexes, $[CpFe(CO)(PMe_3)(BNCy_2)]^+[BAr^f_4]^-$ (**5.8**), $[CpFe(CO)(PPh_3)(BNCy_2)]^+[BAr^f_4]^-$ (**5.9**), $[CpFe(CO)\{P(OMe)_3\}(BNCy_2)]^+[BAr^f_4]^-$ (**5.10**), and $[\{CpFe(CO)(BNCy_2)\}_2(\mu\text{-dmpe})]^{2+}[BAr^f_4]^{2-}$ (**5.11**). Substitution of one carbonyl ligand leads to a shortening of the Fe-B bond as expected due to an increase in the electron density on the transition metal which is π back-donated to the borylene ligand, whilst changes in the BN bond lengths are not statistically significant.

Replacing the sterically bulky cyclohexyl groups in the aminoboryl precursor for smaller methyl groups allowed for the substitution of the second carbonyl group by irradiation of $[CpFe(CO)_2B(NMe_2)Cl]$ with PMe_3/dmpe in toluene, forming $[CpFe(PR_3)_2B(NMe_2)Cl]$ (**5.13**: $PR_3 = PMe_3$, **5.16**: PR_3 = ½ dmpe). However, unlike the analogous dicyclohexyl substituted mono(phosphine) complexes which crystallize from a saturated pentane solution, **5.13** and **5.14** are not extracted into pentane, and instead form the cationic terminal borylene, $[CpFe(PR_3)_2(BNCy_2)]^+Cl^-$ (**5.14**: $PR_3 = PMe_3$, **5.17**: PR_3 = ½ dmpe) in dichloromethane by spontaneous halide ejection. Unfortunately, molecular structures of **5.14**/**5.17** could not be obtained despite attempts to vary both the counterion and layering solvents. However, a structure of $[CpFe(dmpe)(BNMe_2)]^+[BPh_4]^-$ was subsequently obtained in the group giving credence to the inferences made on the basis of spectroscopic data.

An extended comparison of structural and computational data can be drawn up for the newly formed complexes. From the table, we can see that substituting a carbonyl ligand for a phosphine group leads to a shortening in the M-B bond and results in an increase in σ:π contributions to the covalent bond. The bis(phosphine) complex, $[CpFe(dmpe)(BNMe_2)]^+[BPh_4]^-$ which was subsequently structurally characterized and found to have a significantly shorter Fe-B bond, 1.811(3) Å.

Table 5.7 Comparison of Fe-B bond length and σ:π bonding contribution for a range of cationic terminal borylene complexes with varying borylene substituent, transition metal and ancillary ligands.

	d(Fe-B) / Å	σ:π	
$[Cp^*Fe(CO)_2(BMes)]^+$	1.792(8)	62:38	M=B double bond
$[Cp'Fe(CO)_2(BN^iPr_2)]^+$	**1.835(3)**	**70:30**	
$[CpFe(CO)_2(BNCy_2)]^+$	1.859(6)	71:29	
$[CpRu(CO)_2(BNCy_2)]^+$	1.960(6)	68:32	
$[CpFe(CO)(PMe_3)(BNCy_2)]^+$	**1.821(4)**	**67:33**	
$[CpRu(CO)(PMe_3)(BNCy_2)]^+$	1.928(4)	65:35	
$[\{CpFe(CO)(BNCy_2)\}_2(\mu\text{-dmpe})]_2^+$	**1.830(7)**	***a***	
	1.828(7)		
$[CpFe(dmpe)(BNMe_2)]^+$	**1.811(3)**	***a***	
$[CpFe(CO)_2(BCp^*)]^+$	1.977(3)	86:14	M-B single bond

[a]Data not available.

It would be interesting to see the effect on the Fe=B bond length by subtle variation in the phosphine substituent by repeating the reaction of $[CpFe(CO)_2B(NCy_2)Cl]$ with both dimethylphenyl and diphenylmethyl phosphine.

Modification of the cationic terminal borylene whether by variation in the borylene substituent or the metal centre, not only affects the electronic structure of the complex, but also affects the nature of reactivity. Whereas the nature of the borylene substituent has a profound effect, variation in the metal/ancillary ligands would presumably not have as great

an effect. Neverthless, it would be interesting to investigate the reactivity of the mono(phosphine) $[CpFe(CO)(PR_3)B(NCy)_2]^+$ and the bis(phosphine) complex, $[CpFe(PMe_3)_2(BNMe_2)]^+$ with a variety of different nucleophiles in order to compare the reactivity, and reduced electrophilicity of the boron centre to that of the dicarbonyl analogues. Furthermore, it would be interesting to react both the mono- and bis(substituted) complexes with dicyclohexylcarbodiimide, given their different electronic structure, to see whether an initial insertion reaction would occur into the B=N bond rather than into the Fe=B bond (Chapter Three).

5.5 References for Chapter Five

1. (a) H. Braunschweig, *Angew. Chem. Int. Ed*., 1998, **37**, 1786. (b) H. Braunschweig, M. Colling, *J. Organomet. Chem*., 2000, **614**, 18. (c) H. Braunschweig, M. Colling, *Coord. Chem. Rev*., 2001, **223**, 1. (d) H. Braunschweig, M. Colling, *Eur. J. Inorg. Chem*., 2003, 393. (e) H. Braunschweig, *Adv. Organomet. Chem*. 2004, 51, 163. (f) S. Aldridge, D. L. Coombs, *Coord. Chem. Rev*., 2004, **248**, 535. (g) H. Braunschweig, D. Rais, *Heteroatom Chem*., 2005, **16**, 566. (h) H. Braunschweig, G. R. Whittell, *Chem. Eur. J*., 2005, **11**, 6128. (i) H. Braunschweig, C. Kollann, D. Rais, *Angew. Chem. Int. Ed*., 2006, **45**, 5254. (j) S. Aldridge, D. L. Kays, *Main Group Chem*., 2006, **5**, 223. (k) H. Braunschweig, C. Kollann, F. Seeler, *Contemporary Metal Boron Chemistry I*, eds. T. B. Marder, Z. Lin, Springer, 2008, Vol. 130, p 1. (l) D. Vidovic G. A. Pierce, S. Aldridge, *Chem. Comm*., 2009, 1157.
2. (a) D. L. Coombs, S. Aldridge, C. Jones, D. J. Willock, *J. Am. Chem. Soc*., 2003, **125**, 6356. (b) D. L. Coombs, S. Aldridge, A. Rossin, C. Jones, D. J. Willock, *Organometallics*, 2004, **23**, 2911.
3. S. Aldridge, C. Jones, T. Gans-Eichler, A. Stasch, D. L. Kays (née Combs), N. D. Coombs, D. J. Willock, *Angew. Chem. Int. Ed*., 2006, **45**, 6118.
4. D. Vidovic, M. Findlater, G. Reeske, A. H. Cowley, *Chem. Comm*., 2006, 3786.
5. R. A. Fischer, J. Weiß, *Angew. Chem. Int. Ed*., 1999, **38**, 2830
6. R. Waterman, P. G. Hayes, T. D. Tilley, *Acc. Chem. Res.*, 2007, **40**, 712.
7. (a) D. L. Kays (née Coombs), J. K. Day, L-L. Ooi, S. Aldridge, *Angew. Chem. Int. Ed*., 2005, **44**, 7457. (b) D. L. Kays (née Coombs), J. K. Day, S. Aldridge, R. W. Harrington, W. Clegg, *Angew. Chem. Int. Ed*., 2006, **45**, 3513. (c) G. A. Pierce, S.

Aldridge, C. Jones, T. Gans-Eichler, A. Stasch, N. D. Coombs, D. J. Willock, *Angew. Chem. Int, Ed.*, 2007, **46**, 2043. (d) G. A. Pierce, N. D. Coombs, D. J. Willock, J. K. Day, A. Stasch, S. Aldridge, *Dalton Trans*., 2007, 4405. (e) G. A. Pierce, D. Vidovic, D. L. Kays, N. D. Coombs, A. L. Thompson, D. J. Willock, E. D. Jemmis, S. De, S. Aldridge, *Organometallics*, 2009, **28**, 2947.

8. J. Emsley, *The Elements*, Oxford University Press: Oxford, 1991.
9. B. Blank, M. Colling-Hendelkens, C. Kollann, K. Radacki, D. Rais, K. Uttinger, G. R. Whittell, H. Braunschweig, *Chem. Eur. J*., 2007, **13**, 4770.
10. K. M. Waltz, C. N. Muhuro, J. F. Hartwig, *Organometallics*, 1999, 3383.
11. (a) A. A. Dickinson, D. J. Willock, R. J. Calder, S. Aldridge, *Organometallics*, 2002, **21**, 1146. (b) S. Aldridge, A. Rossin, D. L. Coombs, D. J. Willock, *Dalton Trans*., 2004, 2649.
12. G. C. A. Bellinger, H. B. Friedrich, J. R. Moss, *J. Organomet. Chem*. 1989, **366**, 175.
13. (a) H. Braunchweig, C. Kollann, U. Englert, *Eur. J. Inorg. Chem*., 1998, 465. (b) H. Bruanchweig, C. Kollann, K. W. Klinkhammer, *Eur. J. Inorg. Chem*., 1999, 1523.
14. T. Yamaguchi, K. Ueno, H. Ogino, *Organometallics*, 2001, **20**, 501.
15. P. J. Hore, *Nuclear Magnetic Resonance*, Oxford University Press: Oxford, 1995.
16. S. E. Kegley, M. Brookhart, G. R. Husk, *Organometallics*, 1982, **1**, 760.
17. T. E. Müller, D. M. P. Mingos, *Transition Met. Chem*., 1995, **20**, 533.
18. C. A. Tolman, *Chem. Rev*., 1977, **77**, 31.
19. T-Y Luh, Coord. *Chem, Rev*, 1984, **60**, 255.
20. D. J. Blumer, K. W. Barnett, T. L. Brown, *J. Organomet. Chem*., 1979, **173**, 71.
21. S. G. Davies, *J. Organomet. Chem*., 1979, **179**, C5.

22. K. Ueno, M. Hirotsu, N. Hatori, *J. Organomet. Chem*., 2007, **692**, 88.

23. N. D. Coombs, W. Clegg, A. L. Thompson, D. J. Willock, S. Aldridge, *J. Am. Chem. Soc*, 2008, **130**, 5449.

24. D. R. Senn, A. Wong, A. T. Patton, M. Marsi, C. E. Strouse, J. A. Gladysz, *J. Am. Chem. Soc*., 1988, **110**, 6096.

25. P. B. Glaser, P. W. Wanandi, T. D. Tilley, *Organometallics*, 2004, **23**, 693.

26. S. Aldridge, D. L. Kays (née Coombs), A. Al-Fawaz, K. M. Jones, P. N. Horton, M. B. Hursthouse, R. W. Harrington, W. Clegg, *Chem. Comm*., 2006, 2578.

Appendix One

Computational Methodology

Details of the computational methodology used in this study are similar to those reported recently, and salient points are outlined here.[1]

Gradient corrected DFT calculations were carried out using the ADF2000.01 code,[2] with functionals for exchange and correlation due to Becke[3] and Lee, Yang and Parr,[4] respectively. A basis set constructed from Slater type orbitals at the triple zeta with polarization functions level was used for all calculations (ADF IV). The level of frozen core approximation for B, C, N, O and F was the 1s orbital and for P, Cl and Fe was the 2p orbital. All structures, unless otherwise stated, were fully optimised with no symmetry restrictions. Convergence was accepted when the following limits were met: (i) energy change on next step < $1x10^{-3}$ Ha; (ii) gradient < $1x10^{-3}$ Ha $Å^{-1}$; and (iii) uncertainty in cartesian coordinates < $1x10^{-2}$ Å. The multiplicity of each structure was determined by using unrestricted calculations with spin states set to reasonable alternatives to determine the lowest energy configuration which conformed to the aufbau principle.

To calculate the degree of σ and π-bonding between the metal centre and boron atom the optimised structures were re-orientated so that the bond was aligned with the *z*-axis. A bonding analysis was then carried out following the approach discussed below to give contributions to the bonding density segregated according to the symmetry of the atomic orbitals involved.

The one electron wavefunctions, ψ_i, used to represent the density in these DFT calculations are constructed in the usual manner as a linear combination of atomic basis functions, ϕ:

$$\psi_i = \sum_k^M c_{ik}\phi_k \tag{1}$$

where c_{ik} is the coefficient of the k^{th} basis function in the i^{th} molecular orbital and there are a total of *M* basis functions. The density, ρ, is then given by summation over the occupied orbitals of the one electron densities:

$$\rho = 2\sum_i^{N/2}\sum_l^M c_{il}\phi_l \sum_k^M c_{ik}\phi_k = 2\sum_l^M\sum_k^M \phi_l\phi_k \sum_i^{N/2} c_{il}c_{ik} \tag{2}$$

Where *N* is the total number of electrons and we only consider the restricted spin paired situation for simplicity, extension to the spin unrestricted case is straightforward. The rearranged form of the density expression allows the calculation to be performed *via* the definition of two square matrices with the dimension *M*. The first is usually referred to as the density matrix, **P**, and its components depend only on the calculated coefficients:

$$P_{lk} = \sum_i^{N/2} c_{il}c_{ik} \tag{3}$$

The second, the overlap matrix, **S**, depends on the basis set and the geometry of the molecule:

$$S_{lk} = \phi_l \phi_k \tag{4}$$

The density can then be represented as a matrix multiplication:

$$\rho = 2\sum_{l}^{M}\sum_{k}^{M} S_{lk} P_{kl} \tag{5}$$

Since the basis set consists of atom centred functions, **P** and **S** will contain some contributions which are wholly centred on a given atom and some which are due to the overlap of basis functions on pairs of atoms. The latter contribution is related to the bonding between atoms and the most straightforward way to address the character of bonding is to examine this portion in isolation. By identifying the basis functions centred on a pair of atoms, *A* and *B* say, we can identify the bonding density, ρ_{AB}, by summing only the relevant contributions in equation 5:

$$\rho_{AB} = 2\sum_{l\in A}\sum_{k\in B} S_{lk} P_{kl} \tag{6}$$

This is the bonding density as defined by Mulliken.[5] To differentiate π and σ contributions to the bonding density we simply align the bond of interest with the *z*-direction and separate the basis

functions according to their symmetry, *e.g.* p_z is of σ type and p_x and p_y are of π type. Equation 6 can then be further sub-divided:

$$\rho_{AB} = 2\sum_{l\in A}^{\sigma}\sum_{k\in B}^{\sigma} S_{lk}P_{kl} + 2\sum_{l\in A}^{\pi}\sum_{k\in B}^{\pi} S_{lk}P_{kl} + 2\sum_{l\in A}^{\delta}\sum_{k\in B}^{\delta} S_{lk}P_{kl} + \ldots\ldots \quad (7)$$

where the symmetry labels on the summations indicate the basis function symmetry to be considered. We report the two terms in equation 7 separately to judge the degree of π bonding in MB bonds.

This decomposition of the molecular orbital representation of the density to give bonding density is not unique and so to ensure the reliability of our analysis we also consider a bonding density analysis proposed by Mayer.[6] In the Mayer analysis the product of the density and overlap matrices is first calculated and then the elements of this product matrix are selected according to the basis functions belonging to the atoms of interest. Again we further partition the matrix in terms of π and σ symmetry:

$$\rho_{AB}^{M} = 2\sum_{l\in A}^{\sigma}\sum_{k\in B}^{\sigma} (\mathrm{PS})_{kl} + 2\sum_{l\in A}^{\pi}\sum_{k\in B}^{\pi} (\mathrm{PS})_{kl} \quad (8)$$

As part of this work the application of equations (7) and (8) to the data provided by an ADF output was automated by the development of a dedicated program. The coding was tested by calculation of the Mulliken atomic densities which are output by ADF and by analysis of simple

test cases such as ethane, ethene, ethyne *etc.* (these analyses are included in reference 1). The Mayer bond order calculation was tested by comparing values obtained from our analysis of ADF outputs and those generated at a similar basis set level by the MSI code, Dmol.[7] The results of decomposition into σ and π contributions from Mulliken and Mayer approaches consistently showed the same trends and so only the former is reported in the main text.

References for Appendix One

1. A. A. Dickinson, D. J. Willock, R. J. Calder, S. Aldridge, *Organometallics*, 2002, **21**, 1146.
2. (a) E. J. Baerends, D. E. Ellis, P. Ros, *Chem. Phys.*, 1973, **2**, 41. (b) L. Versluis, T. Ziegler, *Chem. Phys.*, 1988, **88**, 322. (c) G. te Velde, E. J. Baerends, *J. Comput. Phys.*, 1992, **99**, 84. (d) C. Fonseca Guerra, J. G. Snijders, G. te Velde, E. J. Baerends, *Theor. Chem. Acc.*, 1998, **99**, 391.
3. A. D. Becke, *Phys. Rev. A*, 1988, **38**, 3098.
4. C. Lee, W. Wang, R. G. Parr, *Phys. Rev. B*, 1988, **37**, 785.
5. R. S. Mulliken, *J. Chem. Phys.*, 1955, **23**, 1833.
6. I. Mayer, *Int. J.Quantum Chem.* 1986, **29**, 477.
7. *DMOL*^{3}, Biosym/MSI, San Diego, CA, 1996.

Appendix Two

List of Publications

- Cationic terminal aminoborylene complexes: controlled stepwise insertion into M=B and B=N double bonds, G. A. Pierce, S. Aldridge, C. Jones, T. Gans-Eichler, A. Stasch, N. D. Coombs, D. J. Willock, *Angew. Chem. Int. Ed*., 2007, **46**, 2043.

- Insertion reactions of dicyclohexylcarbodiimide with aminoboranes, -boryls and -borylenes, G. A. Pierce, N. D. Coombs, D. J. Willock, J. K. Day, A. Stasch, S. Aldridge, *Dalton Trans*., 2007, 4405.

- Transition metal borylene complexes: boron analogues of classical organometallic systems, D. Vidovic, G. A. Pierce, S. Aldridge, *Chem. Comm*., 2009, 1157.

- Half-sandwich group 8 borylene complexes: synthetic and structural studies and oxygen atom abstraction chemistry, G. A. Pierce, D. Vidovic, D. L. Kays, N. D. Coombs, A. L. Thompson, D. J. Willock, E. D. Jemmis, S. De, S. Aldridge, *Organometallics*, 2009, **28**, 2947.

- Reactivity of cationic terminal borylene complexes: novel mechanisms for insertion and metathesis chemistry involving strongly lewis acidic ligand systems, S. De, G. A.

Pierce, Drasko Vidovic, D. L. Kays, N. D. Coombs, E. D. Jemmis, S. Aldridge, *Organometallics*, 2009, **28**, 2961.

- Spontaneous borylene generation: evaluation of the thermodynamic factors leading to the formation of an exceptionally short metal-boron bond, D. A. Addy, G. A. Pierce, D. Vidovic, D. Mallick, E. D. Jemmis, S. Aldridge, submitted.